A

THESIS

Entitled

THE EFFECT OF LEAD HALIDES

ON

OXIDATION CATALYSTS

--oOo--

BY

JAMES G. BUCKNELL

Submitted for the

DEGREE OF DOCTOR OF PHILOSOPHY JULY 1977

of the

CITY UNIVERSITY

C O N T E N T S

ABSTRACT

Owing to an increasing awareness over the last few decades, of the importance of vehicle exhaust emissions to the growing problem of air pollution, a number of methods for reducing such emissions have been developed. Of these, the catalytic converter is probably the most important. The function of a catalytic converter is to oxidise completely carbon monoxide and hydrocarbons and also to reduce oxides of nitrogen without the formation of ammonia. However, the presence of various lead compounds resulting from the combustion of lead tetra-alkyl antiknock additives has been found to deactivate or poison the catalysts used in such converters. The purpose of this work has been to investigate the mechanism of deactivation of catalysts by lead compounds.

In the Introduction, an account is given of the general problem of pollution with particular reference to the role of catalysis in the control of automotive air pollution. In addition, the main theories of heterogeneous catalysis, including catalytic poisoning, are summarised together with a description of the main experimental techniques used. Finally a review is given of the current status of heterogeneous catalytic oxidation, as applied to the control of automotive air pollution, with particular emphasis on catalyst deactivation.

The Experimental Section describes the compounds, apparatus and procedures used in this work. The catalysts selected for study were mainly transition metal oxides (both supported and unsupported), the most important of which were nickel (II) oxide and cobalt (II,III,III) oxide. In addition to these, an alumina-

supported platinum catalyst was investigated. The lead compounds chosen were lead (II) bromide and lead (II) chloride. Catalysts were deactivated by use of a specially designed apparatus, which allowed a regulated stream of lead halide vapour to come into contact with the catalyst. The effect of lead halide on catalytic activity with respect to carbon monoxide oxidation was studied using a pulsed-flow micro-reactor. In conjunction with this, a number of physicochemical techniques were employed to examine further the interaction of catalysts with the lead halides.

In the Results Section, the lead halides are shown to deactivate all the catalysts examined, with the supported catalysts showing a significantly greater resistance to deactivation than the unsupported catalysts. Of the unsupported catalysts, cobalt (II,III,III) oxide was clearly the most resistant to deactivation. Furthermore lead (II) chloride was found to be far more effective than lead (II) bromide in deactivating both supported and unsupported cobalt (II,III,III) oxide. Nitrogen adsorption studies have revealed that there is little correlation between the deactivation by lead halides of unsupported catalysts, on the one hand, and the surface properties of these catalysts on the other. However, it has been shown that both surface area and porosity decrease during the deactivation of supported catalysts. Various physicochemical techniques have shown that bulk chemical reaction between the lead halides and the catalysts does not take place.

Finally, in the Discussion, the significance and implications of the experimental results are considered in detail. Adsorption of the lead halides appears to be the principal mode of deactivation both with supported and unsupported catalysts. However, the support provides a large surface area for adsorption of the halides, and this increases the tolerance of the catalyst to deactivation. In addition, with supported catalysts, lead halides appear to be concentrated primarily on the outer surface of the catalyst, without deep penetration into the porous structure, thus causing pore blocking. The mechanism of pore blocking was not found, however, to be important.

ACKNOWLEDGMENTS

My sincere thanks are due to Professor C. F. Cullis who organized this project and whose supervision has been a constant source of help and encouragement. My thanks are also due to Dr. D. J. Hucknall who co-supervised this project and whose help in every aspect of the work has been invaluable.

I am very much indebted to The Associated Octel Company for their most generous sponsorship of this project and also to [redacted], of this company, whose continued interest in this project was most helpful.

I am also indebted to many of the staff of The City University for their assistance and cooperation. In addition my thanks are due to my collegues in The Chemistry Department for many interesting conversations and much practical help and advice.

I would like to thank both of my parents for many years of encouragement during my education and in particular to thank my mother for her generous assistance in typing this thesis.

Finally, my warmest thanks are due to [redacted] who has made many sacrifices during the time spent on this project and whose support and understanding are greatly appreciated.

--oOo--

SECTION 1

INTRODUCTION

SECTION 1

Cont.

Page Number

1.3. HETEROGENEOUS CATALYSIS FOR CONTROL OF AUTOMOTIVE POLLUTION

--oOo--

1.1. POLLUTION

1.1.1. GENERAL

One of the fastest growing areas of technology at the present time is that concerned with pollution control. In the last few decades, the contamination of the environment has reached alarming proportions, resulting in a considerable public outcry. This has stimulated legislation to control pollution levels, which in turn has promoted much research effort directed towards solving these man-made problems.

However, in order to consider the problems of pollution and pollution control from a fair-minded and scientifically-detached viewpoint, it is necessary to look a little further into the background of the subject. It is not particularly uncommon for a subject such as pollution to be presented to the general public, by newspaper articles, television and radio programmes, etc., in such a way as to cast doubt on the validity of our whole modern way of life.

There are in fact numerous examples of ancient civilizations who also had pressing pollution problems. Excavations at the site of Troy indicated that the inhabitants dropped their refuse on the floor and let it accumulate until the level rose so high that doors would not open, whereupon the doors were repositioned. Ancient Athenians improved somewhat on these sanitation habits, disposing of refuse in dumps at the borders of the city. The Romans, also, left masses of refuse, garbage and even human corpses

in open trenches on the city's outskirts, which historians say contributed to the typhoid, typhus, cholera and malaria outbreaks which plagued the city.

There is evidence to show that many countries in the Middle East destroyed their once fertile land by a gradual process of deforestation. At the same time, no attempt was made to protect the soil from the harmful effects of the wind. Furthermore, there was a tendency to burn useful residual matter, so that the value of humus as a fertilizer was lost.

The practice of destroying fertile land was not confined to ancient times. Within living memory, vast tracts of the U.S.A. were laid waste because improvident farmers failed both to sustain the natural humus of their soil and to replenish its nutrients by means of fertilizers.

It can therefore be seen, by looking at a few of the many examples of pollution over the ages, that it is not a new problem but one which is invariably associated with any sizeable community. However, it is encouraging to note that, even as long ago as the thirteenth century, the need to control pollution was recognised in some countries, and legislation was introduced for this purpose. For example in 1273, during the reign of Edward I the first smoke abatement legislation was enacted in England. This law was designed to control the usage of cheaply mined coal for cooking and heating, because there was considerable concern about the effects of coal smoke on health.

With the coming of industrialization some of the most pressing pollution problems began to appear in this country. The problem was

exacerbated by the tendency of industrialization to take place on a large scale in localized areas. In the early years of the Industrial Revolution, the science and technology which created a large proportion of the pollution problem, was ill equipped to provide a solution. Nevertheless, this state of affairs could not last and the technical answers to most of the problems were soon forthcoming. However, the existence of the scientific and technical knowledge required to deal with pollution is only one part of the problem. Coupled with this knowledge there has to be a political will to implement the techniques of pollution control. In short, legislation is necessary to ensure that no industrial manufacturer is tempted to pollute the environment in the search for an economic advantage over its competitors. The legislation necessary to cope with this country's pollution problems has been enacted over a very long period of time, beginning with the first smoke abatement legislation in 1273, although the main Acts such as The Public Health Act 1936, and The Clean Air Act 1956, came into effect only quite recently.

The scope of the modern-day pollution problem may be conveniently dealt with under the classifications land, water, and air pollution, which, whilst not including all types of pollution such as noise pollution for example, do cover most areas of concern. Each of these classifications is thus dealt with separately and in turn in the subsequent sections.

1.1.2. LAND POLLUTION

Land pollution is brought about almost entirely from the dumping of solid wastes, which have a harmful effect upon the land. Occasionally these wastes can become sufficiently dispersed by the wind and rain to contribute to pollution of the waterways and also to air pollution,

although this is a relatively insignificant effect.

Land pollution can be divided into three main areas:- agricultural, mineral, and municipal land pollution. Agricultural wastes and mineral wastes, derived principally from mining operations, make up a very large proportion of the total solid wastes in all countries. However, these constitute a proportionately less harmful pollution effect than municipal solid wastes because they are spread over wide areas. Agricultural solid wastes make up the largest single source of solid wastes and include animal manures and wastes from slaughter houses and from all forms of crop harvesting. Food animals generate 1,000 times more manure than does the total human population (1). In the past, this manure was returned to the soil quite naturally by the animals. However, with modern methods of intensive farming, the manure has tended to be concentrated in local areas. In order to prevent the problems of high concentrations of animal manure, it is merely necessary to spread the manure over the land, where it can be usefully returned to the soil. At the same time this minimises the possibility of water pollution. Modern agricultural fertilizers have also contributed to eutrophication of water, either when more fertilizer is applied to the land than the crops can absorb, or when heavy rains wash off the fertilizer. This problem can be controlled by obtaining a greater understanding of the movement of fertilizers and the use of the latest slow-release nitrogen fertilizers, as well as by using improved techniques of application, designed to minimize the loss of fertilizer from the land.

Mineral solid wastes are produced mainly from the extraction of minerals and fossil fuels. These wastes constitute a pollution problem

in several ways. Their presence affects visual amenity and prevents the useful and normal agricultural use of the land; some of the mineral wastes run off the land and pollute rivers and streams; and surface dust causes air pollution. Control and prevention of this form of pollution can be brought about by land reclamation schemes e.g. building parks and cattle farms. However, one of the essential prerequisits for land reclamation is the use of strict planning controls by local authorities.

Municipal land pollution is brought about by the dumping of large amounts of solid wastes generated by both residential and industrial sources. If the dumping of the solid wastes is properly controlled, the site should not give rise to air, water or severe land pollution. Furthermore once operations have ceased, it is quite possible to reclaim tipping land for other uses. Technological means for meeting the municipal waste problem include improved collection as well as improved incineration, the resulting heat being used for power generation and recycling. Furthermore, recycling, which is already extensively used in Japan for waste paper recovery, has the dual advantages of dealing with the solid waste problem and alleviating the ever-growing pressure on raw material resources.

1.1.3. WATER POLLUTION

Pollution of natural waters i.e. rivers, lakes and the sea, is caused by the release of domestic sewage and industrial effluents.

The discharge from domestic premises, either directly into the streets, or into the nearest streams or rivers was, during earlier centuries, an important cause of the spread of diseases. Today it is no longer permissible to deposit sewage into the streets or to discharge it directly into the nearest water course. As a result of

the laws preventing such practices, the spread of harmful water-borne bacteria, such as those responsible for cholera, typhoid, and enteric fever, has ceased. However, although the processes for purifying water contaminated from domestic sources have been understood for many years, it is still the practice of most local authorities to discharge untreated sewage directly into water courses.

The main processes used to deal with domestic effluents include filtration, biological action, sedimentation and sterilization. In recent years, this comparatively simple method has been complicated by the use of detergents, which are not capable of being broken down by biological action. This problem has now fortunately been overcome by the gradual replacement of these detergents by their biodegradable equivalents. It is of interest to note that this change was accomplished largely as a result of public opinion but also due to the efforts of scientists who have discovered the more recently developed biodegradable materials.

The treatment of industrial effluents is a much more complicated problem than that of domestic effluent treatment. Industrial wastes produce organic pollution almost equal to that caused by the living processes of the population as a whole (2). Much of this organic pollution is caused by chemicals, which are far more difficult to degrade biologically than those present in domestic sewage. In addition, industry produces substantial quantities of persistently damaging pollutants i.e. phenol, dissolved metal salts, oil products, radio-active substances, etc., which are discharged both in solution and in suspension into water courses. These discharges, rather than the more natural domestic sewage flows, have been the cause of massive and deadly pollution of natural waters throughout the industrialized world. It is for these reasons that regulations concerning the

discharge of industrial effluents have been introduced e.g. in Britain a new Public Health Act came into force in 1936. Although the regulations regarding industrial effluents in many countries are still inadequate, particularly in the United States, it has been clearly established that only stringent control of industrial effluents will improve the problem.

If industrial water is to be discharged into public sewers or water courses, it is, therefore, absolutely necessary that it is adequately purified beforehand. The technical problems of purifying industrial effluents are relatively simple, provided that treatment is carried out, at source, by the Company concerned. Furthermore it is desirable that different effluents should be dealt with before being mixed together, as the mixing of dissimilar effluents can cause difficulties in treatment procedures. In addition, some effluents, when mixed together, may constitute an immediate health hazard to the plant workers.

1.1.4. AIR POLLUTION

1.1.4.1. GENERAL

Air pollution has been shown beyond all reasonable doubt to have an adverse effect upon health. An extremely large volume of statistical evidence has been published (3), which shows clearly that people living in polluted areas are far more likely to suffer from certain diseases than people living in clean-air conditions. Constant air pollution has other far from pleasant effects on the environment. Many plants are affected by the acidity of rainwater and the deposition of solids on leaves. Air pollution causes far-reaching structural and surface damage to buildings, ruins clothing

and other fabrics and induces heavy corrosion of metal structures ranging from bridges to motor vehicles. Again, as in the other main areas of pollution, the technical means are available for eliminating air pollution. However, in order to induce manufacturers and others contributing to air pollution to apply such controls, a well-thought-out legislative programme is needed. Some important steps in this direction have already been taken in this country. Thus the Clean Air Act 1956 has had the effect of reducing air pollution caused by smoke particles over the period 1958 - 1968 by a factor of three (4).

Air pollution falls into two main types, that caused by finely divided solid and liquid particles such as dust, carbon, hydrocarbons etc., which are electrically charged and thus kept in suspension by electrostatic forces; and that caused by gases which are poisonous or otherwise obnoxious in nature e.g. sulphur dioxide, carbon monoxide, oxides of nitrogen, hydrocarbon vapours and other substances. One of the most harmful of such materials is 3.4 - benzpyrene, which is markedly carcinogenic.

Air pollution is caused by three main factors: Domestic fires and domestic refuse incineration; Industry; Motor vehicles, aircraft, ships, and other combustion engines. These three factors are considered in the following two sections.

1.1.4.2. DOMESTIC AND INDUSTRIAL AIR POLLUTION

In the United Kingdom, by far the most important source of air pollution is the open coal fire. Grit and sulphur dioxide emission from domestic fireplaces, not to mention emission of dangerous 3.4 - benzpyrene, greatly exceeds pollution from all other sources. In the U.K., only 20-30 per cent of air pollution is caused by vehicles and industry (5), while the remainder comes from domestic chimneys.

It is interesting to note that the proportion of air pollution generated by the different sources varies considerably from country to country, and even from town to town. For example, in Los Angeles in 1969 (just before the enforcement of anti-pollution laws) road vehicles accounted for about 85 per cent by volume of all man-made toxic emissions (6). One of the reasons for these variations is that cooler regions require more domestic heating. Another cause of the variation is the size of cars, larger engines producing much more pollution than smaller ones.

Despite the improvement in the air pollution situation which has occurred in the U.K. since the Clean Air Act 1956, this country is still far dirtier than many other industrialized countries e.g. those of central and northern Europe and countries under Communist rule. In many of these countries, district heating systems are a major source of urban heating, this method being by far the best way of eliminating air pollution from domestic sources. District heating is so successful, because the need for combustion appliances in individual homes is eliminated by substituting hot water or steam supplied from centralised sources. The type of central station used in district heating can vary from conventional oil or coal burning boiler houses to refuse incinerators or even nuclear energy heating plants. The important advantage of all these methods of heating is that they are all large enough to enable air cleaning of flue gases to be carried out efficiently. With the use of high chimneys, any sulphur dioxide emitted can be carried away from the centres of population. In Britain, unfortunately district heating is still very much in its infancy.

In the United States, heating is carried out mainly by natural gas or oil-fired central heating furnaces; as a result there is little pollution from heating appliances. Nevertheless American cities are at least as dirty as British ones because of the widespread and growing practice of using inefficient small domestic incinerators to burn household waste. Air pollution in American cities could be virtually eliminated if the increase in the number of ineffective domestic garbage incinerators were prevented.

Other methods of preventing domestic air pollution include the use of smokeless fuels, the best known of these being coke, which is produced as a by-product of town gas production by coal carbonization. Smokeless fuels, whatever their source, all suffer from the disadvantages of high cost and low thermal efficiency, and in addition still cause high levels of sulphur dioxide to be produced as a pollutant.

The sulphur content of other fuels, such as oils or coal is also a significant disadvantage, even when these fuels are burnt in efficient central heating systems, designed to eliminate smoke and grit formation. In fact, there are processes for removing sulphur from oil and coal and these have been used with some success with the former but not yet with the latter.

When raw coal is burned in an open domestic fireplace, the flue gases contain both solid particles and obnoxious gases. It is almost impossible to remove these pollutants, as the use of gas cleaning plant in each individual home is totally impracticable. However, the industrial generation of polluted air is an entirely different matter. Methods are available today which make it possible to remove almost all solid, liquid and gaseous pollutants

from waste gases; and the reason why they are not used everywhere is exactly the same as the reason why only a fraction of the waste water produced by home and industry is treated, and virtually none is purified to the degree which present day technology makes possible. Namely, it costs money to instal and operate efficient gas-cleaning plant and, until appropriate legislation is introduced, the problem will remain.

It is not within the scope of this thesis to describe all the methods available for dealing with industrial air pollution but the principal techniques for separating solid and liquid particles from gases may be listed here:

Gravity settling chambers;

Inertial separators;

Cyclones;

Filtration plants;

Electrical precipitation plants;

Liquid scrubbers.

By far the most important gaseous pollutant produced by industry is sulphur dioxide, which can be removed efficiently from flue gases in a number of ways. Most methods of removal are chemical in origin and involve reacting the gas with solids or liquids to produce sulphur-containing compounds or even pure sulphur. Part of the cost of removing sulphur dioxide from flue gases can be recovered by selling the resulting sulphur compounds.

1.1.4.3. AUTOMOTIVE AIR POLLUTION

Mobile sources of air pollution include almost all known forms of transportation: motor cars; diesel engines in heavy road vehicles, buses, and railway engines, as well as ships and aircraft.

Some years ago, pollution from these sources was insignificant compared with air pollution emanating from homes and factories, but with constantly increasing numbers of vehicles of all types, this is no longer the case. The most important mobile source of air pollution is without doubt the motor car, and it is the pollution from such vehicles which is of most interest and to which most of this Section of the thesis specifically applies.

Motor vehicles emit a number of pollutants which give rise to concern, namely carbon monoxide, unburnt hydrocarbons, nitrogen oxides, lead compounds, sulphur dioxide and particulate matter.

Carbon monoxide, unburnt hydrocarbons and oxides of nitrogen are considered to be the most important pollutants emitted from car exhausts by most workers in this field (7, 8). Sulphur dioxide, which is such an important pollutant from domestic and industrial furnaces, is not of major significance as a pollutant from internal combustion engines, as sulphur is removed almost completely from petrol and other fuels during oil refining. The amount of solid particulate matter emitted in the exhausts from petrol engines is not large, and if this matter consisted only of inert materials such as carbon it would cause little concern. However, some workers consider that the lead compounds emitted by car exhausts constitute a serious health hazard (9), whilst others believe that present levels are not dangerous (10).

It is of interest to note that the three main pollutants emitted by car exhausts are produced by natural agencies in far greater quantities, on a global basis, than the entire quantity produced by all man-made agencies. There exist however natural

cycles for the control of these pollutants (11,12). For this reason it would seem that efforts to control pollution by exhaust emissions should be directed towards reducing high localised concentrations, rather than towards controlling the global situation.

High localised concentrations of exhaust emissions can occur only in urban districts, where a large number of vehicles are moving relatively slowly. This can give rise to particularly high levels of pollutants at street level. A very well known location for this type of pollution is the city of Los Angeles, U.S.A., where not only are high localised concentrations of exhaust emissions found at street level, but owing to the unusual geographical and climatic conditions, a photochemical smog can build up. Such a smog is characterized by decreased visibility, crop damage, eye irritation and increased mortality amongst sufferers from heart and chest conditions.

The country most affected by pollution from car exhaust emissions is the U.S.A., where recent legislation has resulted in the imposition of stringent limits on the permissible concentration of car exhaust emissions. This legislation has stimulated a number of technological developments and scientific discoveries designed to reduce pollution from car exhausts.

These developments may be classified into two rather broad groups: those relying on engine modifications; and those based on treatment of the exhaust emissions of unmodified and conventional engines. In the first of these groups are two developments (13,14), the "Vapipe" and the stratified charge engine, which are already showing considerable promise. Both of these devices have made use of the characteristic variation of exhaust emissions with air:fuel ratio for combustion engines (figure 1.1.) in order drastically to

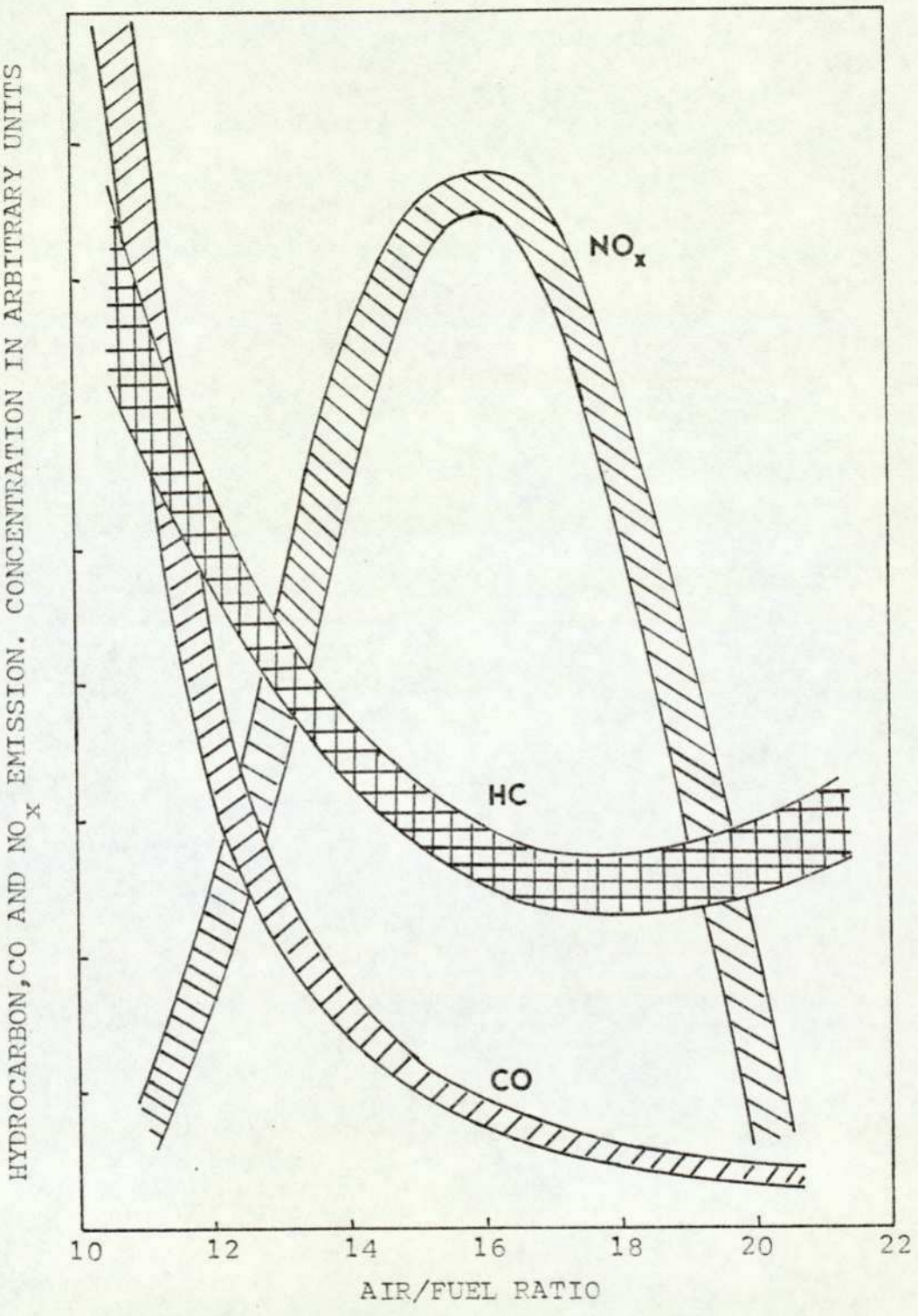

FIGURE 1.1. VARIATION OF MIXTURE STRENGTH WITH EXHAUST POLLUTANT CONCENTRATION

reduce pollution levels. Conventional engines have in the past, always been forced to operate at an air:fuel ratio of about 14 to 1 in order to achieve a suitable compromise of power and economy and also to prevent misfiring. At this mixture composition, which is slightly "rich", all three principal pollutants are present in a relatively high concentration. It can be clearly seen, from figure 1.1., that, if an engine could be made to operate at an air:fuel ratio of 20 to 1, then the levels of exhaust emissions would fall significantly.

The first of these developments, the Vapipe, is a fuel vaporizer located between the carburettor and inlet manifold of a car engine. It is designed to supply a much more homogeneous fuel-air mixture to the engine, thus overcoming the problem of misfiring which normally occurs under these conditions. The stratified charge engine, which unlike the Vapipe, is not a recent invention (although its usefulness with regard to pollution control has only recently been discovered) operates in a similar manner to a conventional four-cycle internal combustion engine, but differs in the manner in which the fuel-air mixture is introduced into the combustion chamber. A small but concentrated quantity of combustible fuel-air mixture is introduced around the sparking plug together with a very "lean" fuel-air mixture which is introduced into the remaining volume of the combustion chamber. The effect of this procedure is effectively to raise the fuel-air ratio to the desirable 20 to 1 value, which results in low levels of exhaust emissions.

Of the two inventions previously described, the Vapipe is of more immediate usefulness, since it may be used to modify existing engines.

The stratified charge engine cannot, however, be introduced generally until all currently used engines, or engines at present being manufactured, are replaced. This replacement process would, even if it were decided on by manufacturers, take a number of years to implement.

Despite the success of the Vapipe, the stratified charge engine and other novel engine modifications, it is unlikely that this approach to the problems of exhaust emission controls would on its own result in the attainment of the very low limits laid down by the U.S.A. and other countries. It is probable that the second group of exhaust control methods, i.e. those which reduce exhaust emissions after they have left the combustion chamber, would be used, either in conjunction with modified or redesigned engines, or indeed on their own.

The main principle used in most methods of removing exhaust pollutants is to oxidise fully the unburnt hydrocarbons and carbon monoxide to carbon dioxide and water, although nitrogen oxides and particulate materials require a different approach. The thermal reactor (15), or the exhaust gas after-burner, operates by allowing the exhaust gases to come into contact with a metered quantity of air. The temperature of the gases is sufficiently high for partial oxidation of carbon monoxide and hydrocarbons to take place, although some devices employ a sparking plug to ensure that combustion occurs. The thermal reactor and other similar devices have achieved overall reductions in emissions of up to 80% (17) but they are only partially successful for the removal of unburnt hydrocarbons and carbon monoxide and indeed do not remove nitrogen oxides at all.

Particulate matter can be removed in a variety of ways, the most common of which is filtration, although a recently developed technique employs exhaust cooling. For this, an air-cooled heat exchanger is used to lower the temperature of the exhaust; the water formed by combustion condenses and in its turn removes, in solution, such pollutants as nitrogen oxides, some of the hydrocarbons and particulate matter, including lead compounds (16).

However, perhaps the most important method of reducing exhaust emissions is to use a catalytic converter in the exhaust system. Many American cars are already fitted with such a device. There are a variety of different designs, one of which is a two-stage apparatus, in which the exhaust gases are first passed over a catalyst bed, where nitrogen oxides are reduced to nitrogen, although reduction to ammonia may be a problem at this stage. The gases are then passed over an oxidising catalyst bed, together with secondary air from an engine-driven pump. The carbon monoxide and hydrocarbons are thus fully oxidised to carbon dioxide and water.

Catalytic converters are much more effective than thermal reactors and the other devices mentioned, for the removal of all three principal pollutants from car exhaust; and they have the additional advantage, compared with thermal reactors, of being able to operate at temperatures as low as 200°C. It is for these reasons that it is difficult to imagine a system of emission control which does not include a catalytic unit. However, catalytic converters suffer from the disadvantages of relatively high initial cost and, more importantly, from a limited useful life. The useful life of the

catalysts used in practical catalytic converters are believed to be decreased by several effects (18). The catalysts may be sintered, or undergo crystal growth due to continual exposure to the high temperatures developed in exhaust systems. The catalyst support material may lose surface area, from the effect not only of temperature but also of the water vapour present in the exhaust gases. Phase transitions which can lead to the break-up of the support material can occur due to severe thermal treatment. Finally, as in the case where leaded fuel is used, deactivation of the catalyst can take place as a result of the deposition of lead on the catalyst from the exhaust gases.

It is the influence on catalysts of the lead compounds found in the exhaust gases, which is of particular interest in the present investigation. Indeed this work is devoted to acquiring an understanding of the mechanism of catalyst deactivation by the lead compounds found in exhaust gases.

1.2. HETEROGENEOUS CATALYSIS

1.2.1. GENERAL

A catalyst is a substance which increases the rate at which a chemical reaction attains equilibrium. Catalysis describes the mode of action of such a substance. The nature of catalysis has been studied for at least a century and a half, and in addition the phenomenon has been used for a much longer period. In the study of catalysis it is usual to classify reactions as either homogeneous, i.e. taking place in a single phase, or heterogeneous, which means that reactions take place at the interface between two phases. By far the most important class of heterogeneous catalytic reactions consist of those which occur at the interface between solids and gases. It is this latter type of reaction which is considered almost exclusively in this thesis.

A catalyst, by increasing the rate at which a chemical reaction reaches equilibrium, must therefore increase the rates of both forward and backward reactions. This principle has been used in the determination, at room temperature, of the heats of reaction of processes (e.g. hydrogenation) which, in the absence of a catalyst, proceed only very slowly. In the study of catalysis it has become abundantly apparent that a catalyst cannot affect the position of chemical equilibrium, and that a catalyst can increase the rate only of a process which is thermodynamically feasible. However, for a given reactant there are sometimes several permissible reaction paths, and the type of catalyst used may determine which path is taken (19). It can be concluded therefore, that the catalyst plays an active, rather than a passive, part in the catalysed

reaction, and its chemical nature is of the utmost importance.

1.2.2. ADSORPTION

The importance of adsorption to the study of heterogeneous catalysis has been understood for a long time. For a reaction to occur at the surface of a catalyst then adsorption must take place. If an atom at the surface is joined by chemical forces to other atoms in the same plane and also below it, there will be a net resultant force on the surface atom, attracting it towards the bulk. If the surface atom has the same valency as any other atom in the bulk, then the unused valencies must be available at the surface.

There exists therefore a certain energy at the surface of a solid. This energy can be used to attract molecules to be adsorbed. An adsorbed molecule must lose entropy as its motion on the surface is more restricted than in the gas phase. In addition the free energy of the system also decreases as the surface valencies become saturated. Now for an isothermal process:-

$$\Delta G = \Delta H - T\Delta S$$

so that adsorption should be an exothermic process. However, there exists some experimental evidence which shows that endothermic adsorption can take place (20).

A very great deal of experimental work over the last 50 years has shown that there are two quite distinct types of adsorption. In the first type, termed physical or Van der Waals adsorption, the adsorbed molecule is held to the surface by weak forces of the type responsible for cohesion in non-hydrogen bonded liquids. Physical adsorption is therefore akin to the liquefaction of gases and for this reason is characterized, chiefly, by relatively low heats of adsorption, roughly 5 to 10 k cal per mole of gas. In

addition, physical adsorption is associated with a relatively rapid rate of adsorption, frequently leading to multi-layer formation, a temperature range for this process close to the boiling point of the gas, and finally non-specificity with regard to the nature of the adsorbent.

In the second type of adsorption, termed chemical adsorption or chemisorption, there is a chemical reaction between the molecule being adsorbed and the solid surface. Since chemisorption involves the formation of chemical bonds with the surface, it is characterized by significantly higher heats of adsorption, the values generally lying within the range 10 to 100 k cal per mole. Furthermore, chemisorption, like most chemical processes, requires activation, and for this reason often occurs at a lower rate than physical adsorption. In addition chemisorption can occur at temperatures much higher than the boiling point of the gas, and it is a specific process, even to the extent of a localised action occurring at the surface of a particular adsorbent. Indeed, this phenomenon of localised action i.e. adsorption at definite points, often referred to as active sites, has been a significant factor in the explanation of many catalytic processes.

All the differences between the two types of adsorption outlined here can, at least in theory, be individually used as tests to distinguish between them. However, it is usually considered necessary to complete most, if not all of these tests before reaching any firm conclusions about the nature of adsorption, even though experimentally it is often rather difficult to do this. However, there are one or two exceptions to this general rule. Thus, for

example, if the number of layers of adsorbate formed can be ascertained, then this, on its own, can be a reliable indication. The reason for this, is that it is generally accepted that chemisorption cannot exceed more than a monolayer, whereas physical adsorption can extend to multilayers (21).

For efficient catalysis, the strength of adsorption of the reactant or reactants must lie within certain fairly wide limits. If a reactant is too strongly adsorbed, it will be correspondingly difficult to remove, and it may then constitute a poison. On the other hand, if it is too weakly adsorbed, it will have little chance of remaining on the surface long enough to react. However, it is often the case that weak physical adsorption can be an essential preliminary to chemical adsorption, the strength of which is of the correct value for catalysis to take place efficiently.

1.2.2.1. ADSORPTION ISOTHERMS

It has been understood for a long time that the equilibrium distribution of adsorbate molecules between the surface of the adsorbent and the gas phase is dependent upon pressure, temperature, nature and area of the adsorbent, and the nature of the adsorbate. The adsorption isotherm is by far the most convenient method, although not the only one, of defining an experimentally determined adsorption equilibrium. Furthermore it is possible to derive theoretical isotherms based on various physical models, and to compare these with the experimentally obtained isotherms. This procedure enables the particular physical model which is operative under certain experimental conditions to be established.

There are a number of well known theoretical isotherms which can be represented by simple equations expressing directly the

variation of the concentration of the adsorbed species with the gas pressure. Most of these isotherms are associated with both chemisorption and physical adsorption, and of these, the most frequently used isotherm is that derived by Langmuir (65). The essential assumptions in the derivation of the Langmuir equation are that: (I) adsorption is localised and takes place only through collision of gaseous molecules with vacant sites. (II) each site accommodates only one adsorbed species. (III) the surface is homogeneous and adsorption sites are not perturbed by their closest neighbours, i.e. the heat of chemisorption is constant and independent of coverage.

Although the Langmuir adsorption isotherm is used extensively in kinetic interpretations of surface reactions, and also for the determination of surface areas (22), the validity of the second and third assumptions, particularly with respect to metals and oxides, is doubtful. It is interesting to note that it is this failure of the Langmuir isotherm which has contributed almost as much to the advancement of catalytic-theory as its limited success. For example, Brunauer (23) has stated that many experimentally observed anomalies can be explained if the surface is heterogeneous. Other workers have argued that these anomalies can also be explained, if there is interaction between molecules which are adsorbed close to one another on a surface (24). Since these objections to the Langmuir model were first made, substantial evidence has come to light to confirm that both surface heterogeneity and surface interactions are factors of considerable importance in the surface chemistry of solids. Indeed the idea of surface heterogeneity in the form of active sites, has long been accepted as a likely explanation of many catalytic phenomenon e.g. Pease and Stewart (25)

explained the poisoning action of mercury on a copper catalyst in terms of strong adsorption of the poison on active sites. More recently direct evidence concerning the actual structure of active sites at solid surfaces has emanated from such techniques as electron microscopy (26), field ion microscopy (26, 27) and electron-probe micro analysis (26).

In summary, then, it can be argued that the failure of an experimentally obtained isotherm to conform to the Langmuir equation can be considered as evidence to support the idea of heterogeneous surfaces, and therefore the existence of active sites.

The first isotherm to account successfully for physical adsorption from the submonolayer to the multilayer stage was that of Brunauer, Emmett, and Teller (53) (The BET isotherm). This isotherm was derived by making assumptions identical to those of Langmuir, but in addition it was assumed that the localised monolayer treatment could be extended to multilayers. The BET equation is capable, under the correct conditions, of yielding the shapes of all five types of physical adsorption which are generally agreed to occur. Indeed it was Brunauer (23) who first clearly recognised these five types of physical adsorption isotherm. Furthermore, apart from the success of the BET isotherm in clarifying the process of physical adsorption, probably its greatest achievement was to enable the surface area of solid catalysts to be measured reliably.

1.2.3. THEORIES OF HETEROGENEOUS CATALYSIS

1.2.3.1. GENERAL

In the scheme of heterogeneous catalytic reaction initially proposed by Sabatier (28) there are five stages:

(a) Diffusion of the reactants from the gas phase to the surface of the catalyst.

(b) Chemisorption of the reactants and migration to active sites.

(c) Chemical reaction of the adsorbed species to form adsorbed products. (The reaction may proceed via intermediate steps).

(d) Desorption of the products from the catalyst surface.

(e) Diffusion of the products into the gas phase.

Steps (b), (c) and (d) involve the making and breaking of chemical bonds with the surface of the catalyst, and as such it is to be expected that the catalytic properties may be related to the electronic properties of the surface and to some extent to the electronic properties of the bulk solid.

Furthermore, the way in which a reactant molecule is chemisorbed and subsequently migrates over the catalyst surface might be expected to be influenced by such factors as the lattice dimensions, the orientation of the crystallite faces, and surface imperfections such as grain boundaries, and stacking faults (geometric factor).

These two approaches have led, over the last twenty or thirty years, to attempts to explain catalytic activity and selectivity first on a geometric basis and recently by means of an electronic approach using band theory and Pauling's valence bond theory. However, the more recent developments have tended to show that these two factors (geometric and electronic) are closely inter-related and attempts have been made to obtain more unifying concepts using the crystal field extension of molecular orbital theory.

Oxidation-reduction catalysts consist primarily of the transition metals and their various semiconducting compounds, especially the oxides and mixed oxide compounds. Theories of catalysis which have been used to relate catalytic properties to the behaviour of solids may be classified as: (I) band theory, (II) Pauling's bond theory, (III) molecular orbital theory, and more recently (IV) crystal field theory.

1.2.3.2. BAND THEORY

This theory explains the electrical properties of metals and semiconductor materials, in terms of the formation of energy bands from the original atomic orbitals of the individual atoms, and the way in which these are filled by the available electrons. At absolute zero, the electrons occupy the lowest energy band, but at higher temperatures electrons may be excited to a higher-energy conduction band. If the energy gap between the filled band and conduction band is too great for such an excitation to occur at normal temperatures, then the solid would be an insulator. But, if the energy gap is not too great, then the solid would be a conductor or a semiconductor.

Imperfections in the crystal lattice result in the formation of discrete energy levels between the filled and conduction bands. Such imperfections may be caused by the presence of an impurity ion or may result from non-stoichiometry. The effect of the impurity ion may be such that it has electrons associated with it which are more easily excited to the conduction band. Alternatively, the impurity may give rise to an empty energy level into which an electron may be excited in preference to the conduction band. Thus there are three reasons why a solid may be a semiconductor.

Firstly, the energy gap may be of such width that electrons may be excited to the conduction band (intrinsic semiconductor). Secondly an impurity ion may produce an electron in an energy level close to the conduction band into which it may be excited (extrinsic n-type semiconductor). Thirdly, the impurity may produce an empty energy level close to the filled band and so form discrete levels into which electrons may be excited (extrinsic p-type semiconductor).

The excitation of an electron from the filled band to the conduction band (intrinsic semiconductor) leaves a "positive hole" in the filled band. Conduction arises from the movement of both the electrons in the conduction band and the "positive holes" in the filled band. For an n-type semiconductor, electrons are donated from an intermediate energy level to the conduction band and electrical conductivity arises from the movement of these electrons under the influence of an applied electric field. For a p-type semiconductor, electrons are excited to an intermediate acceptor energy level, resulting in the formation of "positive holes" in the filled band. Electrical conductivity arises from the movement of the "positive holes".

When for example oxygen is chemisorbed on the surface of a catalyst, negative ions are produced (47) i.e. electrons are donated from the solid to the oxygen. Adsorption on an n-type semiconductor would, then, lower the semiconductivity as the electrons are donated from the conduction band to the adsorbate. Adsorption on a p-type semiconductor would increase the semiconductivity as the electron would be donated from the valence band, increasing the number of "positive holes". Adsorption of a gas which formed cations would have the opposite effect, as electrons would be donated from the adsorbate to the solid. It is of interest to note that, in the decomposition of nitrous oxide, in which adsorbed oxygen ions are

formed, the order of activity is: p-type oxides $\rangle$ insulators $\rangle$ n-type oxides.

The electronic theory of catalysis has been extended by the ideas of Wolkenstein (48), who differentiated between "weak" and "strong" chemisorption and emphasised the differing reactivities of the strongly and weakly chemisorbed species. Weak adsorption would occur when an electron of the adsorbate is attracted to a lattice cation or an electron of a lattice anion is attracted to the adsorbate. The adsorbed species, however, remain electrically neutral. Strong adsorption occurs when the electrons or "positive holes" interact with the adsorbed species, forming chemical bonds. In both cases, localisation of either the electrons or "positive holes" occurs, which means that the adsorbed species are able to change the character of their bonding to the surface. Thus a radial may react with a free electron to form an anion and so change its reactivity.

The electronic theories of catalysis have been successful in explaining many observations, but fail in a number of ways. For example, the chemisorption of a reacting molecule at a particular site is not explained, and certain activity patterns also cannot be explained.

1.2.3.3. PAULING'S BOND THEORY

The introduction of this theory added an important dimension to the catalitic theory, although it offers only qualitative information.

Pauling suggested that the bonds between metal atoms were essentially covalent and that the d-orbitals associated with each atom in the solid can be divided into (a) bonding d-orbitals (in dsp hybrids), (b) metallic d-orbitals, involved in electronic conduction and (c) atomic d-orbitals which are non-bonding and into

which electrons may be transferred. The transition elements were suggested to have vacant atomic d-orbitals and the concept of "percentage d character" was used to represent the extent to which d electrons participate in dsp hybrid orbitals. Thus the percentage d character is a measure of the availability of d orbital electrons. Typical values are: Ni 40%, Pt 44%, Pd 46% and Rh 50%. Various workers have established correlations between catalytic activity of a series of transition metals and percentage d character (29).

1.2.3.4. MOLECULAR ORBITAL THEORY

The ideas of the valence bond theory, developed by Pauling, can be extended in more realistic terms by the molecular orbital theory, as applied to the covalent bonds formed between a metal atom and the chemisorbed neutral reactants. Using concepts originally developed for metal complexes in solution, two types of bond (σ and π) have been postulated and identified upon combination of the s, p, d metal orbitals and the sp orbitals of the adsorbate. Sigma (σ) bonds involve only the d_γ (d_{z^2}, $d_{x^2-y^2}$), s and p orbitals of the transition metal and the sp hybrid orbitals of the adsorbate; the d_ε orbitals (d_{xy}, d_{xz}, d_{yz}) of the metal are not used. Combination of the above metal and adsorbate orbitals produces a set of bonding σ orbitals and a set of antibonding σ^* orbitals separated by an energy gap. These are filled by the available electrons to give a lower energy arrangement than with the individual atoms or molecules. Pi (π) bonds can be formed when the symmetry is such that overlap of the p orbitals of the adsorbate with the d_ε metal orbitals occurs to give a set of π (bonding) and π^* (antibonding) orbitals.

Chemisorption and catalysis is suggested to involve the

formation of σ and or π bonded complexes which can react with each other (or re-arrange internally) to give an adsorbate of different structure, possibly bonded in a different way, but certainly with an overall lower energy.

1.2.3.5. CRYSTAL FIELD THEORY

This theory was first applied to the surface of heterogeneous catalysts by Dowden (30, 31) in an attempt to explain the patterns of activity displayed by the oxides of the first transition metal series for several reactions which could not be satisfactorily explained using an electrostatic or ionic molecular orbital model for the surface bonds. This approach is potentially more useful in that it allows an extension of the principles of inorganic complex chemistry to explain the role of surface intermediates in heterogeneous catalysis.

Crystal field theory predicts that the energy of the adsorbent/adsorbate system can be reduced by an amount called the crystal field stabilisation energy (C.F.S.E.) due to the splitting of the energy levels of the five atomic d orbitals of the metal in the electrostatic field of the adsorbate ion (ligand).

The exact effect of the ligands will depend upon the symmetry of the complex. Generally the two d_{γ} orbitals are placed in a higher energy level, and the three d_{ε} orbitals in a lower energy level. The total energy with all bonds equally filled will of necessity remain constant.

The actual value of the energy split depends on the strength of the ligand field. Two distinct cases are known:

(1) Weak field; all 5 d levels are filled with single electrons according to Hund's rule, and resulting in a high spin complex.

(II) Strong field; the Hund rule applies to each group of d levels i.e. the electrons are paired and a low spin complex results.

Thus the C.F.S.E. is zero for weak fields at d^0, d^5 and d^{10} configurations, is zero for strong fields at d^0 and d^{10}, and reaches a maximum value for d^6 in strong fields. In general the differences in C.F.S.E. for different symmetries are small, and reversible changes between say, octahedral, tetragonal, square pyramidal and square planar complexes may well occur.

At the surface of a catalyst the coordination number (C.N.) of the metal atoms will be lower than in the bulk, and chemisorption of reactants (ligands) to bring the C.N. up to the bulk value (the surface analogue of inorganic complex formation in solution) will be energetically favourable.

Quantitative calculations are usually difficult for real catalytic reactions on account of a lack of knowledge of the indices of the active crystal faces for chemisorption and subsequent chemical reaction and also due to covalent contributions to the bonding. In some well defined cases, the C.F.S.E. for chemisorption has been calculated. For example, on a nickel surface, Dowden (31) has calculated that the C.F.S.E. for chemisorption of water on the 100 face is 5 k cal per mole, and Haber and Stone (32) have calculated C.F.S.E. values for oxygen adsorption (as O^{2-}) of 10.4 k cal per mole for the 100 plane, 21.8 k cal per mole for the 100 plane and 2.1 k cal per mole for the 111 plane.

In considering less well-defined catalytic reactions, qualitative analysis can still be used to predict patterns of catalytic activity and chemisorption. It should be noted, however, that conditions suitable for reactant chemisorption are not necessarily optimal for catalytic activity, since desorption of

products and surface migration may also affect the possibility of reaction.

For weak field ligands the C.F.S.E. for chemisorption will be zero for d^0, d^5 and d^{10} transition elements and a maximum for d^6. These correspond to the ions Ti^{4+}, (Mn^{2+} and Fe^{3+}), Zn^{2+} and Co^{3+} respectively. The results of several reactions over oxides of the first transition series (Hydrogen-deuterium exchange, cyclohexane disproportionation and propane dehydrogenation) give patterns of activity which are in accord with the above observations, i.e. minimum activity at d^0, d^5 and d^{10} and maximum activity at d^6 (with a smaller maximum at d^3 (Cr^{3+})).

The crystal field theory has proved successful in explaining certain observations, and in predicting the course of catalysed reactions (49). However, there have been criticisms of this theory (50), and indeed criticisms of some of the data upon which the theory is based (51). However, it is to be expected that any theory of catalysis will be criticised, and indeed criticism of many theories has in the past led to an improved understanding of the subject as new theories have been developed. It is not possible at this stage to identify any single theory of catalysis which is universally acceptable. Indeed it is probable that this is not a worthwhile goal, and that each catalytic system or group of systems should be considered separately using such theories as are applicable and relevant.

1.2.3.6. CATALYST POISONS

It is well known that a number of substances can effectively inhibit the catalytic activity of catalyst surfaces. Such substances are known as catalyst poisons and function by blocking

the reaction between the reactant and the surface, thus being themselves strongly chemisorbed by the surface (33). It has usually been assumed that poisons are strongly chemisorbed on the sites which would otherwise be active in the catalytic process, and indeed the striking action of mercury as a poison has been used to advance the idea of active sites (see section 1.2.2.1.).

The action of mercury as a poison has received further attention since the early work of Pease and Stewart. For example Campbell and Thomson (34), using isotopic techniques in the study of cyclopropane hydrogenation over a nickel catalyst, found that mercury was an effective poison. In addition, these workers showed that multilayer adsorption took place on the catalyst, but that mercury could not displace all of a preadsorbed hydrogen layer. It was concluded that the mercury must preferentially be adsorbed on those sites active in the catalytic reaction.

The idea of surface heterogeneity, implicit in the theory of active sites, was further advanced for a thiophene-poisoned palladium catalyst on the basis of results obtained during a study of adsorption and hydrogenation of crotonic acid and vinyl acetic acid (35). Again the work involved the use of isotopic tracer techniques. The results showed that the extent of adsorption of the acids was not affected by the presence of the poison, although the hydrogenation rates were drastically reduced. It was concluded that only a small fraction of the adsorbed molecules of acid takes part in the catalytic hydrogenation and that the catalyst surface must be heterogeneous. Finally, another similar study involving the hydrogenation of ethylene on nickel also, for identical reasons, established that the ethylene-nickel surface is heterogeneous (36).

Maxted and others have carried out a most systematic quantitative treatment of poisoning (37). This work has led to results for the inhibition of the hydrogenation of cyclohexane on platinum, by dimethyl sulphide, which can be expressed in the form of a simple equation, i.e.

$$Vp = Vo\ (1 - \alpha P)$$

Where Vp is the rate inhibited by an amount P (moles) of poison, and α is the sensitivity constant or poisoning coefficient. The surface is fully poisoned when $P = 1/\alpha$. Kwan (38) has calculated that, for the same reaction but poisoned by hydrogen sulphide, the number of poison molecules necessary for complete poisoning is close to the number of surface platinum atoms available. Maxted demonstrated in an early paper that the size of the poison is important, less of a poison with larger molecules being required (39). Furthermore, it was also shown that, for a homologous series of dialkyl sulphides, the poisoning coefficient (α) increased with the alkyl radical chain length. Finally, the effect of a given poison on the rate of hydrogenation of several different substrates was examined. It was found that the same relative reduction of the rates of hydrogenation of benzene, nitrobenzene, crotonic acid, oleic acid and benzoic acid were observed for both carbon disulphide and mercuric chloride.

Ashmore has pointed out that, for a large number of liquid phase reactions, the activation energy does not change with the extent of poisoning (46). It was concluded that these catalyst surfaces must be homogeneous, and supports the argument by pointing out that many solutes are adsorbed on metals from solution in such a way as to obey the Langmuir equation. A possible reason for this effect, it is

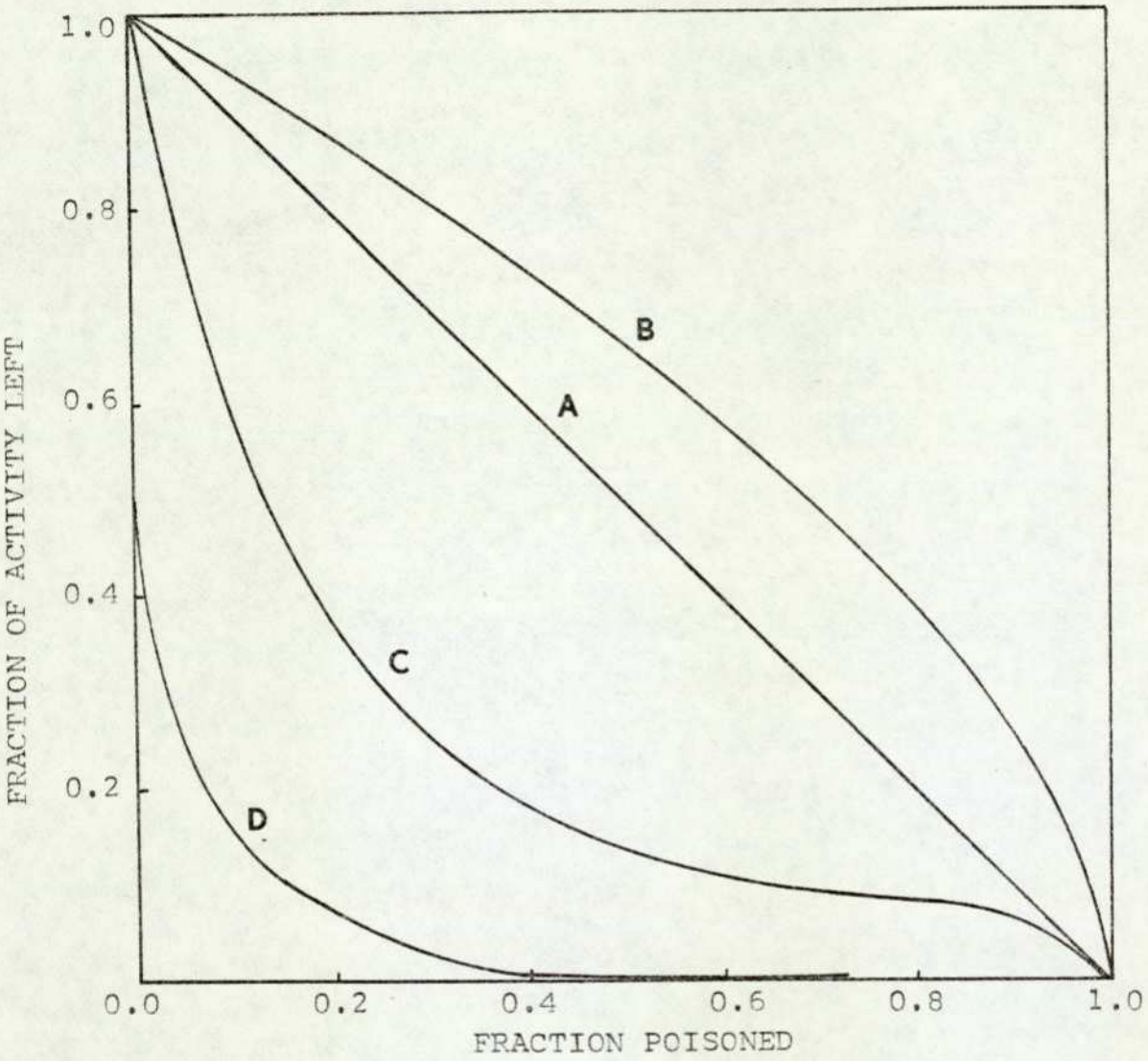

FIGURE 1.2. POISONING CURVES FOR POROUS CATALYSTS (40)

suggested, may be connected in some way with the solvent; perhaps displacement of the solvent from the adsorption site produces some levelling effect in the energetics of adsorption in solution.

One of the most important theoretical treatments of the poisoning of catalysts was carried out by Wheeler (40), who considered in some detail the poisoning of porous catalysts. The effect was first examined of a poison which is adsorbed uniformly over the external and the internal (i.e. pore) surface of the catalyst. An example of a poison of this type is one which would be rather inefficient, and would collide many times with the surface before being adsorbed, and so penetrate into the catalyst pores. The way in which the catalyst activity varies with the fraction of the surface covered with poison is shown in Figure 1.2. Curves A and B represent a slow and a fast reaction respectively.

Wheeler also examined the effect of a poison which is rapidly adsorbed by the catalyst. In this case the mouths of the pores would be selectively poisoned, and the rate of approach to the internal surface would be controlled by diffusion at the pore mouth.

This type of selective poisoning gives rise to curves C and D, curve D, representing the extreme case of very small pores. It would therefore appear probable that the extreme effectiveness of some poisons, e.g. those which follow curve D, may be due to the adsorption of the poison at the pore mouths of porous catalysts.

Finally, Wheeler also showed that the true activation energy of the catalytic reaction on a porous catalyst, could be measured only within a narrow range of low temperatures, where the reaction was not diffusion-controlled.

1.2.4. HETEROGENEOUS CATALYTIC OXIDATION

This topic covers a very wide area of heterogeneous reactions which are important both from scientific and economic points of view. These reactions may be classified into two groups:

(I) Oxidation of simple inorganic compounds

(II) Oxidation of organic compounds

The catalysts which, in general, are the most effective for these reactions, are transition metal oxides and noble metals.

The reactions included in group (I) are the catalytic oxidations of hydrogen, carbon monoxide, sulphur dioxide, and ammonia. Some of these reactions have been extensively studied because of their industrial importance, whilst the oxidation of carbon monoxide has, for example been a popular choice for workers studying the electronic theory of catalysis (66) and catalyst selection rules for oxidation - reduction reactions (41).

In contrast to the relatively simple compounds considered in group (I), the organic compounds in group (II) are either oxidised completely to carbon dioxide and water or, under milder conditions, give valuable intermediate oxygen - containing products, e.g. alcohols, acids, aldehydes, and ketones. The value of complete oxidation,by way of contrast, lies not in the usefulness of the products (which is practically zero) but in applications such as the detection of potentially explosive hydrocarbon/air mixtures, and of course the removal of harmful exhaust products from internal combustion engines.

The literature is full of studies of catalyst selection rules for the oxidation of organic compounds (41). Furthermore it has become possible to lay down certain general principles which are of value in this respect. For example certain physical effects such as

diffusion in porous catalysts have been shown to have a profound influence on selectivity (42). In addition it has been shown that highly porous catalysts are to be preferred for complete oxidation, whereas, if high selectivity for the formation of some partially oxygenated product is required, then a non-porous catalyst is preferred. Chemical factors have also been shown to be of importance in laying down selection rules. The band theory has been of use in this area, as p-type oxides have been shown to be very active catalysts with low selectivity, and n-type oxides are generally very selective catalysts but are of low activity. There are of course many other examples of both physical and chemical factors which are of use in determining the principles of catalyst selection.

In general, the order of activity of catalysts for the complete oxidation of hydrocarbons on the one hand and for the oxidation of carbon monoxide on the other, (i.e. those catalysts with direct relevance to this project) is the same (43, 44). Those catalysts with the highest activity are platinum, palladium, cobalt (II, III, III) oxide, chromium (VI) oxide, manganese (IV) oxide, copper (II) oxide and nickel (II) oxide. Catalysts with low activity include zinc oxide, vanadium (V) oxide, molybdenum (VI) oxide and titanium (IV) oxide. It is of particular interest, in relation to this project, to note that lead (II) oxide (a major constituent of lead compounds emitted by car exhausts) has been found to have some activity (albeit rather low) with respect to the complete oxidation of propylene (45).

1.2.5. EXPERIMENTAL TECHNIQUES IN HETEROGENEOUS CATALYSIS

1.2.5.1. INTRODUCTION

There are a large number of techniques which may be employed in the studies of catalysis. These techniques are conveniently classified into: (I) Adsorption studies and (II) Studies of physicochemical phenomena associated with catalysis. In addition to these classifications there is also the consideration of catalytic reactor systems. Each of these topics is dealt with in turn, in the following Sections. Those techniques which were actually used in this investigation are considered in some depth. However, it is not within the scope of this review to detail all the possible techniques (or indeed to include them all) and therefore some of these are mentioned without individual discussion.

1.2.5.2. ADSORPTION STUDIES

Physical adsorption constitutes a particularly important method of investigating the surface properties of heterogeneous catalysts. As already mentioned, the appearance of the BET equation resulted in a reliable method of estimating the total surface area of most types of catalyst. The BET equation is applied to the physical adsorption of inert gases, such as nitrogen and krypton, at temperatures close to their boiling points. Physical adsorption can also be used to determine the porosity of solid catalysts. A number of methods have been developed for measuring the porosity (i.e. the pore-size distribution) of a porous solid from physical adsorption data. One of the most important of these is that of Barrett, Joiner and Halenda (52), who developed a method based on the Kelvin equation, which relates vapour pressure

depression to capillary radius. Other methods have been developed by Pierce (55) and Ettre (56).

Chemisorption, as it is specific in nature, goes one stage further than physical adsorption, in that it provides information about the "active" rather than the total surface area. However, in some cases, the active and total surface areas may be the same.

Normally, in chemisorption studies, the surface of the solid must be outgassed and clean. If this were not the case, then true chemisorption between adsorbate and adsorbent might not take place, as the chemical forces involved in this process are operative only when the adsorbate and adsorbent are in very close contact. Furthermore, the surface of the adsorbent should be reproducible; in other words, the surface must not be significantly altered by the chemisorption process. If an irreproducible surface is encountered, then it may be necessary for some conditioning procedure to be invoked in order to rectify the situation.

In contrast to the detailed surface preparations required in chemisorption studies, it is sufficient, in the case of physical adsorption, to use some simple outgassing procedure. Various techniques are available for the preparation of clean surfaces and detailed descriptions of most of these may be found in reference (57).

It is possible to determine the amount of gas adsorbed by a solid in several ways: volumetrically, gravimetrically, and by a flow method. Detailed accounts of the volumetric and flow methods are given in Sections 2.2.1.8., 2.2.3.1. and 2.3.1.

The gravimetric method involves measuring the weight of the adsorbent during the course of adsorption. In order to facilitate this, very sensitive microbalances have been developed which can detect changes as small as 10^{-8}g (58).

In addition to the experimental aspects of adsorption already mentioned, significant information may be obtained from other adsorption measurements. For example, measurements of the heat of adsorption can determine the influence of a reactant, product, or intermediate product on the course of a catalytic reaction. Those substances with large heats of adsorption tending to hinder the catalytic process by remaining for too long on the surface, and those substances with low heats of adsorption may not be present on the surface for sufficient time for reaction to take place. Another useful technique is that of flash desorption in which an adsorbed species is desorbed from the surface by a rapid temperature increase; this can be used to investigate surface heterogeneity. In this method the adsorbate molecules desorbed from sites with a low heat of adsorption will be observed to be removed at lower temperatures than those from sites with high heats of adsorption.

1.2.5.3. STUDIES OF PHYSICOCHEMICAL PHENOMENA

One of the most successful methods of investigating the processes taking place at the surface of a catalyst is the application of spectroscopic techniques. Infra-red spectroscopy for example is particularly useful in determining whether chemisorption or physical adsorption has occurred.

If a new absorption band is observed then this may be taken as positive evidence of chemisorption. However, the converse is not necessarily true. In other words, if no new band is

observed, then it is possible that a bond may have been formed which is not active in the infra-red region. Infra-red spectroscopy has been used, mainly in the study of relatively simple molecules such as carbon monoxide (59). On the other hand, ultra-violet spectroscopy, which is an equally useful technique, has a greater applicability in the study of larger species (particularly intermediate compounds in a catalytic reaction (60)). Other spectroscopic techniques which have had, an as yet, rather limited applicability in catalytic studies include: nuclear magnetic resonance (n.m.r.) and electron spin resonance (e.s.r.).

Another useful technique in the study of catalysis is that of magnetic susceptibility measurements. This can be used to measure the number of unpaired electrons present in the adsorbents and adsorbates taking part in chemisorption. For this reason, changes in the electronic structure of catalytic systems may be followed.

Electrical conductance measurements have been informative in studies of catalysis, particularly with regard to chemisorption processes. If chemisorption, on for example, an n-type catalyst, involves the donation of electrons from the adsorbate to the conduction band, then an increase in conductivity would be expected. Conversely a p-type conductor would behave in an opposite manner under those conditions. The practical difficulties associated with conductance measurements include the problem of ensuring that a large proportion of the catalyst atoms reside at the surface (i.e. using a high surface area catalyst) where conduction changes may be expected to be significant. In addition the electrical supply should be a high frequency alternating current, in order to

eliminate polarization effects.

In recent years, there has been a significant advance in the practicalities of examining catalysts, using information gathered by X-ray irradiation, or bombardment by an electron beam. The irradiation of catalyst surfaces with X-rays leads to the formation of photo electrons, the analysis of their energy forms the basis of electron spectroscopy for chemical analysis (ESCA) developed by Siegbahn (61). ESCA is useful in the study of catalysis as it is applicable to only the first few surface layers of the sample. The direct study of non-metallic catalysts, i.e. those with relatively poor electrical conductivity, is complicated somewhat by the build-up of an electrical charge at the catalyst surface. This is a limiting factor in the study of these catalysts (62).

The bombardment of solids by an electron beam of high energy, and the subsequent spectrochemical analysis of the liberated X-rays, constitute the principle of electron-probe microanalysis (63). This technique enables both qualitative and quantitative analysis of samples at depths up to 3μm. Modern instruments frequently combine this technique with electron microscopy, in order to select the exact area to be analysed. The use of an instrument combining both facilities is outlined in Section 2.3.6. Other techniques which utilise the effects of an electron beam include: low-energy electron diffraction, which can yield information concerning the arrangement of foreign atoms adsorbed as a monolayer on a crystal surface, and Auger spectroscopy, which involves the analysis of liberated Auger electrons.

Information concerning the topographical features of catalyst surfaces can be obtained from electron microscopy. Both replication techniques and transmission electron microscopy are of considerable importance. However, the transmission technique is the more useful for a number of reasons, the most important of these being its greater resolving power (64).

The ability to identify the various phases of solid catalysts is important and may be achieved by X-ray diffraction. However, this technique is limited to the investigation of catalysts of relatively low surface area. The reason for this is that X-ray diffraction patterns become increasingly diffuse with increase in surface area (line broadening effect).

A useful method of investigating solid phase reactions (which can occur in both catalyst preparation and use) is that of differential thermal analysis(DTA). In DTA two identical crucibles are heated at the same rate under the same environmental conditions. The sample under test is placed in one crucible and an inert standard substance in the other. When the two crucibles are heated, the thermal effects due to the reactions or phase changes occurring in the sample may be determined by measuring the difference in temperature between the two crucibles.

Other important methods used in the study of catalysis include: X-ray spectroscopy, X-ray fluorescence spectroscopy, field-emission microscopy and work function measurement techniques.

1.2.5.4. CATALYTIC REACTOR SYSTEMS

There are a number of reactor systems which may be used in laboratory scale investigations of catalytic reactions; and these

include the following:

(a) Tubular reactors

(b) Stirred continuous flow reactors

(c) Re-circulating static reactors

(d) Pulsed flow micro-reactors

(e) Static reactors

(f) Heated wires and beads

Each system has been developed for specific applications, for example the static reactor is useful for systems involving long contact times and low reaction rates. On the other hand, heated catalyst beads are suitable for the study of rapid reactions. A comprehensive review of all of these catalytic reactors has been carried out by Keene (67).

The pulsed flow micro-reactor (described in detail in Section 2.2.1.) was developed as a logical step in the chromatographic analysis of reaction products from catalytic reactions (68), since the micro-reactor was placed directly in the carrier gas flow of a gas chromatograph.

This reactor was chosen for use in this project on account of its versatility and ease of operation. The design of the micro-reactor system allows the change of both the reactant mixture (previously made up and stored) and the catalyst bed to be effected conveniently and quickly. The analysis of reactants and products, facilitated by the gas chromatography system, is also a rapid operation, which may be carried out accurately even for small amounts of these substances, since the entire quantity of the reacting mixture is withdrawn for analysis. Furthermore the micro-reactor is suitable for "in situ" chemisorption studies (for "active" surface area determination), Kinetic studies and also "in situ" catalyst poisoning.

1.3. HETEROGENEOUS CATALYSIS FOR CONTROL OF AUTOMOTIVE POLLUTION

1.3.1. GENERAL

The importance of catalysis in the control of automotive pollution has already been outlined in Section 1.1.4.3. In the present Section it was mentioned that a two-stage catalytic converter has been designed, the object of which is to reduce catalytically nitrogen oxides to nitrogen in the first stage and to oxidise catalytically carbon monoxide and hydrocarbons to carbon dioxide and water in the second stage. In the current state of development, this approach would seem to be the most practicable. However, other systems have been proposed. Thus, for example, a single-stage converter which will catalyze both reactions simultaneously has been suggested (69, 70); this design is, however, of limited applicability at present, because narrowly defined carburation conditions are needed for its efficient operation, which is a serious disadvantage.

The development of catalysts suitable for this type of operation is by no means easy. Firstly the catalyst must exhibit high efficiencies under transient conditions. Secondly it should be effective at temperatures varying from ambient to 900°C, and finally it must be able to withstand the poisoning action of additives in petrol. The severe physical condition to which catalysts tend to be exposed have been mentioned previously, but in addition to the need to withstand both chemical and physical "shocks" the catalyst should be able to retain its activity for use over a distance of at least 50,000 miles. In the following Sections the catalysts which have been found to be suitable for this application are described.

In addition, the difficulties associated with their use with particular emphasis on the problems relevant to the present project, are discussed.

1.3.2. OXIDATION OF CARBON MONOXIDE

The mechanism of oxidation of carbon monoxide has been studied for many years, and in recent years has been used to investigate the catalytic properties of semiconductors. One of the most important contributions to the study of the catalytic oxidation of carbon monoxide was that of Roginskii (71, 72), who studied manganese (IV) oxide as the catalyst. The mechanism proposed postulates the catalyst as an oxygen donor regenerated by the oxygen in the reactant stream, as well as a site for the interaction of carbon monoxide and oxygen in the adsorbed phase. In a later study (73), this reaction was presented as being consistent with a Rideal mechanism, although the catalyst was still depicted as an oxygen donor.

Copper (II) oxide is recognised to be a very active catalyst for the oxidation of carbon monoxide and, an early study of its behaviour (74) resulted in a mechanism consistent with the Roginskii scheme (71, 72). A later study of carbon monoxide oxidation over alumina-supported copper (II) oxide (75) also indicated that oxidation and reduction of the catalyst may take place at temperatures above 160°C.

A recent infra-red spectroscopic study of the oxidation of carbon monoxide by Hertl (76), using cobalt (II, III, III) oxide, has indicated the formation of surface carbonate groups as intermediate species. Again, the catalyst was stated to undergo an oxidation-reduction cycle during the reaction, the

source of the oxygen required to form the surface carbonate group being the cobalt oxide surface. This oxygen was in turn replaced by oxygen from the gas phase. Another recent study of carbon monoxide oxidation over both manganese (IV) oxide and manganese hydroxide oxide catalysts (77), also yielded results which were consistent with successive oxidation and reduction of the surface.

As a result of interest in nitrogen oxide reduction in the first stage of a two-stage catalytic converter, the simultaneous reduction of nitrogen monoxide and oxidation of carbon monoxide has been investigated. Fuller et al (78) examined a tin oxide/copper oxide gel catalyst which was found to be suitable for this reaction. These workers suggested that the mode of action was a "catalyst redox mechanism".

It can be seen therefore, that for the transition metal oxide mechanisms examined so far a common characteristic step exists throughout. This step is a redox mechanism in which the catalyst participates directly in the reaction. However, there is not universal agreement that this mechanism operates for all transition metal oxides under all conditions. Indeed several workers have proposed mechanisms in which adsorbed oxygen rather than lattice oxygen plays the major role during catalysis (139, 140, 141). Thus it can be seen that there exists some difficulty in proposing a generalized mechanism for carbon monoxide oxidation on transition metal oxides, and indeed it is probable that an attempt to do this would be a misleading over simplification.

In the case of the other important class of carbon monoxide oxidation catalysts, namely noble metals, a somewhat different situation is revealed. For example, Pacia et al (79), employing

a platinum catalyst, proposed that adsorbed oxygen was attacked by carbon monoxide (either in the gas phase or loosely adsorbed) in an Eley-Rideal mechanism, and was also attacked by strongly adsorbed carbon monoxide in a Langmuir-Hinshelwood reaction. McCarthy et al (80) have proposed a very similar theory for the catalytic oxidation of carbon monoxide using a platinum catalyst. Using powdered silver, Keulks and Chang (81), from their kinetic studies and tracer experiments, proposed a reaction mechanism whereby the rate-determining step involved the interaction of weakly chemisorbed carbon monoxide with adsorbed oxygen. The mechanism for carbon monoxide oxidation over palladium catalysts has been presented as involving a reaction between carbon monoxide and adsorbed oxygen (82, 83).

The mechanisms proposed for noble metal catalysts, all involve the direct interaction of the adsorbed species, carbon monoxide and oxygen, but with no possibility of direct catalyst participation during this stage. An interesting consequence of the difference between those reaction mechanisms of transition metal oxides, which involve direct participation of lattice oxygen, and the reaction mechanisms of noble metals, arises in the poisoning of oxidation catalysts by carbon monoxide. For the transition metal oxide catalysts a reaction could take place which removes oxygen from the catalyst, and this may lead to irreversible changes taking place. However, carbon monoxide poisoning would be a temporary process in the case of a noble metal catalyst since the adsorbed carbon monoxide could be rapidly removed if sufficient oxygen was available.

1.3.3. OXIDATION OF HYDROCARBONS

There has been comparatively little research on the complete catalytic oxidation of hydrocarbons, most of the work on hydrocarbons being restricted to partial oxidation. Furthermore, the work which has been done has involved a somewhat different approach to that adopted during studies of carbon monoxide oxidation. Most investigations appear to have been aimed at identifying the rate-determining step in the oxidation, based on kinetic studies,and at correlating the overall catalytic activity with intrinsic chemical properties of the catalyst.

It would appear that there are some similarities between carbon monoxide oxidation over transition metal oxides and the complete oxidation of hydrocarbons. For example Hertl (76) found that hydrocarbon oxidation over cobalt (II, III, III) oxide proceeded in a similar manner to carbon monoxide oxidation, i.e. by the formation of surface carbonate groups and by a redox mechanism involving surface oxygen. Grodsel (84) also reported the formation of surface carbonate groups in an adsorption study of carbon monoxide and various hydrocarbons. However, by way of contrast, Yu Yao (85) reported in a recent study that neither hydrocarbons or carbon monoxide would react with the surface lattice oxygen for a chromium oxide catalyst. The mechanism of hydrocarbon oxidation over noble metals, as well as for transition metal oxides , would also appear to follow similar principles to those for carbon monoxide oxidation. Mezaki and Watson (86), for example, proposed that the complete oxidation of methane over a platinum catalyst took place by reaction of gaseous methane with adsorbed oxygen.

Ahuja and Mathur (87) proposed a similar mechanism for this reaction using a palladium catalyst. Hiam et al (88) studied the catalytic oxidation of various alkanes over a platinum filament catalyst, and reported the relative ease of oxidation of the different hydrocarbons; in addition it was concluded that dissociative adsorption of the hydrocarbon was the rate-determining step.

As has already been mentioned, various attempts have been made to correlate the activity of catalysts for the complete oxidation of hydrocarbons, with some intrinsic chemical property of the catalyst. Cant and Hall (29) have correlated the activity of various noble metal catalysts with per cent d character. Similarly Sazanov et al (89) related the catalytic activity of transition metal oxides to the oxygen bond energy of the adsorbed layer. Other correlations include that of activation energy with activity (90) and of enthalpy of catalyst oxide formation with activity (91).

In an as yet rather rare attempt to provide useful and relevant kinetic and mechanistic data, with direct application to automotive emission control, Yu Yao (85, 92, 93) studied the complete oxidation of both carbon monoxide and hydrocarbons over various transition metal oxide catalysts. In addition to providing useful data on the lines mentioned, additional information concerning the interaction of oxidizable species (mutual retardation was observed in all the tried combinations) was obtained.

1.3.4. CATALYSTS FOR NITROGEN OXIDE REMOVAL

The principal oxide of nitrogen found in automotive exhaust emissions is nitrogen monoxide (NO), although some nitrogen dioxide is normally also present. The combination of these two oxides is frequently referred to as NO_x, but they are simply referred to as "nitrogen oxides" in this Section.

There are two methods at least in theory, which may be employed for the removal of nitrogen oxides: decomposition and reduction. The catalytic decomposition of nitrogen oxides was reported in 1906, by Jellinek (96), to be achieved using platinum and iridium at temperatures above 670°C. Since then no catalyst has been found which will operate at a significantly lower temperature. For this reason nitrogen oxide decomposition is not a practical possibility for this application.

The reduction of nitrogen oxides is, in contrast to the decomposition reaction, a practical possibility. The catalysts which are effective for reduction of nitrogen oxides are in general similar to those used to catalyze the oxidation of carbon monoxide and of hydrocarbons. In addition, some transition metals such as copper, nickel and even the alloy, stainless steel, have been successfully used.

An important mechanism for nitrogen monoxide reduction by carbon monoxide over transition metal oxides is thought to be a redox reaction (78, 94, 95), whereby carbon monoxide reacts to form carbon dioxide and a reduced catalyst surface, the reduced surface then being oxidized by nitrogen monoxide to form nitrogen in the rate-determining step. Shelef et al (97) have reported an order of reactivities for various transition metal oxides, which has been correlated with the strength of the oxygen to surface bond. Dwyer (94) has suggested that the mechanism of nitrogen monoxide reduction by hydrogen over transition metal oxides may proceed by a redox mechanism at high temperatures, but suggests that the formation of ammonia at lower temperatures is indicative of an interaction between adsorbed hydrogen and nitrogen monoxide. The latter suggestion is

supported, in the case of an iron oxide catalyst, by the work of Clay and Lynn (98), who proposed a mechanism involving adsorbed molecules for the reduction of nitrogen monoxide by both carbon monoxide and hydrogen at temperatures in the range 370-540°C. Furthermore, as a result of an extensive study of nitrogen monoxide reduction by carbon monoxide over supported platinum and a number of transition metal oxides, Force and Ayen (99) proposed a mechanism involving the reaction of adsorbed nitrogen monoxide and carbon monoxide on adjacent sites. These workers were also operating in a relatively low temperature range i.e. 240-500°C. Finally an adsorption mechanism for nitrogen monoxide reduction by carbon monoxide over copper, has also recently been proposed by Rewick and Wise (100).

The preceding work has all been completed on pure reactant systems. However, the effects of both oxygen and water, present in exhaust gases, has also been investigated. Oxygen has been shown to be an inhibitor for the reduction of nitrogen monoxide as a result of its preferential reaction with the reducing agent carbon monoxide (101). In this way, the extent of the desired reaction is reduced. Water on the other hand, has been shown to have a beneficial effect i.e. the catalytic activity is enhanced. This was explained by Klimisch and Barnes (102), who argued that hydrogen is produced by the water gas shift reaction, and that the hydrogen in turn reduced nitrogen monoxide to nitrogen. Meguerian and Lang (103) reported that a great number of catalysts, both noble metals and transition metal oxides, were effective in reducing nitrogen oxides, but most of them yielded 40-50% ammonia in the product. In an actual converter system, the nitrogen oxide

converter would be followed by a hydrocarbon-carbon monoxide converter which would also oxidise any ammonia formed to nitrogen monoxide and thus render the process ineffective. At present only ruthenium is known to be able to convert nitrogen monoxide directly to nitrogen and to exhibit the required selectivity at temperatures below 500°C (104,105,106). However, rhodium and nickel catalysts operate successfully at temperatures above 600°C (107, 108).

1.3.5. CATALYST SUPPORTS

The catalyst support, as in all other applications in heterogeneous catalysis, is used to stabilize the catalytic component, increase the surface area of the catalyst, and increase the degree of dispersion of the catalytic component. Dwyer (109) has reported that chromites exhibit a particularly high thermal stability when supported on alumina, and also that noble metals benefit particularly from the improved dispersion provided by support materials. The catalyst support is capable, under certain conditions, of undergoing solid-state reactions with the active catalyst (110). This effect may be observed both during catalyst preparation and also during catalyst use. The existence of this effect can obviously modify the activity of the catalyst, both beneficially and deleteriously, and there are numerous examples of this in the literature.

The materials which are used as catalyst supports are usually alumina and to a lesser extent silica. Other materials such as stainless steel (111) have also been used but these are rather less commonly encountered.

Various methods of preparing catalyst support materials are

employed. Thus in pelleting, for example, spherical pellets of approximately 1/4" diameter are formed and their use has been found to be desirable (110). One of the more common methods of preparing a catalyst support is to form a honeycomb structure (known in general as a "monolith") of low surface area (112) and to coat this with a very high-surface-area substrate (i.e. washcoat) before the catalyst itself is deposited.

In addition to the properties already mentioned, the catalyst support has to provide the mechanical strength necessary to withstand vibration, sufficient resistance to thermal effects of a cyclical nature, as well as a low pressure path for the exhaust gases.

1.3.6. CATALYST DEACTIVATION

In Section 1.1.4.3. a brief outline was given of the problem of deactivation in automotive exhaust catalysis. In that Section various modes of deactivation were mentioned, including that resulting from lead poisoning. However, in the present Section the current status of chemical poisoning is more fully discussed. Furthermore the discussion includes the effects of substances other than lead, as recent studies have shown that several other potential poisons are present in exhaust gases. The problem of lead poisoning arises because petrol contains tetraethyl or tetramethyl lead as antiknock additives. These combine with ethylene dibromide or dichloride "scavengers" to form a mixture of halides, oxyhalides and other compounds. Both phosphorus, present in oil additives, and sulphur, often present in natural petroleum, are also important poisons. Other potential poisons include zinc, manganese, iron and calcium.

There is a wealth of literature available, covering the period from the late fifties to the early seventies (113,114,115), which reports the poisoning effects of lead compounds in automotive catalysts. In general this work was not as useful as it might have been, as no real attempt was made to offer an explanation for the reported effects. Indeed in some of these evaluations, the catalysts were not identified, which made the interpretation of the results somewhat difficult for those other than the researchers themselves.

In 1971, Yolles and Wise (116) summarised the main ideas concerning the mechanism or mechanisms of lead poisoning, although surprisingly no mention was made of chemisorption of the poison at active sites. These ideas were: physical adsorption on the catalyst with monolayer formation, pore plugging of porous catalysts, and reaction with the catalyst or support to produce an inactive phase or compound. However, despite the reasonable nature of these theories, and the existence of a great deal of data which strongly indicated that lead was a catalyst poison, there was also some apparently contradictory evidence i.e. the existence of lead promoted oxidation catalysts for automotive application (117). Since then there have been several reported cases of oxidation catalysts containing lead (118, 119, 120). Furthermore, in 1971, Roth (121) published data which formed the first significant contribution towards understanding the mechanisms involved in catalyst deactivation. It was concluded from these results, obtained from catalysts used in actual road tests, that the deposition of lead sulphate and lead oxyhalides (formed by reactions in the engine or exhaust system) on the surface of the catalyst constituted one mechanism. Migration of the active constituent

(copper (II) oxide) away from the surface, and the formation of a compound between copper (II) oxide and the alumina support were other contributing factors. Furthermore, Roth conducted laboratory reactor experiments, using a synthetic exhaust gas mixture containing, apart from the expected gases, organic halogen compounds. Various halogen compounds were used including ethylene dibromide. With all the halides used it was found that severe deactivation of the catalyst occurred due to volatile copper halide formation. It was further suggested that the formation of volatile halides could be responsible for the deactivation of a number of other transition metal compounds commonly used in automotive catalysis i.e. nickel, cobalt and iron.

Since the work of Roth, there have been other important advances towards a better understanding of the mechanisms of chemical poisoning of automotive catalysts. Most of this work has been directed towards noble metal catalysts, with comparatively little emphasis on the other types of catalyst. One of the theories of catalyst deactivation considered by Yolles and Wise (116) was that of "pore plugging" and this aspect has received attention from several workers. For example Hegedus and Baron (122), using an alumina-supported platinum catalyst, reported that lead (II) oxide and lead (II) sulphate poisons reduced the pore volume of the catalyst in both the micropore and macropore regions. Similarly Bomback et al (123) reported that lead, phosphorus and sulphur had penetrated the micro porous structure of an alumina-supported platinum catalyst. Other workers have also shown that there is a correlation between the reduction of pore volume and surface area on the one hand and the degree of poisoning by lead compounds on the other (124, 125). An interesting and important recent development

in the field of chemical deactivation has been the discovery that both phosphorus and sulphur are significant poisoning agents. It is also of interest to note that the interaction of these elements with lead and other substances has a profound effect upon the extent of the poisoning process. For example Bomback et al (123) investigated the concentrations and distribution of lead, zinc, iron, phosphorus and sulphur on a series of automotive catalysts (alumina-supported platinum). It was found that lead formed both sulphate and phosphate salts on the surface of the washcoat. These salts then coalesced to form a continuous layer which smothered the catalyst. In addition, the formation was reported of a branching "treelike" structure growing to several hundred microns in height. Iron and zinc were found not to penetrate the surface of the catalyst, which contrasted with the behaviour of lead, sulphur and phosphorus previously mentioned. Thus the poisoning effect was concluded to be caused by the dual mechanisms of impervious layer formation and penetration by the poisons of the microporous structure. Other workers such as Klimisch et al (126) have reported the formation of lead (II) sulphate and lead (II) phosphate at the surfaces of supported noble metal catalysts (both platinum and palladium). However Klimisch and his co-workers found that the poisons were deposited exclusively at the surface of the catalyst, and furthermore suggested that regeneration of catalytic activity could be achieved by redistribution of the contaminants throughout the whole of the catalyst.

The distribution on catalysts of a wide variety of potential poisons such as lead, phosphorus, sulphur and also calcium and zinc was very thoroughly investigated by McArthur (127). This study

involved only catalysts for the reduction of nitrogen oxides under reducing conditions. These catalysts included noble metals and transition metals such as copper and nickel. All of the catalysts investigated were supported on alumina. It was found that the extent of the retention of contaminants was P $\rangle$ Pb $\rangle$ Zn $\rangle$ Ca $\rangle$ S. The distribution of the poisons was found to vary in a most complicated manner depending on various factors, such as the composition of the exhaust gases at any given position, the geometric position of the particular section of the catalyst and also the design of the catalyst monolith (i.e. the rigid support). However, some general conclusions can be drawn from McArthur's results. Firstly, the bulk of the contaminants concentrated at the front of the catalyst bed, although variations of the extent of this trend exist for the different elements. Secondly the radial distribution of lead was rather random at any particular point in the catalyst bed. In general, the metal was thought to be present as either the sulphate or phosphate, although lead (II) bromide phosphate was identified at the surface of the catalyst, and also on the surface of the container. Finally, phosphorus was found to be very heavily concentrated at the surface of the catalyst at the rear of the bed. This was thought to be due to the formation of aluminium phosphate. However, this effect did not occur at the front of the catalyst bed and the reason for this is not known.

A further example of the importance of the interaction of the various poisons present in exhaust gases has been provided by Acres et al (128). These workers, using a supported platinum oxidation catalyst, reported that deactivation due to lead and phosphorus was more serious when the poisons were present alone.

On the other hand catalyst activity was maintained for longer times when both lead and phosphorus were present in the fuel, and also when phosphorus was initially combined with zinc (this form of phosphorus is one of several possible alternative lubricating oil additives). In a similar vein, Fitzgerald and Wilson (129) have reported that the presence of metals such as calcium or zinc in a lubricant inhibits the poisoning effect of phosphorus on noble metal oxidation catalysts. Acres and his co-workers concluded that lead and phosphorus combine together to form lead (II) phosphate particles which are only loosely held or physically adsorbed by the catalyst and are therefore relatively non-toxic. This mechanism would also appear to operate in the case of zinc (and other metals) and phosphorus. Acres et al also reported that deactivation due to phosphorus would be explained by a mechanism involving selective poisoning at the pore mouths; in other words, phosphorus accumulates exclusively at the surface of the catalyst. Furthermore, lead poisoning was believed to be due to some volatile compound (the nature of this was not identified, but halides are precluded as the fuel used was halide-free) which penetrated throughout the porous structure of the catalyst. The effect of sulphur was reported by these workers to be insignificant compared with that of lead and phosphorus.

Another recent and very interesting investigation of the interaction of lead, sulphur and phosphorus on platinum and palladium foils has been reported by Williams and Baron (130). These workers investigated this system using Auger electron spectroscopy and, although the catalytic activities were not measured, the work represents an important advance in this field. From the results of this study a mechanism was proposed for the poisoning of platinum (although no specific mechanism was proposed for palladium). The proposed

mechanism involved the transport of lead in the form of a halide (lead halides are generally recognised to be the principal volatile carriers of lead) to the catalyst surface, the halide then undergoing decomposition on the noble metal to form a strong lead-platinum bond. The lead formed in this way was thought subsequently to become oxidised and then to react with sulphur trioxide to form lead (II) sulphate. In the view of these workers, halides were thought unlikely to contribute to irreversible deactivation of noble metal catalysts. In addition to proposing this specific mechanism, the behaviour of platinum and palladium was compared. In general, these two noble metals behaved similarly, both accumulating various oxidised forms of lead, sulphur and phosphorus on the surface. However, at the initial stage of exposure to these contaminants, it was found that lead(probably as the oxide) is formed on the surface of platinum but not of palladium. This effect was explained by suggesting that lead (II) oxide is drawn into the bulk of the oxidised palladium, on account of the solubility of lead (II) oxide in palladium oxide.

As has been previously mentioned, the poisoning of transition metal oxides in automotive catalysis has received very little attention, the work of Roth (121) being an important exception. However, in a recent study by Wheeler and Bettman (131), the deactivation of cobalt (II, III, III) oxide when supported on alumina was suggested to be due to the dissolution of the active compound in the substrate during catalyst preparation. Compound formation under certain conditions was also reported.

Possibly one of the most important discoveries concerning "lead poisoning" of noble metal catalysts was made recently by workers at the Chrysler Corporation (132), who discovered that ethylene dibromide, rather than lead, is the important poison. In the work

reported by Chrysler, the effects, on platinum and palladium catalysts, of fuels containing tetraethyl lead and ethylene dichloride but no ethylene dibromide, were compared with fuels containing ethylene dibromide with, and without, tetraethyl lead. Only fuels containing ethylene dibromide were found to exert a significant poisoning effect. In fact a fuel containing no lead but only ethylene dibromide was the most effective poisoning agent. However, the use of a fuel containing no additives was found to restore catalytic activity even after the most severe poisoning had occurred. Similar results, confirming the effect of ethylene dibromide as a noble metal catalyst poison have also been published recently (133, 134).

The rejuvenation of catalysts poisoned by lead and other substances has received some attention from workers in this field. Various approaches have been used. For example the redistribution of the poisons which are found predominantly at the surface, and indeed the use of petrol containing no additives, have already been mentioned in this Section. Other methods have involved chemical cleaning (135) and the use of high operating temperatures to facilitate the more complete removal of volatile poisons (136).

There is little doubt in the near future, as a result of the advances in the understanding of poisoning mechanisms which have been reported in the past and are likely to be reported in the future the rejuvenation of catalysts will become an important aspect of work in this field.

1.3.7. SUMMARY

The development of catalysts for the oxidation of hydrocarbons and carbon monoxide has reached an advanced stage, although no system has actually been reported to be satisfactory for 50,000 miles at the

1976, American Federal Emission standards. The development of oxidation catalysts has reached this advanced stage, on account of the wealth of fundamental studies on catalyst mechanisms and the characteristics of the catalyst. In addition to this, a great volume of work has been completed in the last five years, mainly by industrial concerns. This work has dealt with, amongst other things, the problem of chemical poisoning. In the preceding Section, the success of this effort particularly with regard to the poisoning of noble metals has been outlined. The elucidation of some of the poisoning mechanisms and the isolation of new and hitherto unsuspected poisoning agents, has enabled the problem to be solved to a substantial extent, as the conditions affecting oxidation catalysts can now be chosen to minimise the effects of catalytic poisoning.

However, there are a great many unsolved problems in the field of automotive catalyst poisoning. For example, the poisoning of transition metal oxides has received very little attention. In addition, the problem of why lead compounds can behave as both poisons and catalysts, has remained unsolved, although it is possible to speculate about this. The latter problem illustrates well the intricacies involved in the poisoning of exhaust gas catalysts, as the chemistry of even the lead compounds involved is complicated, and that of the potential catalysts even more so.

The state of development of nitrogen oxide reduction catalysts is far less advanced. This is due, in part, to the relative lack of fundamental studies in this area. Here, again, however, a great deal of more applied work has been completed in the last five years, including some important studies of the lead poisoning of these

catalysts. There remains, however, a great deal of scope for research into the development of a reliable catalyst for nitrogen oxide removal.

1.3.8. THE PRESENT WORK

At the commencement of this project, very little was known about the problem of poisoning of automotive catalysts. The work of Roth (121) had only recently been published, and the knowledge that lead compounds had a deleterious effect on catalysts was only beginning to become significant, largely as a result of the legislative programme of pollution abatement initiated by the U.S.A. Federal Authority.

However, as the result of some excellent work by Lamb, Niebylski et al (137), the chemistry of the lead compounds, both deposited on catalysts and found in the exhaust gas stream, was well known. The main compounds deposited on catalysts were lead (II) halides (PbX_2) and lead (II) oxyhalides ($PbO.\ PbX_2.H_2O$). Furthermore, a number of other compounds such as lead (II) sulphate, lead (II) oxysulphate, lead (II) phosphates and various other compounds (including those actually deposited on catalysts) were emitted as particles in the exhaust gas stream. It would appear likely that these compounds, emitted as particles, would also exist, as minor constituents, in the deposits.(This has been shown to be the case in various studies reported in Section 1.3.6.). In addition, it is evident that the lead compounds apart from their complexity, exist in a state of dynamic equilibrium between gas and solid phases (138), with the position of this equilibrium being affected by a number of factors, e.g. the catalyst bed operating temperature, the fuel composition etc. Finally it was

concluded that, because lead (II) halides were an important class of lead poisoning compound and were convenient to obtain and use, this class of compound was the most suitable for study.

In this work the effect has been studied of lead (II) halides (primarily lead (II) bromide but also lead (II) chloride) on various physical and chemical properties of a number of supported and unsupported transition metal oxide catalysts and of a noble metal catalyst. In conjunction with this, the effect of lead (II) halides on catalytic activity with respect to carbon monoxide oxidation was measured. The choice of carbon monoxide oxidation to monitor the variation of catalytic activity brought about by lead (II) halides was based on several factors. The most important of these was the representative nature of this reaction i.e. the oxidation of carbon monoxide generally follows a pattern similar to that of hydrocarbon oxidation. In addition carbon monoxide represents at least on a quantitative basis, the most important single pollutant found in automotive exhaust gases. Finally, this reaction has the dual advantages of simplicity and reproducibility, as only one reaction product (i.e. carbon dioxide) is possible.

SECTION 2

EXPERIMENTAL

SECTION 2

Cont. Page Number

--oOo--

2.1. MATERIALS

2.1.1. UNSUPPORTED CATALYSTS

Nickel (II) oxide was prepared by the following four methods of which, however, only the first two were extensively used in this investigation.

(I) Nickel (II) hydroxide was precipitated from nickel (II) nitrate solution using an excess of potassium hydroxide solution. The precipitate was washed until neutral, dried by heating in air for 90 minutes at 180°C and finally decomposed by heating in air for twenty-four hours at 630°C. The resulting nickel (II) oxide was then washed with distilled water until the washings contained no detectable quantities of potassium, and was finally dried at 130°C for two hours. The washed catalyst then contained approximately 10 p.p.m. of potassium. The potassium impurity was detected using an Eel flame photometer Mark II (maxiumum sensitivity 3 p.p.m. for potassium).

(II) Nickel (II) nitrate hexahydrate was decomposed to nickel (II) oxide in two stages, the first stage removing the bulk of the water of crystallization, and the second stage removing oxides of nitrogen and any remaining water of crystallization. The first stage consisted of heating the nitrate to 130°C under vacuum for two hours while in the second stage the dehydrated nickel (II) nitrate was heated in air at 630°C for twenty-four hours. It was found that, if the first stage of the preparation was omitted, or carried out in such a manner as to allow the water vapour formed to recondense on the nickel (II) nitrate (drying without the vacuum facility encouraged the condensation of water vapour) then the

resulting catalyst had a very low surface area and was consequently of little use.

(III) Nickel (II) oxalate was precipitated from nickel (II) nitrate solution using an excess of ammonium oxalate solution. The precipitate was dried at 130°C for two hours and then decomposed by heating in air for various lengths of time at either 400, 300, or 250°C.

(IV) Nickel (II) formate was decomposed in air at 250°C for three hours.

Of the four methods described for preparing nickel (II) oxide, (I) and (II) were found to be most useful. Both yielded catalysts which had a sufficiently high surface area and could be ground to a convenient mesh size without disintegrating into a powder. However, method (I) exhibited the disadavantages of an inconveniently long preparation route and the presence as an impurity of potassium, which was difficult to remove. Method (III) (oxalate route) yielded a catalyst which had an acceptable surface area, and by virtue of the gaseous nature of the decomposition products of ammonium oxalate, was not contaminated by the breakdown products formed from the reagents used. However, nickel (II) oxide from this source was found to be unsuitable due to its inconvenient powdery physical form. Method (IV) was found to be unsuitable as it yielded a nickel oxide with an unacceptably low surface area.

Cobalt (II, III, III) oxide was prepared by treating cobalt nitrate hexahydrate in exactly the same way as was used for the preparation of nickel (II) oxide from nickel (II) nitrate hexahydrate. Copper (II) oxide was prepared by heating copper nitrate hexahydrate in air at 630°C for twenty-four hours. The copper (II) oxide produced by this method was satisfactory in all respects except surface

area, which was too low for a full investigation of its properties (although some work was completed using this catalyst). It is probable that the surface area of this catalyst could have been improved, if attempts had been made to prepare it via the nitrate along the lines discussed for nickel (II) oxide. Vanadium (V) oxide was prepared by heating ammonium metavanadate in air at 630°C for twenty-four hours.

Manganese (IV) oxide and platinum black were obtained directly from the manufacturers. All the chemicals used in the preparation of the unsupported catalysts were AnalaR grade reagents, supplied by Fisons, with the exception of manganese (IV) oxide which was provided by Hopkins and Williams and platinum black, (spectroscopic grade) which was obtained from Johnson Matthey.

2.1.2. SUPPORTED CATALYSTS

Only one type of catalyst support was used in this work, Actal type A a pseudo boemite phase of alumina, supplied by Laporte Industries. The catalyst particle size as received was 4 - 6 mesh, but this was reduced in a mortar and sieved, the 40 - 60 mesh fraction being used.

A freeze-drying technique was used to prepare the following supported catalysts:

copper (II) oxide

cobalt (II, III, III) oxide

nickel (II) oxide.

Each of these catalysts was prepared in an identical manner. The amount of metal nitrate required in order to make a supported catalyst, containing the required fraction of the active constituent,

was calculated and a highly concentrated aqueous solution of it was made up. A slurry of the nitrate solution and the alumina support was prepared by adding the appropriate quantity of the support to the concentrated metal nitrate solution. This stage was followed by thorough mixing, excess liquid being removed by absorption with filter paper. The slurry was finally frozen using liquid nitrogen and then placed under vacuum until the water vapour had been completely removed. The supported catalyst was decomposed by heating under vacuum at 250°C, until no further decomposition was apparent, this process normally taking 24 hours. Finally the supported catalyst was heated in air at 630°C for twenty-four hours.

An alumina-supported platinum catalyst was made by freeze-drying a slurry of a concentrated solution of hydrogen hexachloroplatinate (IV) hydrate and the alumina support. The resulting material was then reduced in a stream of hydrogen gas at 90°C for twenty-four hours. Again the final stage was to heat the supported catalyst to 630°C for twenty-four hours in air. The amount of catalyst present in the support was determined in each case by weight increase. This value was also checked in all cases, except that of supported platinum, by dissolving the supported catalyst in nitric acid, or a mixture of nitric and hydrochloric acids and carrying out analysis using a Perkin Elmer 290B Atomic Absorption Spectrophotometer. The hydrogen hexachloroplatinate (IV) hydrate used was an AnalaR grade reagent supplied by Hopkin and Williams.

2.1.3. CATALYST POISONS

Lead (II) bromide and lead (II) chloride were obtained from Fisons. Both chemicals were of a quoted minimum purity of 99% and were used without further purification.

2.1.4. REACTING GASES

Oxygen was supplied by the Britiish Oxygen Company (B.O.C.) and was of a quoted minimum purity of 99.5%. This gas was purified by passing through platinized asbestos at 450°C, which oxidised any hydrocarbons present, and was then passed over copper (II) oxide at 600°C in order to oxidise any remaining impurities. The gas was finally passed through liquid nitrogen at - 196°C to remove any condensable impurities and distilled, the middle fraction only being taken.

Carbon monoxide was supplied by the Matheson Company with a quoted minimum purity of 99.5%. This gas was purified by condensing at - 196°C (using liquid nitrogen) and subliming the middle fraction into evacuated storage globes.

Hydrogen was supplied by B.O.C. with a quoted minimum purity of 99.5%. This gas was purified by passing it first through platinized asbestos at 450°C, then over fine copper wool at 450°C and finally through a cold trap at - 196°C.

2.1.5. CARRIER GASES AND INERT GASES

Helium is an ideal carrier gas to use in a Katharometer detector because it is chemically inert and has a high thermal conductivity (142). The possibility of cumulative catalyst

PLATE 2.1. PULSE FLOW MICRO-REACTOR SYSTEM

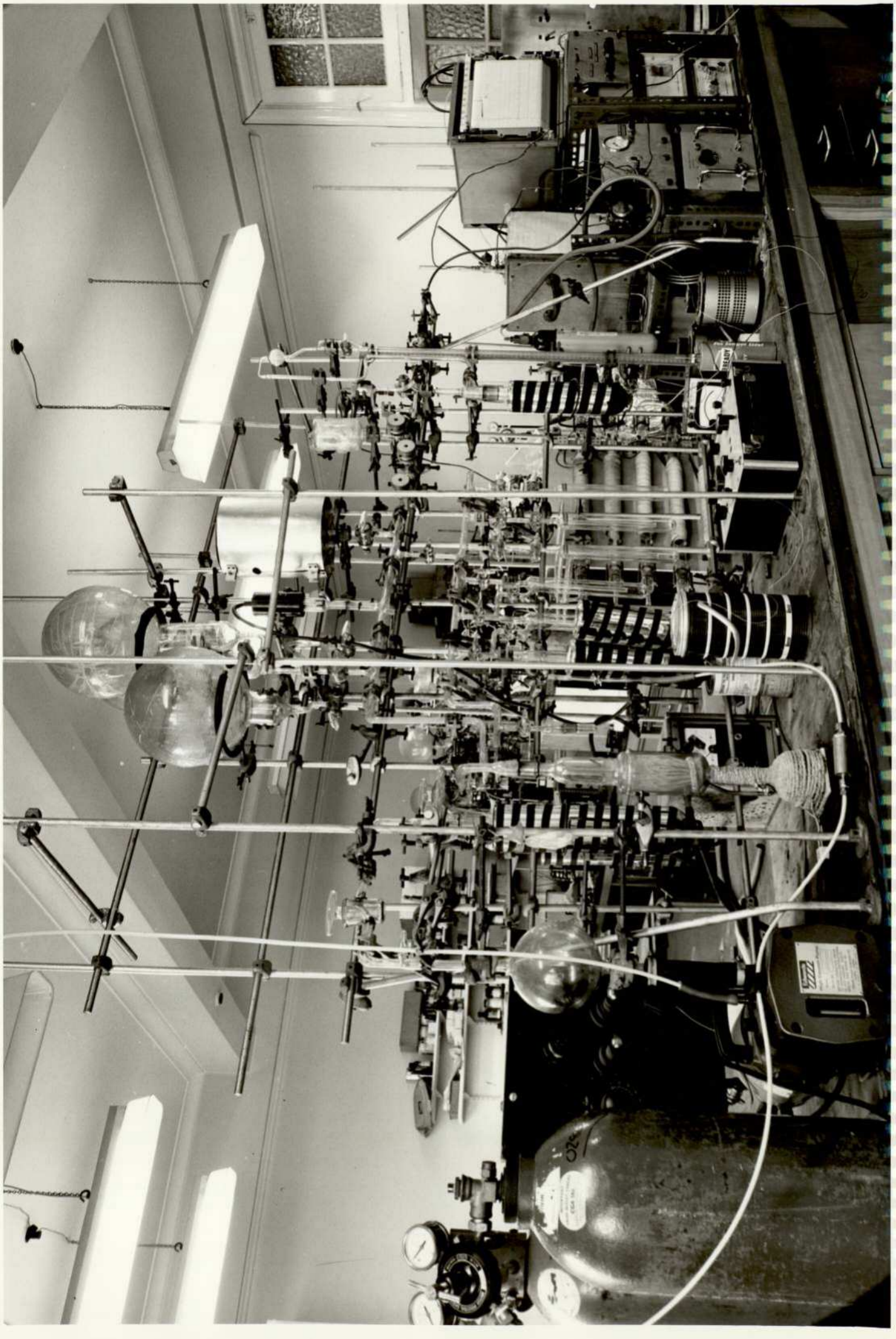

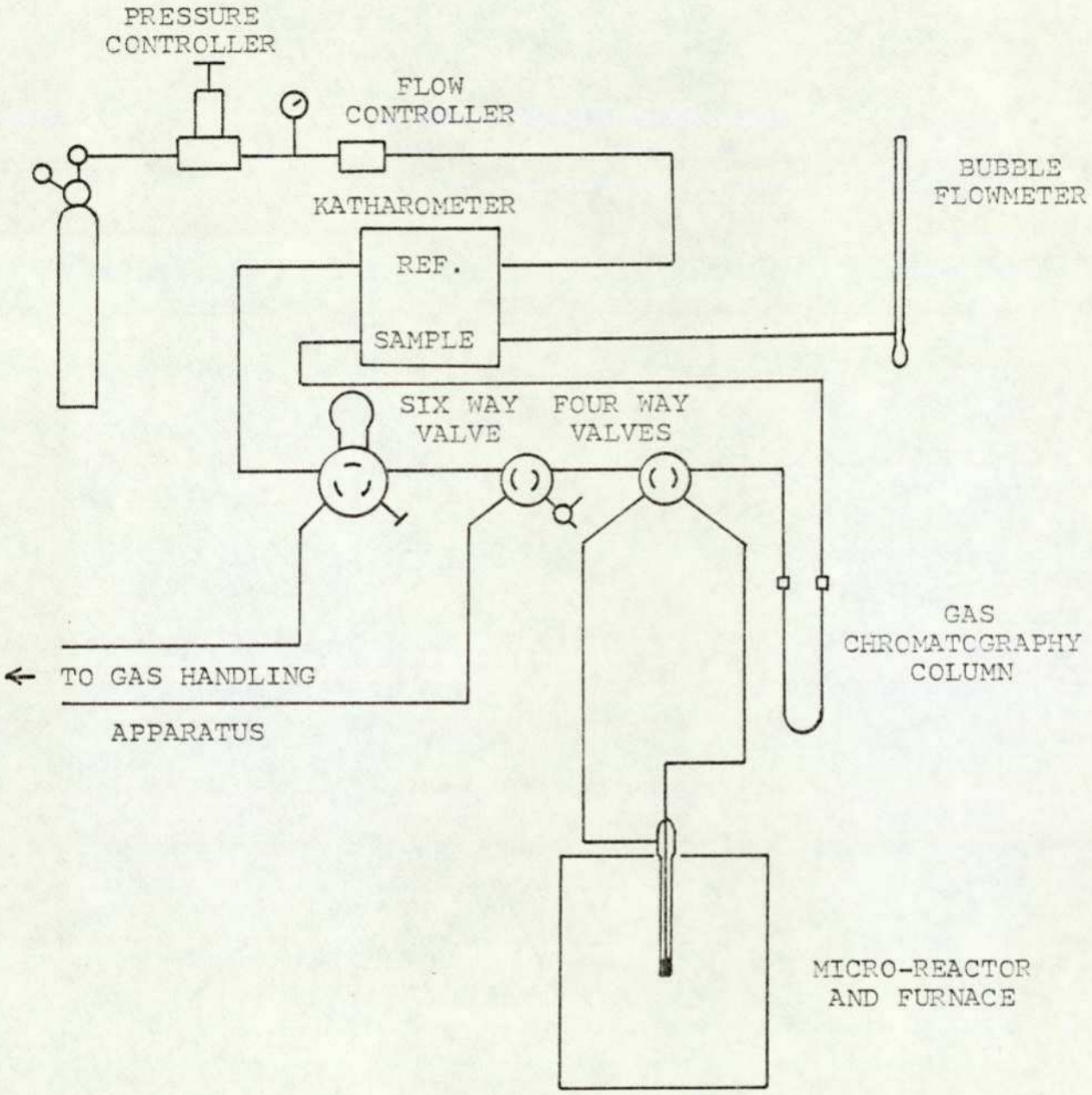

FIGURE 2.1.

SCHEMATIC DIAGRAM OF PULSE FLOW MICRO-REACTOR SYSTEM

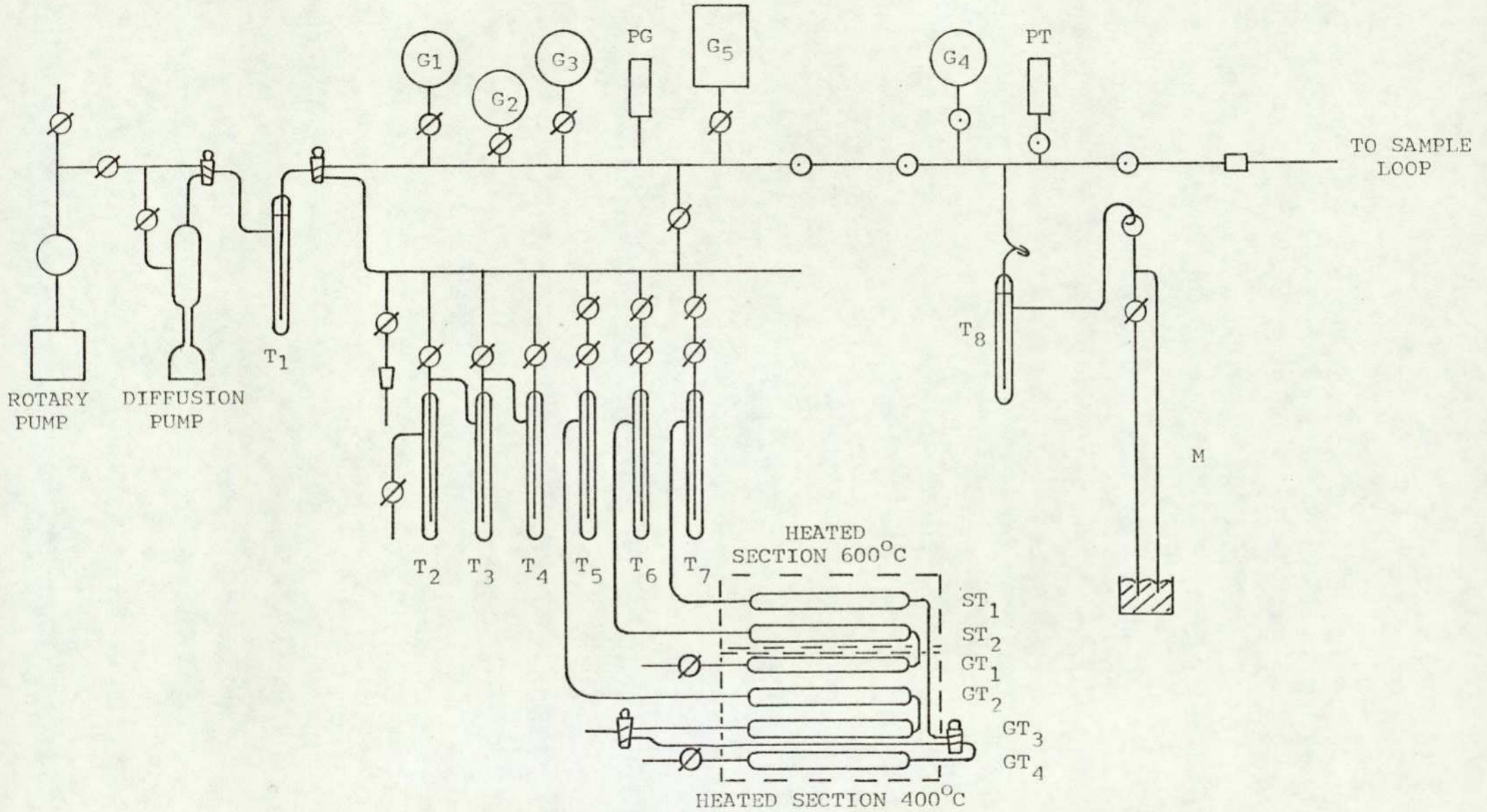

FIGURE 2.2. VACUUM APPARATUS AND GAS PURIFICATION LINE

KEY TO FIGURE 2.2.

COMPONENT		DESCRIPTION
	=	TWO-WAY HIGH VACUUM TAP
	=	HIGH VACUUM TAP
	=	GREASELESS TAP
	=	ROTAFLO TAP
G_1-G_4	=	GAS STORAGE GLOBES
G_5	=	GAS STORAGE GLOBE WITH GUARD
PG	=	PIRANI VACUUM GUAGE
PT	=	PRESSURE TRANSDUCER
T_1-T_8	=	COLD TRAPS
ST_1, ST_2	=	SILICA TUBES CONTAINING COPPER OXIDE
GT_1-GT_3	=	GLASS TUBES CONTAINING PLATINISED ASBESTOS
GT_2-GT_4	=	GLASS TUBES CONTAINING COPPER TURNINGS
M	=	MANOMETER

poisoning required the use of very high purity helium. This was supplied by B.O.C. with a quoted minimum purity of better than 99.99%.

The only other inert gas used was nitrogen; it was used only as a diluent and was supplied by B.O.C. as "white-spot, oxygen-free" grade. This gas was further purified by passing it over fine copper wool at 450°C, then over copper (II) oxide at 600°C, and finally through a cold trap at - 196°C.

2.2 APPARATUS AND PROCEDURE

2.2.1. PULSE FLOW MICRO-REACTOR SYSTEM

2.2.1.1. INTRODUCTION

A substantial part of the experimental work was carried out using a pulsed-flow micro-reactor system. This apparatus was used for determining the activities of poisoned and non-poisoned catalysts, with respect to carbon monoxide oxidation, as well as the "active"surface areas of some supported catalysts.

The pulsed-flow micro-reactor system consisted essentially of a conventional gas chromatograph, with a micro-reactor placed in the carrier gas flow just downstream of the sample injection valve. A schematic representation of the system is shown in figure 2.1., and the separate components are described in detail in the following sections.

2.2.1.2. PREPARATION AND STORAGE OF REACTANTS

The vacuum apparatus shown in figure 2.2. was used for the purification and storage of reacting and inert gases, and additionally for making up mixtures of these gases. Connections were arranged to the sample injection valve and to the gas purification section.

Table 2.1. PRESSURE TRANSDUCER CALIBRATIONS

(a) Manufacturer's specifications

Range 0 - 15 p.s.i. (absolute)

Output 20.52 mV Input voltage ca 5 volts.

(b) On line calibration with a Croydon Precision Instruments potentiometer, maximum sensitivity 0.005 mV.

Input voltage supplied by an Advance PP 34 variable D.C. current/voltage supply unit.

Pressure mm Hg.		Output mV
0.0	-	6.38
1.5	-	6.295
38.0	-	5.21
56.3	-	4.74
82.0	-	3.93
121.17	-	2.975
135.0	-	2.95
171.0	-	1.61
202.0	-	0.98
210.0	-	0.46
235.0	+	0.35
296.0	+	2.15
347.0	+	3.15
412.0	+	5.35
462.0	+	6.76
536.0	+	8.86
567.0	+	9.75
608.0	+	11.08
637.0	+	11.82
665.0	+	12.59
766.6	+	15.35

Gas pressure in the line was measured by a Solartron 0.15 p.s.i. (absolute) pressure transducer. Calibration and other performance details are given in Table 2.1. The mercury manometer was used only for calibration purposes and was normally isolated from the rest of the line. This removed the possible danger of inadvertently poisoning the catalyst with mercury vapour. The signal output from the pressure transducer was measured on a Comark D.C. millivoltmeter, with an estimated probable error of $\pm$ 2% (F.S.D.) and a maximum sensitivity of 1 mV (F.S.D.). The Comark instrument was used only for conveniently and rapidly measuring the approximate value of the signal output, the final value being measured with a Croydon Precision Instruments potentiometer with a maximum sensitivity of 0.005 mV.

The gas pressure in the line at high vacuum was measured using a Pirani vacuum gauge model 8/2, which had a limiting sensitivity of 1×10^{-4} Torr. The pumping system, which consisted of a mercury diffusion pump backed by an Edwards high vacuum rotary pump, model EDM2, was able consistently to achieve a vacuum of ca. 5×10^{-3} Torr. over the whole vacuum line and one of ca. 2×10^{-3} Torr. over the part of the vacuum line necessary for making up mixtures of gaseous reactants.

Mixtures of gaseous reactants, i.e. carbon monoxide, oxygen and an inert gas, were prepared and placed in the storage globes by using the following general procedure.

The minor component was admitted to the pre-evacuated globe to the required pressure, the globe tap was then closed and the manifold was pumped down. The next gas was then admitted slowly into the manifold, and when the pressure had risen above that of the first

component, the globe tap was opened and the second gas was admitted to the required pressure. Further gases were admitted in a similar fashion. Mixture compositions were calculated from the filling pressures and checked by gas chromatographic analysis. Connections from glass to metal tubing were made using modified Simplifix couplings fitted with silicone rubber washers. This form of coupling from metal to glass tubes was found to be very satisfactory, giving vacuum- or pressure-tight seals requiring only hand tightening and with a minimal risk of breaking the glass section.

2.2.1.3.GAS PURIFICATION APPARATUS

The use of the gas purification line has already been described in sections 2.1.4. and 2.1.5. However, its construction, which was quite complex, is described in this section. A detailed diagram is shown in figure 2.2.

The apparatus consisted of two sections. The first and main section for the purification of oxygen, nitrogen and hydrogen, consisted of six heated interconnected glass (pyrex) and silica tubes and three cold traps. Both the glass and silica tubes were mounted in spring clips on an asbestos board, and were heated by nichrome wire elements set into asbestos paper wound on to the tubes. The tubes were finally insulated with several layers of cotton-lined asbestos tape. Power was supplied to the elements by two Variac voltage controllers, one of which controlled all of the glass tube elements, and the other controlled the silica tube elements. The voltages required to achieve the correct temperatures inside the glass and silica tubes, were determined using a probing thermocouple before the

tubes were sealed into the apparatus by glass blowing. The silica tubes were obtained from Quadrant glass and were specially constructed with glass ends using graded glass/silica joints. The second section of the gas purification apparatus was used for the purification of carbon monoxide. This section consisted of three inter-connected cold traps, and carbon monoxide was condensed and purified in them as described in section 2.1.4.

2.2.1.4. SAMPLE INJECTION

A Perkin Elmer six-way gas sampling valve was used to inject gases and reactant mixtures into the micro-reactor or gas chromatograph. The sample loop consisted of a coiled 40 feet length of $\frac{1}{8}$" o.d. stainless steel tubing having a calibrated volume of 21.8 ± 0.3 cm^3 at S.T.P. The calibration was carried out in situ by comparing the detector response to injections of nitrogen gas from the sample loop, with various standard loops supplied by Perkin Elmer. The volumes of the standard sample loops were checked, and found to be accurate, by weighing them empty and after they had been filled with water. The sample loop itself was also checked in this manner. The use of mercury instead of water, although probably yielding more accurate results, was avoided due to the possibility of contamination.

The long narrow bore type of sample loop minimised the amount of mixing of the carrier gas (helium) with the sample during injection. Shorter lengths of larger diameter tubing were found to give poor results in this respect. The concentration profile of the sample pulse was examined by connecting the injection valve directly to the detector and recording the pulse shape directly on a chart recorder. The ideal shape of the signal drawn out by the

FIGURE 2.3. PLOT OF GAS SAMPLE VOLUME AGAINST % SAMPLE VOLUME REMAINING UNDILUTED BY THE CARRIER GAS

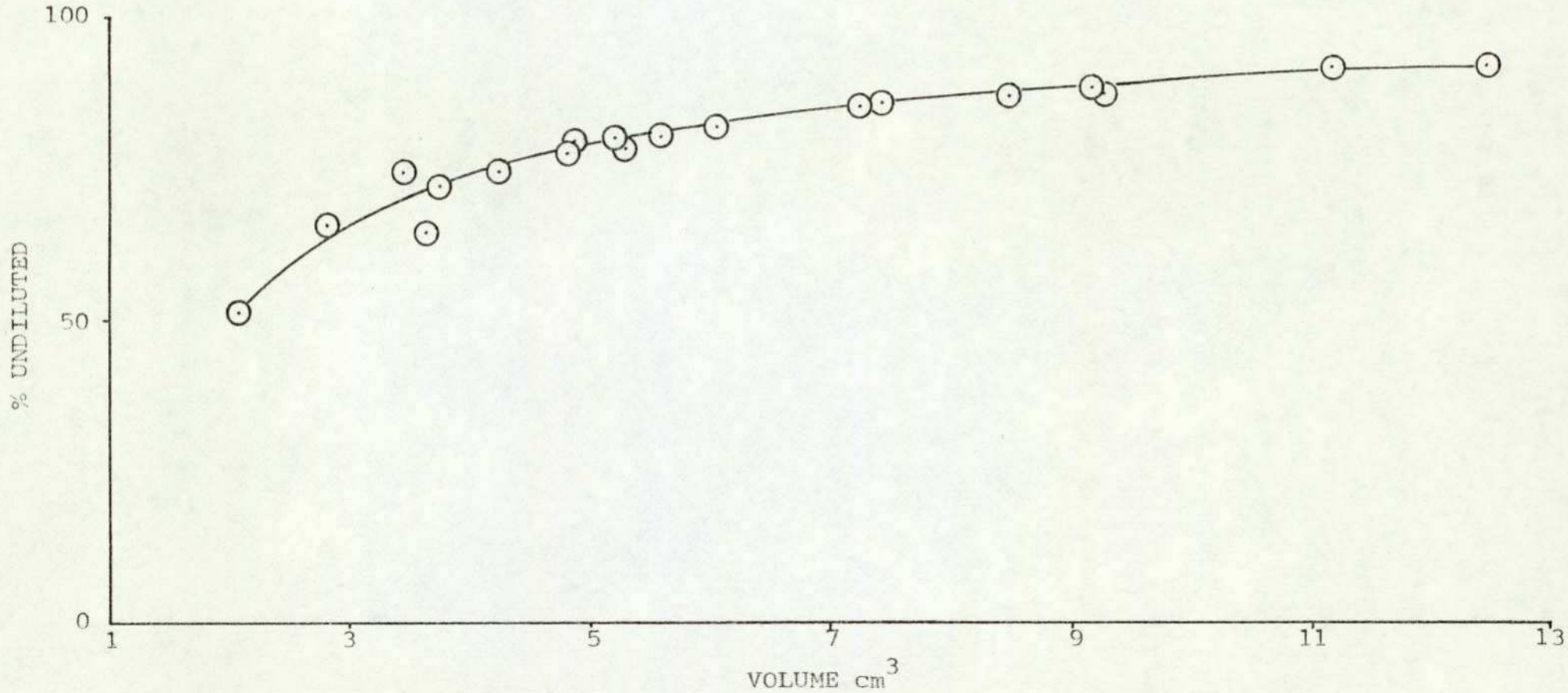

recorder, if no dilution of the sample occurs, is a perfect rectangle, i.e. an instantaneous change in the baseline from a theoretical zero input situation to whatever the new signal level would be, the slope of the leading and trailing edges representing the response time of the system. The volume of the sample injected (calculated at S.T.P.) was varied by altering the introduction pressure. The volume of sample was plotted against the percentage of the sample remaining undiluted, this being calculated by triangulating the leading and trailing edges of the signal and subtracting these from the total. Some typical results are shown in figure 2.3. It was found that for sample volumes of 8 cm^3 and larger, at least 80% of the sample reached the reactor without dilution. Some practical difficulties were encountered during this part of the investigation, in particular the problem of mixing of sample and carrier gas, caused by any unnecessary restrictions or junctions in the connecting pipes. It was therefore found necessary to ensure that the tubing from the six-way gas sample valve to the micro-reactor was as short as possible, without any sharp bends or other restrictions. One particular component, namely a Drallim tap, was an unsuspected source of turbulence and hence sample and carrier gas mixing, for some time, before its effect was discovered and rectified.

Connections from the six-way gas sampling valve and from one component to another in the non-glass part of the apparatus were made mainly with copper tubing; this was normally of $\frac{1}{8}$" o.d. although some $\frac{1}{4}$" o.d. tubing was also used. A small quantity of stainless steel and nylon tubing was also used. Junctions in the tubing and connections from the tubing to components were made with silver-soldered joints, Drallim, Simplifix or Swagelock compression couplings. In general, silver-soldered joints were found to be the best, as once

made and tested for leakage they were completely reliable. The Drallim couplings were easier to use than any other type of joint and furthermore could be made and remade many times without fear of leaks. However, leaks, which resulted in some considerable delay, occurred with Drallim couplings which were located in inaccessible places and were subject to movement. Also Drallim couplings were not suitable for joints in areas which attained temperatures of around 100°C or higher, as the rubber seals were not resistant to sustained use at these temperatures. Swagelock couplings were made of very high quality components, which were both temperature resistant and suitable for joints requiring repeated dismantling and assembly. Their disadvantages included high cost, and less important, an inconvenient bulk if used in a confined space e.g. connections to and from the detector unit. Finally, Simplifix compression couplings were found to be perfectly satisfactory for high temperature use, but could be used only once, and additionally were bulky and not totally reliable, their use resulting again, on occasions, in considerable delays caused by leaks which were difficult to locate.

2.2.1.5. MICRO - CATALYTIC REACTOR

The micro-reactor could be connected with or isolated from, the carrier gas stream with a Perkin-Elmer four-way valve. This arrangement allowed the catalyst to be changed, or if necessary reduced in situ with a negligible disturbance of the carrier gas flow to the gas chromatograph.

The micro-reactor was mounted in a 5cm diameter furnace at a temperature controlled by an A.E.I. proportional controller (day-to-day stability $\pm$ 0.1°C). The reactor temperature was

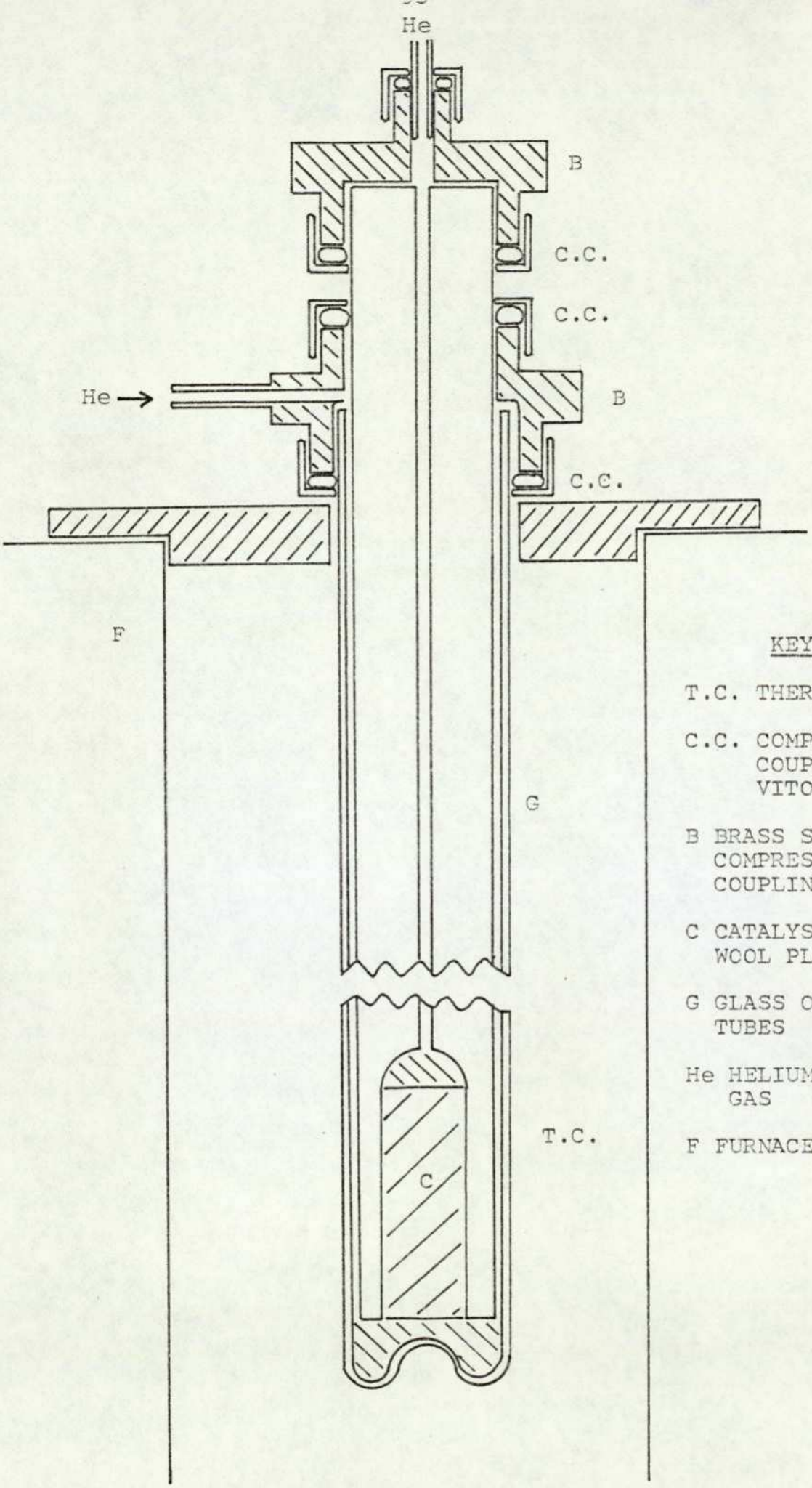

FIGURE 2.4. MICRO-REACTOR

FIGURE 2.5. TEMPERATURE DISTRIBUTION OF MICRO-REACTOR FURNACE

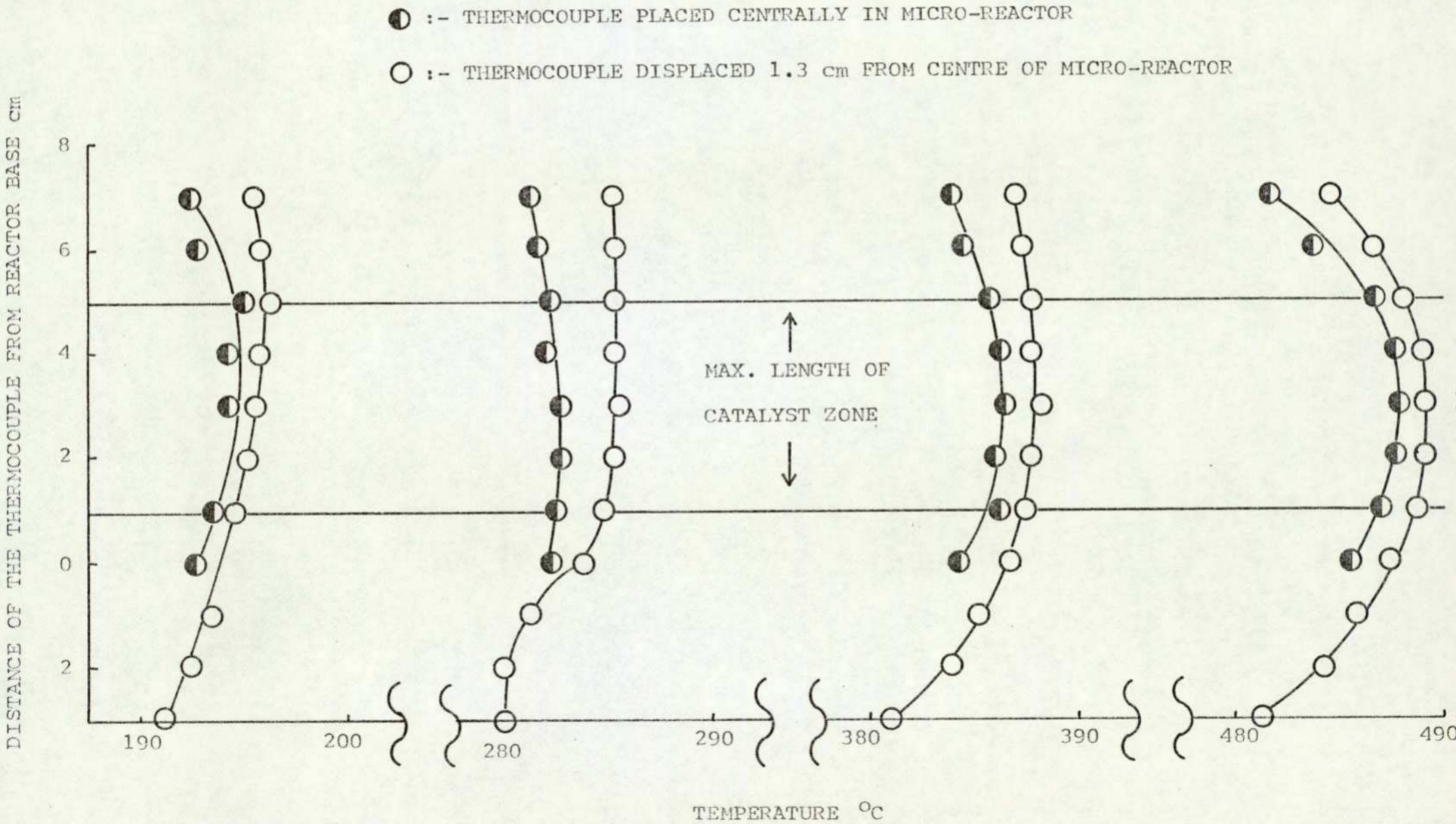

measured by a chromel/alumel thermocouple held adjacent to the catalyst bed.

The micro-reactor is shown in figure 2.4. and was operated at temperatures not exceeding 380°C. The catalyst was positioned between glass wool plugs. The reactor was designed in order to keep dead volume to a minimum. The reactor design also facilitated the rapid removal or replacement of one catalyst with another. This was achieved by constructing at least a dozen different inner tubes (which housed the catalyst bed). An additional advantage of this design was that physical disturbance of the catalyst bed, once packed into the inner tube, was negligible.

The gas flow entered into the annular space between the inner and outer tubes (minimised by selection of tubes with a very close fit), passed through the catalyst bed and accelerated out of the reactor along the 1mm diameter exit tube. The temperature distribution of the furnace was measured with the micro-reactor in situ. Readings were taken along two vertical axes, one coinciding with the vertical axis of the micro-reactor and the other along a vertical axis 1.3cm from the centre of the micro-reactor. The temperature distribution (shown in figure 2.5.) revealed that the region of least temperature variation lay within a zone from 1 to 5 cm above the lower extremity of the reactor. For this reason, catalyst beds were kept within this region.

When the micro-reactor was used for evaluating active surface areas, a modification was made which consisted of making the connections from the four-way valve to the micro-reactor, using two lengths of $\frac{1}{8}$" o.d. nylon tubing. This enabled the convenient transfer of the micro-reactor to a thermostatically-controlled water bath.

2.2.1.6. GAS CHROMATOGRAPH

The gas chromatograph section was of conventional design using helium carrier gas, a single column and a katharometer detector. A flow diagram of the apparatus is shown in figure 2.1. Sample volumes were normally 8 cm^3 (S.T.P.).

In order to analyse for all the reactant, product and inert gases, i.e. oxygen, nitrogen, carbon monoxide and carbon dioxide, a two-column system would have been necessary, as there were no column materials available to resolve a mixture of all four gases. However, as the analysis was strictly necessary for only three gases, only one column was required: either silica gel, which could resolve both oxides of carbon and air, or molecular sieve, which could resolve nitrogen, oxygen and carbon monoxide, leaving carbon dioxide permanently adsorbed on the column. A single-column system was considered desirable, compared with a twin-column system, from the practical viewpoints of ease of construction and ease of operation of the apparatus. The disadvantages, with a single column system, of having to calculate the quantity of oxygen not resolved from mitrogen, when using a silica gel column, or of having to calculate the quantity of carbon dioxide adsorbed permanently on a molecular sieve column, were not considered to be practically or theoretically significant.

For the reasons previously stated it was necessary to compare the relative performances of silica gel and molecular sieve as column materials. It was found in practice that silica gel yielded a relatively poor resolution of carbon monoxide from air, although the oxides of carbon were adequately separated. However, molecular sieve was found to yield a very satisfactory resolution of all the gases except carbon dioxide, which as previously mentioned, was adsorbed permanently. Several grades of molecular sieve were

evaluated, none of which yielded any particular advantage and it was therefore decided, somewhat arbitrarily, to use linde molecular sieve 13 x (60-80 mesh).

The conditions of operation and the column dimensions were chosen to allow the convenient use of sample volumes compatible with the detector sensitivity and with the dimensions of the catalyst bed, and also to allow the use of a carrier gas flow rate of 25 cm^3 $min.^{-1}$ The column was thermostatically controlled at a temperature of 60°C and its length and diameter were 15' and $\frac{1}{4}$" respectively. A column of smaller diameter would have required inconveniently high back pressures to achieve the required flow-rate. The column was conditioned prior to use by purging with helium at 400°C for twenty-four hours at a flow rate of 15 cm^3 $min.^{-1}$ This procedure was repeated from time to time (about every three months) in order to maintain a satisfactory resolution of gases.

The column resolution under these conditions was found to be satisfactory, whilst still allowing the analysis to be completed in a conveniently short time. Typical retention times for oxygen, nitrogen and carbon monoxide were as follows:-

Oxygen - 5.6 min.

Nitrogen - 7.95 min.

Carbon monoxide - 22.5 min.

Retention times were found to vary slightly with sample size. However, as analysis of these gases was quantitative only, the precise values of retention times were of no real significance.

A katharometer detector was chosen as it is the only type of commercially available instrument capable of analysing oxygen, nitrogen and carbon monoxide with a satisfactory sensitivity i.e.

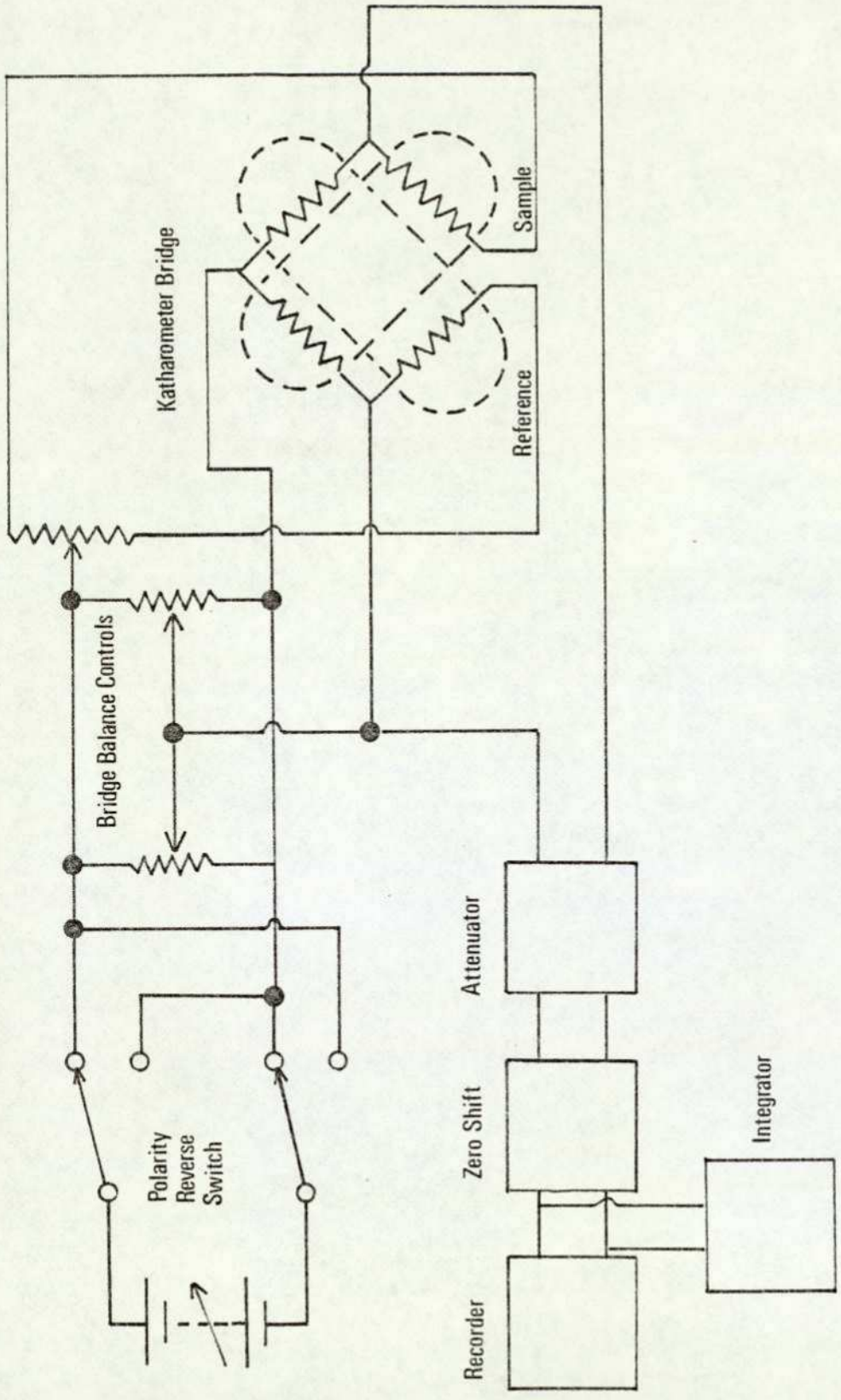

FIGURE 2.10. COMBINED CIRCUIT DIAGRAM OF KATHAROMETER AND BLOCK DIAGRAM OF SIGNAL DISPLAY UNITS

1×10^{-9} g sec^{-1}. The katharometer was a Servomex micro-katharometer MK.158, which the manufacturers claimed to have a sensitivity approaching that of a flame ionization detector, i.e. 1×10^{-12} g sec^{-1} (143) and a response time of the order of 3 milliseconds.

A katharometer is sensitive to changes in temperature, pressure and the carrier gas flow rate. In order to obtain the best results, these must be kept constant. The helium carrier gas flow rate was controlled by a Negretti and Zambra pressure regulator (type R 182 NC) coupled with a Brooks mass flow controller (model 8744). The flow rate was measured with a bubble flowmeter constructed from a 50 cm^3 burette.

The micro-katharometer was housed in a Servomex oven controlled by a Servomex Controller TC 201, which regulated the temperature at $42^{\circ}C \pm 0.25^{\circ}C$. The micro-katharometer filaments were operated at 6 V which was the manufacturer's recommended normal working voltage for use with helium as a carrier gas. The detector output was displayed on a Leeds and Northrup Speedomax W recorder (0 - 1 mV f.s.d.) Peak areas were measured by means of an integrator (Kent Chromologue 1). A combined circuit diagram of the katharometer and control unit together with a block diagram of the signal display units is shown in figure 2.10.

2.2.1.7. OPERATION OF THE MICRO-REACTOR

There are various parameters which can be varied during the operation of the micro-reactor and these parameters are listed below:-

(i) Temperature

(ii) Contact time

(iii) Pulse volume

(iv) Pulse composition

(v) Condition of the catalyst

Temperature was kept constant by means of a proportional temperature controller. The contact time could be varied by either changing the carrier gas flow rate or by changing the quantity of the catalyst.

The pulse volume was not varied for determinations of catalytic activities with respect to carbon monoxide oxidation, the optimum pulse volume having been determined for this system as described in section 2.2.1.4. However, this parameter was varied in the case of the active surface area determinations described in section 2.2.1.8.

The basis for selecting pulse composition depended upon such factors as the quantity of catalyst being used, the practical limitations imposed upon the system by gas storage facilities and also the local temperature rise within the catalyst bed caused by the heat of reaction. With regard to this last factor, some experimental work was initially completed with some of the more active catalysts, in order to estimate the extent of the temperature rise taking place within the catalyst bed. With regard to the information derived from this work, an optimum range of pulse compositions was chosen which caused only a minimal local temperature rise within the catalyst bed for complete oxidation of the carbon monoxide present in the pulse. The temperature was measured during these experiments using an extremely fine thermocouple wire placed directly in the catalyst bed within the micro-reactor. The output of the thermocouple was displayed on a chart recorder which enabled the peak transient temperature attained to be accurately evaluated, even if the time of duration of the peak temperature was of the order of a fraction of a second. Some

FIGURE 2.6. VARIATION OF CATALYST BED TEMPERATURE WITH TIME - SUCCESSIVE REACTANT PULSES

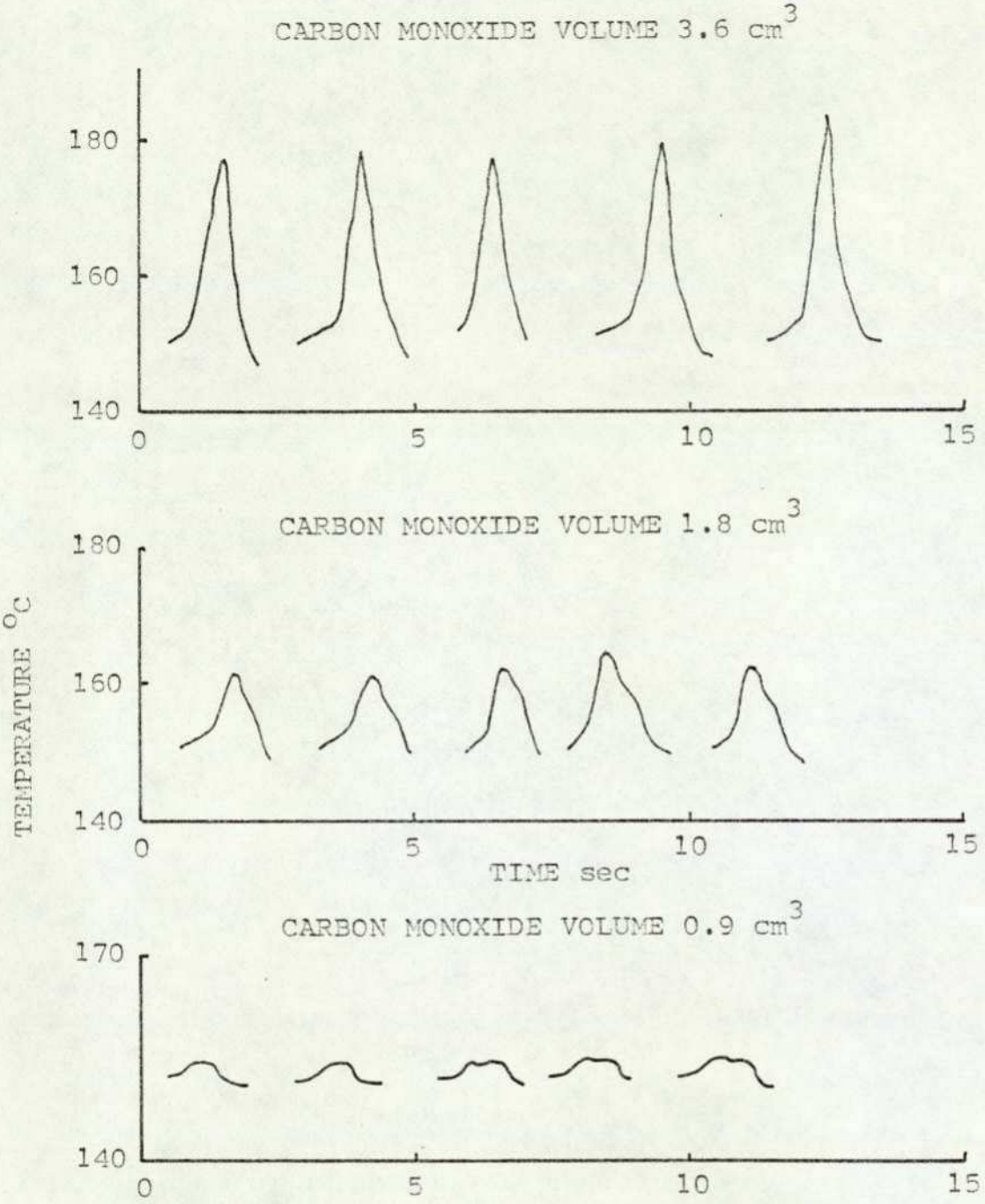

CATALYST DETAILS

COMPOSITION :- NiO

SURFACE AREA :- 34.2 $m^2 g^{-1}$

WEIGHT :- 0.1 g

PULSE DETAILS

CO/O_2 RATIO :- 1.0

DILUENT GAS :- NITROGEN

TOTAL PULSE VOLUME :- 8.0 cm^3

of the results of this investigation are shown in figure 2.6.

The condition of the catalyst whilst "in situ" in the micro-reactor was varied only to the extent of conditioning the catalyst by passing successive identical reactant pulses until the extent of the oxidation was found not to change from one pulse to the next.

This procedure was found to be necessary in almost every case, although the number of pulses required rarely exceeded four or five. However, this was found to be the case only when carbon monoxide was catalytically oxidised in an excess of oxygen. In the oxidation of carbon monoxide with less than the stoichiometric equivalent of oxygen available, successive pulses of reactants normally resulted in reduction of the actual catalyst surface. This condition could be readily diagnosed by a continuing reduction in catalytic activity with each successive pulse. For this reason the catalytic oxidation of carbon monoxide under these reducing conditions was avoided. The variation of the condition of the catalyst with respect to lead halide poisoning was not achieved "in situ" and is fully discussed in section 2.2.2.

2.2.1.8. ACTIVE SURFACE AREA MEASUREMENT

The so called "active" surface areas of supported platinum catalysts were determined by using a flow method based on the chemisorption of carbon monoxide at low temperature (i.e. 30°C) as described by Gruber (144, 145). In order to perform these measurements, the micro-reactor was slightly modified as described in section 2.2.1.5., and in addition the gas chromatograph column was by-passed by connecting the reactor outlet directly to the katharometer detector.

There are four stages in the determination of active surface areas, the first of which is degassing the catalyst and chemically cleaning the surface. The second stage is the determination of the volume of carbon monoxide chemisorbed from a pulse passed over the catalyst. The third stage is desorption and measurement of the desorbed carbon monoxide volume. The final stage is the calculation of the active surface area. In practice the third stage could not be carried out as the temperature required to desorb the carbon monoxide may have melted some of the lead (II) bromide poison. However, the desorption of carbon monoxide, although providing a useful check, was not an essential part of the procedure.

The catalyst was cleaned whilst in situ, first by degassing in the helium carrier stream for a period of one hour at 300°C, and then by reducing the surface by passing a stream of hydrogen over the catalyst at 300°C for a period of one hour. The final stage was a further reduction with three pulses of hydrogen, the volume of which was chosen to be within 4 - 8 times the expected monolayer capacity of the catalyst. The hydrogen pulses were detected by the katharometer and the resulting peaks were examined as a final check on the state of the catalyst. Thus if the catalyst surface was completely reduced, the volume of the hydrogen pulses would remain unchanged and each peak would be identical to the other two.

After the catalyst had been degassed and cleaned, the micro-reactor was cooled and transferred to a thermostatted water bath kept at 30°C. Two identical pulses of carbon monoxide, the volumes of which were precisely known, were passed over the catalyst. The difference in volume between the two pulses represented the volume of carbon monoxide chemisorbed on the surface of the catalyst. In order to check that the catalyst surface was fully saturated with carbon monoxide, several further identical pulses of carbon monoxide were also passed over the catalyst.

It was found from repeated experiments that, if the pulse size was twice the size, or greater than twice the size of the monolayer capacity of the catalyst, then the surface of the catalyst was fully saturated by the first pulse. This method of using two pulses of carbon monoxide was not only found to be convenient, but also eliminated the errors inherent in calculating the volume of chemisorbed carbon monoxide using the volume, pressure and temperature of the sample loop.

The normal procedure after chemisorption of carbon monoxide is, as has been previously mentioned, a desorption stage, which is carried out at approximately 450 - 500°C. However, as this was not possible for the catalysts poisoned with lead (II) bromide an alternative method of removing the carbon monoxide was therefore needed to enable the active surface area determination to be repeated. It was found that a convenient method for removing chemisorbed carbon monoxide was to pass oxygen over the surface of the catalyst at 300°C and remove the carbon monoxide by oxidation to carbon dioxide. Three pulses of oxygen were passed over the catalyst surface at 300°C. The volume of the pulse was chosen to be at least 10 times the quantity required for complete oxidation of the carbon monoxide. The catalyst was then degassed and cleaned in the manner previously described, in preparation for a repeat determination of the active surface area.

Using the quantity of carbon monoxide chemisorbed on the surface of the catalyst the active surface area of the catalyst could be calculated. Alternatively, in the case of a pure platinum catalyst, the total surface area could be calculated. Several

Table 2.2. SURFACE AREA DETERMINATIONS BY CARBON MONOXIDE CHEMISORPTION AND BY THE BET NITROGEN ADSORPTION METHOD

	BET Method	Carbon monoxide chemisorption method
Surface area $m^2 g^{-1}$	7.2	6.5
	7.15	6.76
	7.15	6.6

Details

Sample : - Platinum Black

Weight : - 0.108 g

Carbon monoxide pulse volume : - 1.05 cm^3

BET determination : - Standard conditions

workers have suggested a value for the cross sectional area of the carbon monoxide molecule when chemisorbed on a precious metal catalyst (144, 145, 146). However, it was decided to evaluate the total surface area of a pure platinum catalyst (The total and active surface area of an unsupported platinum catalyst should in theory have the same value) both by the method of carbon monoxide chemisorption and by a dynamic nitrogen adsorption method based on the BET isotherm (this method is fully discussed in section 2.3.1.). It was found that close agreement between the two methods could be achieved if a value of 13.2Å was taken as the cross-sectional area of chemisorbed carbon monoxide (this value was suggested by Van Montfoort (146). Table 2.2. shows the results of this comparison for a platinum black catalyst.

It was found experimentally from many measurements, that the volume of carbon monoxide could be determined with a repeatability of $\pm$ 0.5%. The random error would therefore be within $\pm$ 10% for 10% chemisorption of the carbon monoxide pulse, and within $\pm$ 2% for 50% chemisorption of the carbon monoxide pulse. Several measurements on the same catalyst (see table 2.2.) showed that the random error for 20% chemisorption of the carbon monoxide pulse was not greater than $\pm$ 2%. Admittedly the number of measurements in this case is small, but the order of magnitude of random errors indicated by these measurements is also small. The probable largest single cause of error inherent in the active surface area measurements, was the choice of cross sectional area of the chemisorbed molecule. However, this error was systematically applied to all the results, and would not therefore influence a comparison of surface areas for the same type of catalyst.

2.2.2. LEAD HALIDE POISONING SYSTEM

2.2.2.1. INTRODUCTION

The lead halide poisoning apparatus was constructed to enable the convenient application of either lead (II) bromide or lead (II) chloride to various supported and unsupported catalysts. Several attempts were made to design an apparatus which simulated the conditions occurring in a car exhaust system, whilst at the same time remaining a practical proposition from the point of view both of construction and of operation. The apparatus described in this section was inevitably a compromise between these conflicting factors.

It consisted of a stainless steel reactor, which contained both poison and catalyst, and through which flowed the nitrogen carrier gas. The reactor was heated by a furnace controlled by means of a Variac voltage regulator. The complete assembly was housed in an efficient fume cupboard to ensure that no particular lead halide escaped into the laboratory. A schematic representation of the system is shown in figure 2.8.

2.2.2.2. THE LEAD HALIDE-POISONING REACTOR

The lead halide poisoning reactor was constructed from $\frac{1}{4}$" o.d. stainless steel tubing. The reactor consisted of two sections, a coil of stainless steel in which known quantities of either lead (II) bromide or lead (II) chloride were placed and two or three short lengths of stainless steel into which the catalyst was placed. Each short length of stainless steel tubing was sealed at the bottom with a sintered stainless steel disc, and connections were made with stainless steel Swagelock compression couplings. The temperature of

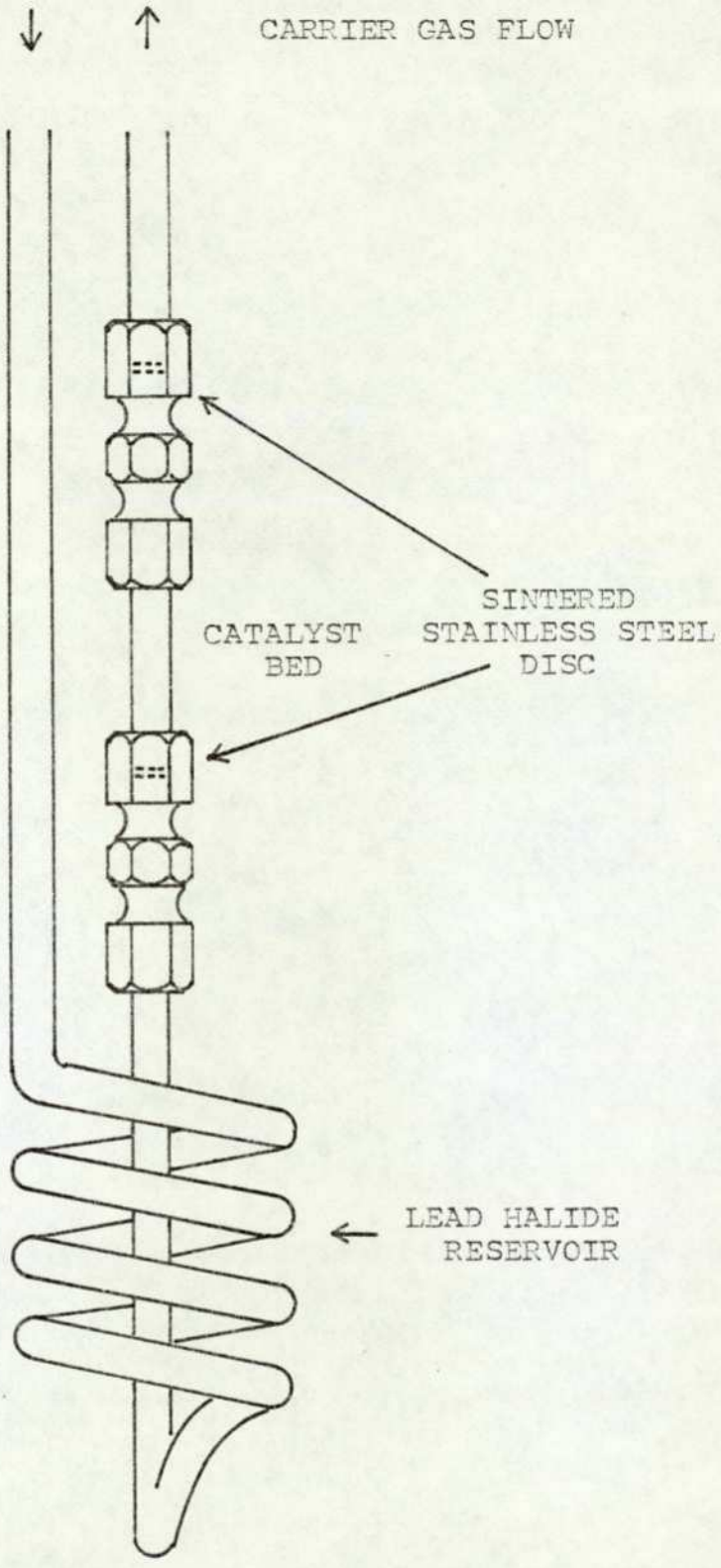

FIGURE 2.7. LEAD HALIDE POISONING REACTOR

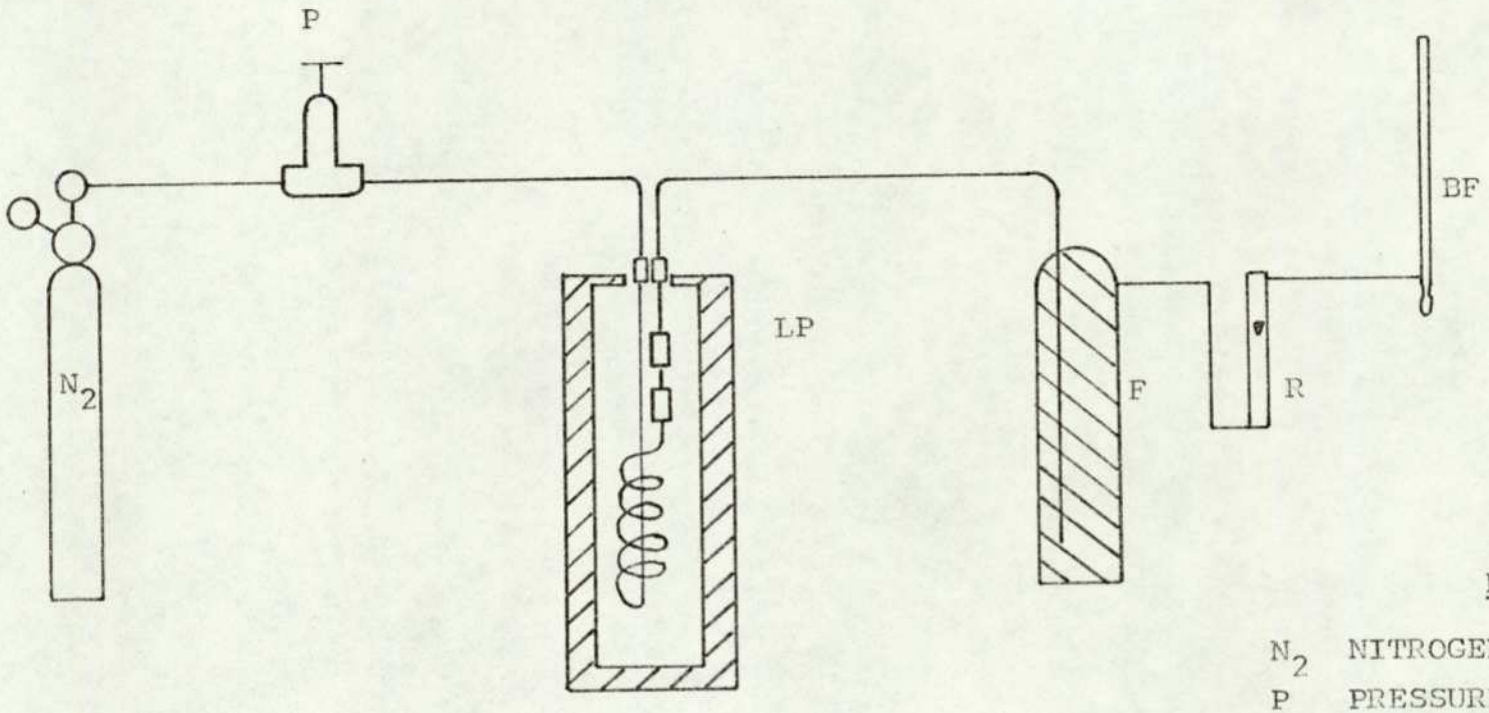

KEY

N_2	NITROGEN CYLINDER
P	PRESSURE CONTROLLER
LP	LEAD POISONING REACTOR AND FURNACE
F	LEAD HALIDE FILTER
BF	BUBBLE FLOWMETER
R	0-15 $dm^3 min^{-1}$ ROTAMETER

FIGURE 2.8. SCHEMATIC DIAGRAM OF LEAD POISONING APPARATUS

the reactor at various different positions along its lengths was measured with chromel-alumel Thermocouples. The reactor was heated using a furnace controlled with a Variac voltage controller. A diagram of the lead halide poisoning reactor is shown in figure 2.7.

2.2.2.3. CONTROL AND MEASUREMENT OF CARRIER GAS FLOW

Nitrogen was used as the carrier gas and was of the same quality as described in section 2.1.5. The nitrogen was dried using an on-line molecular sieve dryer supplied by Perkin-Elmer. The flow of nitrogen carrier gas was used to transfer the lead halide vapour from the stainless steel coil to the catalyst bed in the poisoning reactor. The flow of nitrogen was controlled by the usual B.O.C. two-stage pressure controller (0.30 p.s.i. gauge output) and additionally by a Watts non-relieving pressure controller (0 - 60 p.s.i. gauge output). The nitrogen flow rate was measured using a 0 - 15 litre min^{-1} rotameter or a $50cm^3$ bubble flowmeter, the former for the higher flow rates and the latter for the lower flow rates. A filter packed with glass fibre was placed in the nitrogen stream after the reactor in order to remove excess lead halide. As an additional safety precaution, the outlet of the apparatus was placed adjacent to the fume-cupboard extractor fan. A schematic diagram of the entire apparatus is shown in figure 2.8.

2.2.2.4. OPERATION OF THE POISONING REACTOR

All catalysts used were prepared in particulate form with particles varying within a size range of 40 - 80 mesh. In order to ensure that the poisoning of a catalyst was uniform, the behaviour of the catalyst was examined, under various flow rates, in an apparatus similar to the poisoning reactor, but constructed with a glass section for the catalyst bed. This apparatus enabled the catalyst to be

visually examined while the carrier gas flow rate was varied. It was found after numerous experiments, in which both the type and total weight of catalyst were varied, that fluidisation of the catalyst bed was complete at a maximum flow rate of 0.5 litre min^{-1}. The flow rate used for poisoning catalysts with lead halide was therefore maintained at a value equal to or higher than 0.5 litre min^{-1}. The specific value used in the majority of cases was 2.0 litre min^{-1}. At these flow rates the catalyst bed was completely fluidised, ensuring uniform poisoning of the catalyst.

The temperatures chosen to poison catalysts with lead (II) bromide and lead (II) chloride were respectively 550°C and 580°C. Temperatures were selected at these values for two reasons. First, poisoning could be achieved only with the lead halide vapour, so that temperatures greater than the respective melting points of the two lead halides were necessary (lead (II) bromide M.pt. 398°C, lead (II) chloride M.pt. 581°C). Secondly, the temperature of catalyst preparation (630°C) could not be exceeded during poisoning without risk of a fundamental change in catalyst properties.

The weights of both catalyst and the lead halide poison were determined prior to operating the apparatus. The quantity of lead halide used varied between 2 and 4g. The weight of the catalyst sample varied depending on its density, and in some cases on the total amount available, but was normally of the order of 1g. The lead content of a poisoned catalyst was determined by taking a small aliquot (20-70mg), dissolving it in hot nitric acid, or a mixture of nitric and hydrochloric acids, and then analysing for lead using a Perkin Elmer 290B Atomic Absorption Spectrophotometer. The uniformity of poisoning of the catalyst sample was checked by taking several differnent aliquots from the sample and analysing each aliquot for lead.

Table 2.3. ANALYSES OF CATALYSTS POISONED WITH LEAD (II) BROMIDE

	CATALYST SAMPLES		
	Nickel (II) oxide (A)	Nickel (II) oxide (B)	Copper (II) oxide
Lead Content (% $PbBr_2$)	10.3, 9.2, 9.8	0.635, 0.64 0.65	0.33, 0.34 0.33
Weight of aliquot mg.	51.1, 51.8, 55.0	78.4, 51.9, 35.9	20.0, 49.0, 29.0
Total weight of catalyst mg.	759.0	625.0	837.0

	DETAILS OF CATALYSTS		
	Nickel (II) oxide (A)	Nickel (II) oxide (B)	Copper (II) oxide
Surface area $m^2 g^{-1}$	3.91	2.84	0.145
Method of preparation (see section 2.1.1.)	Via hydroxide	Via nitrate	Via nitrate

The selection of aliquots from a catalyst sample was made randomly by gentle shaking of the sample for at least a minute before selection. Some typical results of lead analyses are shown in table 2.3. It was found that the amount of lead present in different aliquots from the same sample almost invariably lay within a range of $\pm$ 5% from the mean value. In some cases, agreement was within the accuracy of the atomic absorption instrument, i.e. $\pm$ 1%.

2.2.3. CONTINUOUS-FLOW SURFACE AREA APPARATUS

2.2.3.1. INTRODUCTION

The determination of the specific surface area, and other surface properties is an essential requirement of any study of catalysis, and this is particularly true in the present case, as some postulated mechanisms of catalyst poisoning in car exhaust systems involve changes in surface properties (7). For this reason a significant proportion of the time spent on experimental work was devoted to the construction and operation of a continuous-flow surface area apparatus, which operated on the principle of nitrogen adsorption.

The determination of the surface properties of catalysts is frequently achieved by the use of nitrogen adsorption methods. The more common static nitrogen adsorption methods rely on determining the quantity of nitrogen adsorbed and desorbed from a catalyst, at various relative pressures of nitrogen and at the temperature of liquid nitrogen (77.36°K at 1 atmosphere), by detecting weight or pressure-volume changes. This procedure enables a complete adsorption-desorption isotherm to be obtained. From this information

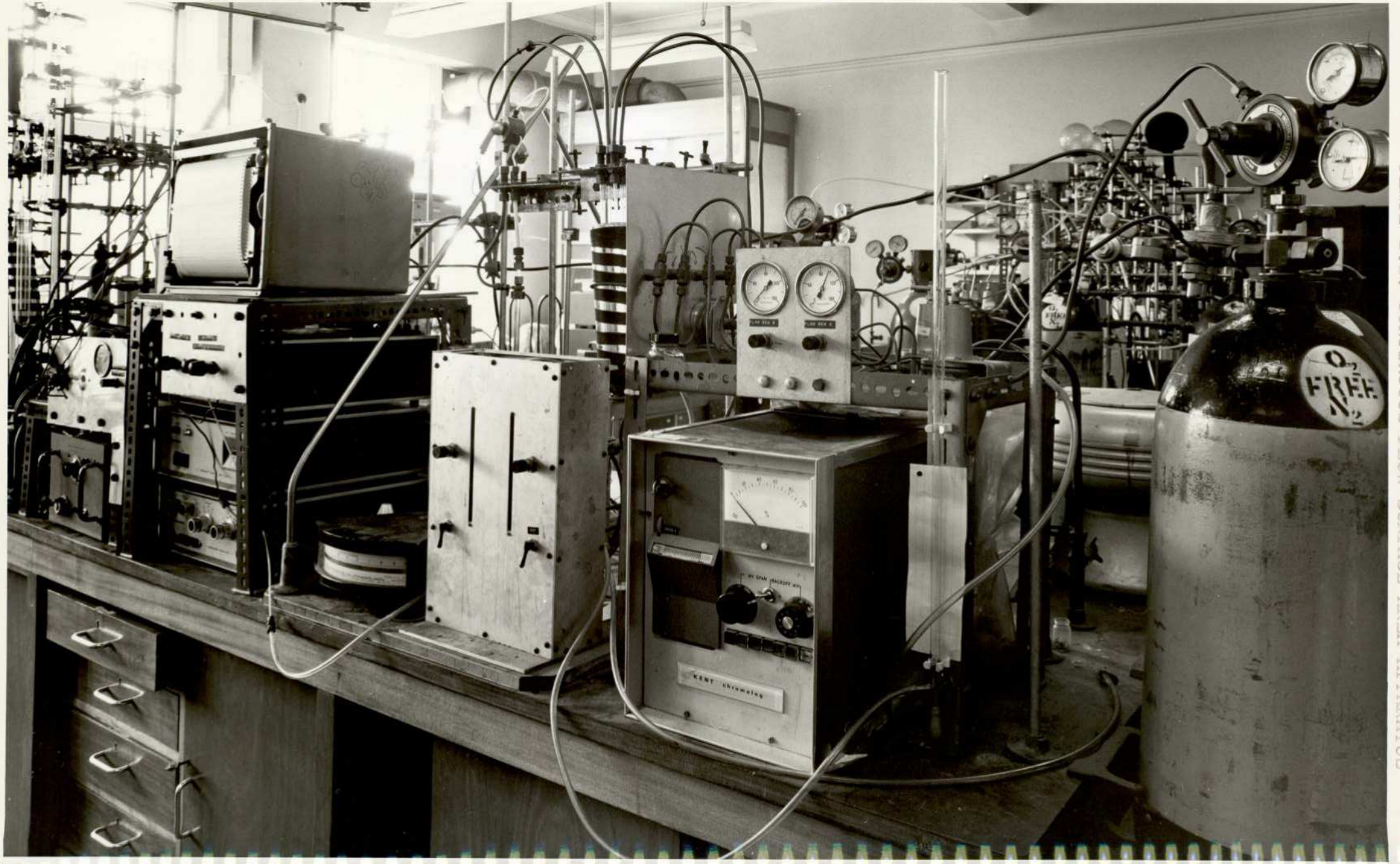

PLATE 2.2. CONTINUOUS-FLOW SURFACE AREA APPARATUS

the surface area may be determined using the well known method of Brunauer, Emmett and Teller (BET) (53). The pore-size distribution may be determined using various methods (52, 55, 56) based on the Kelvin equation and the pore radius may also be calculated. The continuous-flow method utilises the same principle of operation as static methods, but differs in the manner of obtaining adsorption isotherms. In the continuous-flow method, nitrogen is continually passed over the sample, the relative pressure being varied by dilution with helium. The amount of nitrogen adsorbed or desorbed is determined by concentration measurements using a katharometer detector.

The continuous-flow method was introduced by Nelson and Eggertsen (54). These authors found difficulty in controlling the flow of gases and also assumed that detector response was constant over the range of carrier gas compositions used. Later workers (147,148) have improved the operation of the method by successive improvements to flow control and by the investigation of the variation of detector response with change in carrier gas composition. Farey and Tucker (148), having overcome flow control problems by the adoption of modern gas chromatographic techniques, and having also instituted independent gas supplies for the reference and measuring cells of the katharometer detector, showed that this method was suitable for determination of specific surface areas ranging from less than $0.1 m^2 g^{-1}$ to $70 m^2 g^{-1}$ and higher. The method also had the advantages of consuming less time for measurements of specific surface areas than static gas adsorption methods, and of being suitable for the determination of adsorption isotherms.

2.2.3.2. APPARATUS CONSTRUCTION

Figure 2.9. gives a schematic diagram of the apparatus and indicates the gas pressures at various points. Gases were supplied from cylinders equipped with two-stage regulators (0.200 p.s.i.g. output) adjusted to give an output pressure of 120 p.s.i.g. via drying tubes containing Linde 4A molecular sieve. Pressure controller E was a Negretti and Zambra pressure regulator (type R 182 NC), and controlled outlet pressure from -10 p.s.i.g. to + 65 p.s.i.g. Pressure controllers A and B, were Watts non-relieving air regulators (Type 15-Z) controlling outlet pressure from 0-120 p.s.i.g. Mass-flow controllers, C and D, were Brooks Model 8743 (0 to 750 $cm^3 min^{-1}$). Mass-flow controllers G and F, were Brooks model 8744 (0 to 750$cm^3 min^{-1}$). For the correct operations of the mass-flow controllers, a mininum pressure drop of 10 p.s.i.g. was required. The katharometer detector, control and signal display units (Circuit diagram figure 2.10.) were the same instruments, operated under the same conditions as used in the pulse flow micro-reactor described in section 2.2.1.6. The transfer of the detector and its associated units from one instrument to the other, was achieved by means of a system of Drallim valves which could be operated to isolate either instrument.

Both sample and reference lines incorporated liquid nitrogen traps (H, J), which ensured that no condensable impurities reached either the sample or the katharometer. The sample tube I was originally matched with an identical "dummy" tube in the reference line. The "dummy" tube was incorporated to ensure that the thermal history of the two limbs was identical. However, it was found in practice that the "dummy" tube actually caused additional baseline instability and extraneous peaks due to thermal diffusion effects (56, 149). In view of these disadvantages the "dummy" tube in the

reference line was removed without impairing the operation of the apparatus.

It was also found that the time taken for the sample stream gas to pass from the sample tube to the katharometer was insufficient for the gas to attain ambient temperature. This resulted in the sample stream gas failing to reach the temperature of the katharometer ($42^{\circ}C$). Hence the gas analysis was significantly in error due to the reduction in thermal conductivity of the cooled gases. In order to overcome this source of error, the apparatus was modified by passing the gases through lengths of copper tubing (10' x $\frac{1}{8}$" o.d.), immersed in a thermostatically controlled water bath at $42^{\circ}C$, before they entered the katharometer. Gas flow measurements were made with a soap film flowmeter. Gas connections in the system were made with copper tubing. These copper connecting tubes were joined to one another mainly with silver soldered joints, although some compression and captive seal couplings were also used. The advantages and disadvantages of these different types of connectors are discussed in section 2.2.1.4.

The sample holder was originally constructed from a simple glass U-tube, which was connected into the sample gas stream with modified simplifix compression couplings. Various modifications to the design of the sample holder were made, partly in order to increase the convenience of operation and partly to investigate the effect of changes in sample size on surface area results. However, it was finally decided to use the pulse flow micro-catalytic reactor in place of the original sample U-tube. Use of the micro-catalytic reactor for the dual purposes of surface area measurement and for the determination of

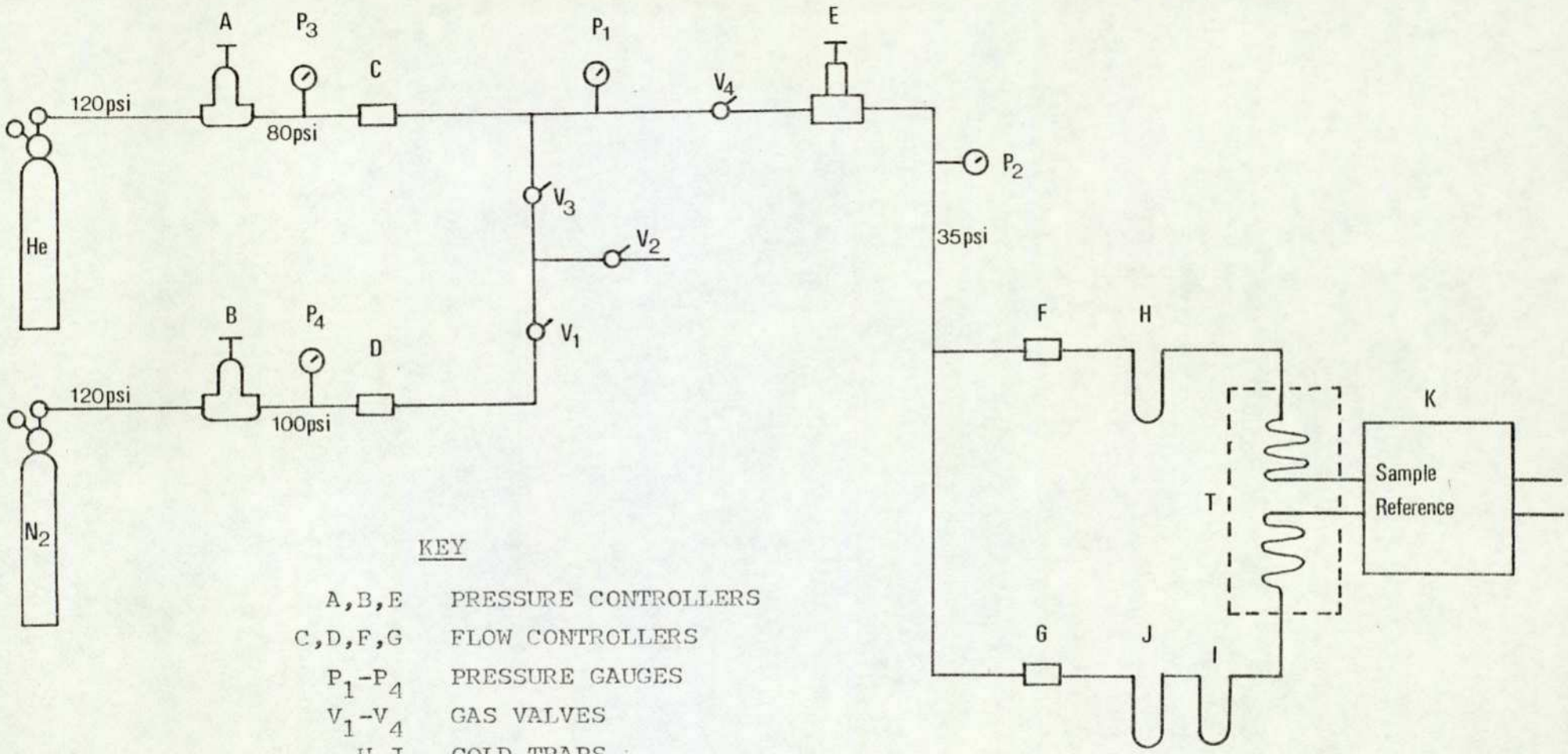

KEY

A,B,E	PRESSURE CONTROLLERS
C,D,F,G	FLOW CONTROLLERS
P_1-P_4	PRESSURE GAUGES
V_1-V_4	GAS VALVES
H,J	COLD TRAPS
I	SAMPLE TUBE
T	THERMOSTATED WATER BATH
K	KATHAROMETER

FIGURE 2.9. SCHEMATIC DIAGRAM OF CONTINUOUS FLOW SURFACE AREA APPARATUS

catalytic activity enabled the convenient transfer of catalyst from one instrument to the other, without the catalyst bed being disturbed or impurities being inadvertently introduced into the catalyst. Experiments to compare surface areas of catalysts, determined using both the original sample U-tube and the micro-reactor as sample holders, showed that the use of the micro-reactor did not affect the accuracy of surface area determinations.

2.2.3.3. OPERATION OF THE CONTINUOUS-FLOW SURFACE AREA APPARATUS

The following section describes the detailed operation of the continuous-flow apparatus in three main stages. The first stage deals with the setting up of the instrument, the second stage with its calibration, and the final stage with its operation to obtain an adsorption isotherm.

The nitrogen flow rate was set by adjusting flow controller D with valve V_3 closed and the flow through valves V_1 and V_2 was then measured. The normal range required was 2 to 20 $cm^3 min^{-1}$. Valve V_3 was opened and valves V_4 and V_1 were closed, and the helium flow-rate was then set by adjusting flow controller C. Finally valve V_1 was opened and the combined nitrogen plus helium flow rate was checked.

The combined flow rate of nitrogen and helium was normally set at a value of 25 $cm^3 min^{-1}$. Once the flow rates of nitrogen and helium had been set, valve V_2 was closed and valve V_4 was opened to admit the gas mixture to the measurement section. Pressure regulator E was set to give a downstream pressure of 35 p.s.i.g. and flow controllers F and G were adjusted to give flow rates of 12.5 $cm^3 min^{-1}$ each, measured at the detector outlets. In order to ensure maximum reliability of the system, very careful attention was needed to balance the various flow controllers as exactly as possible; if the

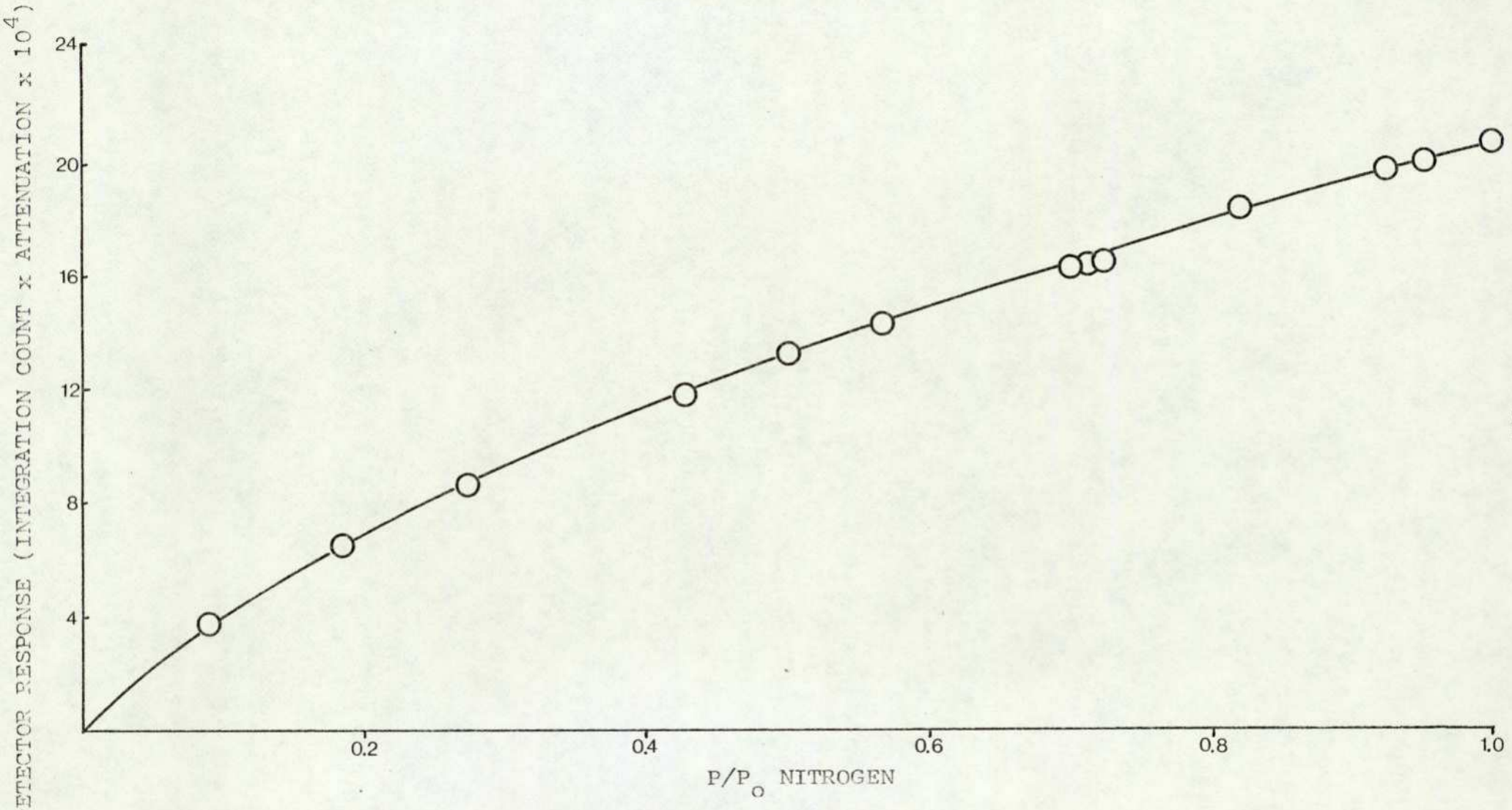

FIGURE 2.11. KATHAROMETER CALIBRATION FOR INJECTION OF $1cm^3$ (STP) OF NITROGEN

flow controllers were set slightly out of balance, i.e. the sum of the gas flows from controllers C and D did not exactly match the sum of the gas flows from controllers F and G, then the gas pressure at point P would change from its correct value. This in turn would subsequently cause one or other or both of the two sets of mass flow controllers to operate at incorrect flow rates. The behaviour of the gas pressure at various points in the system acted as a check on the correct functioning of the apparatus. Furthermore, if unusual difficulty was experienced in balancing the gas flows in the system, then this indicated the probability of a gas leak in the system, which could be located and eliminated if necessary.

In order to carry out a nitrogen adsorption determination with a different gas mixture, i.e. at a different relative pressure of nitrogen, the system required purging for about 15 minutes. The stabilization of the recorder baseline indicated the moment when all the old gas mixture was flushed from the system. Each nitrogen adsorption determination was normally carried out four to six times in order to check repeatability.

The detector was calibrated by the injection of known volumes of nitrogen, using a Perkin Elmer six-way gas sampling valve, which replaced the normal sample holder for the calibration procedure. Calibrations were performed throughout the entire range of relative pressures of nitrogen (i.e. of partial pressure of nitrogen in helium). A plot of detector response against the relative pressure of nitrogen (P/Po) in the carrier gas is shown in figure 2.11. Various Perkin Elmer sample loops of known volume were used for the

Table 2.4. A COMPARISON OF THE SURFACE AREAS OF SOME POROUS SUBSTANCES

Sample	Surface Area ($m^2\ g^{-1}$)			
	(1)	(2)	(3)	(4)
Alumina (I) *	103.2	100	-	-
Alumina (II)	256	-	-	244
Alumina (III)	204	-	-	184
Silica (I) *	4.3	4.1	-	-
Silica (II)	3.7	3.9	-	-
Kaolinite	17.0	-	24.5	-
Poisoned alumina-supported Copper (II) oxide	111.0	-	-	109

*Different alumina and silica samples

(1) Continuous-flow nitrogen adsorption apparatus

(2) Independent determination, similar apparatus

(3) Independent determination, vacuum microbalance

(4) Independent determination, Carlo Erba Sorptomatic Series 1800

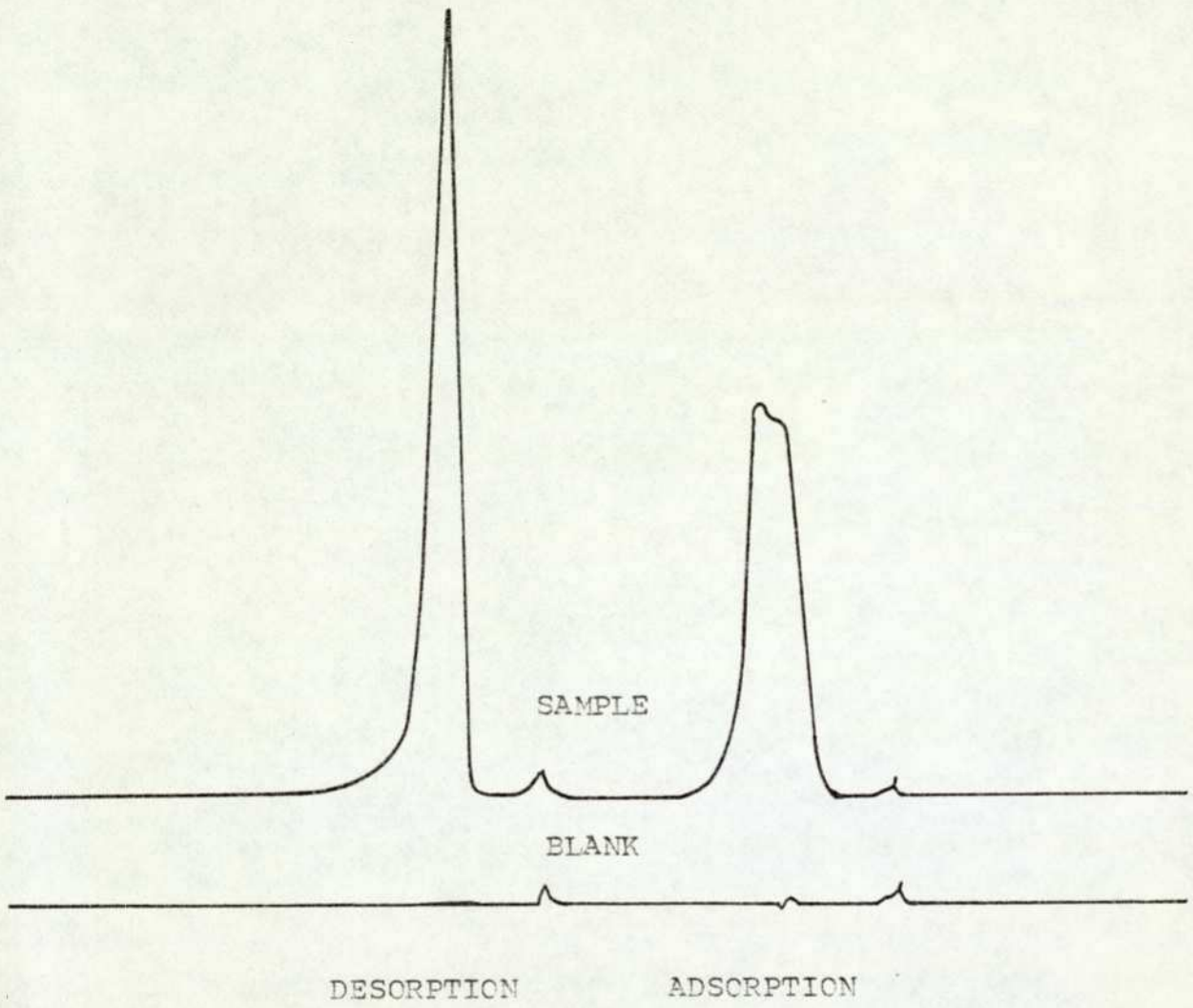

FIGURE 2.12. TYPICAL ADSORPTION-DESORPTION PEAKS

calibration. The volumes of these standard loops were checked as described in section 2.2.1.4.

In order to check that the continuous-flow apparatus was functioning satisfactorily, the surface areas of a number of porous substances, whose areas had already been independently measured, were determined. The results of these determinations and the values of the independently measured surface areas are shown in Table 2.4.

Samples ranging in size from 0.1g to 5g were placed in the sample holder (several sample holders were used, chosen according to the bulk of the sample). Sample beds were located with glass wool plugs. The samples were normally degassed for $1\frac{1}{2}$ hours at 150°C, whilst being purged with helium. Adsorption measurements were made by immersing the sample holder to a predetermined level in liquid nitrogen, chosen to cover the sample adequately without excessive cooling of the sample holder. The sample was maintained in liquid nitrogen until the adsorption peak appeared on the recorder trace. Desorption was simply accomplished, by removing the liquid nitrogen from the sample holder and reversing the katharometer control unit polarity switch (the desorption peak occurs in the opposite direction to that of the adsorption peak). The desorption measurement was used for surface area calculations in preference to adsorption. The main reason for using desorption rather than adsorption, is that desorption and calibration are similar processes, both involving injection of nitrogen into the gas stream, whereas adsorption involves depletion of the nitrogen concentration. Furthermore the shapes of desorption and calibration peaks were similar, both being sharp and narrow and contrasting with the relatively broad flat adsorption peak. The shapes of some typical adsorption, desorption peaks are shown in

figure 2.12.

The value of the saturation pressure of nitrogen (Po) has a profound influence on the BET calculation, according to Ettre (56), and for this reason the value of Po was accurately determined using the following procedure. In order to find the value of Po, the temperature of the liquid nitrogen was first determined (the relationship between temperature and Po is given by Ettre (56)). The temperature of liquid nitrogen, i.e. its boiling point, was again not measured directly but was calculated by first determining its specific gravity and then consulting a series of calibration charts as described in the following paragraph.

The specific gravity of liquid nitrogen was determined using a set of specially calibrated hydrometers supplied by Philips who also manufactured the equipment for liquid nitrogen production. The percentage purity of the liquid nitrogen was then obtained by referring to a series of calibration tables supplied with the hydrometers. The particular table used was selected according to the barometric pressure measured using a standard mercury barometer. The only significant impurity present in liquid nitrogen is oxygen dissolved from the air. The temperature of the liquid nitrogen was finally obtained, by consulting a table relating the elevation of the boiling point with the percentage dissolved oxygen (150). In practice the liquid nitrogen used was invariably sufficiently pure (99.9%) so that its temperature and hence saturation pressure Po were not significantly affected. However, due to the very small quantity of dissolved oxygen normally present in liquid nitrogen, the maximum relative pressure of nitrogen is often very slightly less than unity. For this reason the relative pressure of unity is shown

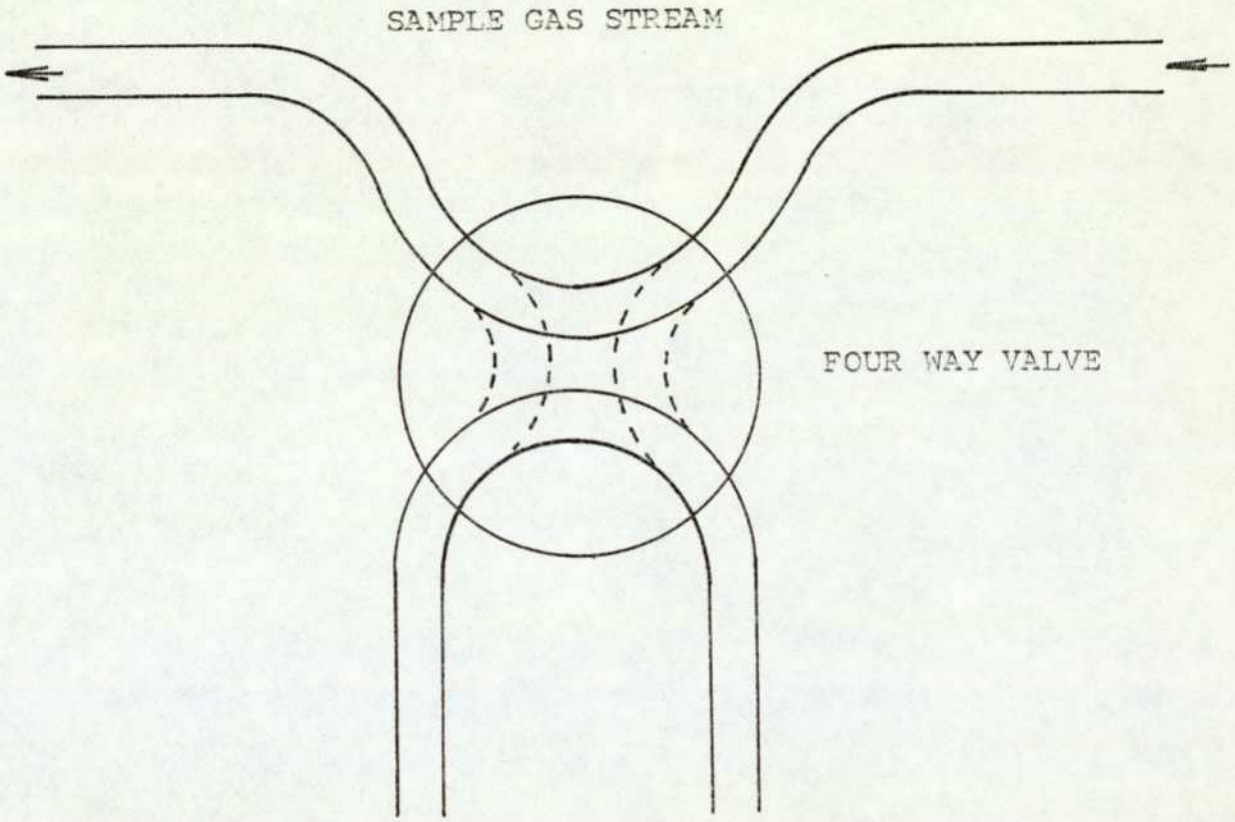

FIGURE 2.13. MODIFIED SAMPLE HOLDER IN BYPASS POSITION

as less than or equal to unity i.e. $P/Po \leq 1$.

The volumes of nitrogen adsorbed at three partial pressures of nitrogen (within the range P/Po = 0.05 - 0.30) were used to calculate surface areas of samples by the BET method. The results of surface area determinations, obtained from the continuous-flow apparatus and independent measurements (Table 2.4.), show excellent agreement with those obtained from a similar apparatus and generally good agreement with results from static adsorption systems.

The method for obtaining the final point of an isotherm, i.e. $P/Po \leq 1$ was somewhat different from the usual procedure and also rather more complex. This procedure involved the isolation of the sample holder from the sample gas line, using a Perkin Elmer four-way valve. A schematic diagram of the valve is shown in figure 2.13. In order to obtain this final measurement, the nitrogen gas flow was set at 25cm $^{3}min^{-1}$ and the helium gas flow was set at zero. The four-way valve was switched to the normal position, i.e. allowing the sample gas stream through the sample holder. Nitrogen was then adsorbed onto the sample, allowing sufficient time for equilibration to take place. The four way valve was then switched over to the by-pass position and the nitrogen gas stream was replaced by a helium gas stream set at 25cm $^{3}min.^{-1}$ The helium stream was allowed to flush out the nitrogen completely and nitrogen was then desorbed from the sample. In order to allow desorption to take place, the four-way valve was switched back to the normal position, whilst the liquid nitrogen was simultaneously removed from the sample. This determination differed from the normal procedure in that nitrogen was adsorbed from a continuously flowing stream of pure nitrogen and desorbed into pure helium. The volume of the desorbed nitrogen obtained in this way was the sum of two values; the nitrogen taken up by the sample and the

nitrogen gas which filled the tube above the sample. In order to measure the latter volume, a blank determination was necessary. The blank determination was a reversal of the adsorption procedure in that "adsorption" of pure helium and "desorption" into pure nitrogen was necessary. The practical details of the blank run were similar to those already described for the nitrogen adsorption measurement. In addition to the blank determination, a calibration of the katharometer detector response was carried out for helium injected into nitrogen, using the previously mentioned six-way gas sample valve and several sample loops of known volume. Since at the temperature of liquid nitrogen, helium does not condense into pores, the volume of "desorbed" helium will be identical to the free space in the holder unoccupied by the sample. The volume of nitrogen desorbed at $P/Po \ll 1$ could therefore be calculated by subtracting the correction obtained in the blank run from the volume of desorbed nitrogen obtained in the first step.

2.3. EXPERIMENTAL MEASUREMENTS ON CATALYSTS

2.3.1. SURFACE PROPERTIES

The importance of surface properties in a study of catalysis with particular reference to the present system has already been outlined and a description has been given of the construction and use of a continuous-flow BET apparatus. However, this apparatus, although it has the advantages of speed of use in determining surface areas and can also be used to measure extremely low surface areas, can not be operated quickly to determine complete adsorption isotherms, nor can it ever be used to obtain a complete adsorption-desorption isotherm. With respect to the former disadvantage, the problem lies mainly in the time consumed in adjusting the many

different gas flow rates necessary and also in the complex procedure for determining the last point on the isotherm (see section 2.2.3.3.). However, the latter disadvantage is an inherent characteristic of the flow system, as both adsorption and desorption at a particular relative pressure (P/Po) have to be carried out together. Hence the typical hysteresis cycle of the adsorption-desorption isotherm (for porous solids) cannot be obtained. A static system does not however suffer this disadvantage, as all adsorption measurements, throughout the entire range of relative pressures, are carried out by successive introductions of nitrogen gas until $P/Po \ll 1$; successive aliquots of nitrogen are then removed for the desorption cycle. For this reason a static BET method will yield results which are more suited to the calculation of pore size distributions than those from a continuous-flow apparatus.

It was with some good fortune that during the latter half of this project, the full-time use of a static BET apparatus was made available. This apparatus was a Carlo Erba Series 1800 Sorptomatic. With this instrument the complete adsorption-desorption isotherm could be obtained automatically. In order to obtain such an isotherm, the sample was weighed into a glass sample holder and degassed under high vacuum, in situ, in the instrument for a period of 24 hours. The apparatus was then switched onto automatic operation which normally took another 24 hours. Finally the sample was removed from the apparatus and the weight of the catalyst was again determined.

A Carlo Erba Sorptomatic apparatus operates on the principle of introducing extremely accurately measured volumes of nitrogen into the sample holder, the resultant pressure changes being automatically measured and recorded. The time lapse between successive volume introductions could be varied between the limits of 2 seconds and 2 hours,

the precise period chosen depending on the time required for pressure equilibration to take place. The temperature of the sample was kept at 77.36 K by immersion in liquid nitrogen, maintained at a constant level. The detailed procedures of operation and calibration of the Carlo Erba Sorptomatic are described in the manufacturer's handbook.

From the record of the pressure changes, the weight of catalyst and the barometric pressure and also certain instrument constants, determined by calibration, the entire adsorption-desorption isotherm surface area, mean pore radius and pore-size distribution could be calculated. To facilitate rapid and convenient calculation of this data, some time was allocated to attending a computer programming course and the subsequent writing of a computer programme to deal with the information. A second computer programme was also written, to facilitate the rapid calculation of pore-size distributions from data obtained from the Dynamic BET apparatus. Both computer programmes are included in the Appendix Section.

2.3.2. ELECTRICAL CONDUCTIVITY

The specific conductance of catalysts was measured, using a simple conductivity cell, consisting of a glass tube, with an internal diameter of 1.6 mm, into which the sample was compressed with steel pistons machined to fit the glass tube with a sliding clearance. The pressure was applied to the cell by rotating a screw thread set in a G- clamp. The pressure developed was detected with a strain gauge, accurately calibrated, and the signal was displayed on a Philips PR 9307 Carrier Frequency Bridge. The electrical

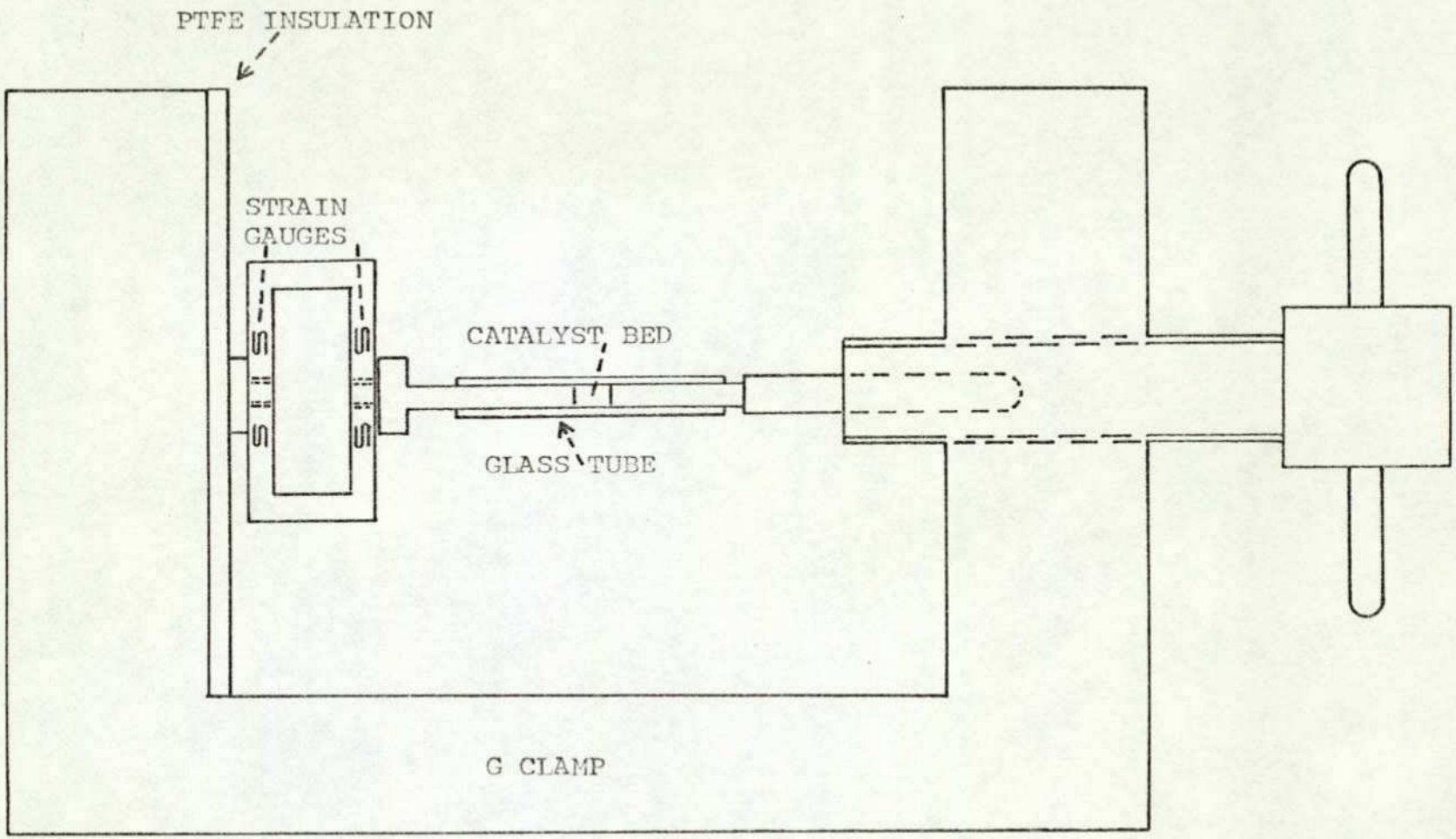

FIGURE 2.14. ELECTRICAL CONDUCTIVITY CELL

conductivity of the sample was measured using a Cambridge Instrument conductivity bridge, operating at a frequency of 1 kHz. A diagram of this instrument is shown in figure 2.14. Samples were normally dried by storing in a desiccator (desiccant phosphorus pentoxide) for one week prior to readings being taken. The internal diameter of the glass tube was measured using vernier calipers and a magnifying glass. Several readings were taken in order to obtain a mean value. However, in practice it was found that readings were too close to discern differences. The thickness of the catalyst sample was measured with a micrometer, provided that the compressed pellet could be removed without breaking. However, if this was not possible, vernier calipers and a magnifying glass were used. It was not found practicable to measure the thickness of the catalyst sample while in situ, say with a travelling microscope, as some of the catalyst was invariably squeezed between the steel pistons and the glass tube, resulting in a "blurring" of the boundary between catalyst and piston. The measurement of the physical size of the catalyst bed probably represented the greatest source of error of the electrical conductivity measurements. The estimated magnitude of the error from this source could be as much as $\pm$ 5% in relation to the thickness of the catalyst pellet, plus a systematic error of $\pm$ 5% in relation to the internal diameter of the glass tube.

In order to take a reading of electrical conductivity the catalyst was poured into the glass tube with the lower piston in position in the tube. The upper piston was then placed in the glass tube and the apparatus was assembled. Set pressure was applied to the cell by rotating the screw in the G-clamp. When the pressure reached the desired (but arbitrarily chosen) value of 50 p.s.i.g., the catalyst was left for a few minutes and the pressure was reset if

necessary. It was almost invariably found that the catalyst compacted slightly under the pressure, and it normally took about 10 minutes before a constant pressure of 50 p.s.i.g. was obtained. All the readings for a particular series of catalysts were completed on the same occasion, the time taken to make all the measurements not normally exceeding 3 - 4 hours. The combined temperature and relative humidity were noted at the beginning and end of each series of readings. However, no significant changes of either of these parameters were ever recorded during a series of readings.

2.3.3. THERMOGRAVIMETRY

A Mettler Thermoanalyzer II thermobalance was used to obtain both thermogravimetric analysis (TGA) and Differential Thermal Analysis (DTA), for catalysts, poisoned catalysts and mixtures of catalysts and lead halides. The maximum sensitivity of the instrument for TGA was 0.02 mg, the full scale deflection being 1 mg.

The maximum sensitivity of the instrument for DTA was 0.5 μV, with a full-scale deflection of 20 μV. Variation of the sample size between 20 and 200 mg was found not to affect the recorded weight changes for TGA. The sample size used for DTA was normally 40 mg (depending on density) and α-alumina (specpure grade, Johnson Matthey) was used as a standard. Details of the construction and operation of this instrument are supplied in the manufacturer's handbook.

2.3.4. X - RAY DIFFRACTION

Both pure and poisoned catalyst samples were analysed using X - ray diffraction. The instrument used was a Philips PW 1010 diffraction apparatus. Copper K_α radiation (wave length 0.1542 nm) was produced from a copper tube operated at a voltage of 40 kV and

a current of 14 mA. A nickel filter was used in all cases. Each sample was reduced in size in an agate mortar and placed in an 0.2 mm Lindemana glass tube before mounting in a Philips powder camera (diameter 11.46 cm). The camera employed the Straumanis type of film mounting and the sample was rotated.

2.3.5. SPECTROSCOPIC MEASUREMENTS

Various pure and poisoned catalysts were investigated by the following spectroscopic techniques:
infra-red, ultra-violet and visible absorption spectroscopy.
The infra-red absorption properties of catalysts were investigated using a Perkin-Elmer 457 grating infra-red spectrophotometer. Samples were reduced in size and mixed with potassium bromide in an agate mortar. The resulting mixture was pressed into a disc for examination. Ultra-violet, visible and near infra-red spectra were recorded, using the reflectance technique, on a Hitachi Perkin-Elmer EPS - 37 recording spectrophotometer, range 170 mμ - 2600 mμ.

2.3.6. ELECTRON MICROSCOPY

Samples were examined at magnifications of up to 50,000 x using a JEM 100 B Analytical Electron Microscope. Analyses were performed in situ with an Energy Dispersive Analysis of X - rays unit (EDAX). Samples were mounted for investigation on 2 mm diameter carbon grids. They were first prepared by dispersal in methyl alcohol using an ultrasonic vibrator, the dispersed sample then being transferred to the carbon grid by pipette and the solvent being allowed to evaporate.

2.3.7. AUGER ELECTRON SPECTROSCOPY

Samples were examined using a Vacuum Generator standard 3-grid retarding field analyser, which was an extension to a LEED (low energy electron diffraction) system. The details of operation and

specification of this instrument are very complex and the details are described by Duckworth (151).

SECTION 3

RESULTS

SECTION 3

3.1. GENERAL SURVEY

The behaviour of five different catalysts, both supported and unsupported, was investigated in order to evaluate the effects of lead halide poisons on catalytic activity with respect to carbon monoxide oxidation.

The variation of catalytic activity with the weight of lead halide deposited, was determined for all catalysts studied. In addition, in several individual cases, studies were made of the effect on catalytic activity of the removal of lead halide from an already poisoned catalyst.

Surface areas were calculated, using nitrogen adsorption data, for most of the unsupported catalysts and for all the supported catalysts. Nitrogen adsorption data were also used to elucidate the effect of lead halides on the pore structure of supported catalysts. Further evidence as to the effect of lead halides on the structure of supported and unsupported catalysts was obtained in a few cases, using electron microscopy. In situ elemental analysis of catalyst samples, examined by electron microscopy, yielded additional information regarding the structure and composition of such catalysts.

Differential thermal analysis and X-ray diffraction data were obtained for most catalysts, in order to investigate the possibility of bulk-scale chemical reaction between catalyst and lead halide. Unsupported catalysts, poisoned with lead halide, were also subjected to thermogravimetric analysis. Infra-red, ultra-violet and visible spectroscopy were used to investigate the structure of both unpoisoned and poisoned nickel (II) oxide catalysts. Electrical conductivity measurements were carried out on several

unsupported catalysts which had been poisoned with varying amounts of lead halide.

Auger spectroscopy and Electron Spectroscopy for Chemical Analysis (ESCA), were both considered as possible methods of studying the surfaces of catalysts used in this work. In the case of Auger spectroscopy the technique was found to be, at least, potentially useful, as some preliminary spectra of lead (II) bromide treated nickel (II) oxide indicated the possibility of lead being present on the surface of this sample. However, the spectra were difficult to interpret and a number of practical difficulties associated with this method, did not allow, in an unfortunately limited time, the production of any further spectra. On the other hand ESCA was found to be suitable only for examining conducting catalysts such as unsupported metals. The non-conducting catalysts investigated in this work are known to build up large static charges under the influence of the electron beam. Such a charge build up would shift the electron energy distribution considerably, masking any shift in the energy spectrum of emitted electrons and thus making elucidation of the results impossible.

3.2. NICKEL (II) OXIDE CATALYSTS

Figures 3.1. and 3.2. show the variation of catalytic activity with the lead (II) bromide content of two nickel (II) oxide catalysts, which had been prepared by decomposition of nickel (II) hydroxide and nickel (II) nitrate respectively. The sample size of the catalysts used for oxidation of carbon monoxide was 0.14 g of nickel (II) oxide, excluding the mass of the associated lead (II) bromide. The total mass of catalyst and poison was calculated from the percentage composition of the solid phase, as determined by

analysis.

The effect on the catalytic activity of nickel (II) oxide, of a blank poisoning operation, i.e. one in which no lead (II) bromide was deposited, was investigated by passing nitrogen over a nickel (II) oxide sample maintained at 550°C for 30 minutes. These conditions represented the maximum period of time and the maximum temperature employed during the poisoning process. The catalytic activity of nickel (II) oxide was found to be unchanged after this procedure. Figure 3.3. shows the effect on catalytic activity of attempting to remove lead (II) bromide, by passing nitrogen over poisoned nickel (II) oxide catalysts. Each stage of lead (II) bromide removal was accomplished by passing gas over the catalyst for one hour at 550°C.

The specific surface areas of nickel (II) oxide catalysts poisoned with lead (II) bromide were determined by means of a continuous-flow BET apparatus. Some of the results obtained are shown in figures 3.4. and 3.5. Surface areas were calculated neglecting the mass of lead (II) bromide incorporated. The continuous-flow BET apparatus was also used to obtain differential pore-size distributions (figures 3.6. and 3.7.) for unpoisoned and poisoned nickel (II) oxide.

The results of thermogravimetric analysis (TGA) of pure nickel (II) oxide, pure lead (II) bromide and nickel (II) oxide samples poisoned with lead (II) bromide are shown in figures 3.8.- 3.11. Nearly all these samples were examined in an atmosphere of nitrogen. The only exception was the first of the pure nickel (II) oxide samples (figure 3.8.a) which was analyzed in air. The entire series of nickel (II) oxide samples examined by TGA, both unpoisoned and poisoned, were prepared from a single batch of nickel (II) oxide, which had

been produced from the nitrate.

Differential Thermal Analysis (DTA) of a physical mixture of nickel (II) oxide and lead (II) bromide (containing 50% by weight of each constituent) was completed using an equal volume of α - alumina as the reference material. DTA of the following samples was also completed for reference purposes:- nickel (II) oxide; lead (II) bromide; α - alumina and calcium oxalate. Figures 3.12. and 3.13. show the results of the DTA of a nickel (II) oxide - lead (II) bromide mixture and of pure lead (II) bromide respectively. Figures 3.14. and 3.15. show the same results, but these were obtained on a Stanton Redcroft instrument of similar sensitivity to that of the Mettler instrument normally used, but capable of accommodating a larger sample.

The ultra-violet, visible and near infra-red spectra of lead (II) bromide poisoned nickel (II) oxide, pure lead (II) bromide and pure nickel (II) oxide are shown in figures 3.16., 3.17. and 3.18., and the infra-red spectra of lead (II) bromide-poisoned nickel (II) oxide and of pure nickel (II) oxide are shown in figures 3.19. and 3.20.

Figure 3.21. shows the relationship between the electrical conductivity of various lead (II) bromide-poisoned nickel (II) oxide catalysts, and the quantity of lead (II) bromide present.

Plate 3.1. shows an electron micrograph (40,000 x magnification) of pure nickel (II) oxide prepared from the hydroxide. Plates 3.2. and 3.3. are electron micrographs (10,000 x and 40,000 x magnification respectively) of the same batch of nickel (II) oxide, treated with 31 weight % of lead (II) bromide.

X-ray powder photographs were obtained of nickel (II) oxide, lead (II) bromide and a mixture of both nickel (II) oxide and lead (II) bromide (containing 50% by weight of each constituent) which had been heated to 550°C for 30 minutes. The X-ray photograph of the heated mixture of nickel (II) oxide and lead (II) bromide showed the same lines, with the same relative intensities, as for the pure constituents; no new lines were observed.

3.3. COPPER (II) OXIDE CATALYSTS

Copper (II) oxide catalysts were prepared in both unsupported and supported forms. However, few results were obtained for the unsupported catalyst, despite its high catalytic activity with respect to carbon monoxide oxidation. Using data from the continuous flow BET apparatus, the specific surface area of the unsupported catalyst was found to be very low (0.145 m^2g^{-1}) and it was not possible to prepare samples with a higher surface area which would be thermally stable at temperatures up to 550°C. Attempts to poison the unsupported copper (II) oxide catalyst resulted in total loss of activity even when the smallest quantity of lead (II) bromide (0.32 weight %) was applied.

Figure 3.22. shows the variation of catalytic activity with the lead (II) bromide content of copper (II) oxide supported on alumina. The supported catalyst contained 21 weight % of copper (II) oxide. The mass of the catalyst samples used for activity measurements was 0.17 g, ignoring the mass of lead (II) bromide present.

The effects on the catalytic activity of the supported copper(II) oxide, of a blank poisoning operation similar to that described in Section 3.2., for nickel (II) oxide, was investigated. Nitrogen

was passed over the catalyst for 2 hours at 550°C and the catalytic activity was found to be unchanged after this treatment.

Figures 3.23. and 3.24. show the variation with lead II bromide content of catalyst surface area, determined using the continuous-flow BET apparatus and the Carlo Erba Sorptomatic apparatus respectively. The differential pore size distributions of poisoned and unpoisoned supported copper (II) oxide catalysts, as determined from nitrogen adsorption data, are shown in figures 3.25. - 3.27.

Table 3.1. shows DTA data for the samples from the Mettler Thermoanalyzer (II) thermobalance, which had a sensitivity of 50 μv (f.s.d). The maximum temperature attained was 600°C and the atmosphere contained only nitrogen. Only one endothermic peak was observed with those samples containing lead (II) bromide and this was due to melting of the lead compound. No other peaks were observed for any of the samples.

X-ray powder diffraction studies were made of copper (II) oxide, lead (II) bromide and a mixture of copper (II) oxide and lead (II) bromide (containing initially 50% by weight of each compound) which had been heated to 610°C during a DTA run. The X-ray photograph of heated mixtures contained a sufficient number of strong lines clearly to identify copper (II) oxide, but the intensity of the remaining lines was too weak to identify them positively. The weak lines which could be distinguished were however not inconsistent with those of lead (II) bromide. No new lines, attributable to a compound other than copper (II) oxide or lead (II) bromide, could be observed.

X-ray powder photographs of alumina and alumina-supported copper (II) oxide were also obtained. In the case of alumina a few diffuse and very broad lines were observed, which were consistent with

a material of very high surface area. The X-ray powder photograph of copper (II) oxide supported on alumina yielded only two lines of sufficient clarity and intensity to be measured. These corresponded exactly with the two strongest lines of pure copper (II) oxide. Examination of a lead (II) bromide-poisoned, supported copper (II) oxide catalyst containing 89 weight % of lead (II) bromide revealed the presence of lead (II) bromide only.

3.4. ALUMINA-SUPPORTED PLATINUM CATALYSTS

Figure 3.28. shows the variation of catalytic activity, at several temperatures, with the lead (II) bromide content of an alumina-supported platinum catalyst. The catalyst was made from the theoretical quantities of hydrogen hexachloroplatinate (IV) hydrate and alumina support which would yield a supported catalyst containing 10 weight % of platinum. This figure was not however checked by analysis. The mass of each catalyst sample used for an activity measurement was 0.15 g, not including the mass of lead (II) bromide present.

The effect on the catalytic activity of the supported platinum, of a blank poisoning operation, was investigated. Nitrogen was passed over the catalyst for 4 hours at 550°C and the catalytic activity at the lowest temperature used for this catalyst (220°C) was found to be unchanged by this procedure.

Measurements were made of the total and active surface areas of the supported platinum catalyst containing varying quantities of lead (II) bromide (figures 3.29. and 3.30.). Figures 3.31. - 3.34. show the pore-size distributions of the supported platinum catalyst poisoned with varying quantities of lead (II) bromide.

3.5. COBALT (II,III,III) OXIDE CATALYSTS

Unsupported cobalt (II,III,III) oxide and alumina-supported

cobalt oxide catalysts were prepared. Both catalysts were poisoned with lead (II) bromide and lead (II) chloride.

The variation of the catalytic activity of cobalt (II,III,III) oxide, at various temperatures, with lead (II) bromide and lead (II) chloride contents, is shown in figures 3.34. and 3.35. respectively. Similarly, the variation of the catalytic activity of the supported catalysts, at different temperatures, with lead (II) bromide and lead (II) chloride contents, is shown in figures 3.36. and 3.37. respectively. The mass of supported or unsupported catalyst, used for activity determinations, was 0.15 g in all cases, although this amount did not include the mass of lead halide poison.

Investigations were made of the effect on the catalytic activity of the unsupported cobalt (II,III,III) oxide catalyst, of a blank poisoning experiment. Nitrogen was passed over the catalyst at 580°C for 1 hour. A similar blank poisoning operation was carried out for the supported catalyst, nitrogen being passed over the catalyst at 590°C for 1 hour. These sets of conditions represented the maximum times and temperatures used in the lead halide poisoning procedures. The catalytic activities of both catalysts were found to be unchanged after the blank poisoning runs.

An attempt was made to remove lead (II) bromide from poisoned cobalt (II,II,III) oxide catalysts by means of flowing nitrogen. The effect on catalytic activity is shown in Figures 3.38. and 3.39. Each stage of the lead (II) bromide removal was accomplished by passing nitrogen over the catalyst for 1 hour at 550°C. Similarly Figures 3.40. and 3.41 show the effect of attempts to remove lead (II) bromide (using a procedure identical to that mentioned previously) on both the catalytic activity and the surface area of a poisoned

alumina-supported cobalt (II, III, III) oxide catalyst. The influence of this procedure on the pore size distribution of the poisoned catalyst is shown in figure 3.47.

The specific surface areas, determined using the continuous-flow BET apparatus, of lead (II) bromide-poisoned and unpoisoned cobalt (II,III,III) oxide samples are shown in figure 3.42. Figures 3.43. and 3.44. show the variation, with lead (II) bromide and lead (II) chloride contents, of the surface area (determined using the Carlo Erba Sorptomatic apparatus) of supported cobalt (II, III,III) oxide. Pore-size distribution results for the supported cobalt (II, III,III) oxide catalyst poisoned both with lead (II) bromide and with lead (II) chloride, which were also obtained using the Carlo Erba Sorptomatic apparatus, are shown in figures 3.45. - 3.49.

The results of thermogravimetric analysis, in a nitrogen atmosphere, of unpoisoned and lead (II) bromide-poisoned cobalt (II, III,III) oxide are shown in figures 3.50.-3.51.

Figures 3.52. - 3.57. show the results of DTA, in an atmosphere of nitrogen, on the following samples:- cobalt (II,III,III) oxide; lead (II) chloride; alumina-supported cobalt (II,III,III) oxide; a mixture of cobalt (II,III,III) oxide and lead (II) bromide; a mixture of alumina-supported cobalt (II,III,III) oxide and lead (II) bromide; a mixture of alumina-supported cobalt (II,III,III) oxide and lead (II) chloride.

The amount of lead (II) bromide lost from several poisoned catalyst samples during TGA, was calculated, both from the weight loss and by direct analysis. Some results are shown in Table 3.3.

X-ray powder photographs were obtained of cobalt (II,III,III) oxide and a mixture of cobalt (II,III,III) oxide and lead (II) bromide (containing initially 50% by weight of each compound) which had been heated to 550°C for 30 minutes. The X-ray photograph of the heated mixture contained all the lines, clearly defined, typical of cobalt (II,III,III) oxide, but no other lines were present.

X-ray powder photographs were also obtained of lead (II) chloride, an alumina-supported cobalt (II,III,III) oxide catalyst and a mixture of these two substances (containing initially 50% by weight of each) which had been heated for one hour at 600°C. The X-ray photograph of the mixture indicated only those lines generated by lead (II) chloride and no other lines were observed. The X-ray photograph of the supported cobalt (II,III,III) oxide showed only those lines attributable to this oxide.

An X-ray diffraction photograph was also obtained of a mixture of the pure alumina support and lead (II) chloride (containing 50% by weight of each constituent) which had been heated to 600°C for one hour. The lines on this photograph showed the presence of lead (II) chloride, although a significant line-broadening effect was noticeable. No lines other than those attributable to lead (II) chloride, were present.

Plates 3.4. and 3.5. are electron micrographs of unsupported cobalt (II,III,III) oxide and lead (II) bromide-poisoned cobalt (II,III,III) oxide (both 20,000 x magnification). Plates 3.6. - 3.8. are electron micrographs of alumina, alumina-supported cobalt (II,III,III) oxide (50,000 x magnification) and alumina-supported cobalt (II,III,III) oxide (20,000 x magnification) Plates 3.9. - 3.13. are all electron micrographs of alumina-supported cobalt (II,III,III) oxide poisoned with lead (II) bromide. All of these were taken at a magnification of 50,000 x

except Plate 3.13. which was taken at a magnification of 20,000 x.

Plates 3.4. and 3.5. show the particulate nature of the poisoned and unpoisoned cobalt (II, III,III) oxide catalyst, the particles varying in diameter from approximately 400 to 2000 Å. Plate 3.6. shows the porous structure of the alumina support. The particles are approximately 2000 Å wide and a maximum of 500 Å deep. In Plates 3.7. and 3.8. some small particles (200 - 400 Å diameter) are visible as well as the larger alumina particles. The small particles were shown by in situ analysis (using the Energy Dispersive Analysis of X-rays - EDAX) to be cobalt (II, III, III) oxide. The larger particles were found to be alumina containing some cobalt (II,III,III oxide. Plates 3.9. - 3.13. show various aspects of the same lead (II) bromide-poisoned, alumina-supported cobalt (II,III,III) oxide catalyst. For example, the alumina phase is predominant in Plate 3.10., but Plate 3.13. shows mainly the cobalt (II,III,III) oxide phase, whilst Plate 3.12. shows an agglomerate of both phases and Plate 3.11.shows both phases existing side by side. The appearance of the poisoned catalyst is very similar to that of the unpoisoned catalyst and the existnce of a third phase, i.e. lead (II) bromide, is not evident. However, analysis using EDAX showed both lead and bromine to be present, as well as cobalt and aluminium. Furthermore, considerably more lead and bromine were found to be associated with the alumina phase than with cobalt (II,III,III) oxide. Indeed the lead (II) bromide associated with the cobalt (II,III,III) oxide was only just detectable with the instrument.

Using EDAX, an attempt was made, to determine the lead: bromine ratio in samples both of unsupported cobalt (II,III,III) oxide poisoned with lead (II) bromide, and of a poisoned supported catalyst. It was

felt that the results would confirm, or disprove, the validity of the assumption, that the lead present in a lead (II) bromide treated catalyst was present as lead (II) bromide. The lead (II) bromide content of the unsupported catalyst, calculated in the usual manner from the amount of lead indicated by atomic absorption analysis, was 11.7 % by weight and that of the supported catalyst was 8.9 weight %.

The use of EDAX to determine the lead: bromine ratio of a poisoned catalyst was accompanied by some difficulty which restricted the accuracy of the method. The principal reason for this difficulty resulted from the size of the particles under examination. These particles were in general less than 1 μ (micron) in diameter. Now the examination of very small particles (i.e. less than 1 μ in diameter) of cobalt (II,III,III) oxide contaminated with relatively small quantities of lead (II) bromide resulted in working at the limit of sensitivity of the instrument. However, despite this, the lead: bromine ratio of both the poisoned catalysts and a pure lead (II) bromide standard were compared. This comparison showed that the lead: bromine ratios in the lead (II) bromide treated catalysts were consistent with the presence of lead (II) bromide.

3.6. MANGANESE (IV) OXIDE

The variation of the catalytic activity of manganese (IV) oxide, at various temperatures, with lead (II) bromide content is shown in figure 3.58. The mass of each catalyst sample used for activity measurements was 0.08 g, not including the mass of lead (II) bromide present. Studies were made of the effect on the catalytic activity of the manganese (IV) oxide catalyst, of a blank poisoning operation,

similar to that mentioned for nickel (II) oxide in Section 3.2. This operation consisted in passing nitrogen over manganese (IV) oxide, for 30 minutes at 550°C. The activity of the catalyst was found to be unchanged by this procedure.

The specific surface areas of manganese (IV) oxide catalysts, both unpoisoned and poisoned, are shown in figure 3.59. These were determined using the continuous-flow BET apparatus.

Figures 3.60. and 3.61. show the results of DTA on manganese (IV) oxide and on a mixture of manganese (IV) oxide and lead (II) bromide respectively. Both DTA runs were carried out in an atmosphere of nitrogen.

Figure 3.62. shows the variation of the electrical conductivity of manganese (IV) oxide poisoned with varying quantities of lead (II) bromide. The specific conductivity of pure lead (II) bromide was also determined and found to be 8.75×10^{-8} $ohm^{-1}cm^{-1}$.

Table 3.1. DETAILS OF CATALYST SAMPLES ANALYSED BY DIFFERENTIAL THERMAL ANALYSIS

Sample	Sample Weight mg	Heating Rate $^{o}C\ min^{-1}$
Blank run with α-alumina	38.0	5
Physical mixture of alumina support (50 Wt%) and lead(II)bromide (50 Wt%)	52.1	2
Physical mixture of copper(II)oxide (50 Wt%) and lead(II)bromide (50 Wt%)	104.3	5
Physical mixture of alumina supported copper(II)oxide (50 Wt%) and lead(II)bromide (50 Wt%)	48.5	5
Physical mixture of copper(II)oxide (33⅓ Wt%), lead(II)bromide (33⅓ Wt%) and alumina support (33⅓ Wt%)	49.7	5
Physical mixture of copper(II)oxide (50 Wt%) and alumina support (50 Wt%)	48.7	5

Table 3.2a. THE EFFECT OF THERMAL ANALYSIS ON $PbBr_2$ LEVELS IN DEACTIVATED NICKEL(II)OXIDE

Weight % $PbBr_2$		Surface Area m^2g^{-1}		Max Temperature
Before TGA	After TGA	Before TGA	After TGA	^oC
0.28	0.203	2.85	1.25	1000
0.46	0.41	-	-	1000
0.645	0.31	-	-	1000
1.17	0.52	-	-	1000

Table 3.2b. LEAD(II)BROMIDE LEVELS IN DEACTIVATED NICKEL(II)OXIDE DURING TGA

Weight % $PbBr_2$		% Loss of $PbBr_2$	Number of Figure
Initial	At 600^oC		Showing TGA Result
0.28	0.22	21	3.9b.
0.46	0.39	16	3.9c.
0.645	0.645	0	3.10a.
1.17	0.7	40	3.10b.
1.32	1.32	0	3.10c.
1.76	1.25	29	3.11a.

Table 3.3. THE EFFECT OF THERMOGRAVIMETRIC ANALYSIS (TGA) ON THE LEAD(II)BROMIDE CONTENT OF CATALYSTS

Catalyst	Max. Temperature During TGA °C	Initial $PbBr_2$ Content Weight %	$PbBr_2$ Volatilized (Weight %)	
			Calculated from Chemical Analysis	Calculated from TGA Results
Cobalt(II,III,III)oxide	550	15.1	9.2	9.8
Nickel(II)oxide	550	1.76	0.53	0.61
Cobalt(II,III,III)oxide	800	11.3	9.2	10.1

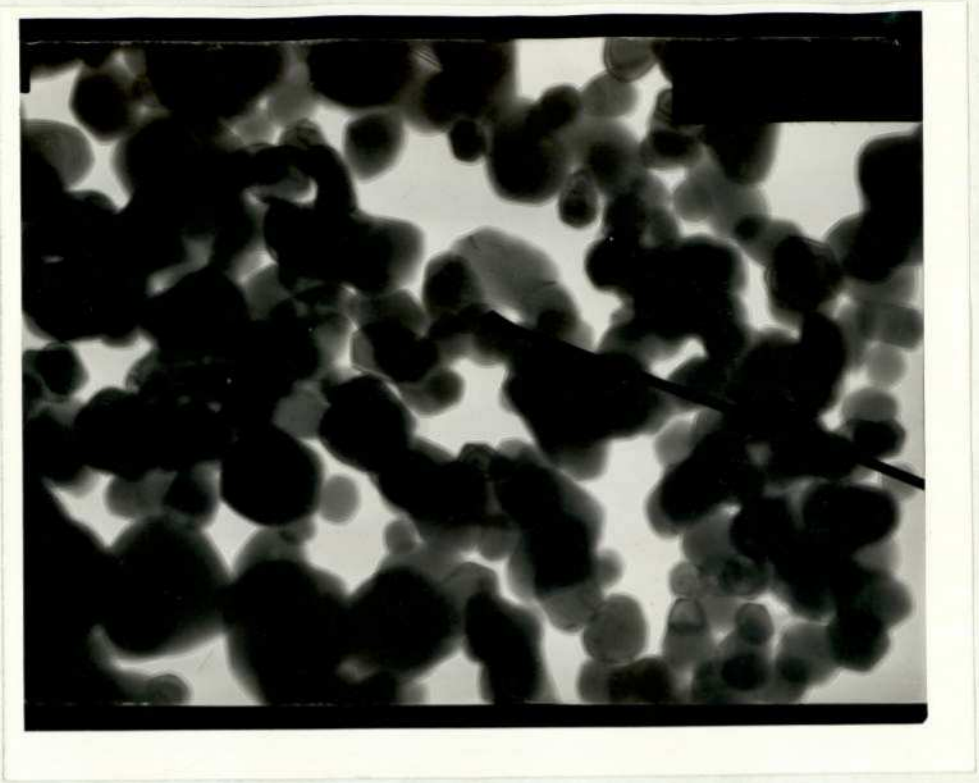

PLATE 3.1. NICKEL(II)OXIDE (40,000 x)

PLATE 3.2.

NICKEL(II)OXIDE WITH 31 WEIGHT % LEAD(II)BROMIDE

(10,000 x)

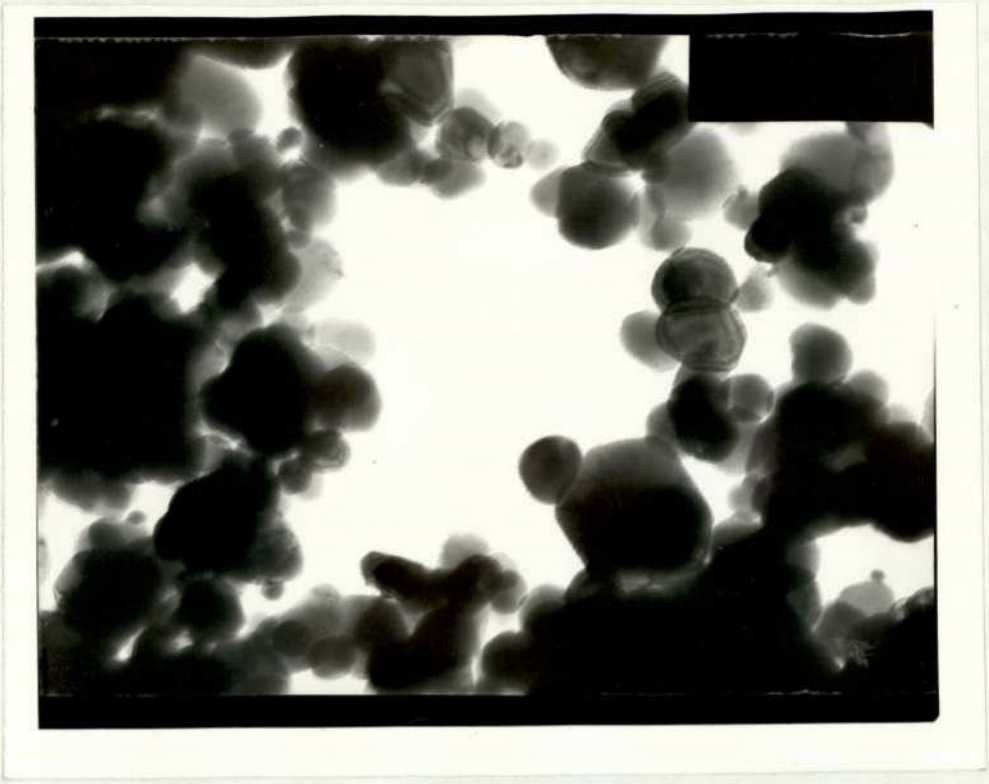

PLATE 3.3.

NICKEL(II)OXIDE WITH 31 WEIGHT % LEAD(II)BROMIDE

(40,000 x)

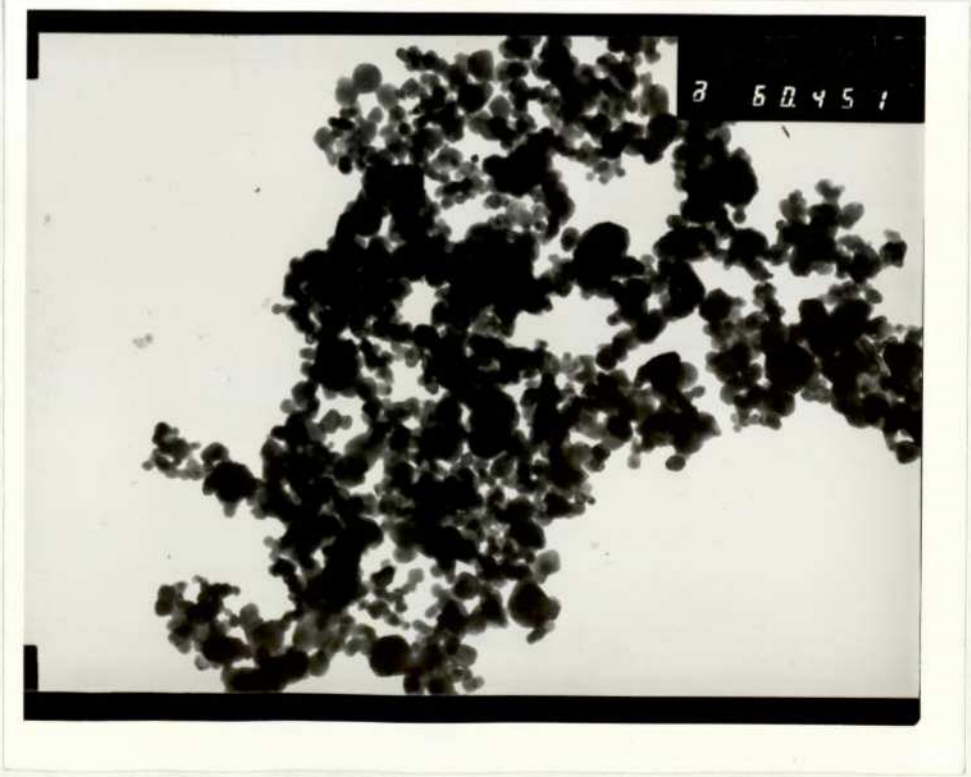

PLATE 3.4. COBALT(II,III,III)OXIDE (20,000 x)

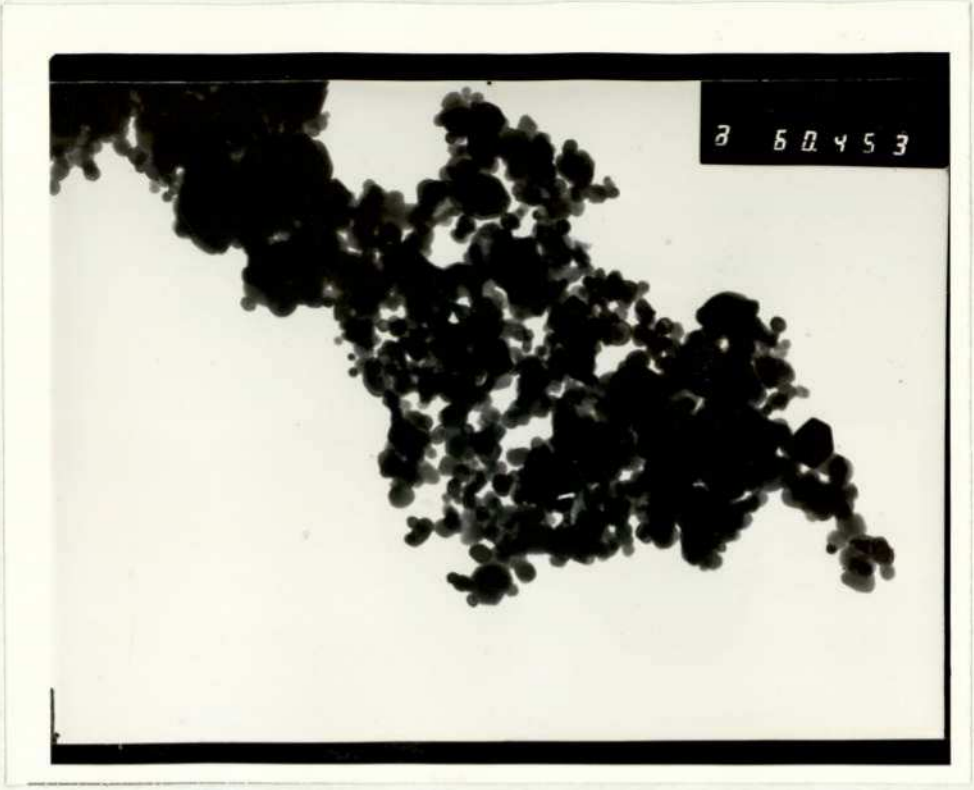

PLATE 3.5.

COBALT(II,III,III)OXIDE WITH 11.7 WEIGHT % LEAD(II)BROMIDE

(20,000 x)

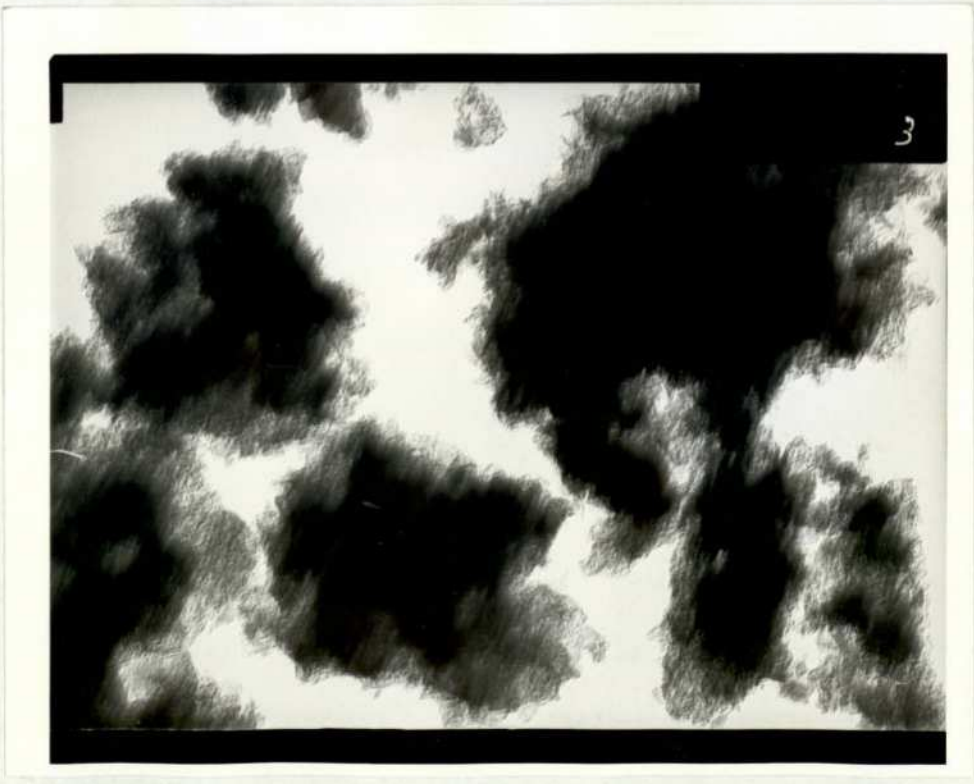

PLATE 3.6. ALUMINA SUPPORT (50,000 x)

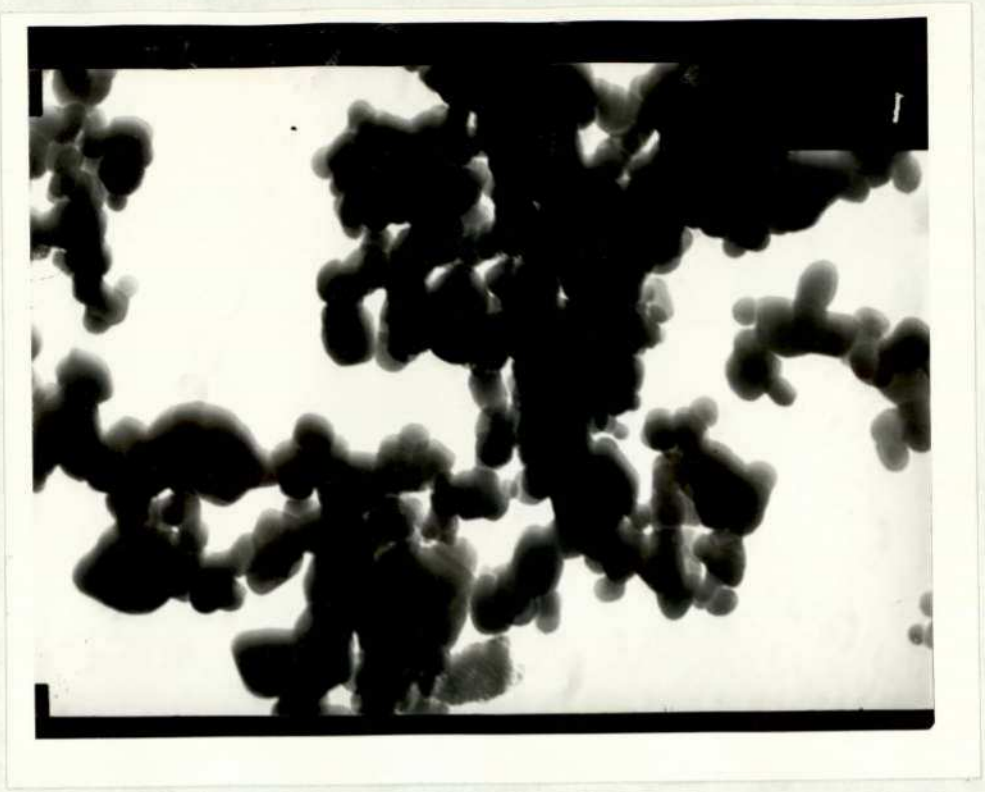

PLATE 3.7.

ALUMINA SUPPORTED COBALT(II,III,III)OXIDE (50,000 x)

PLATE 3.8.

ALUMINA SUPPORTED COBALT(II,III,III)OXIDE (20,000 x)

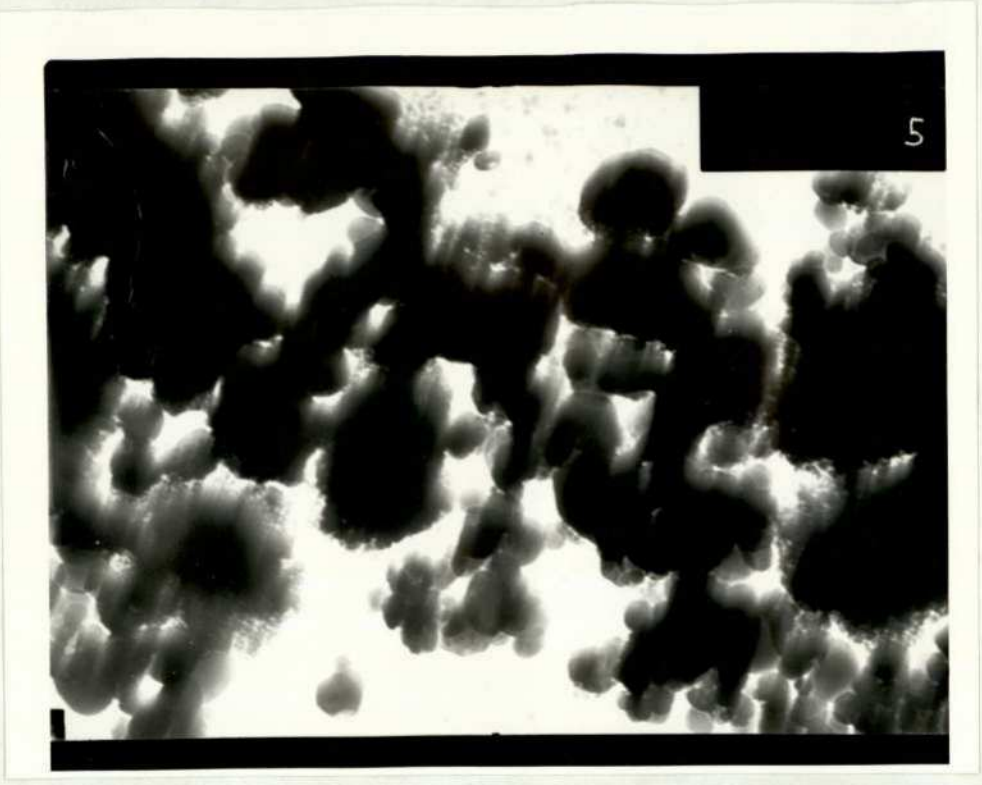

PLATE 3.9. ALUMINA SUPPORTED COBALT(II,III,III)OXIDE WITH 8.9 WEIGHT % LEAD(II)BROMIDE (50,000 x)

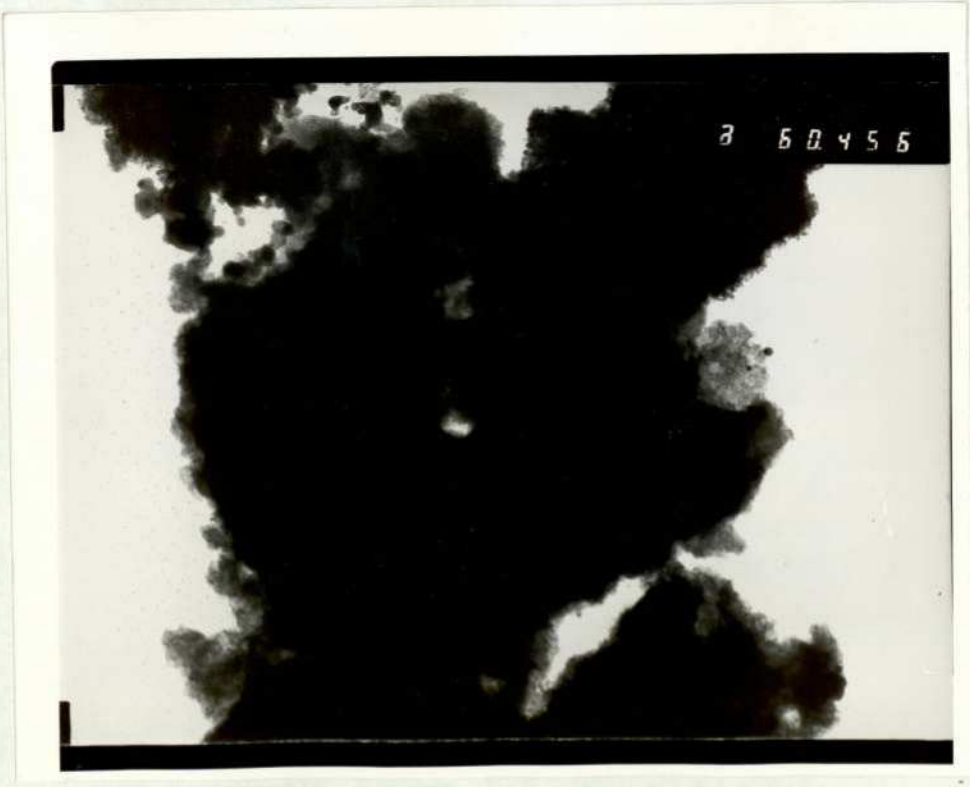

PLATE 3.10. ALUMINA SUPPORTED COBALT(II,III,III)OXIDE WITH 8.9 WEIGHT % LEAD(II)BROMIDE (50,000 x)

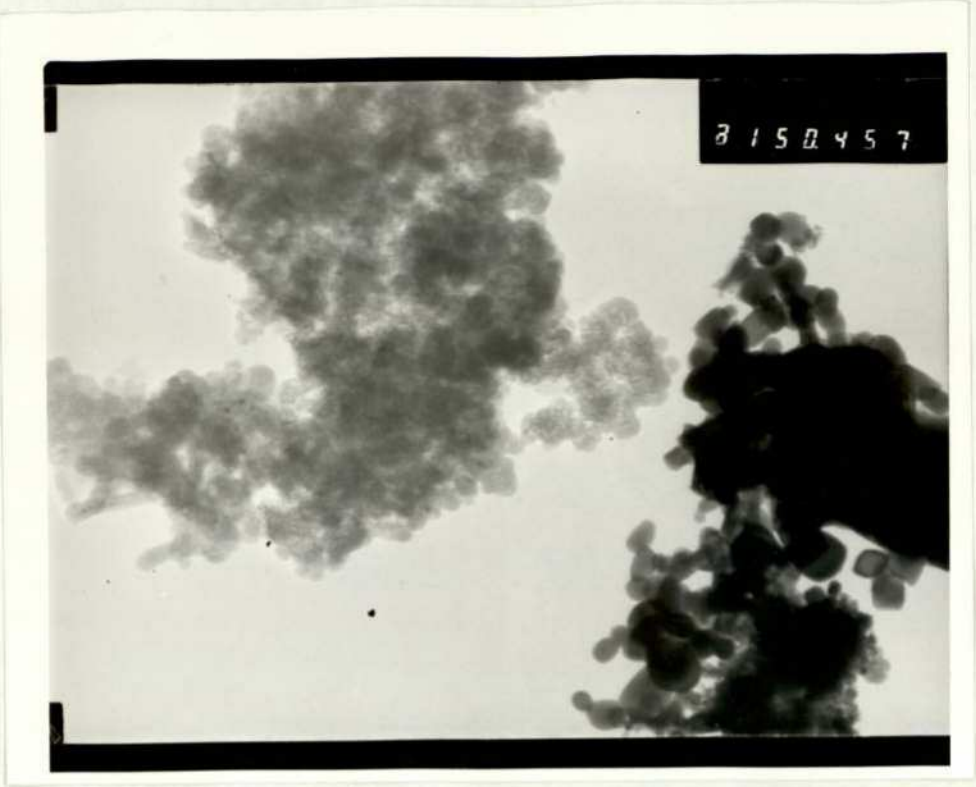

PLATE 3.11. ALUMINA SUPPORTED COBALT(II,III,III)OXIDE WITH 8.9 WEIGHT % LEAD(II)BROMIDE (50,000 x)

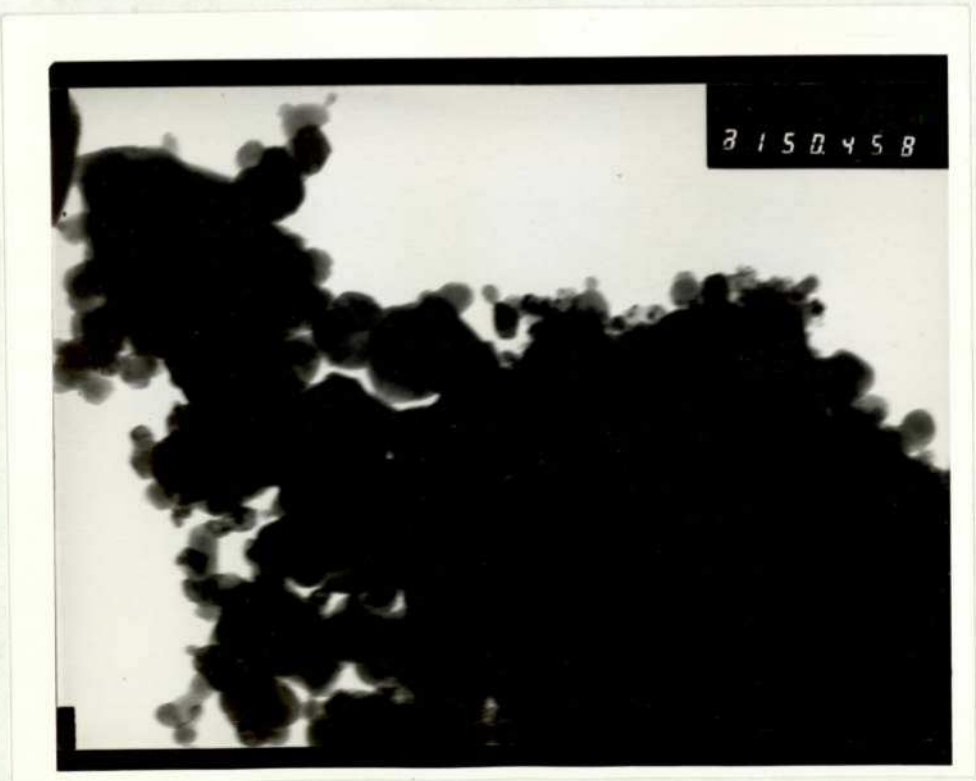

PLATE 3.12. ALUMINA SUPPORTED COBALT(II,III,III)OXIDE WITH 8.9 WEIGHT % LEAD(II)BROMIDE (50,000 x)

PLATE 3.13. ALUMINA SUPPORTED COBALT(II,III,III)OXIDE WITH 8.9 WEIGHT % LEAD(II)BROMIDE (20,000 x)

FIGURE 3.1. CATALYTIC ACTIVITY OF NICKEL(II)OXIDE VARYING WITH LEAD(II)BROMIDE CONTENT

TEMPERATURE 306.5°C

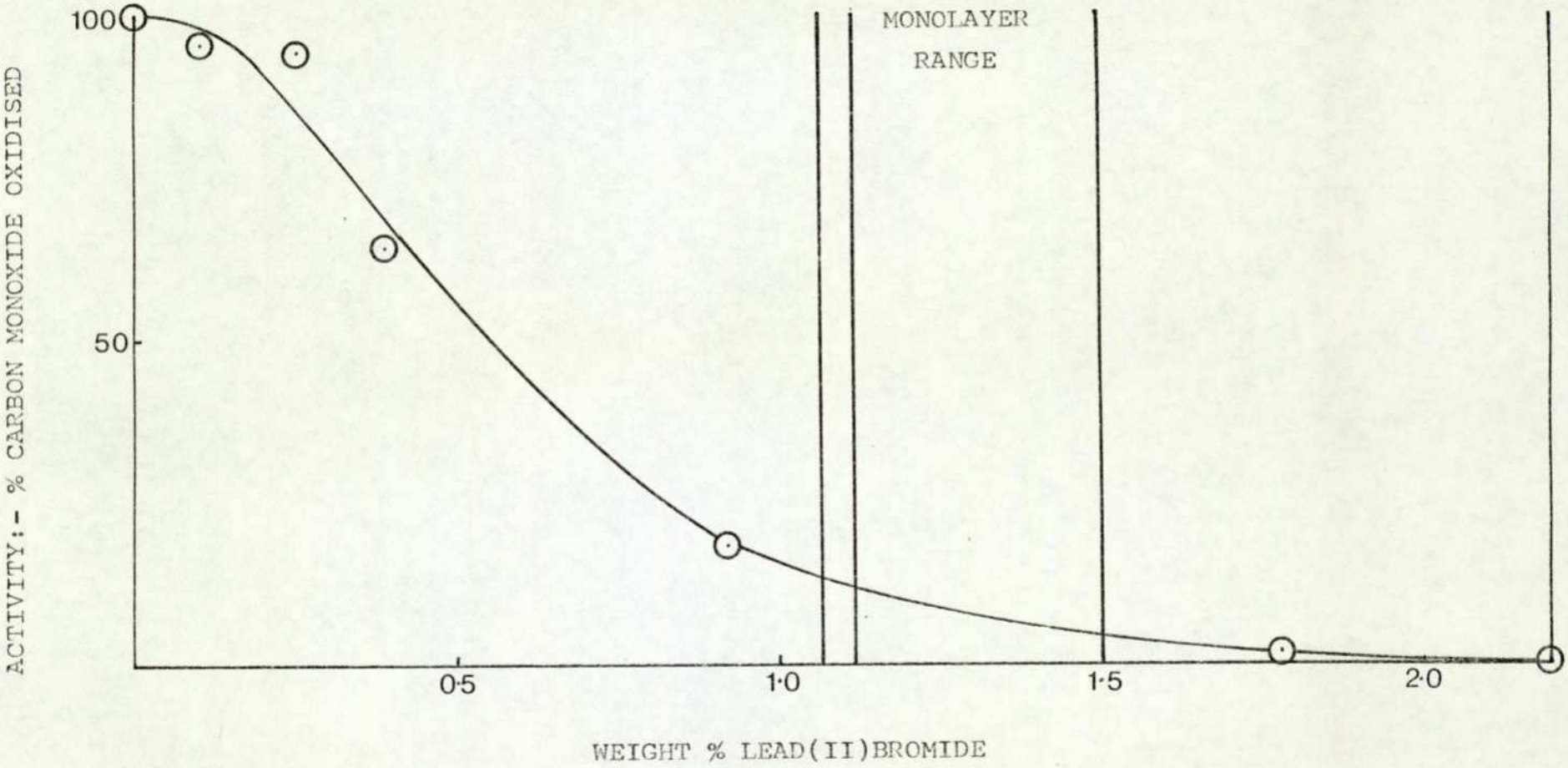

FIGURE 3.2. CATALYTIC ACTIVITY OF NICKEL(II)OXIDE VARYING WITH LEAD(II)BROMIDE CONTENT

TEMPERATURE 306.5°C

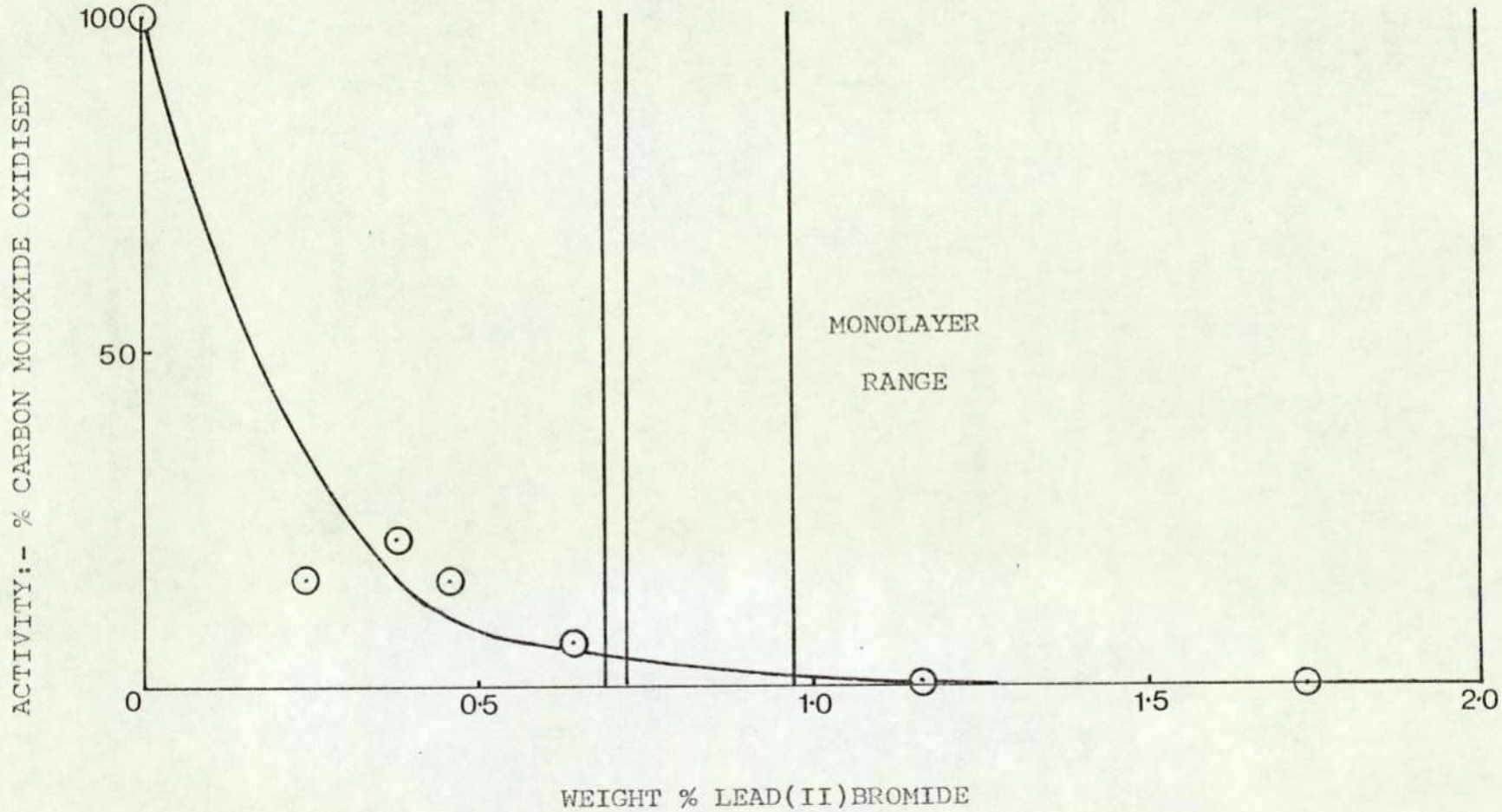

FIGURE 3.3. THE EFFECT OF REMOVAL OF LEAD(II)BROMIDE ON THE CATALYTIC ACTIVITY OF DEACTIVATED NICKEL(II)OXIDE

TEMPERATURE 306.5°C

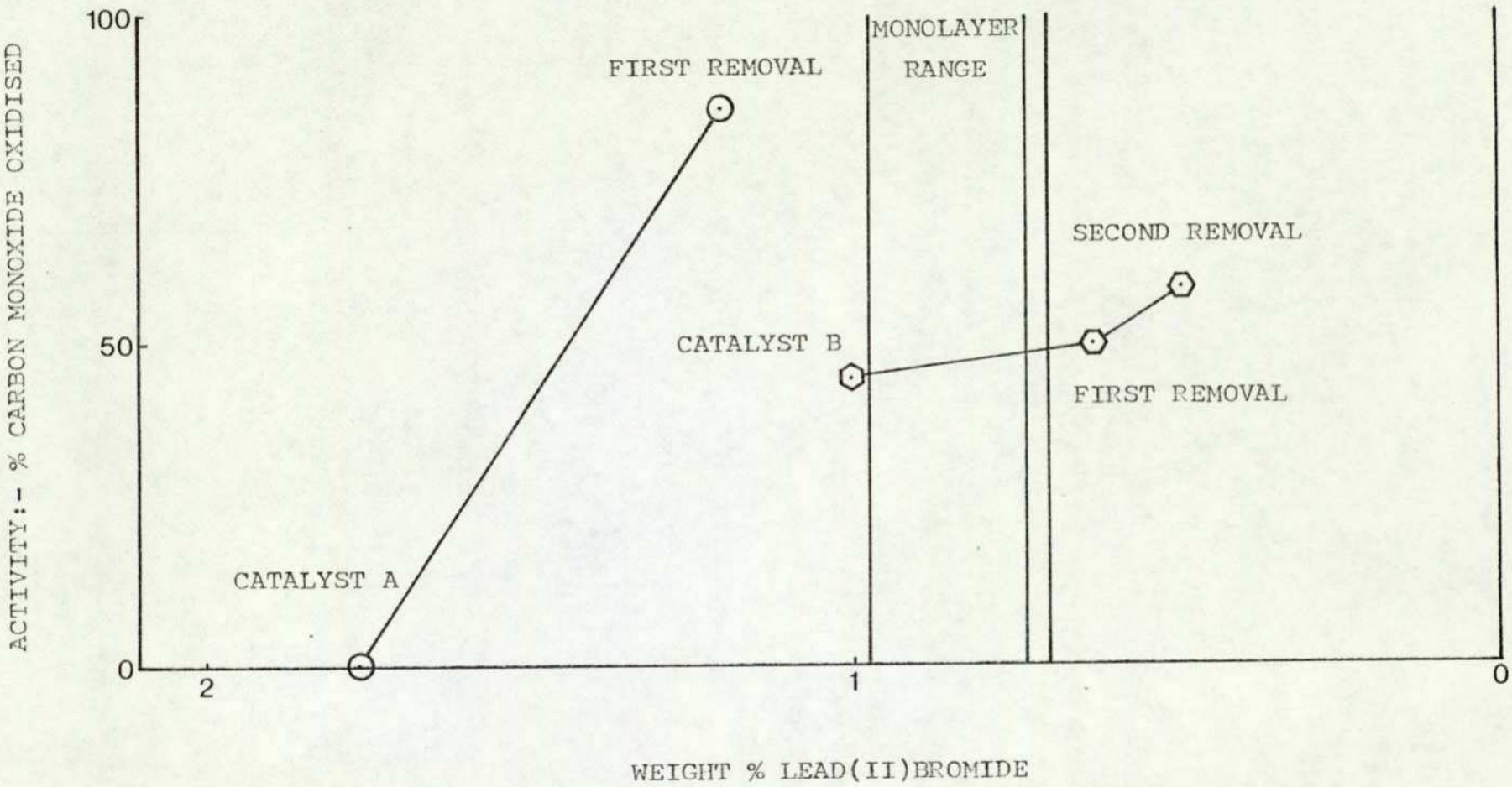

FIGURE 3.4. SURFACE AREA OF NICKEL(II)OXIDE WITH VARYING LEAD(II)BROMIDE CONTENT

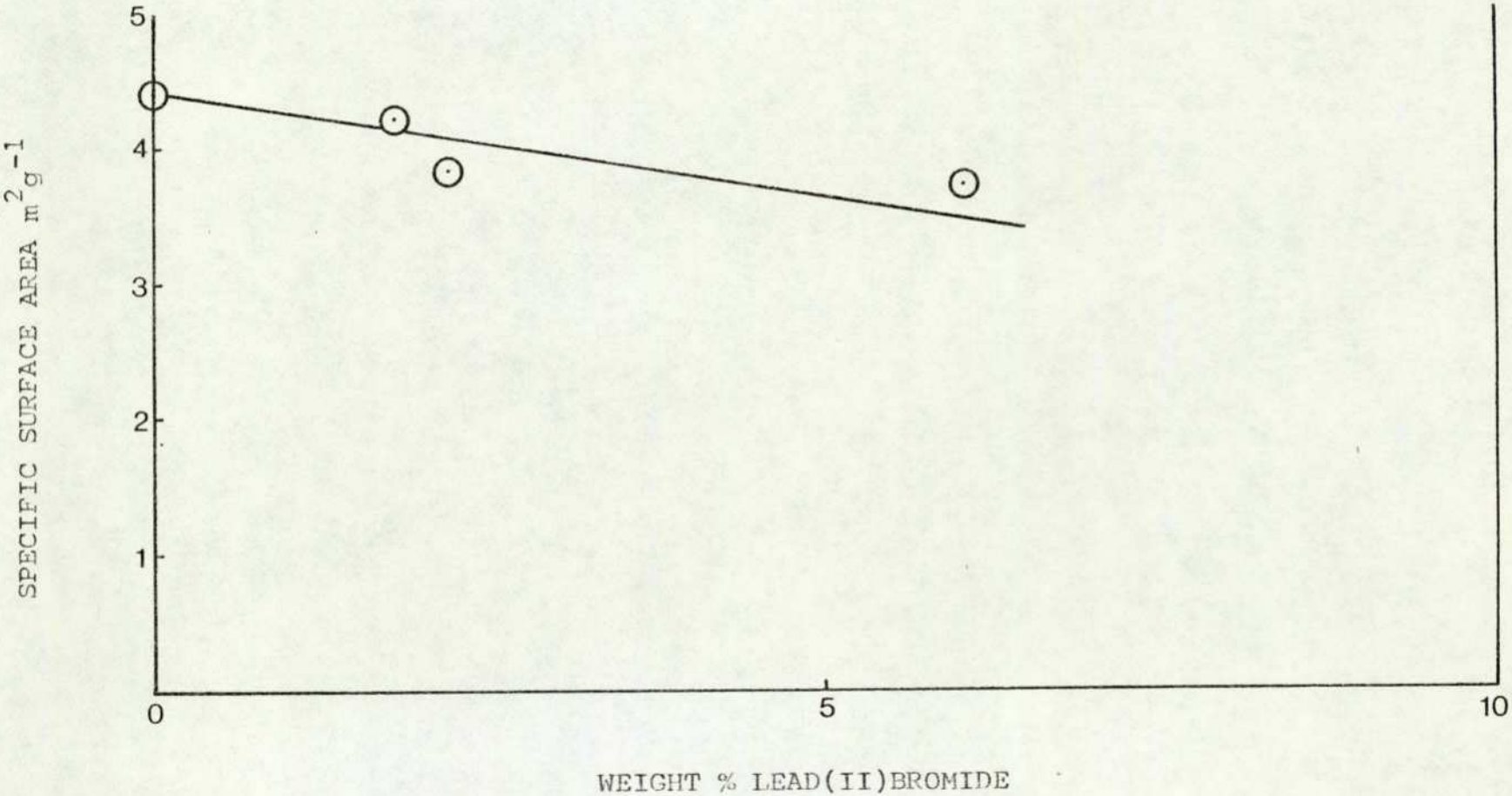

FIGURE 3.5. SURFACE AREA OF NICKEL(II)OXIDE WITH VARYING LEAD(II)BROMIDE CONTENT

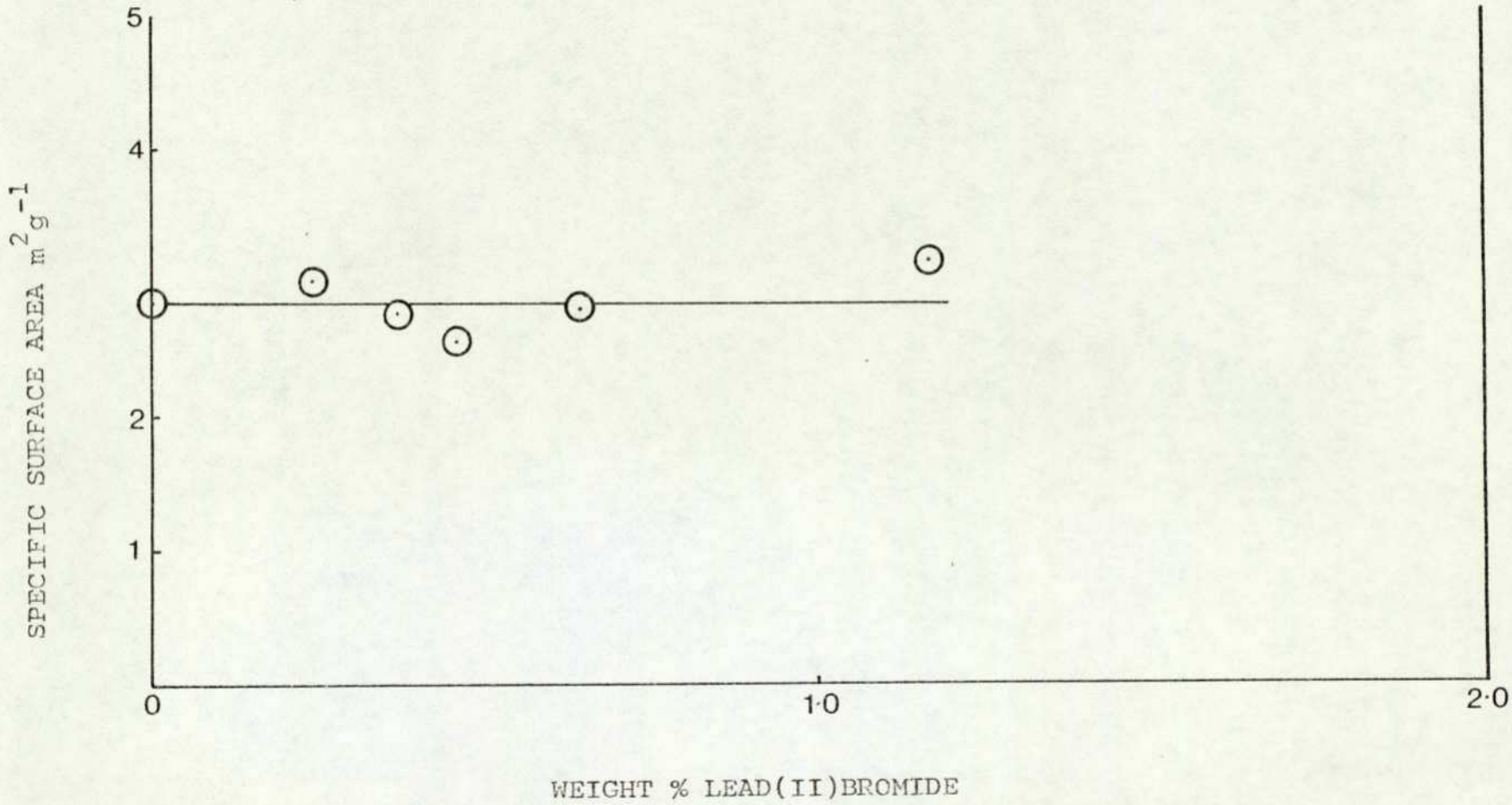

FIGURE 3.6. DIFFERENTIAL PORE SIZE DISTRIBUTION OF NICKEL(II)OXIDE WITH 6.05 WEIGHT % LEAD(II)BROMIDE

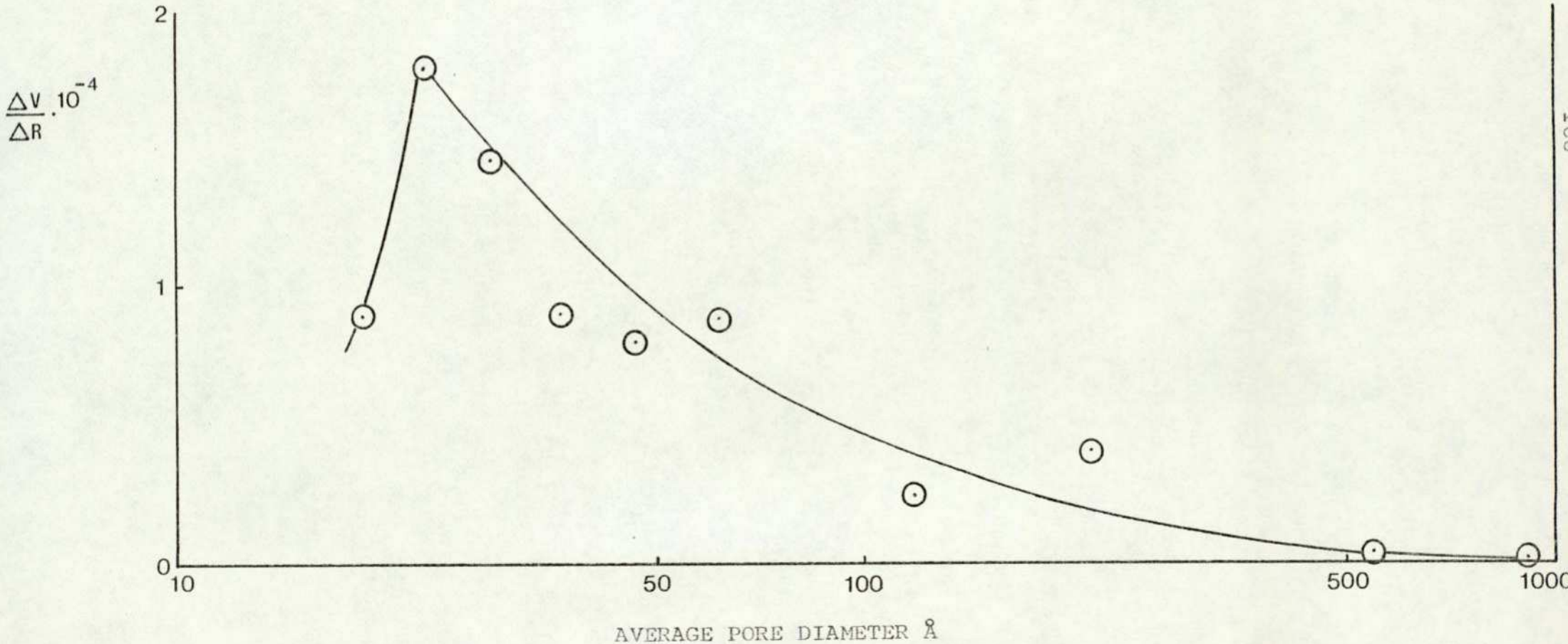

FIGURE 3.7. DIFFERENTIAL PORE SIZE DISTRIBUTION OF NICKEL(II)OXIDE

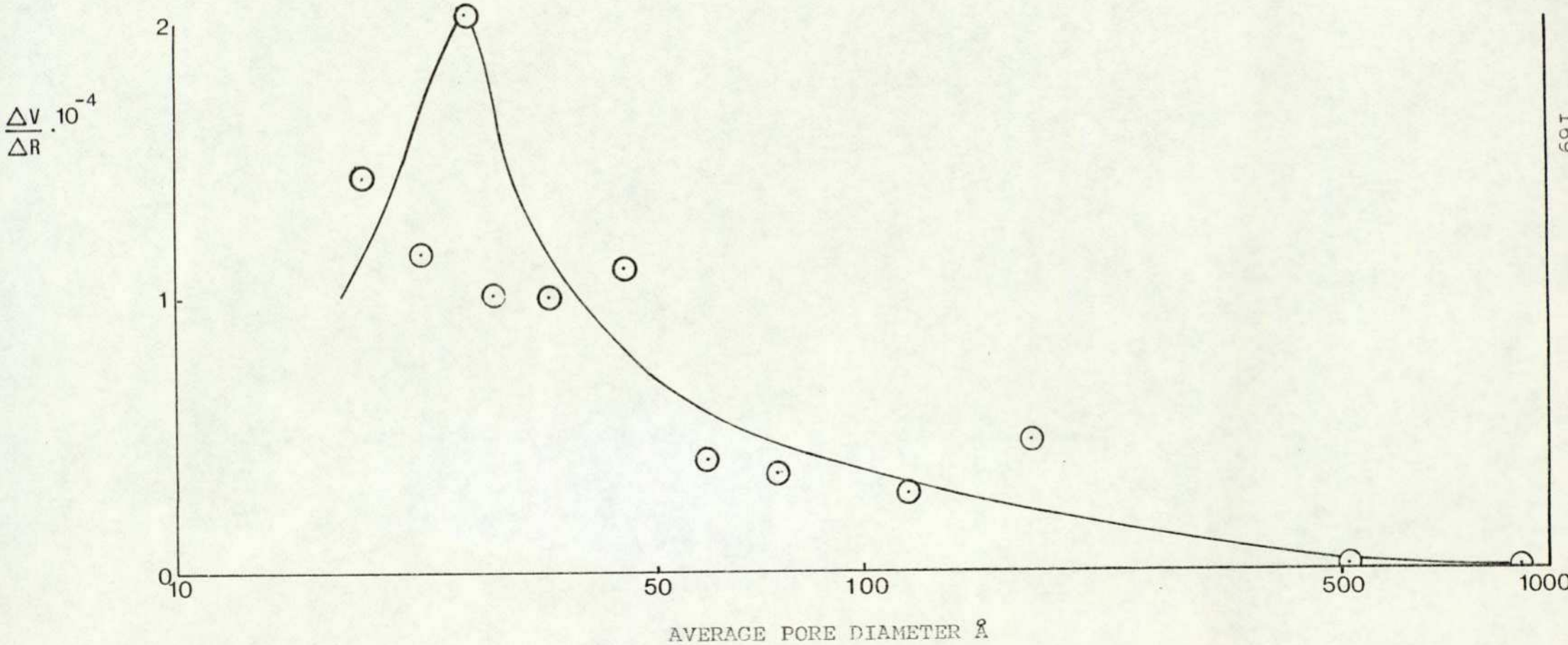

a) NiO SAMPLE Wt 59.6mg

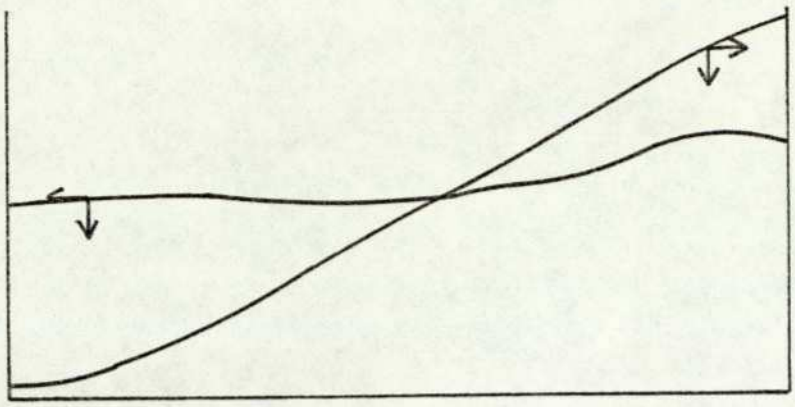

b) EMPTY CRUCIBLE

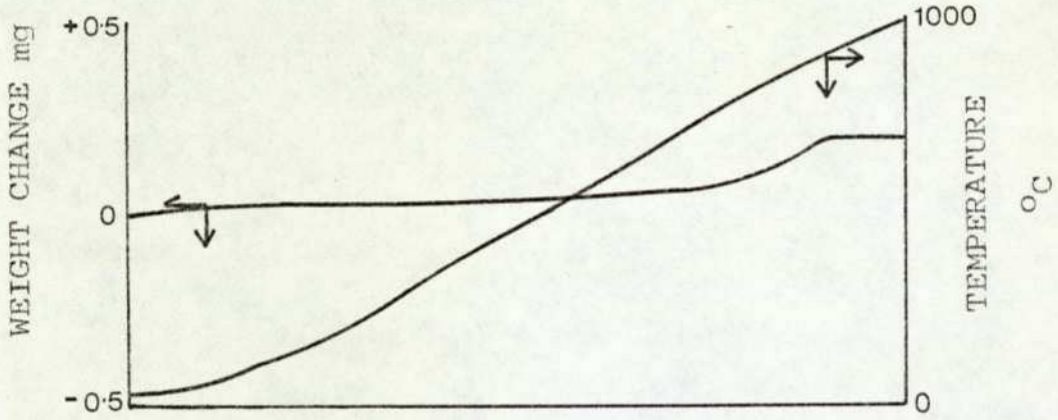

c) NiO SAMPLE Wt 57.3mg

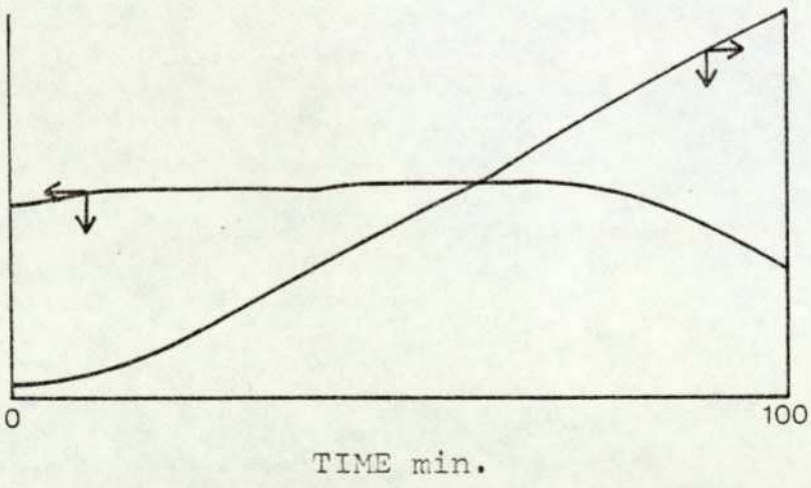

FIGURE 3.8. THERMOGRAVIMETRIC ANALYSIS

HEATING RATE $10^{o}C\ min.^{-1}$

a) $PbBr_2$ SAMPLE Wt 0.9 mg

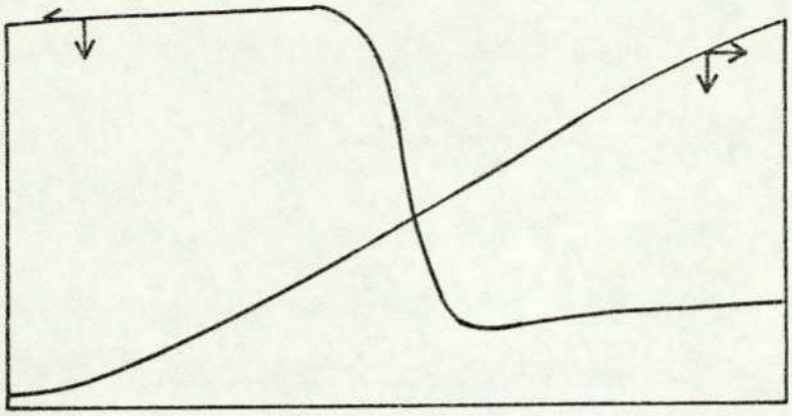

b) NiO WITH 0.28 Wt % $PbBr_2$ SAMPLE Wt 322.2 mg

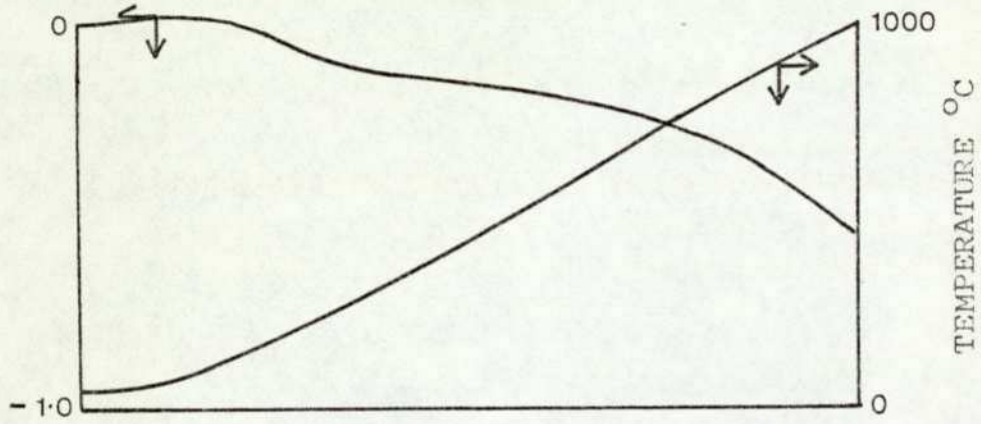

c) NiO WITH 0.46 Wt % $PbBr_2$ SAMPLE Wt 196.5 mg

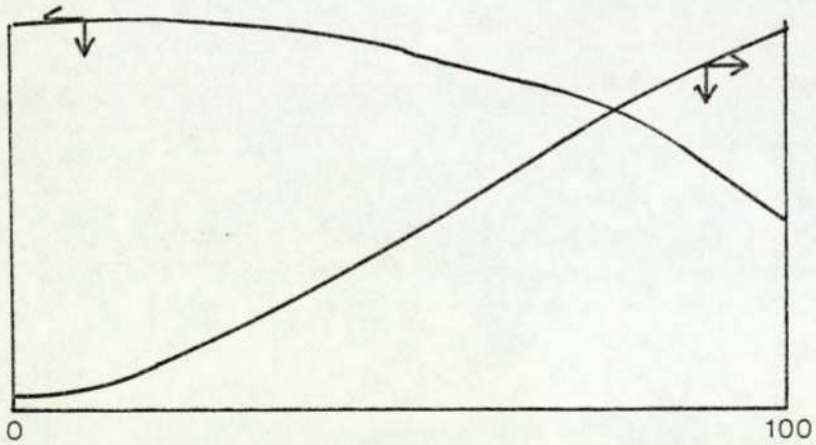

FIGURE 3.9. THERMOGRAVIMETRIC ANALYSIS

HEATING RATE $10^{\circ}C\ min^{-1}$

a) NiO WITH 0.645 Wt % $PbBr_2$ SAMPLE Wt 140 mg

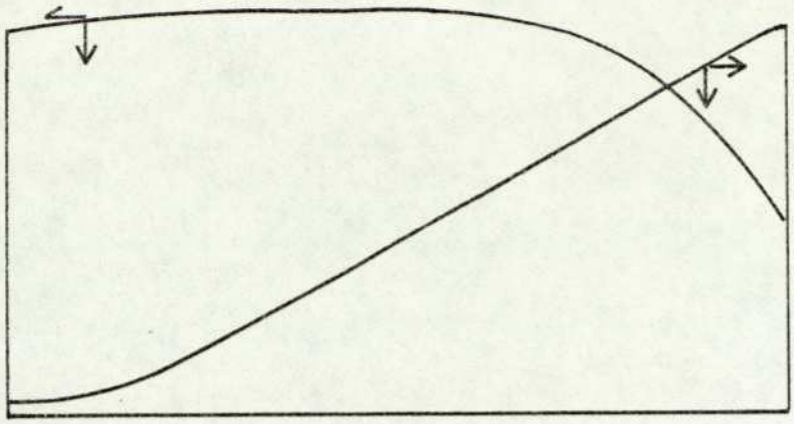

b) NiO WITH 1.17 Wt % $PbBr_2$ SAMPLE Wt 93.17mg

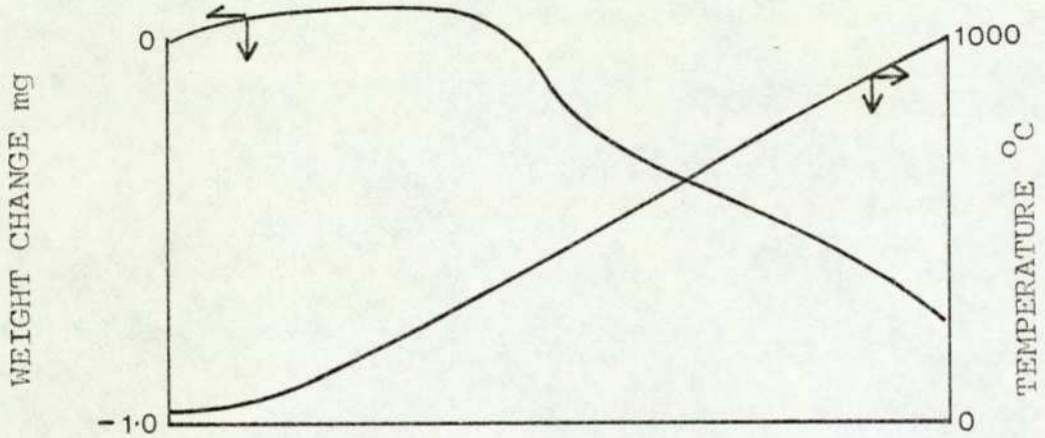

c) NiO WITH 1.32 Wt % $PbBr_2$ SAMPLE Wt 64.86 mg

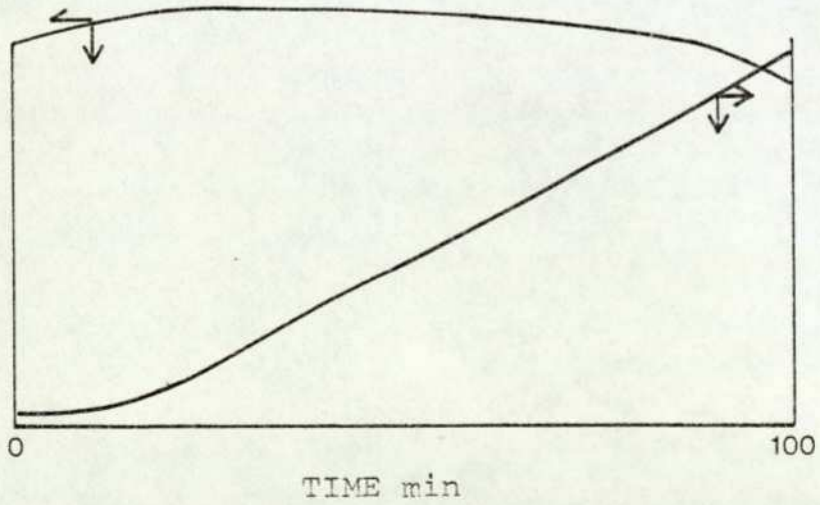

FIGURE 3.10. THERMOGRAVIMETRIC ANALYSIS

HEATING RATE $10^{\circ}C\ min^{-1}$

FIGURE 3.11. a) and b) THERMOGRAVIMETRIC ANALYSIS

HEATING RATE $10^{o}C\ min^{-1}$

a) NiO WITH 1.76 Wt % $PbBr_2$ SAMPLE Wt 47 mg

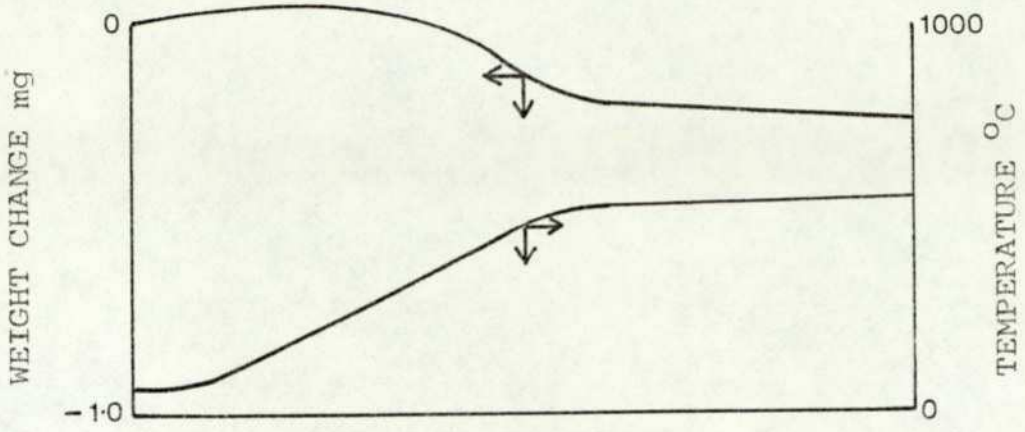

b) NiO WITH 1.76 Wt % $PbBr_2$ SAMPLE Wt 51.2 mg

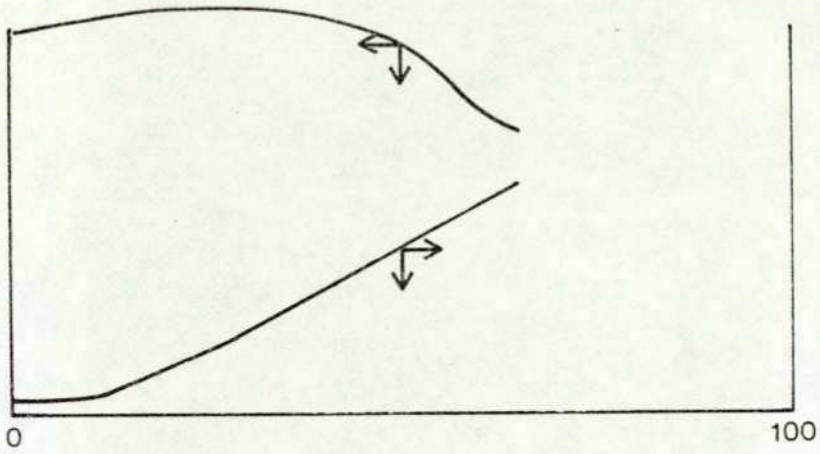

FIGURE 3.11.c VARIATION OF $PbBr_2$ CONTENT OF NiO SAMPLES HEATED TO $1000^{o}C$

MONOLAYER RANGE

BEFORE HEATING AFTER HEATING

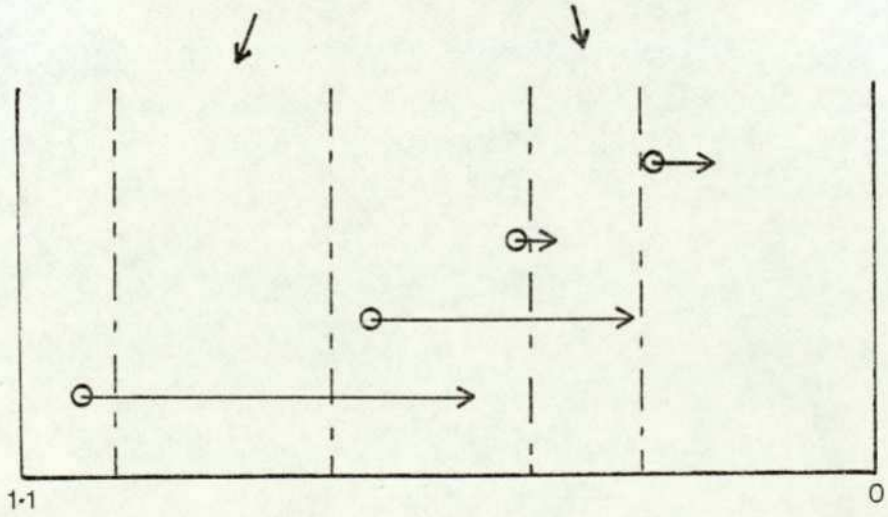

WEIGHT % $PbBr_2$

O INITIAL, → FINAL $PbBr_2$ CONTENT

FIGURE 3.12. DIFFERENTIAL THERMAL ANALYSIS

PHYSICAL MIXTURE OF NICKEL(II)OXIDE (50 WEIGHT %) AND LEAD(II) BROMIDE

SAMPLE WEIGHT 105 mg.HEATING RATE $5^{o}C\ min^{-1}$

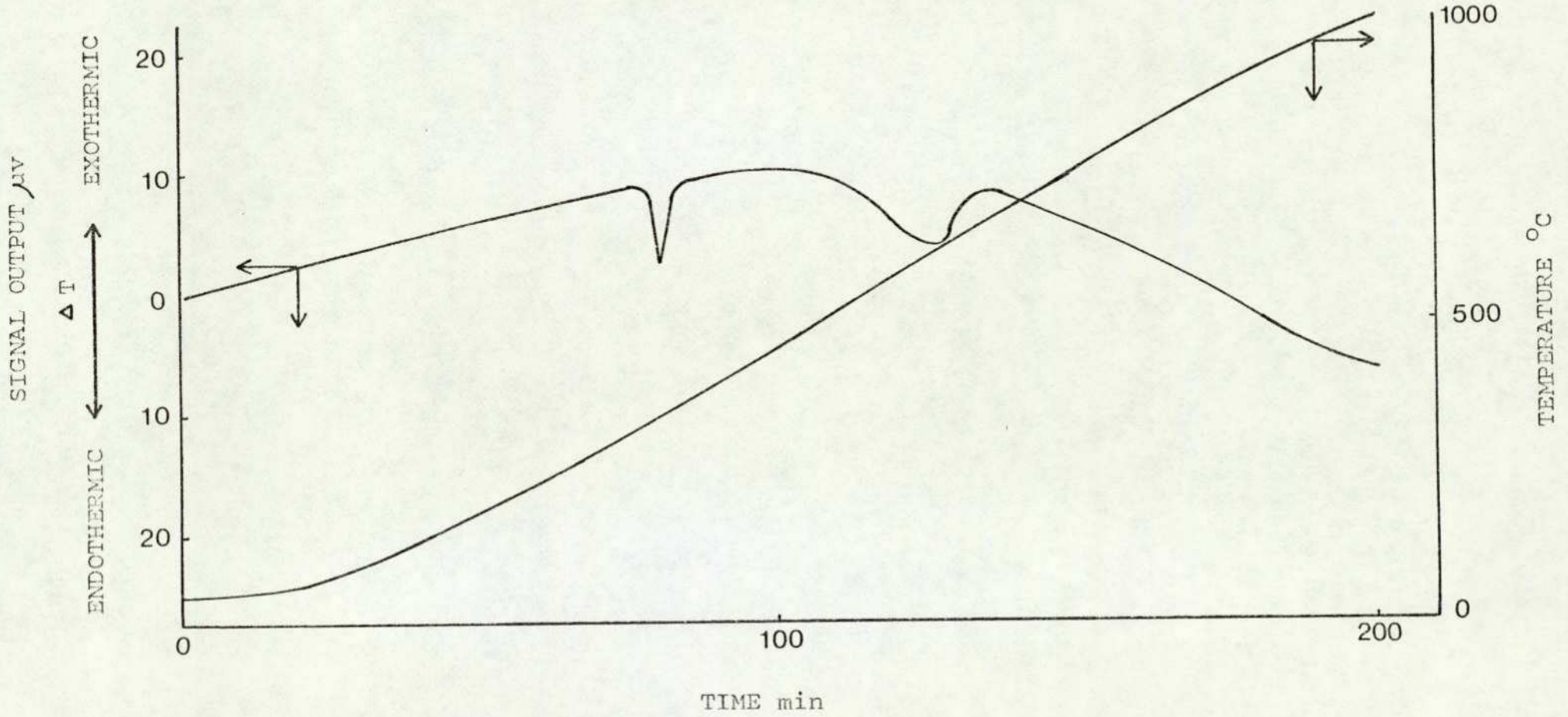

FIGURE 3.13. DIFFERENTIAL THERMAL ANALYSIS:- LEAD(II)BROMIDE

SAMPLE WEIGHT 32.8 mg. HEATING RATE $5^{o}Cmin^{-1}$

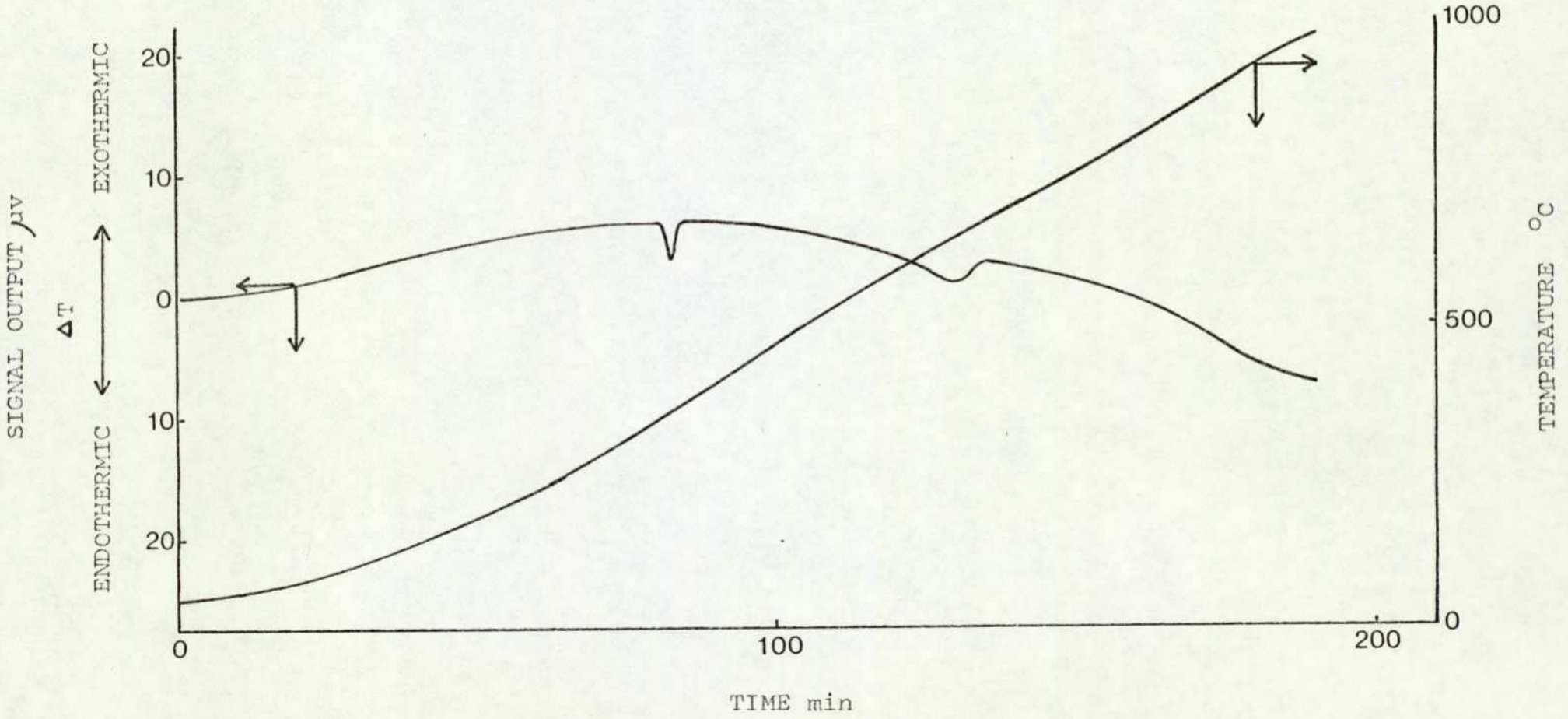

FIGURE 3.14. DIFFERENTIAL THERMAL ANALYSIS

PHYSICAL MIXTURE OF NICKEL(II)OXIDE (50 WEIGHT %) AND LEAD(II) BROMIDE

SAMPLE WEIGHT 202.5 mg. HEATING RATE $5^{\circ}C\ min^{-1}$

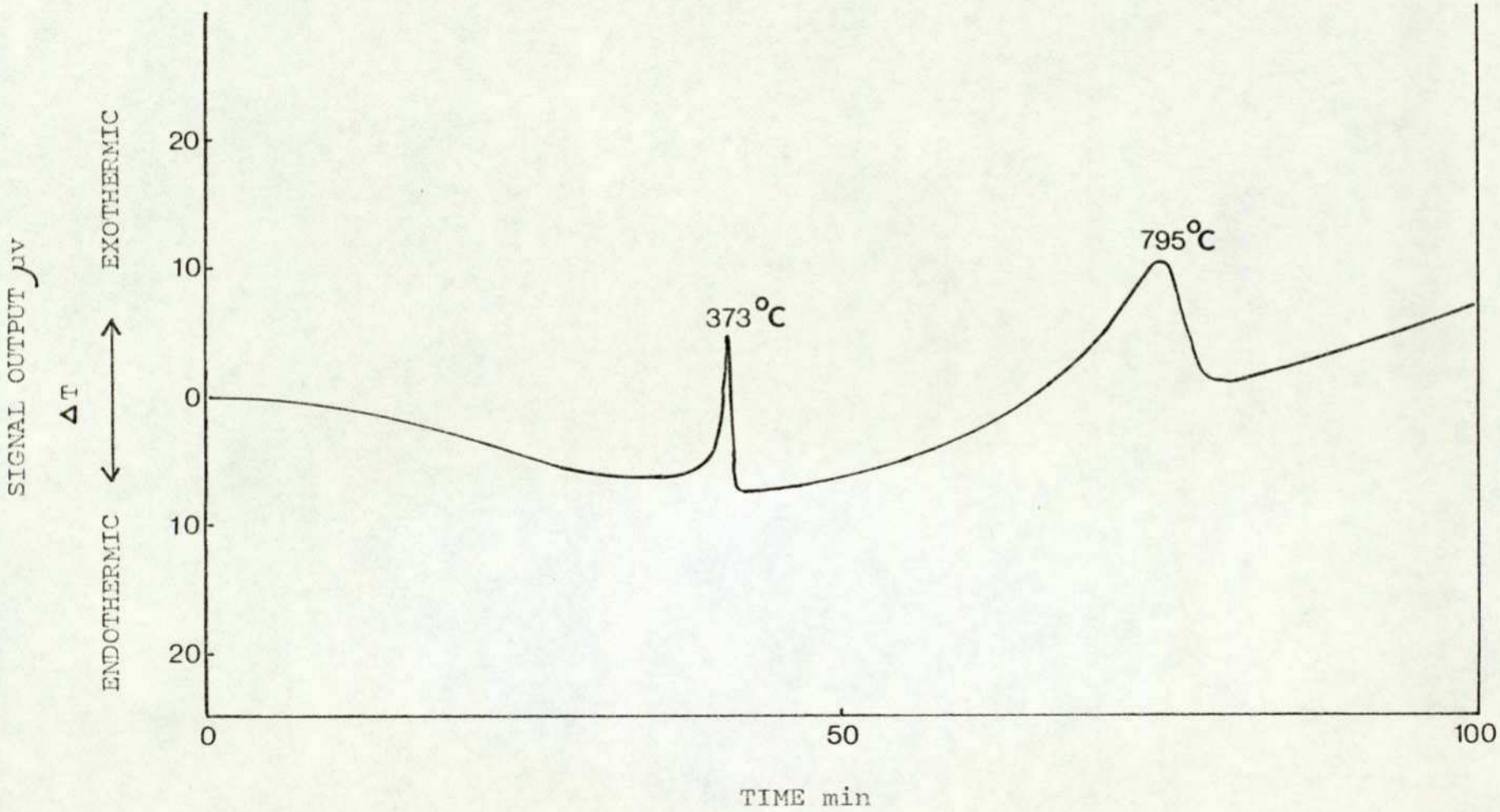

FIGURE 3.15. DIFFERENTIAL THERMAL ANALYSIS:- LEAD(II)BROMIDE

SAMPLE WEIGHT 99.2 mg.HEATING RATE $10^{\circ}C\ min^{-1}$

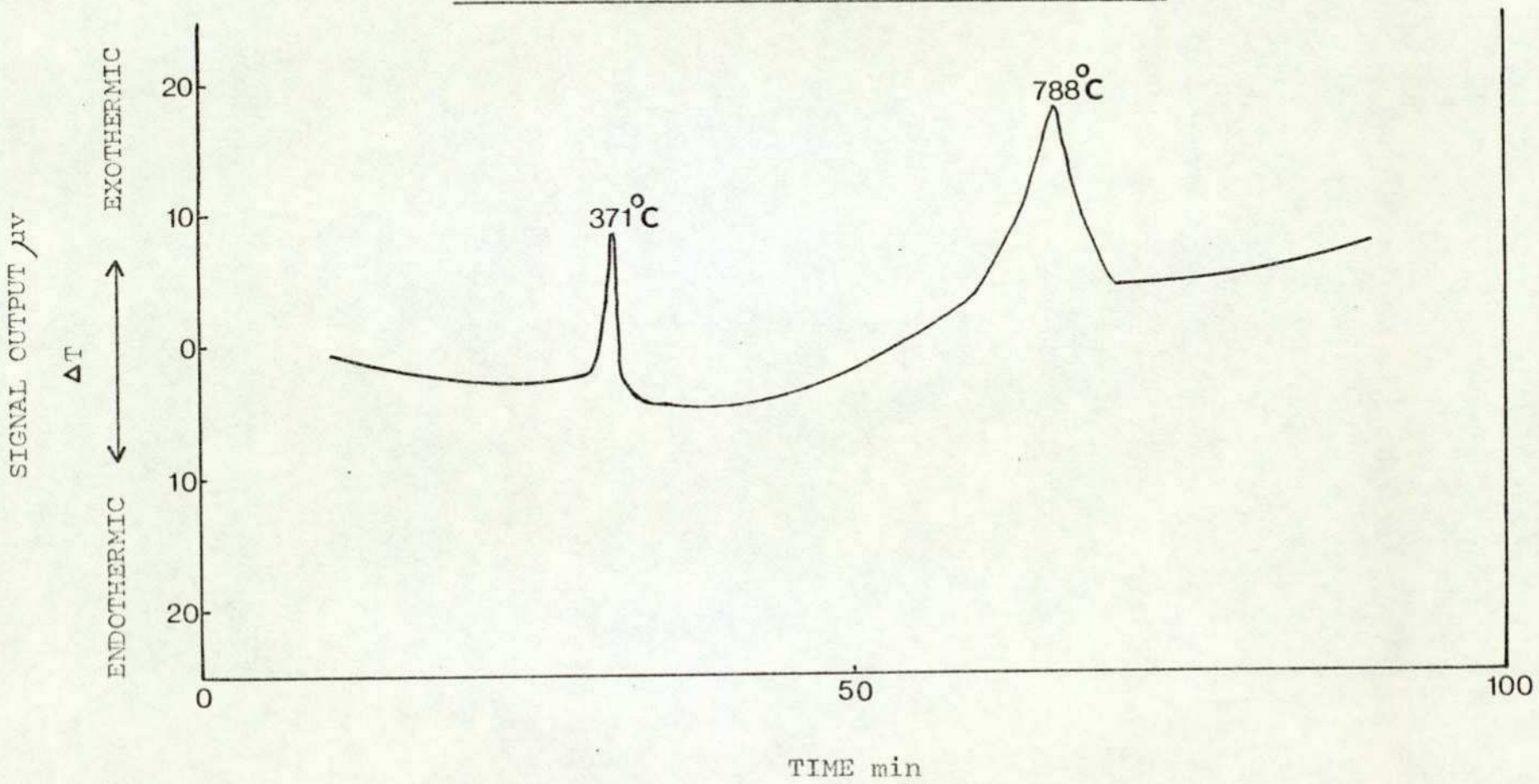

FIGURE 3.16. ULTRA-VIOLET;VISIBLE;NEAR INFRA-RED SPECTRA

NICKEL(II)OXIDE DEACTIVATED WITH 1.76 WEIGHT % LEAD(II)BROMIDE

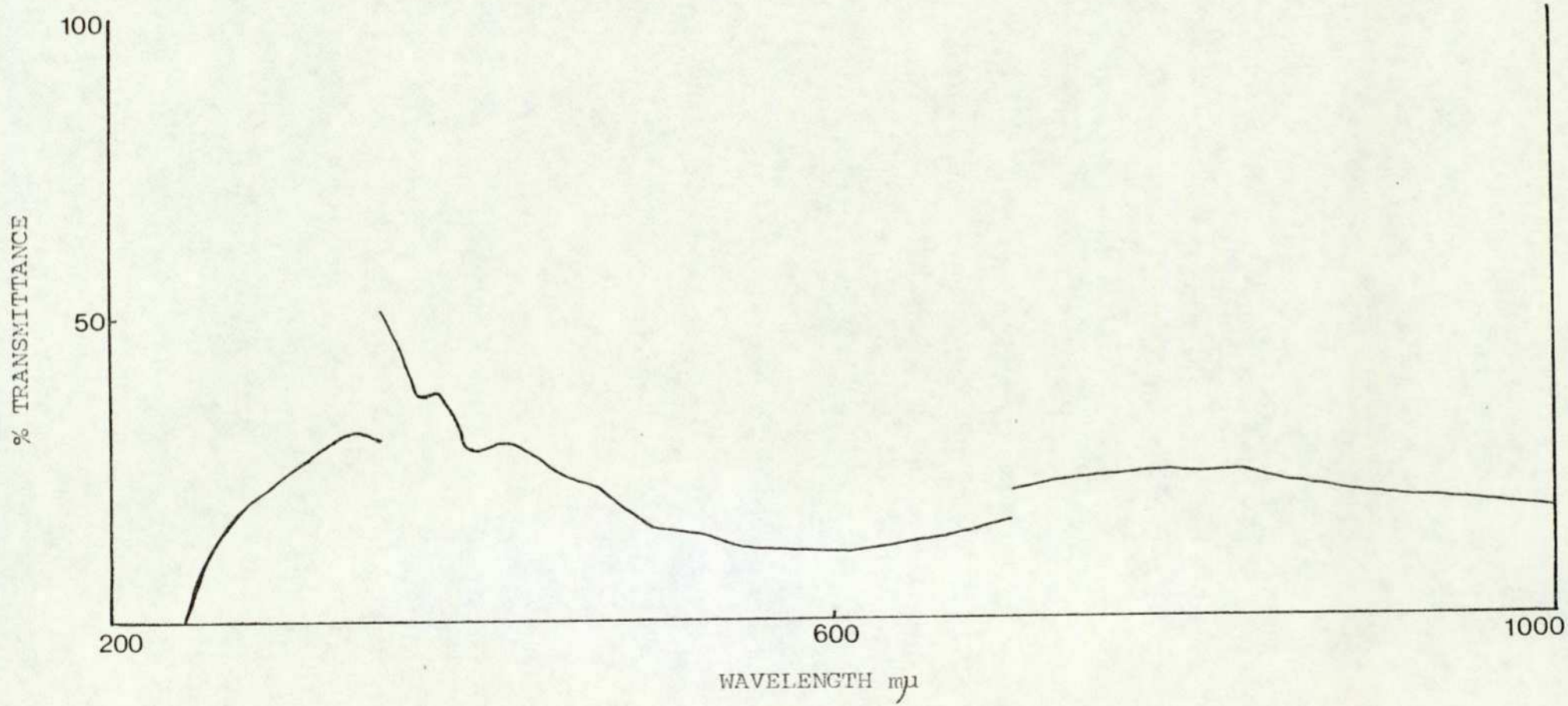

FIGURE 3.17. ULTRA-VIOLET;VISIBLE;NEAR INFRA-RED SPECTRA OF LEAD(II)BROMIDE

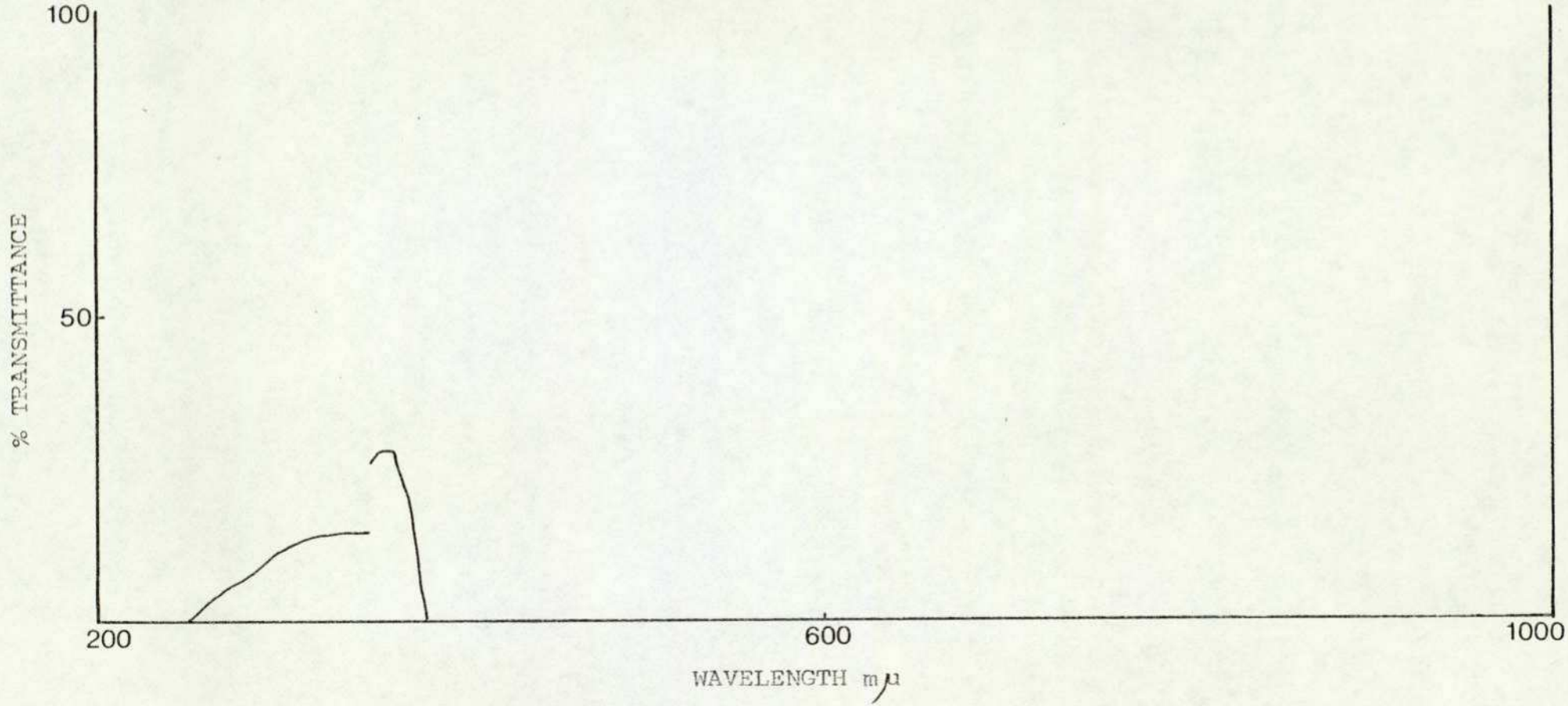

FIGURE 3.18. ULTRA-VIOLET;VISIBLE;NEAR INFRA-RED SPECTRA OF NICKEL(II)OXIDE

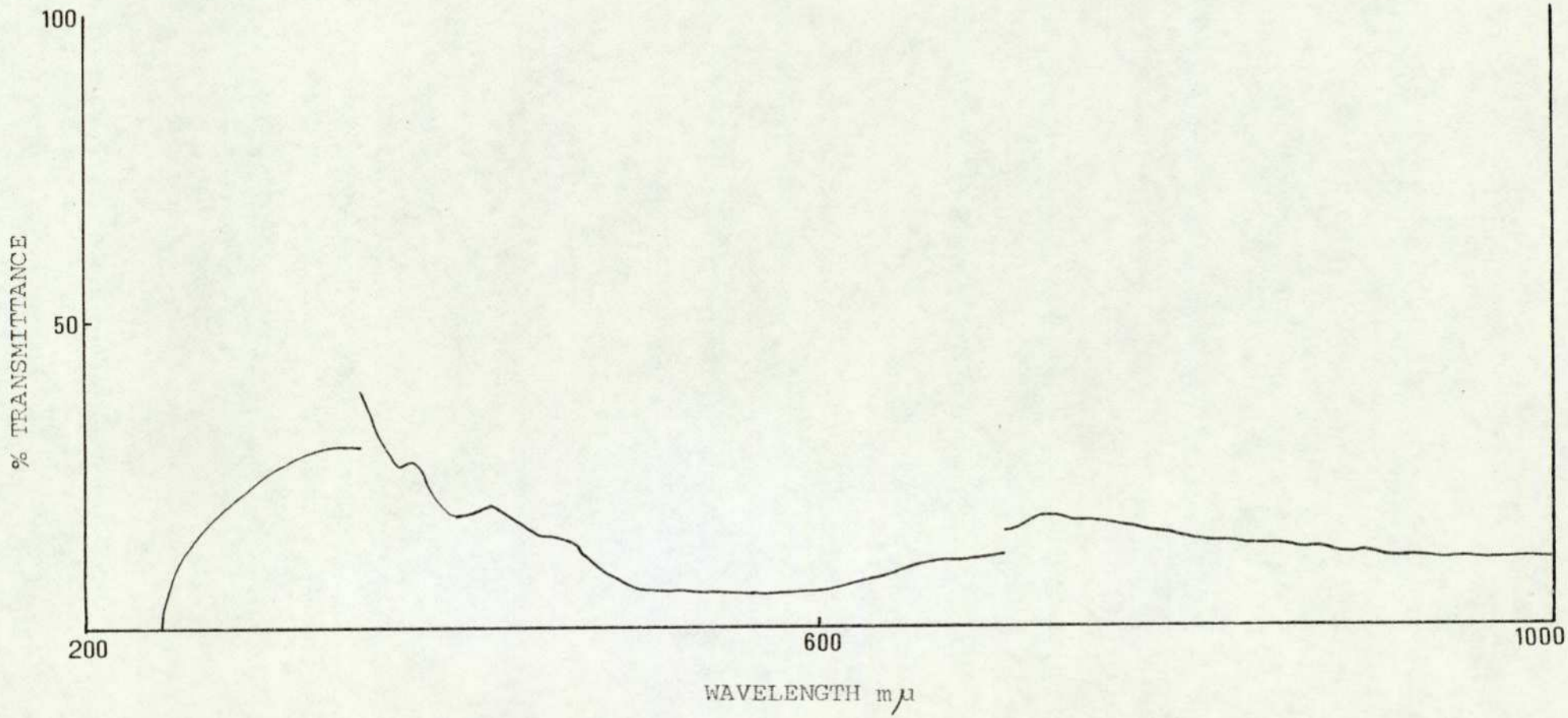

FIGURE 3.19. INFRA-RED SPECTRA

NICKEL(II)OXIDE DEACTIVATED WITH 32.5 WEIGHT % LEAD(II) BROMIDE

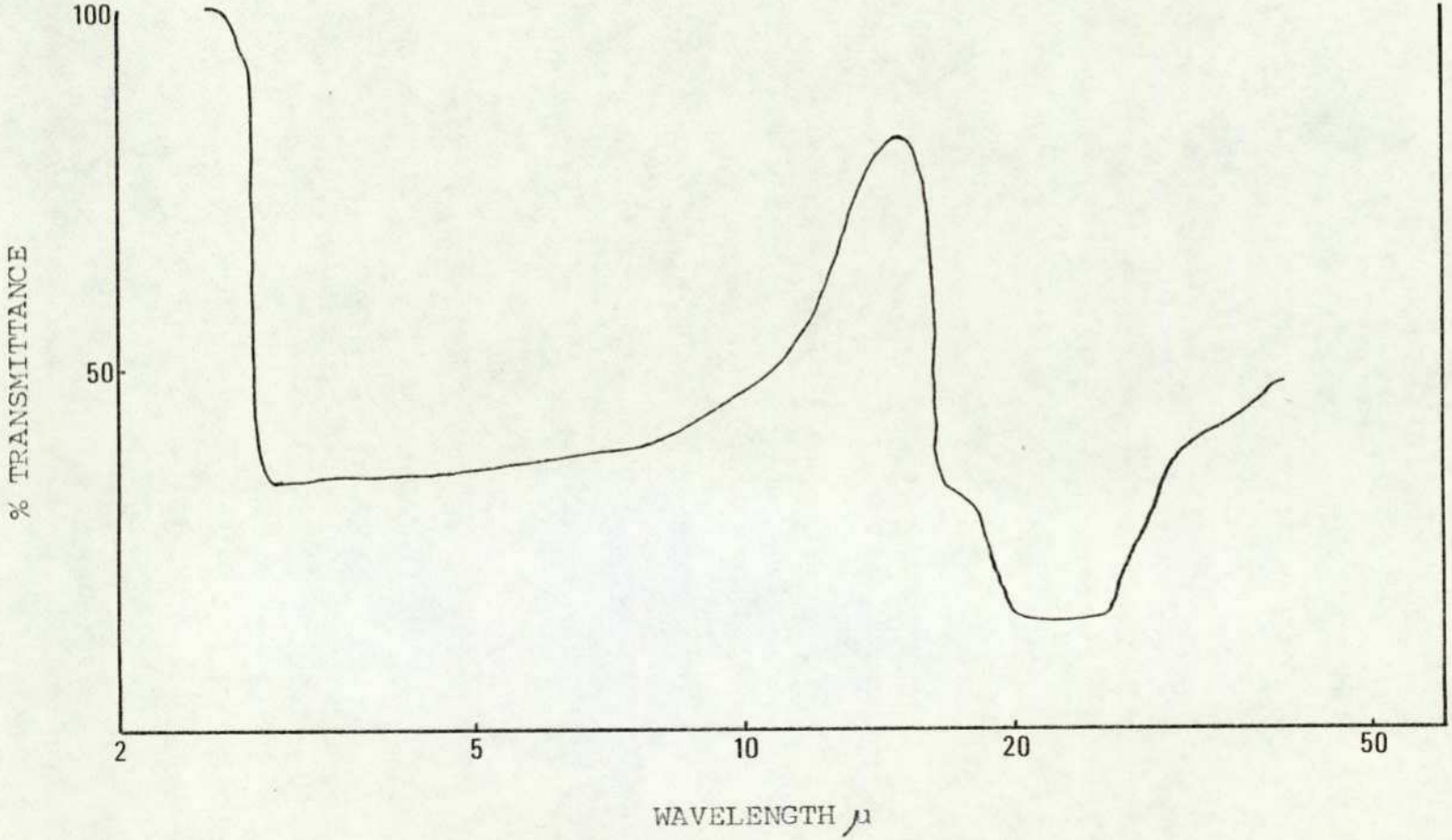

FIGURE 3.20. INFRA-RED SPECTRA OF NICKEL(II)OXIDE

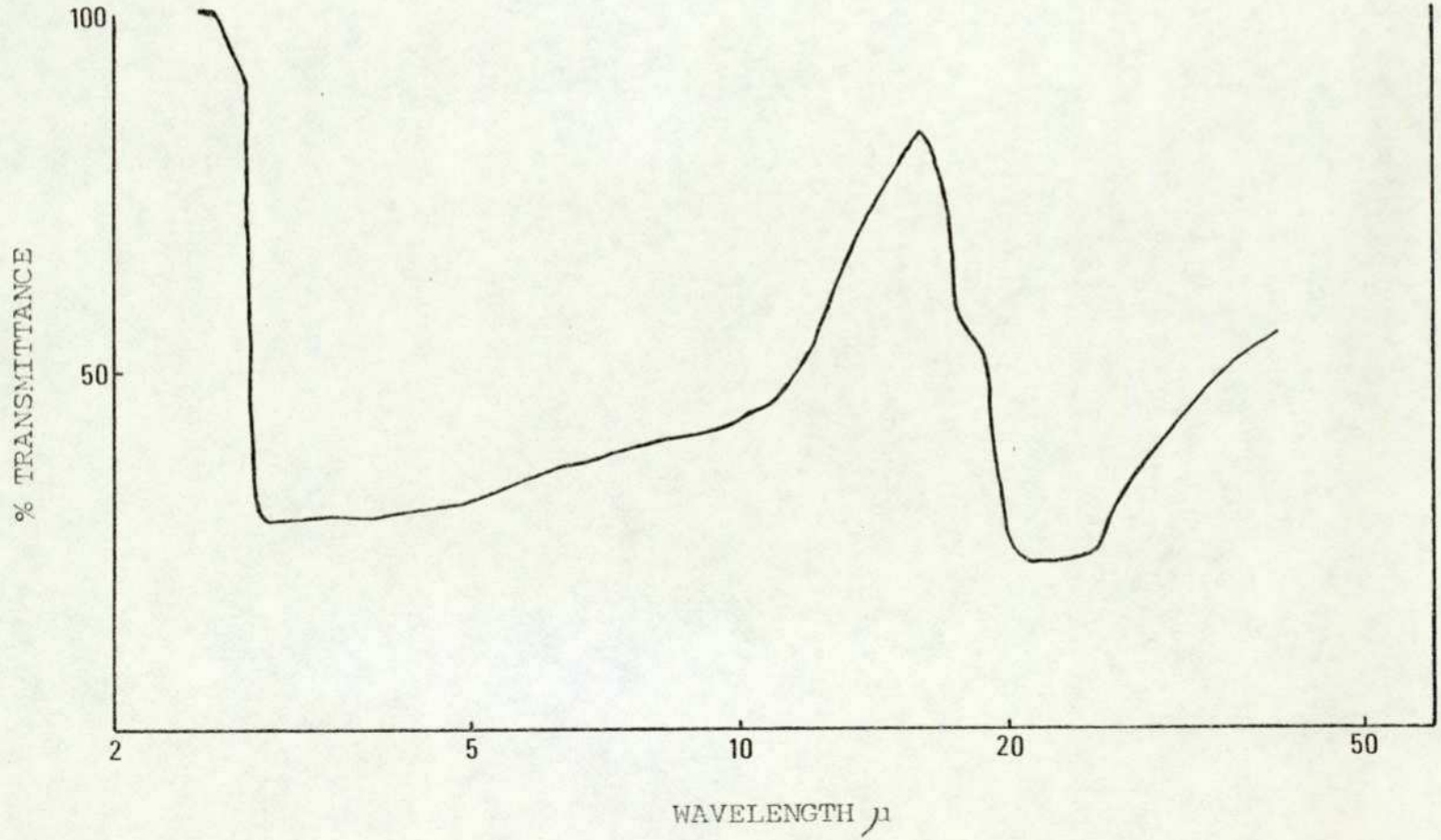

FIGURE 3.21. ELECTRICAL CONDUCTIVITY OF NICKEL(II)OXIDE VARYING WITH LEAD(II)BROMIDE CONTENT

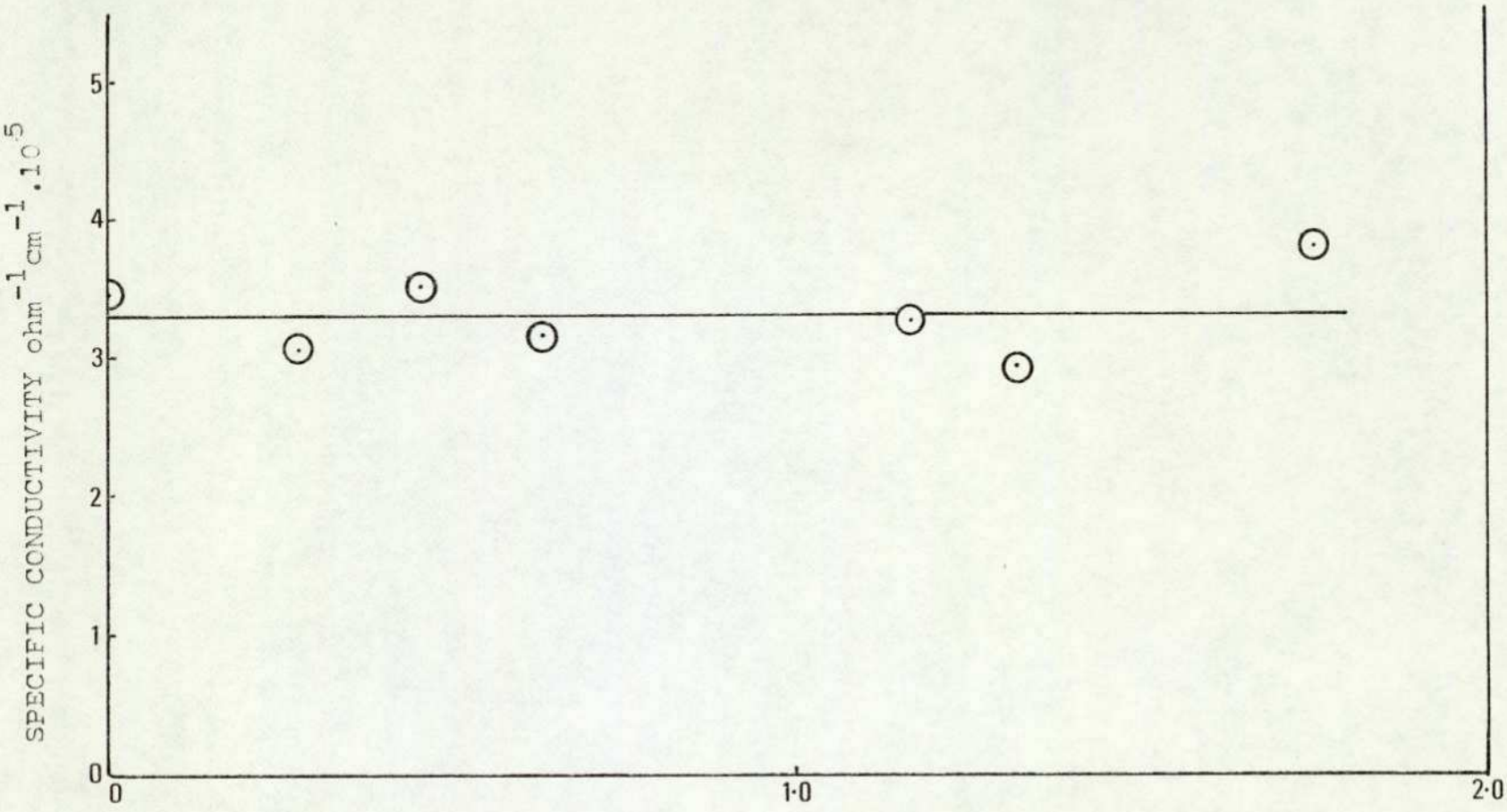

FIGURE 3.22. CATALYTIC ACTIVITY OF ALUMINA SUPPORTED COPPER(II)OXIDE VARYING WITH LEAD(II)BROMIDE CONTENT. TEMPERATURE 241°C

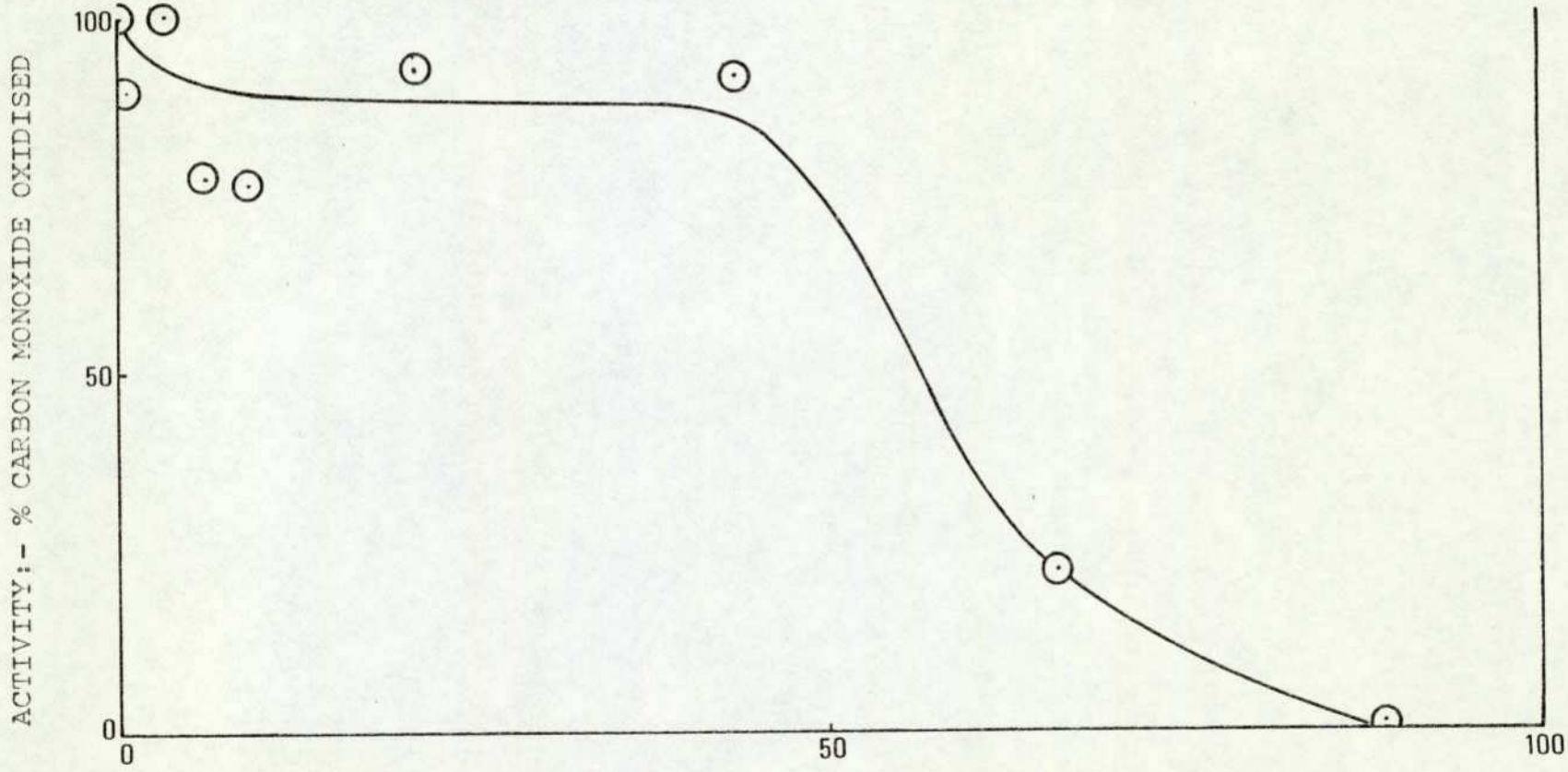

FIGURE 3.23. SURFACE AREA OF ALUMINA SUPPORTED COPPER(II)OXIDE VARYING WITH LEAD(II)BROMIDE CONTENT

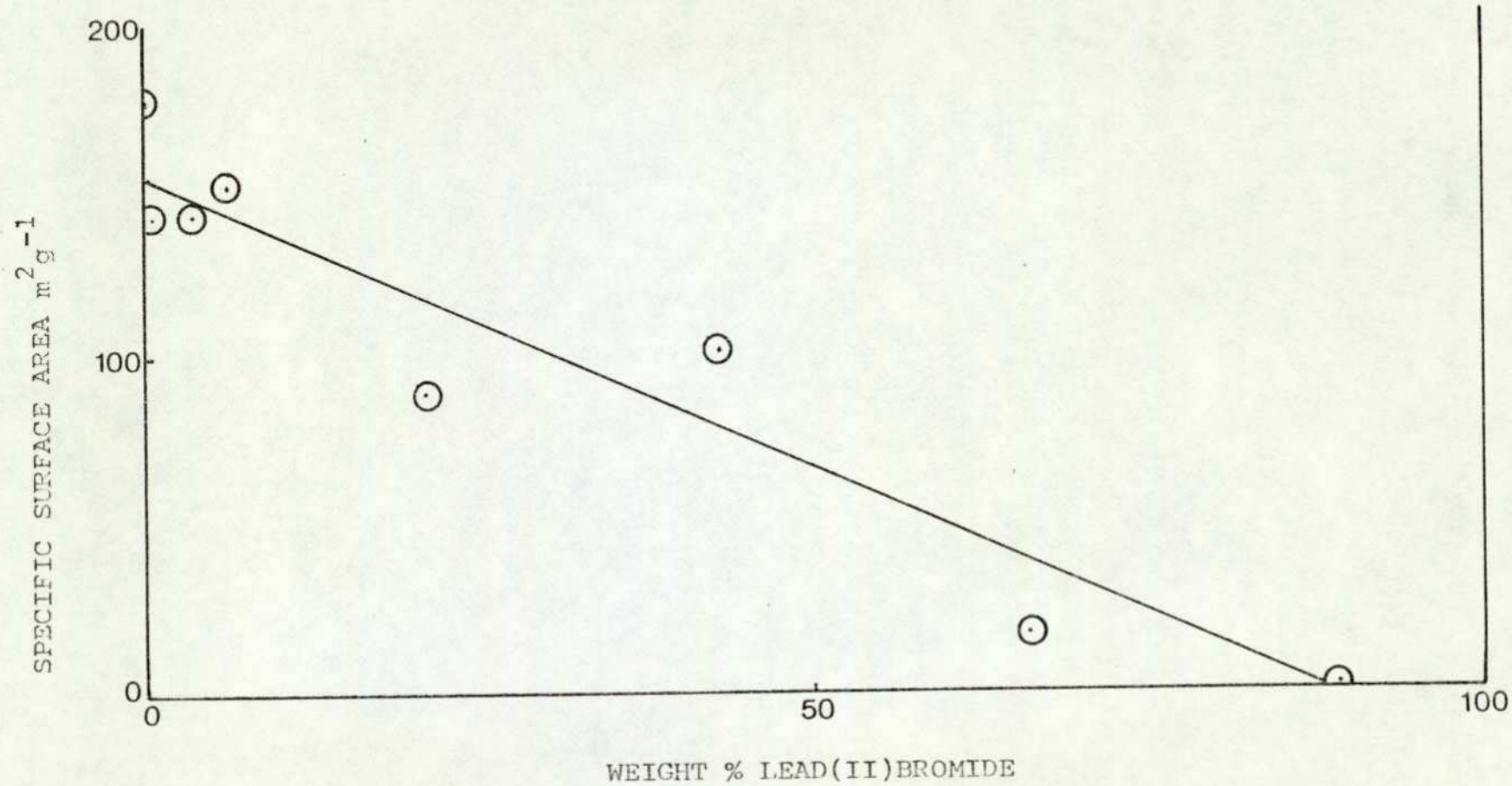

FIGURE 3.24. SURFACE AREA OF ALUMINA SUPPORTED COPPER(II)OXIDE VARYING WITH LEAD(II)BROMIDE CONTENT

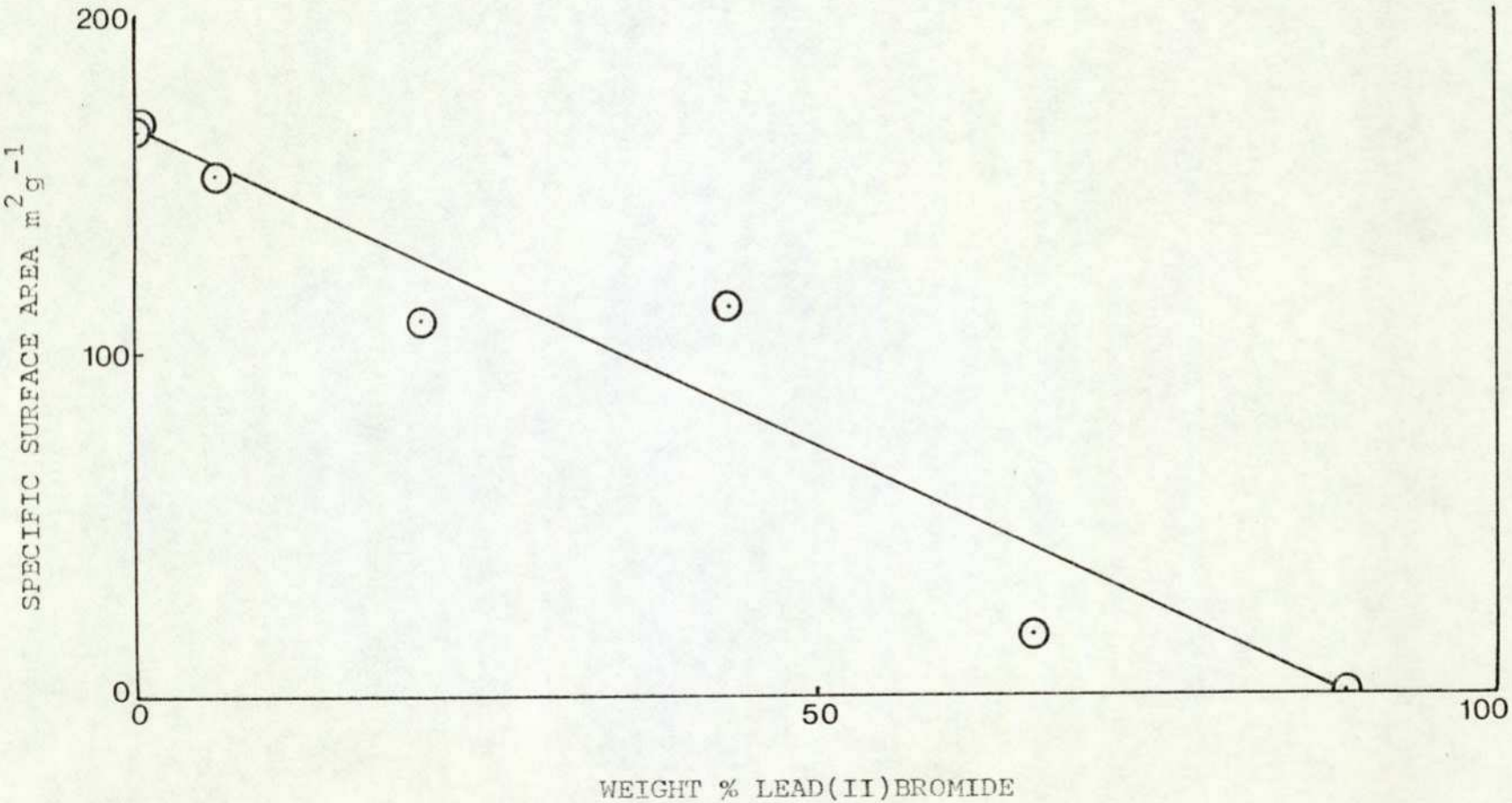

FIGURE 3.25. DIFFERENTIAL PORE SIZE DISTRIBUTIONS:-ALUMINA SUPPORTED COPPER(II)OXIDE

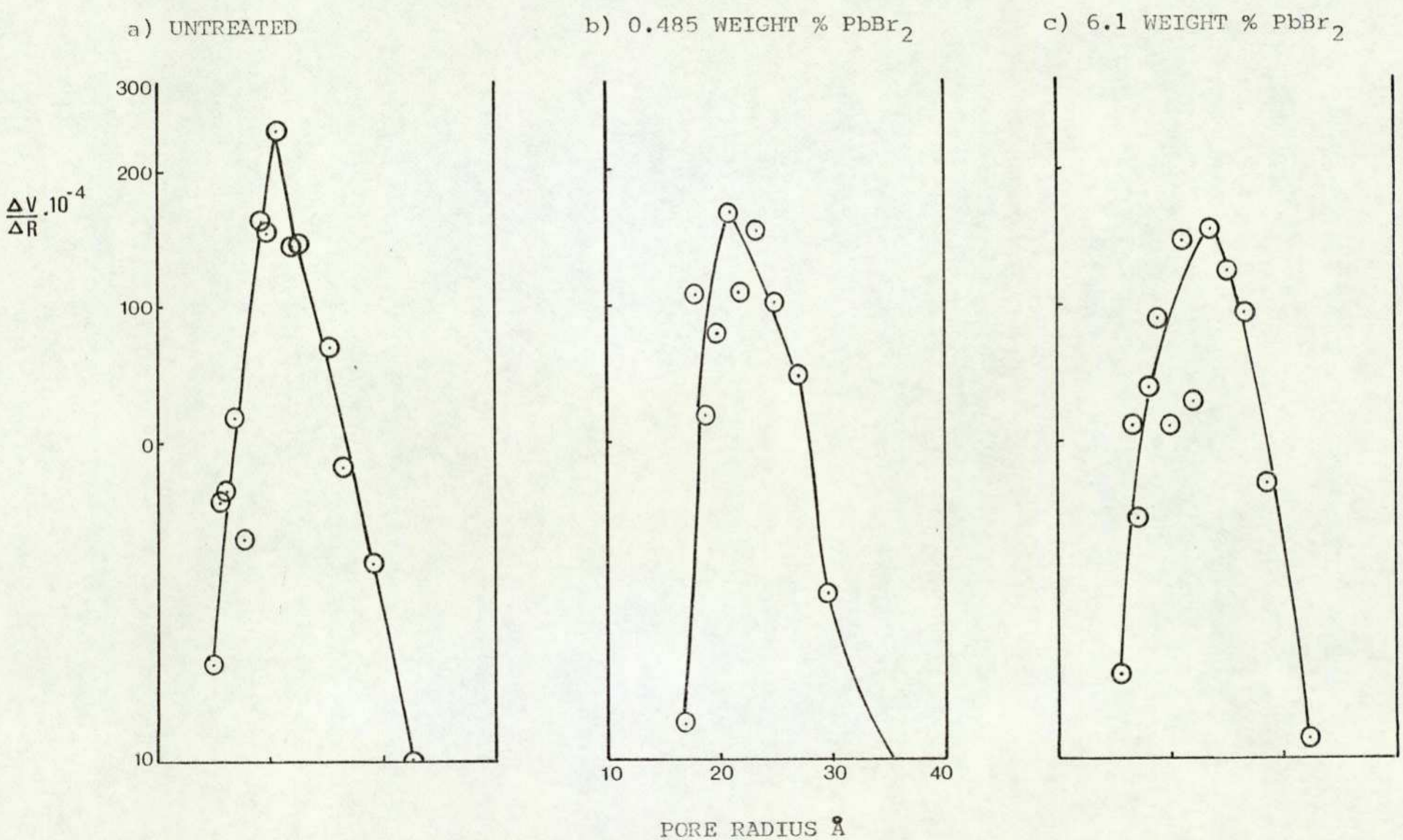

FIGURE 3.26. DIFFERENTIAL PORE SIZE DISTRIBUTIONS:- ALUMINA SUPPORTED COPPER(II)OXIDE

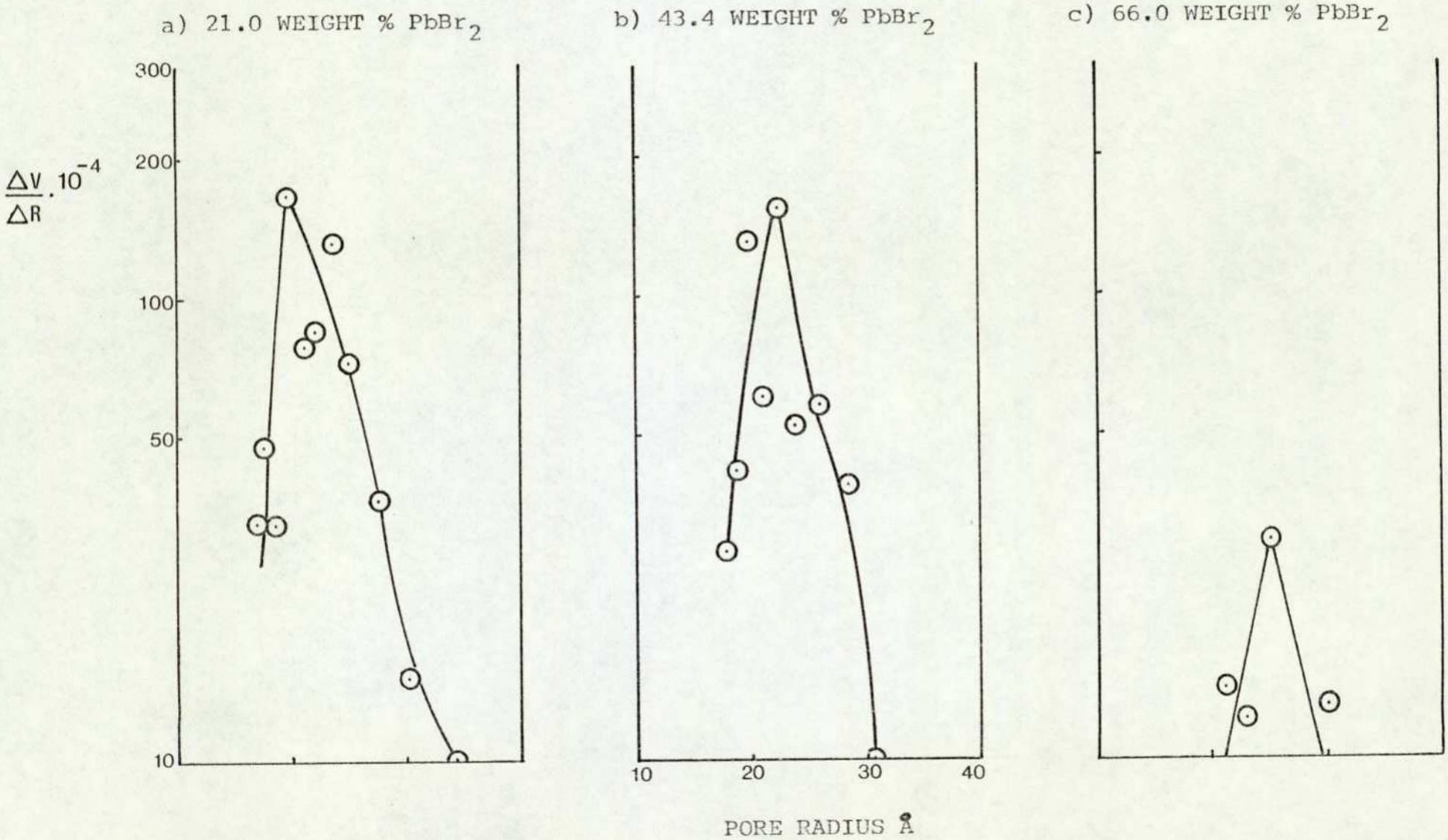

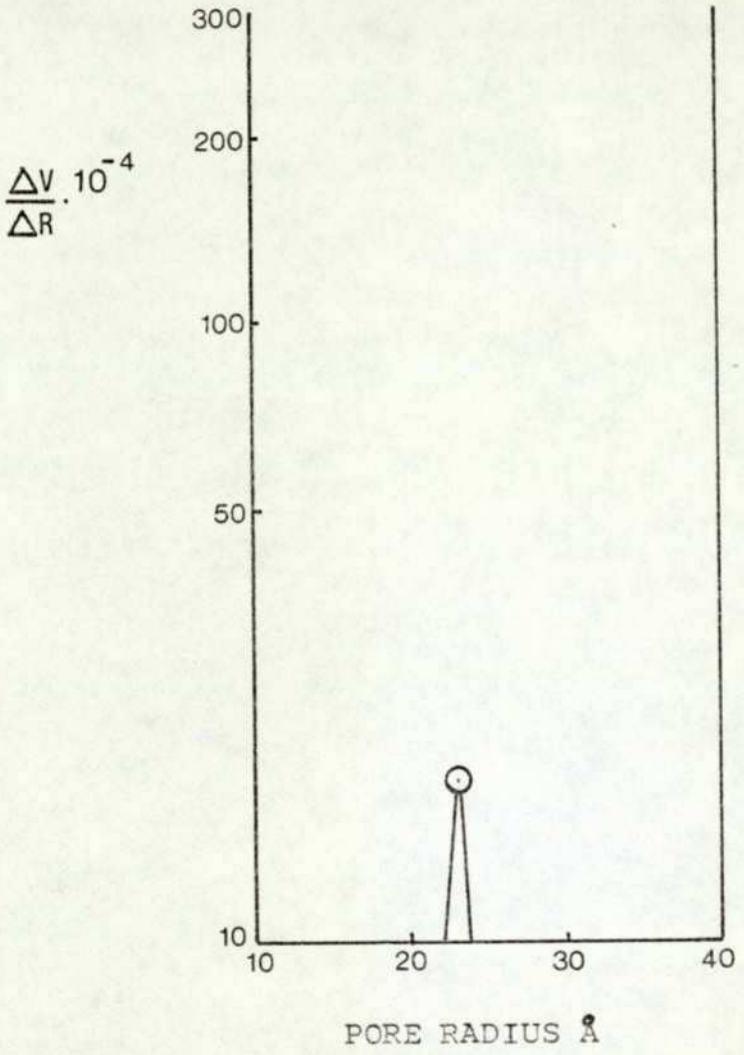

FIGURE 3.27. DIFFERENTIAL PORE SIZE DISTRIBUTION :-

ALUMINA SUPPORTED COPPER(II)OXIDE

WITH 89.0 WEIGHT % LEAD(II)BROMIDE

FIGURE 3.28. CATALYTIC ACTIVITY OF ALUMINA SUPPORTED PLATINUM VARYING WITH LEAD(II)BROMIDE CONTENT

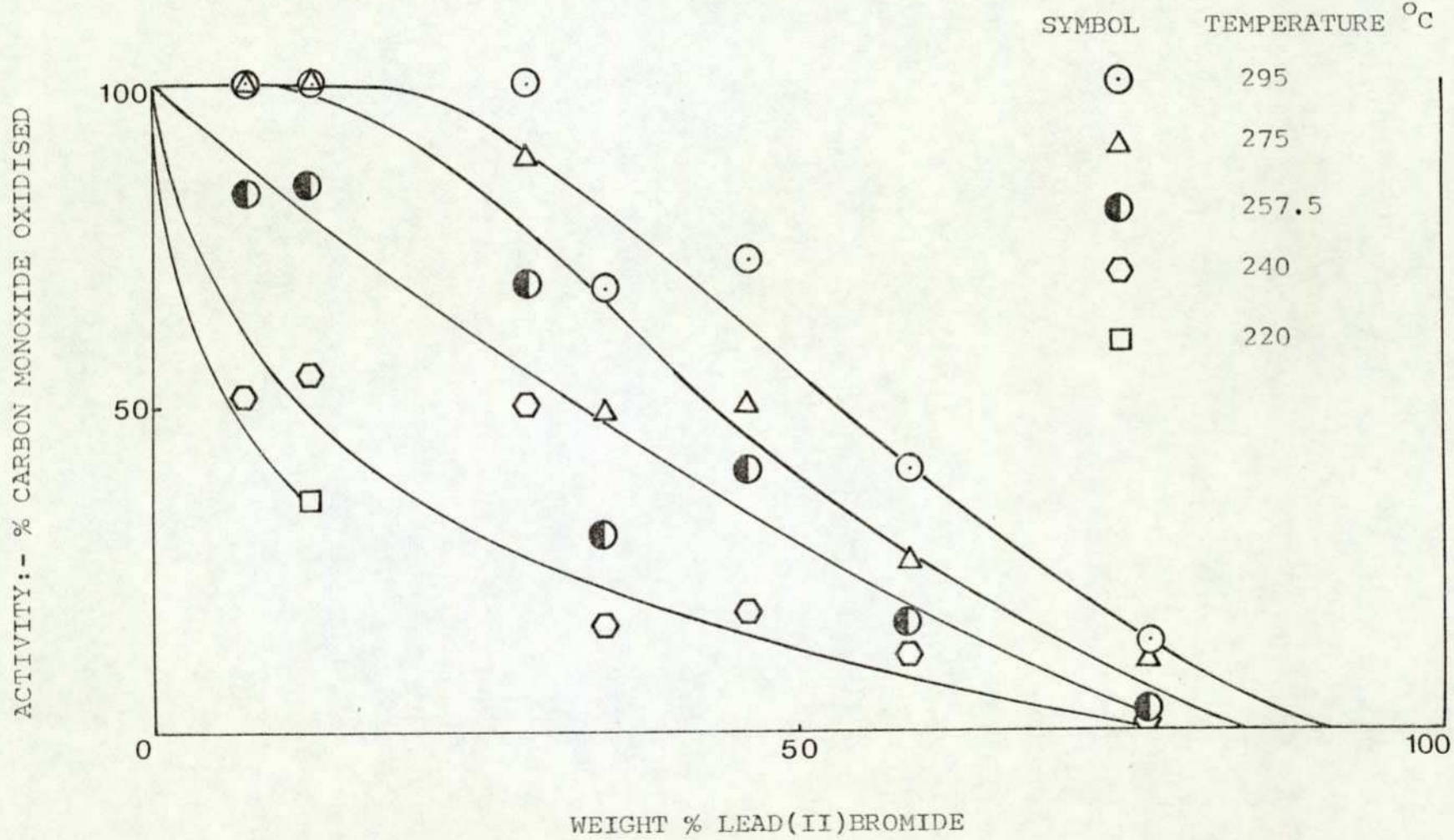

FIGURE 3.29. SURFACE AREA OF ALUMINA SUPPORTED PLATINUM VARYING WITH LEAD(II)BROMIDE CONTENT

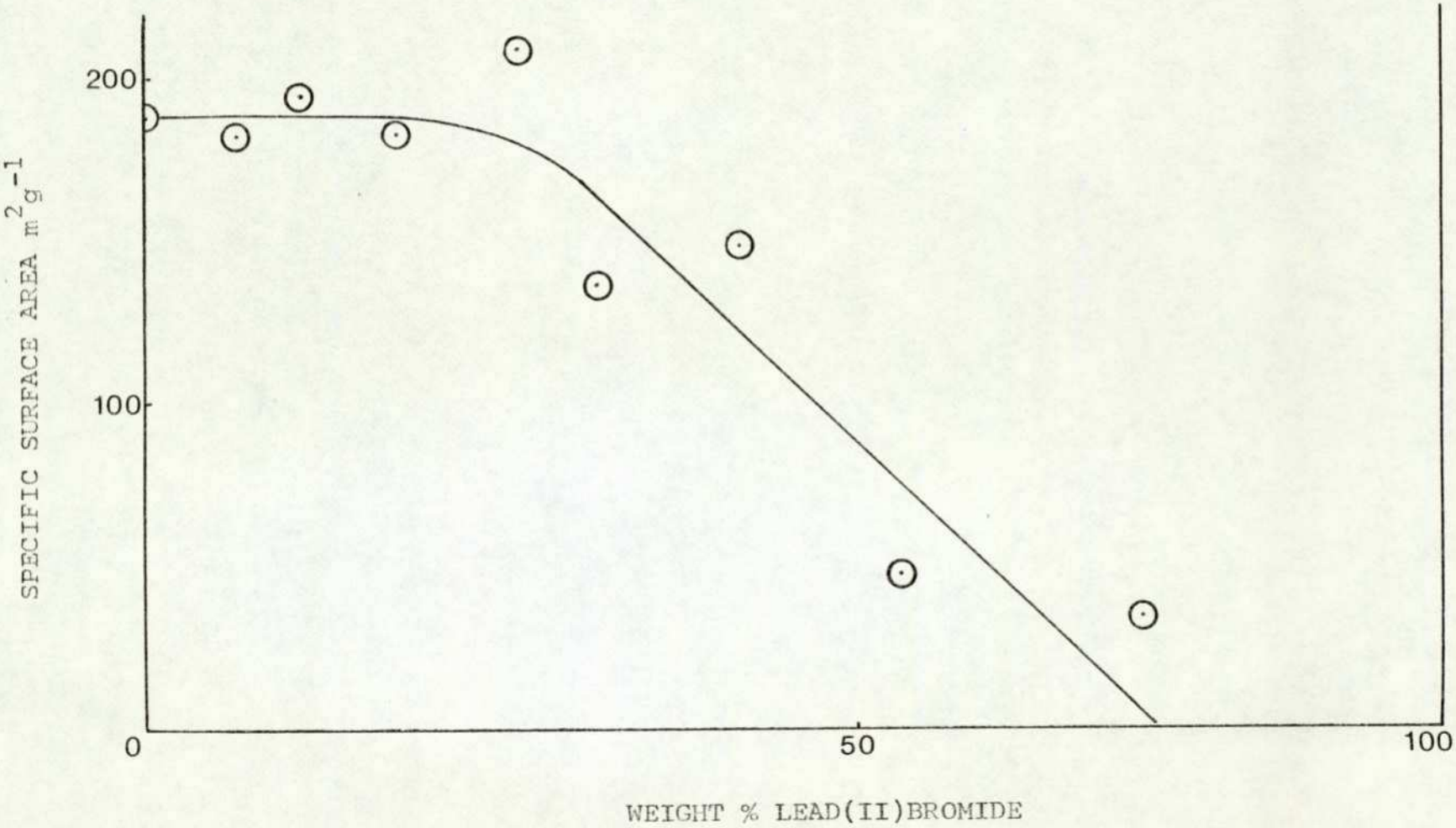

FIGURE 3.30. ACTIVE SURFACE AREA OF ALUMINA SUPPORTED PLATINUM VARYING WITH LEAD(II)BROMIDE CONTENT

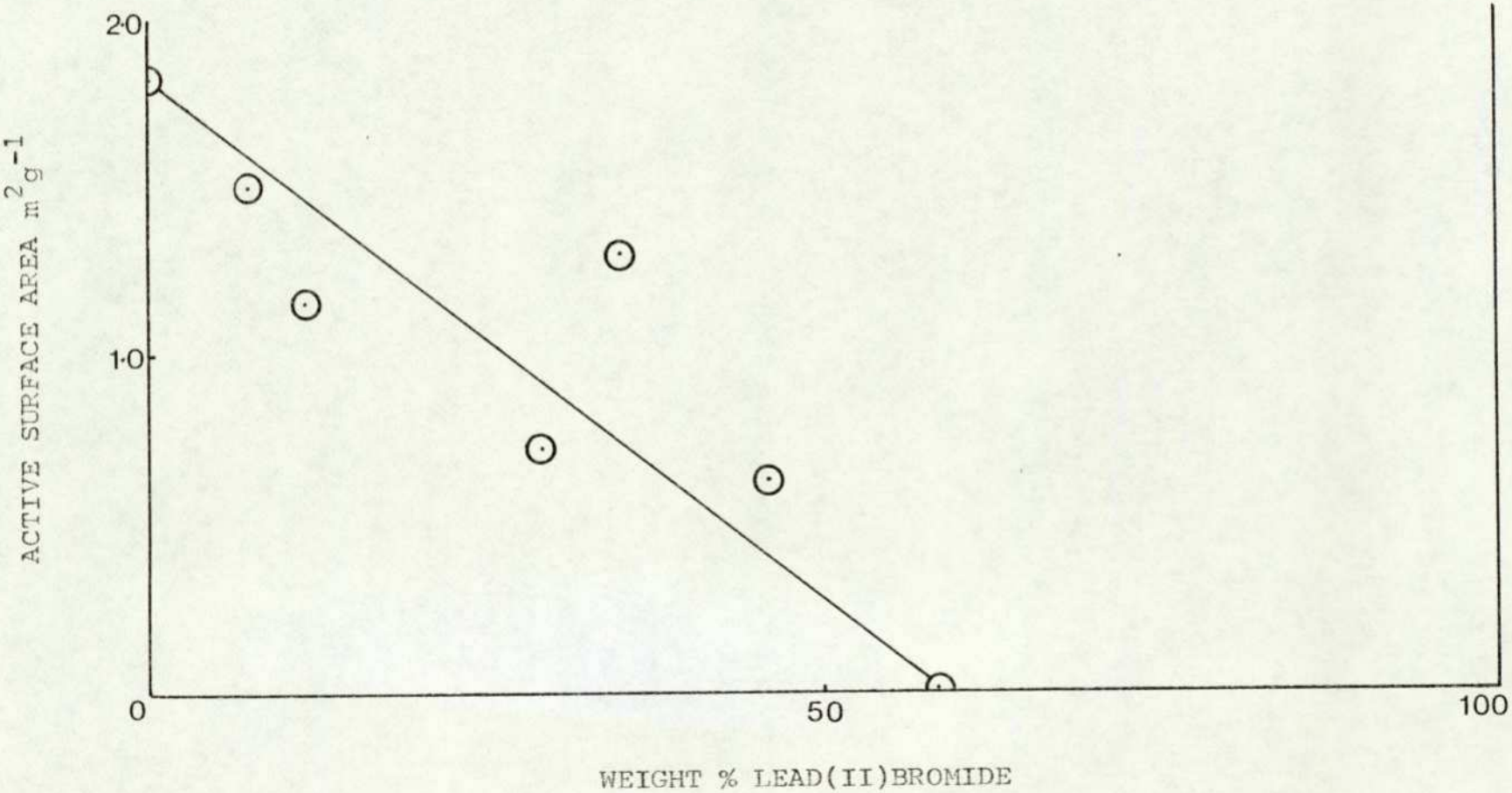

FIGURE 3.31. DIFFERENTIAL PORE SIZE DISTRIBUTION:- ALUMINA SUPPORTED PLATINUM

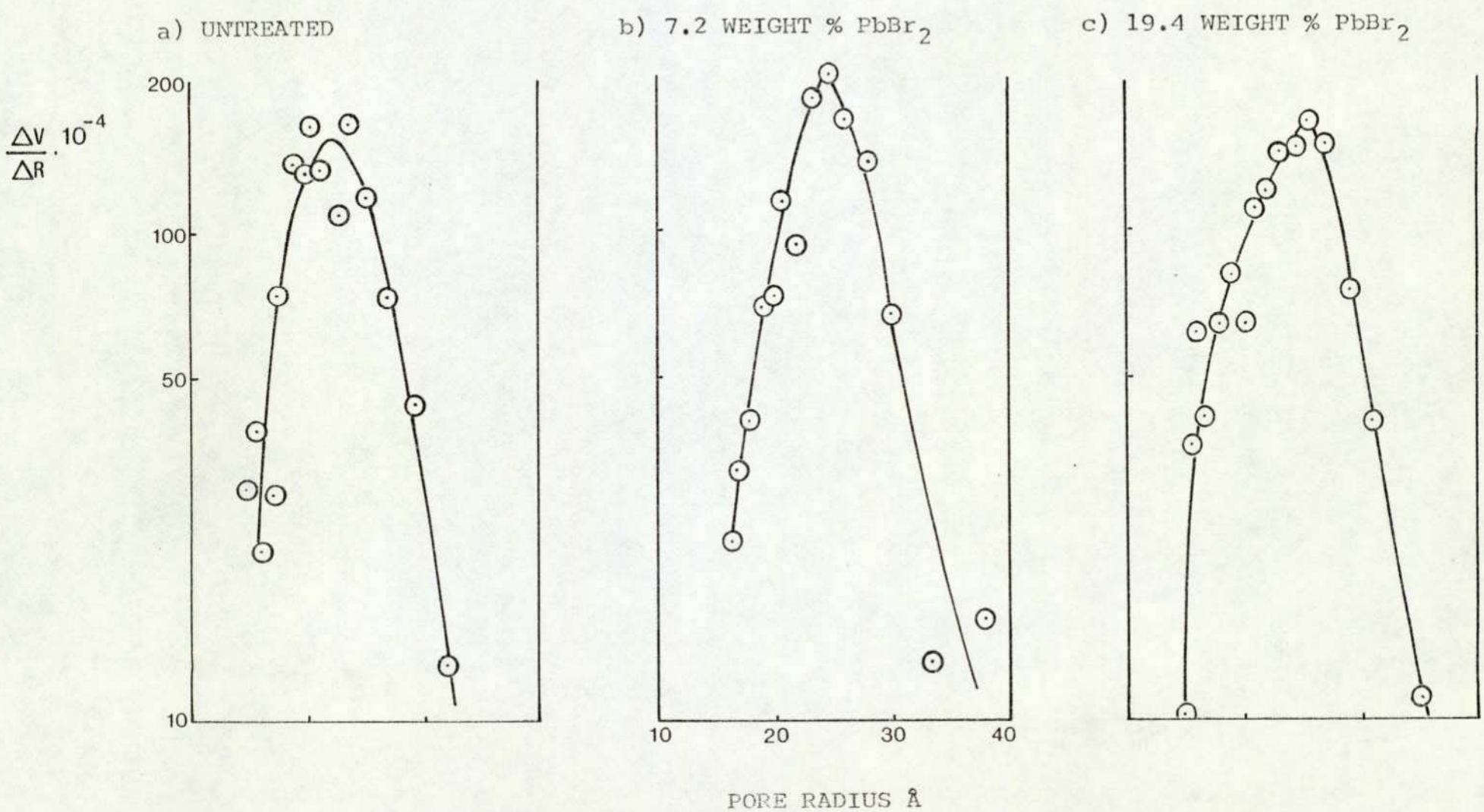

FIGURE 3.32. DIFFERENTIAL PORE SIZE DISTRIBUTION:- ALUMINA SUPPORTED PLATINUM

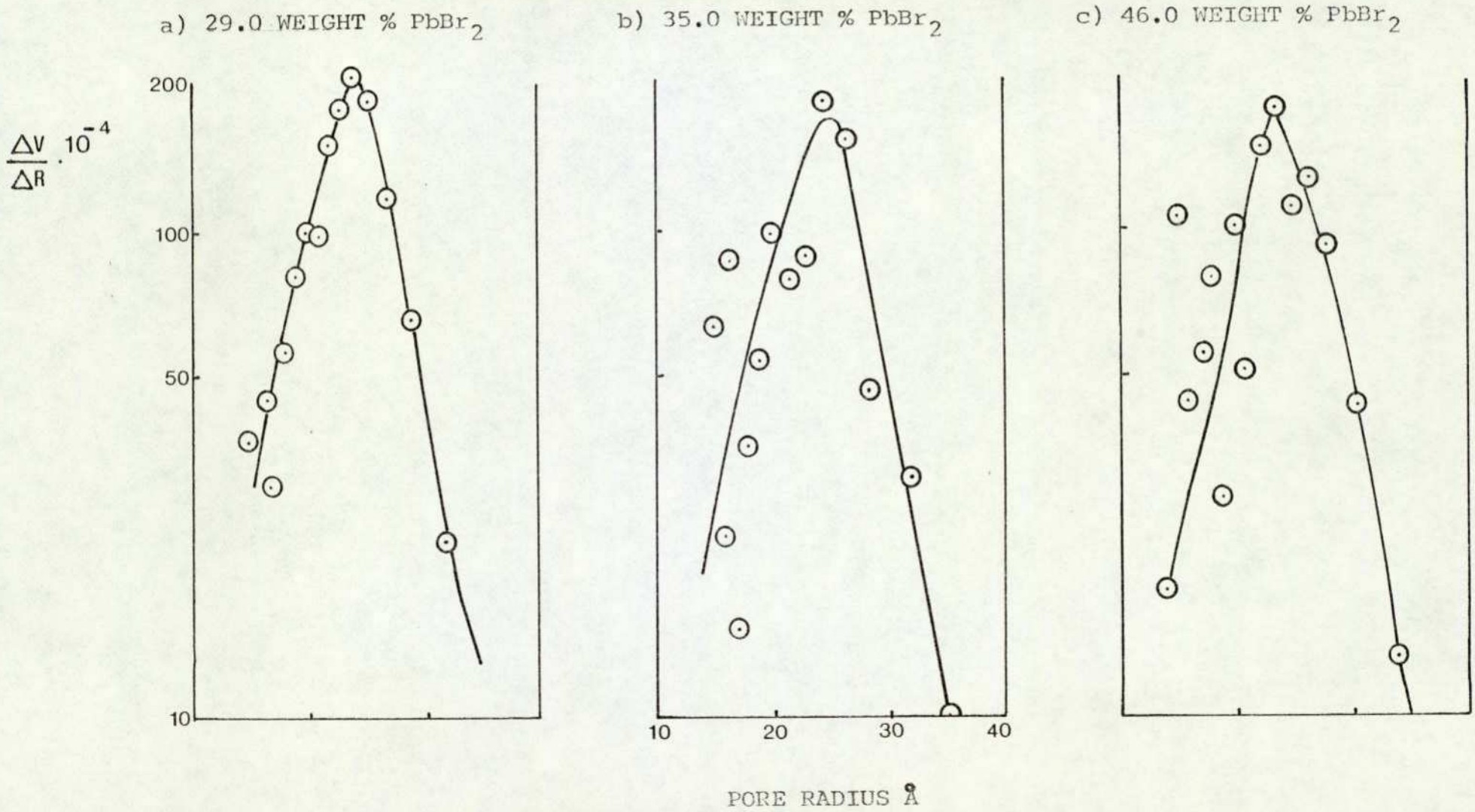

FIGURE 3.33. DIFFERENTIAL PORE SIZE DISTRIBUTION:- ALUMINA SUPPORTED PLATINUM

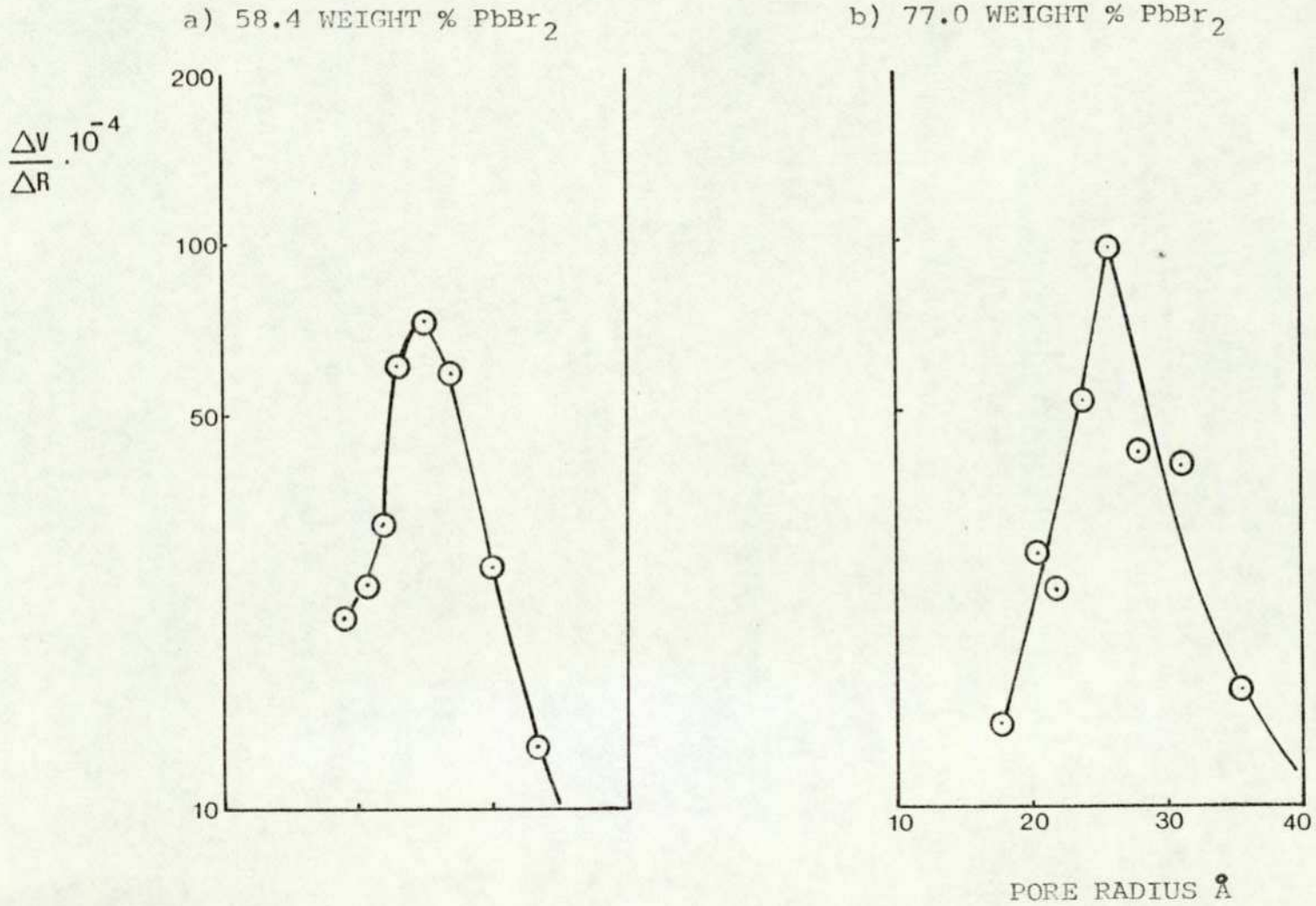

FIGURE 3.34. CATALYTIC ACTIVITY OF COBALT(II,III,III,)OXIDE VARYING WITH LEAD(II)BROMIDE CONTENT

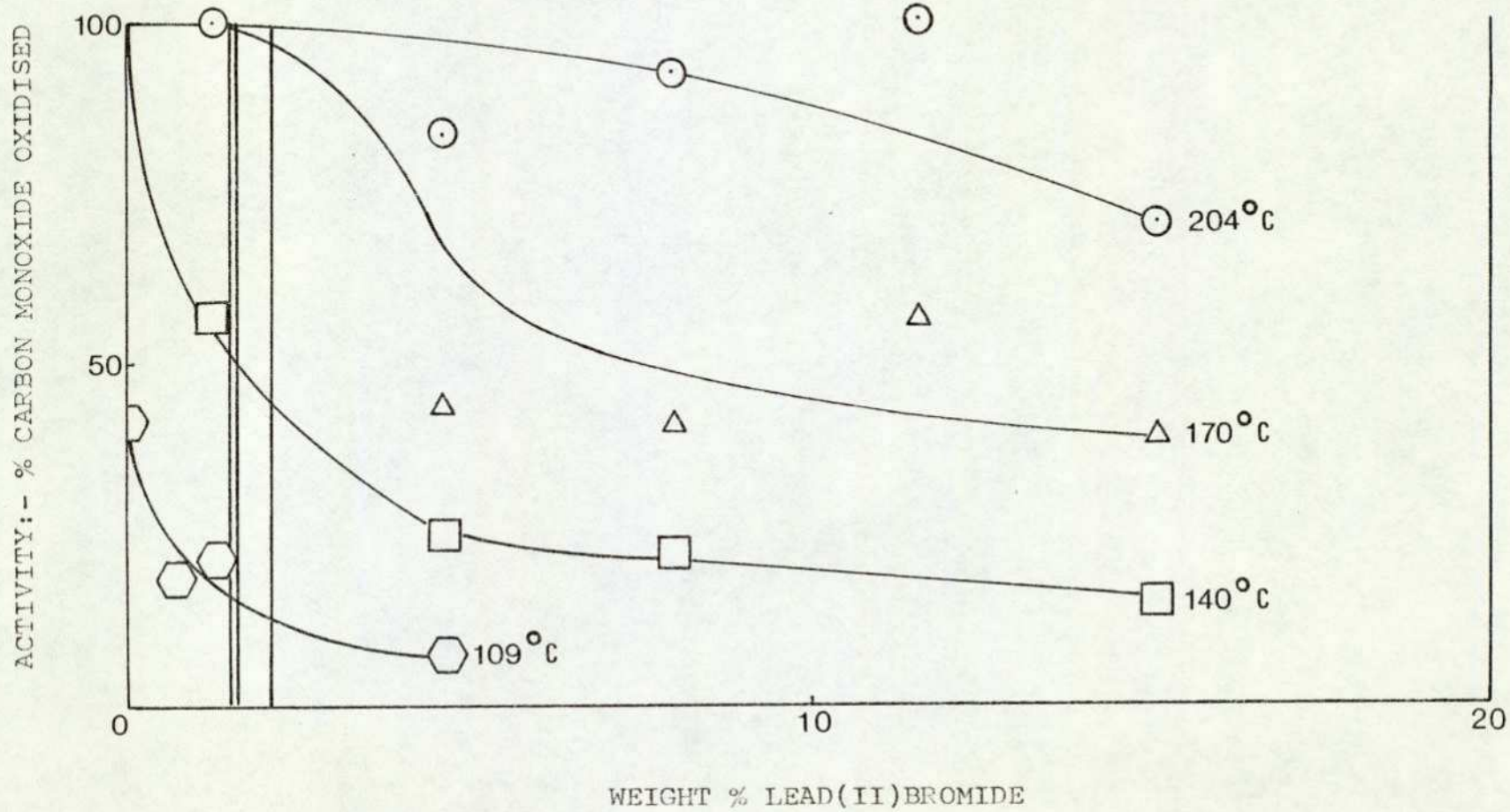

FIGURE 3.35. CATALYTIC ACTIVITY OF COBALT(II,III,III)OXIDE

VARYING WITH LEAD(II)CHLORIDE CONTENT

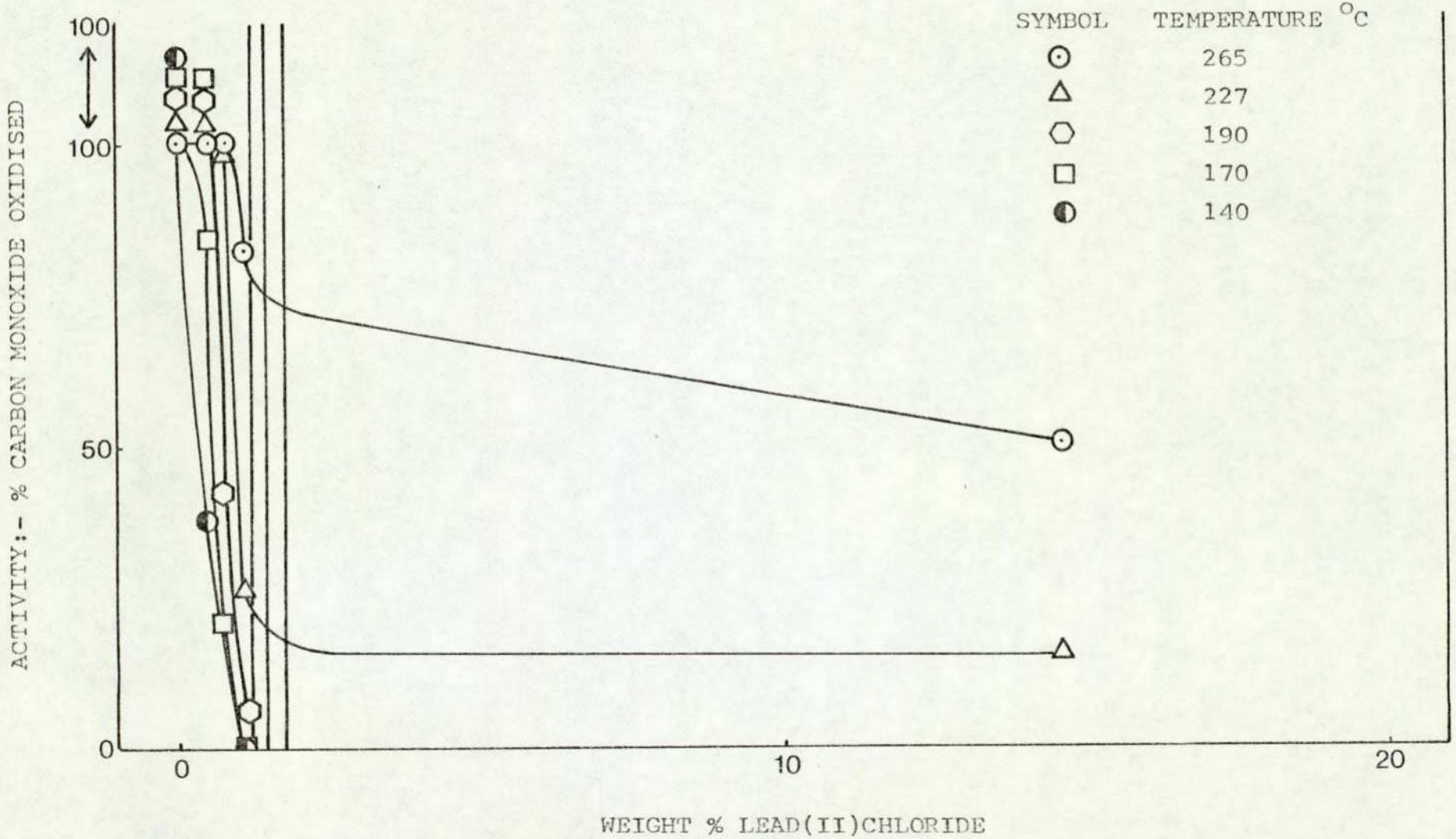

FIGURE 3.36. CATALYTIC ACTIVITY OF ALUMINA SUPPORTED COBALT(II,III,III)OXIDE

VARYING WITH LEAD(II)BROMIDE CONTENT

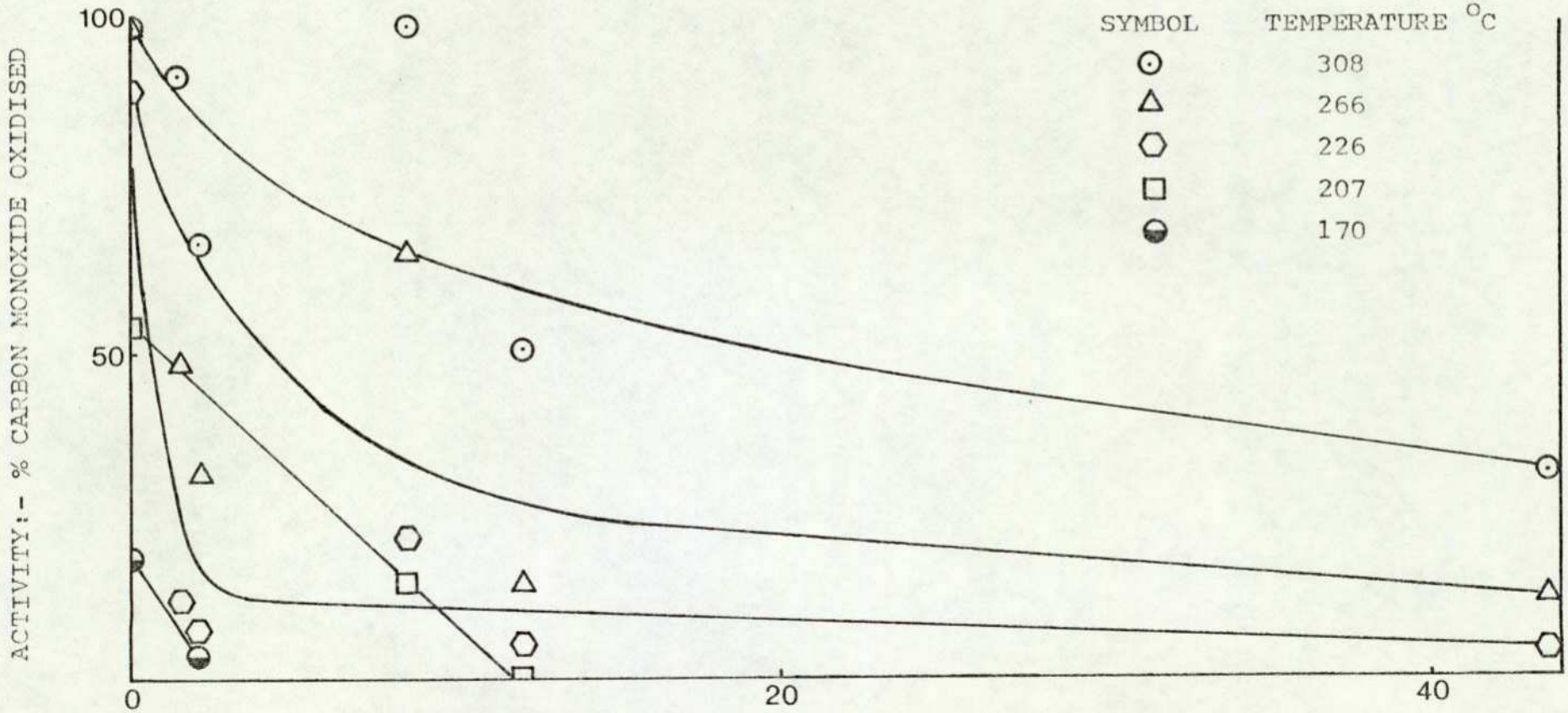

FIGURE 3.37. CATALYTIC ACTIVITY OF ALUMINA SUPPORTED COBALT(II,III,III)OXIDE VARYING WITH LEAD(II)CHLORIDE CONTENT

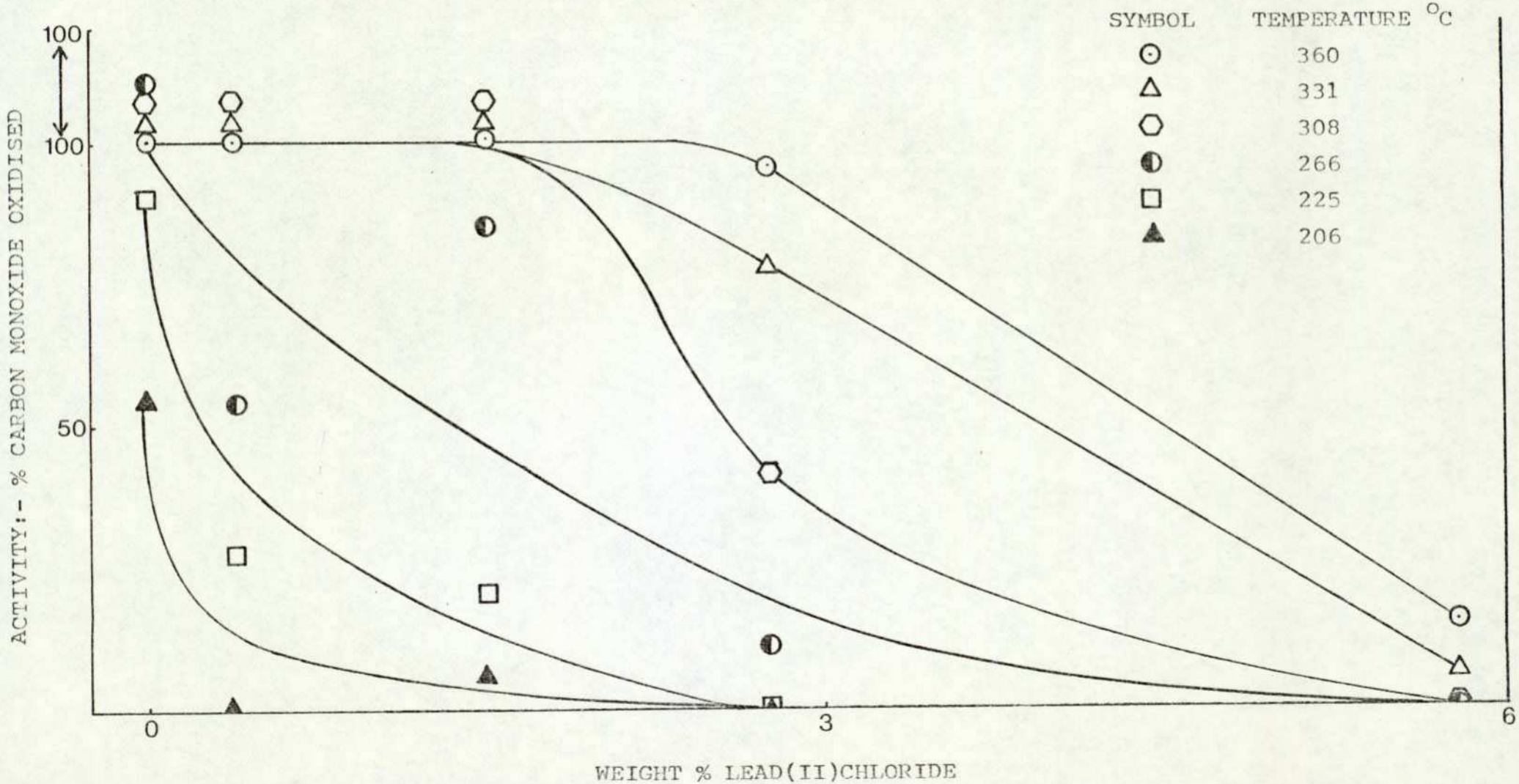

FIGURE 3.38. THE EFFECT OF REMOVAL OF LEAD(II)BROMIDE ON THE CATALYTIC ACTIVITY OF DEACTIVATED COBALT(II,III,III)OXIDE

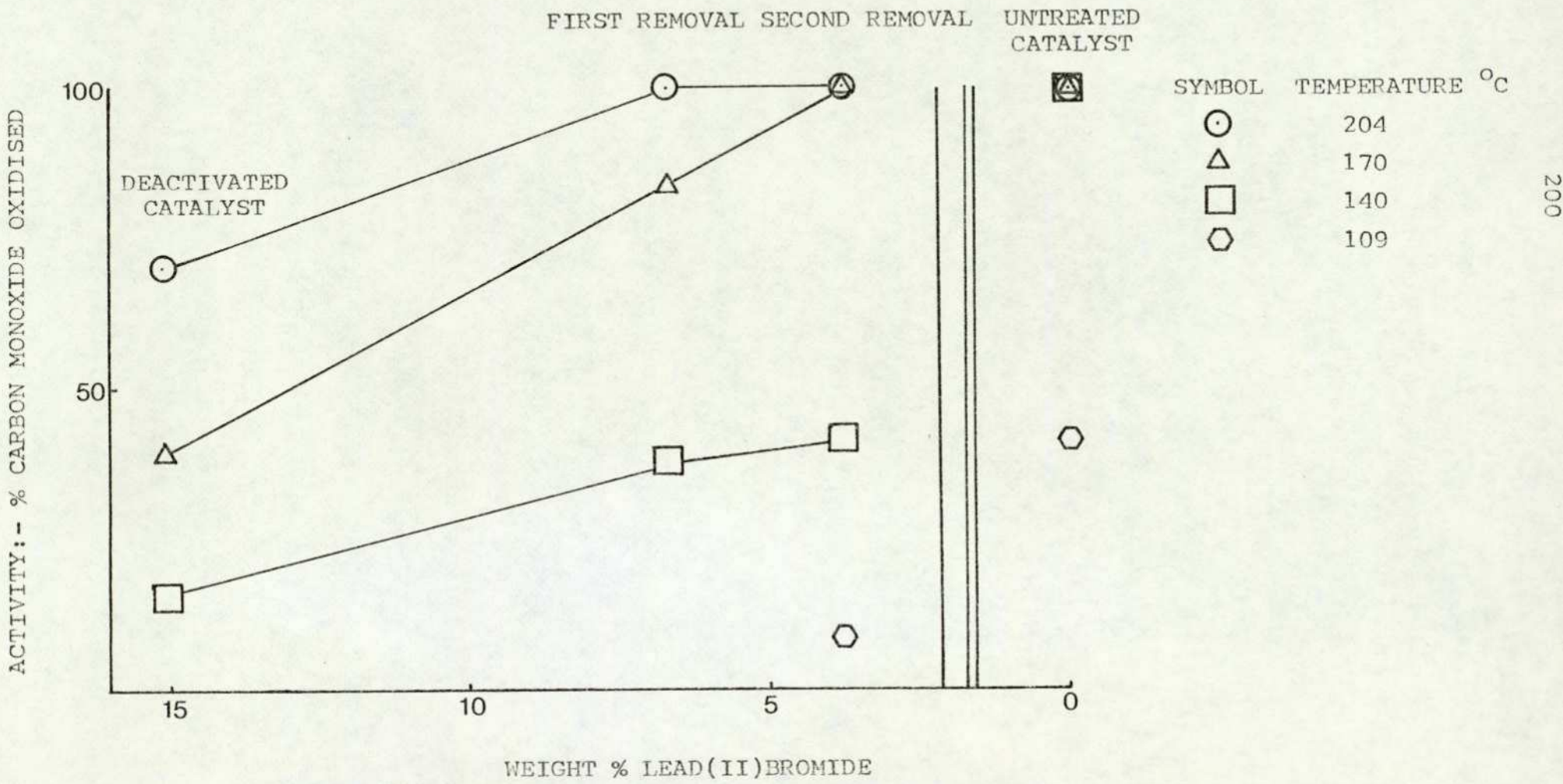

FIGURE 3.39. THE EFFECT OF REMOVAL OF LEAD(II) BROMIDE ON THE CATALYTIC ACTIVITY OF DEACTIVATED COBALT(II,III,III)OXIDE

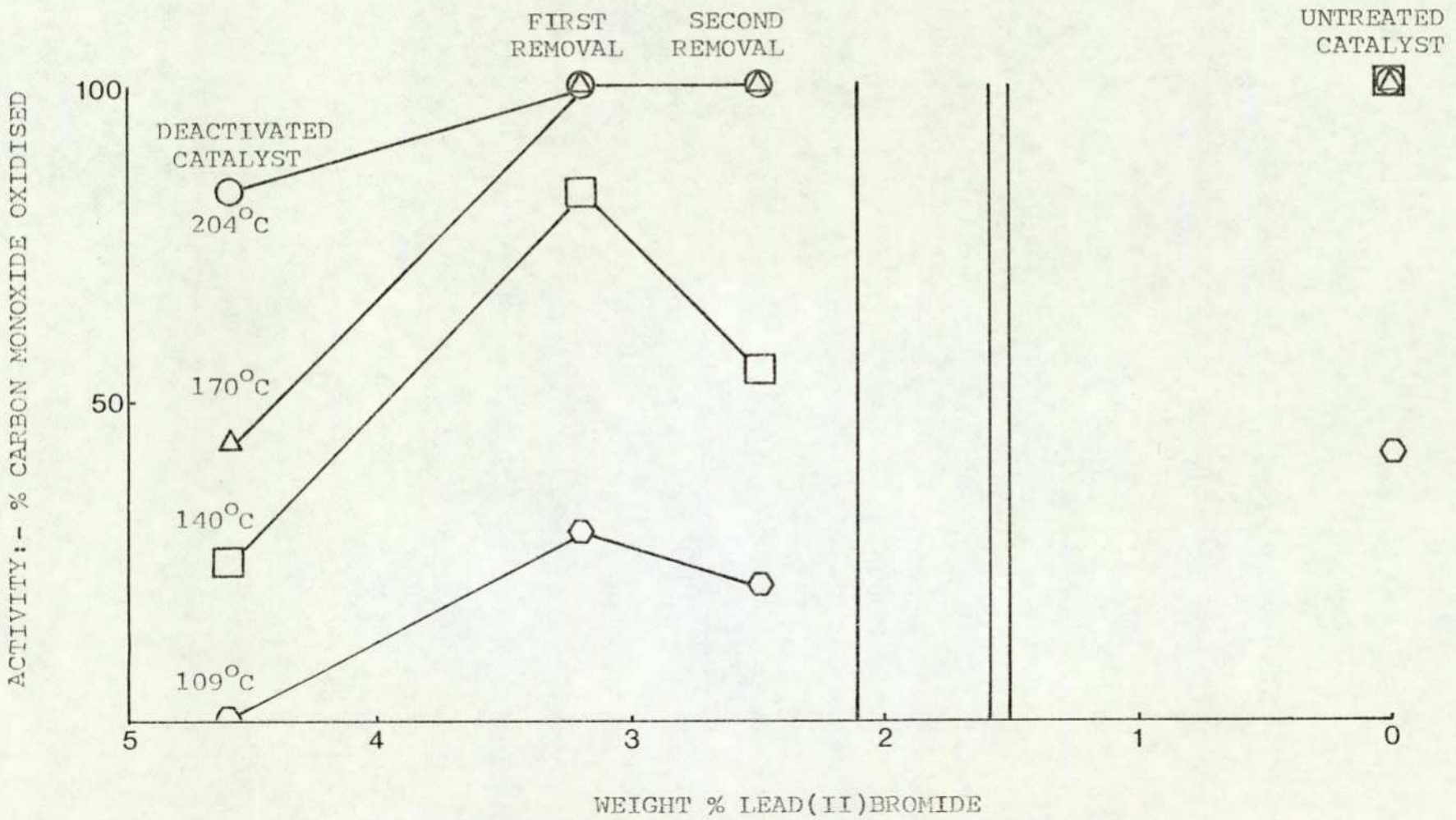

FIGURE 3.40. THE EFFECT OF REMOVAL OF LEAD(II)BROMIDE ON THE CATALYTIC ACTIVITY OF DEACTIVATED ALUMINA SUPPORTED COBALT(II,III,III)OXIDE

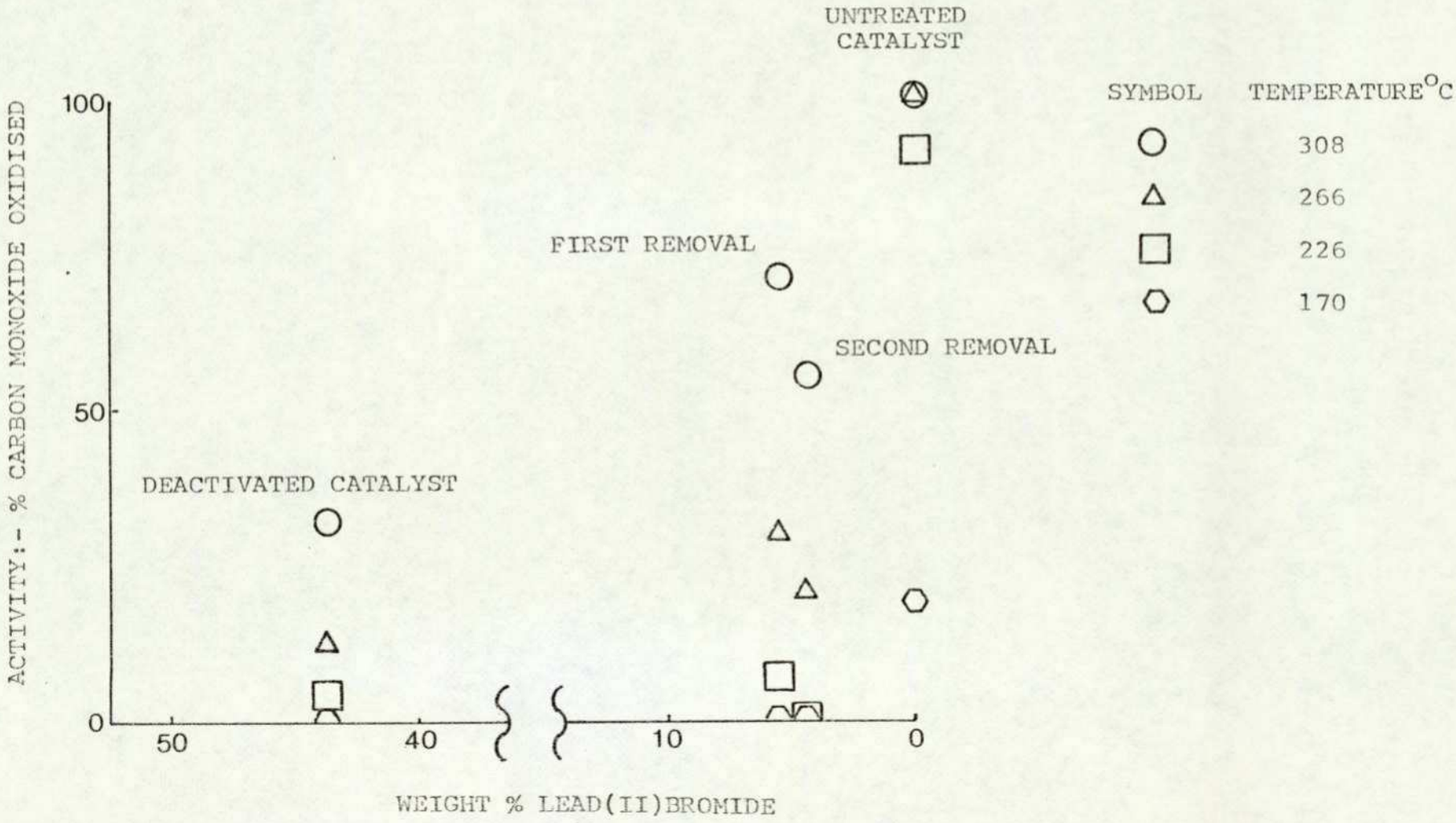

FIGURE 3.41. THE EFFECT OF REMOVAL OF LEAD(II)BROMIDE ON THE SURFACE AREA OF DEACTIVATED ALUMINA SUPPORTED COBALT(II,III,III)OXIDE

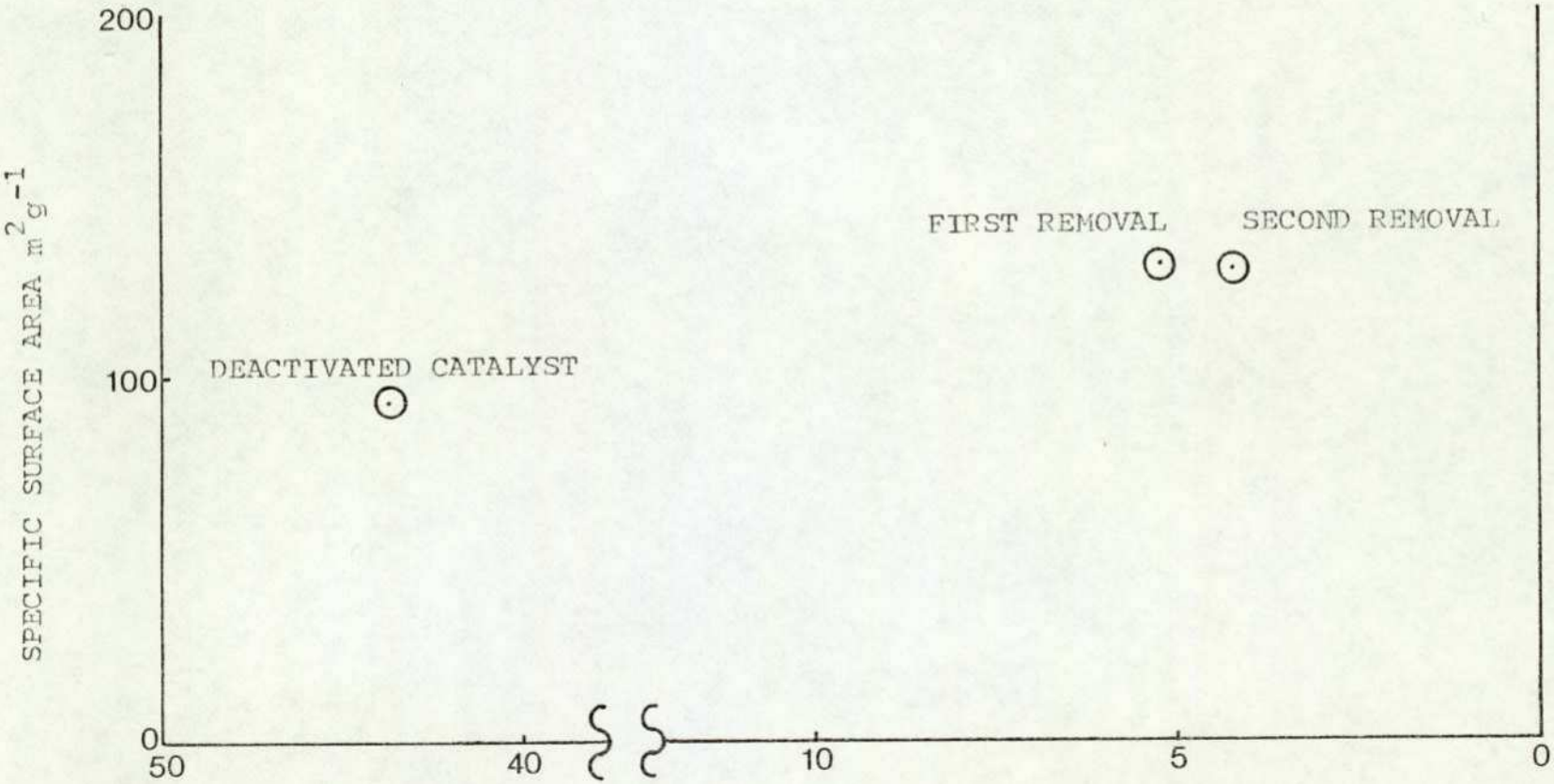

FIGURE 3.42. SURFACE AREA OF COBALT(II,III,III)OXIDE

VARYING WITH LEAD(II)BROMIDE CONTENT

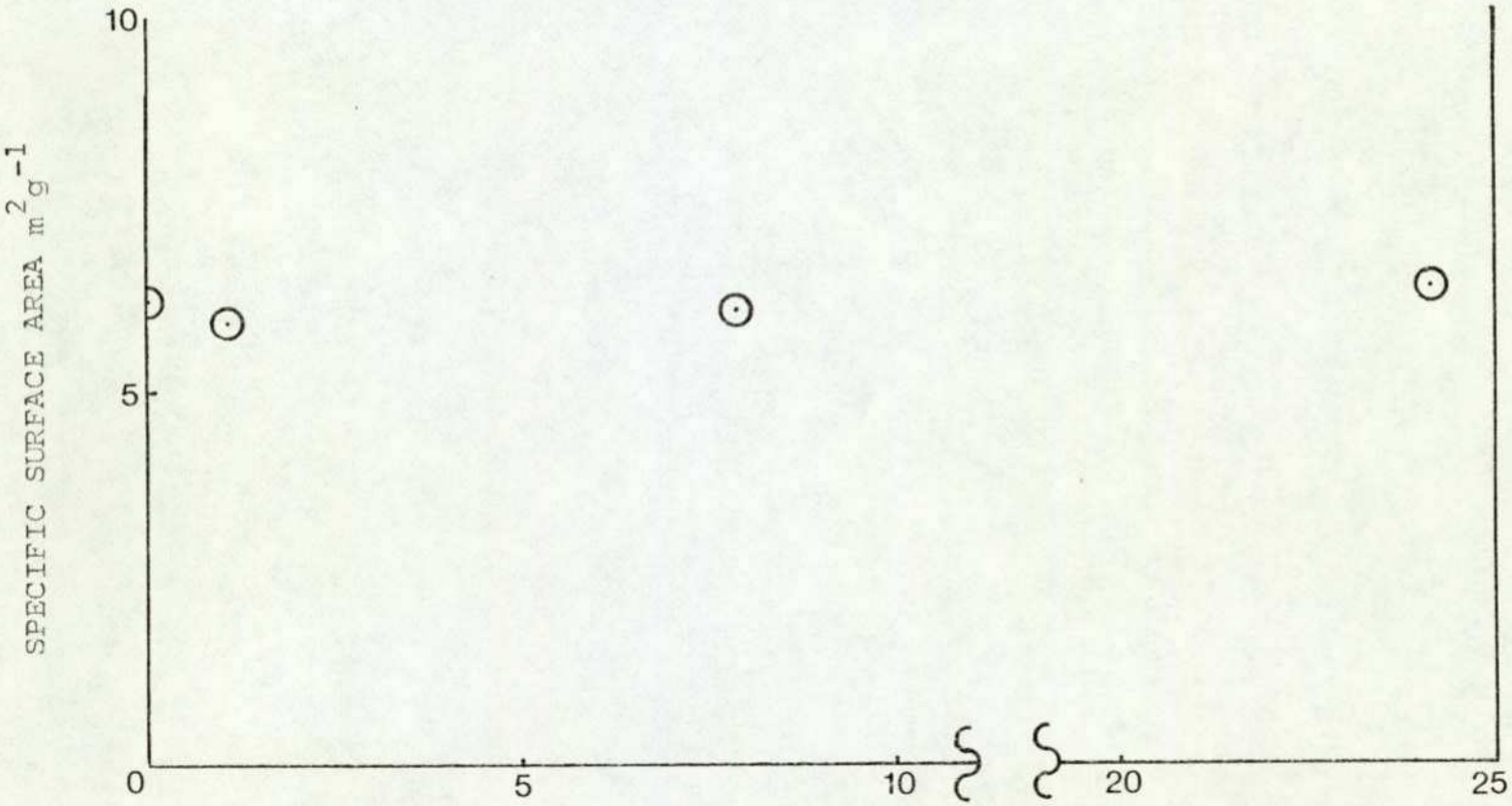

FIGURE 3.43. SURFACE AREA OF ALUMINA SUPPORTED COBALT(II,III,III)OXIDE VARYING WITH LEAD(II)BROMIDE CONTENT

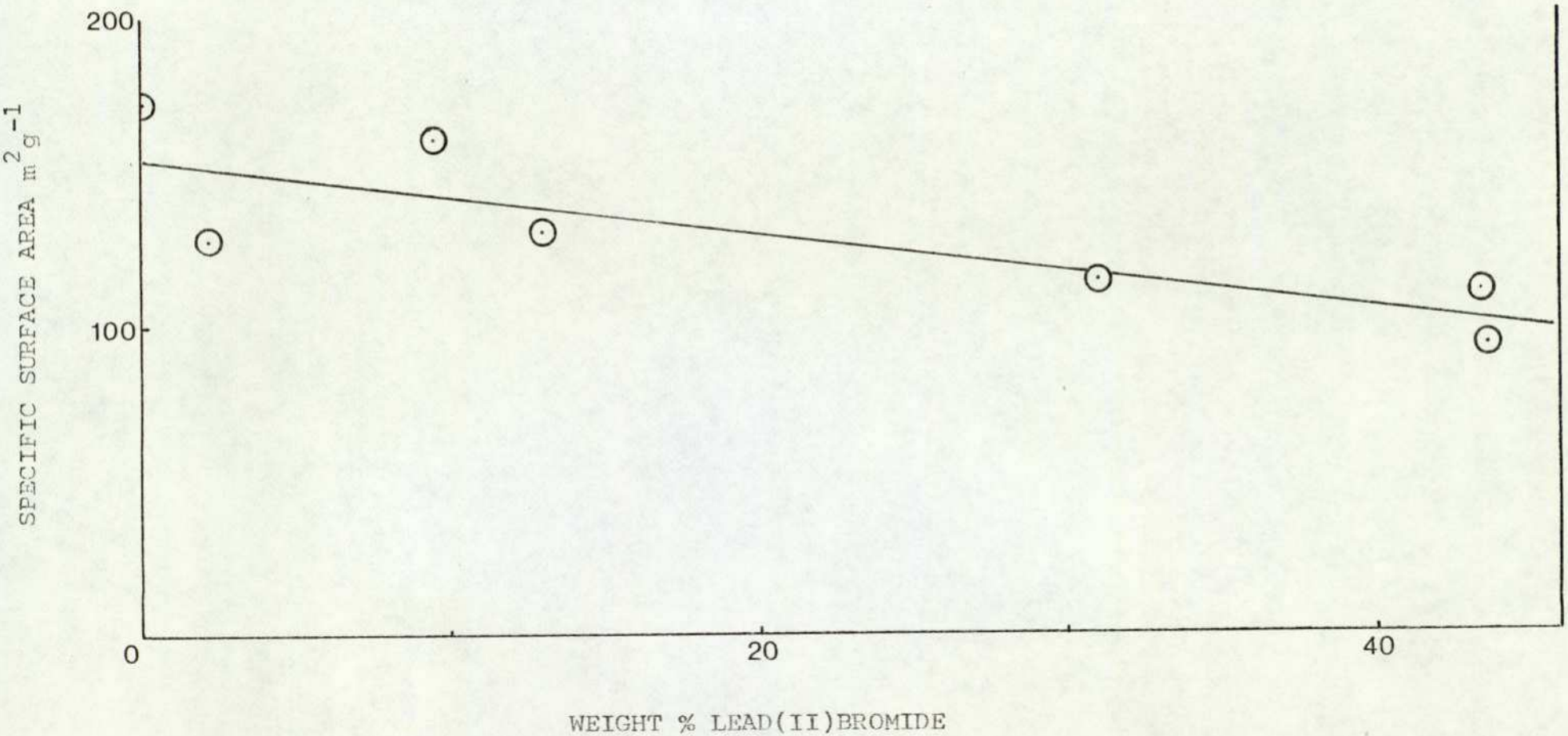

FIGURE 3.44. SURFACE AREA OF ALUMINA SUPPORTED COBALT(II,III,III)OXIDE VARYING WITH LEAD(II)CHLORIDE CONTENT

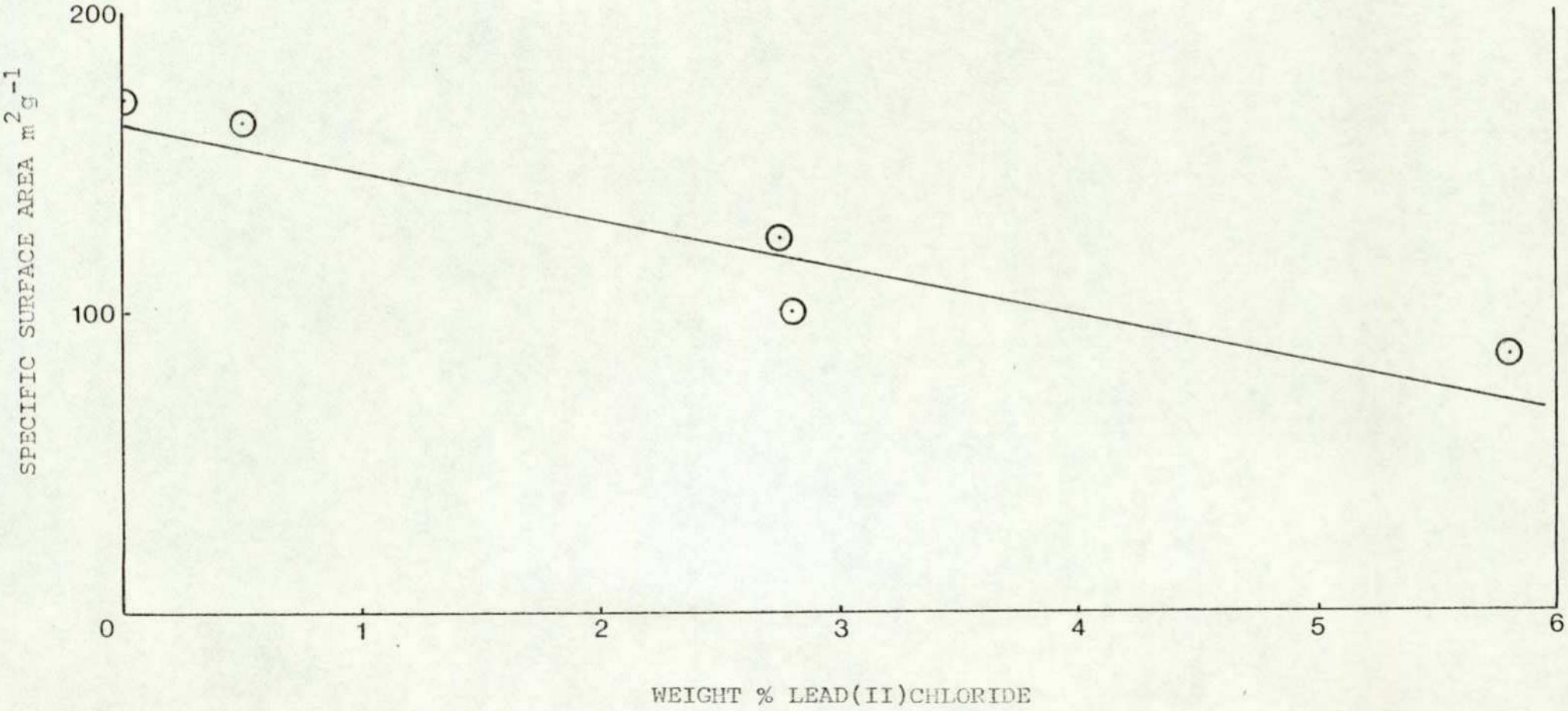

FIGURE 3.45. DIFFERENTIAL PORE SIZE DISTRIBUTION:- ALUMINA SUPPORTED COBALT(II,III,III)OXIDE

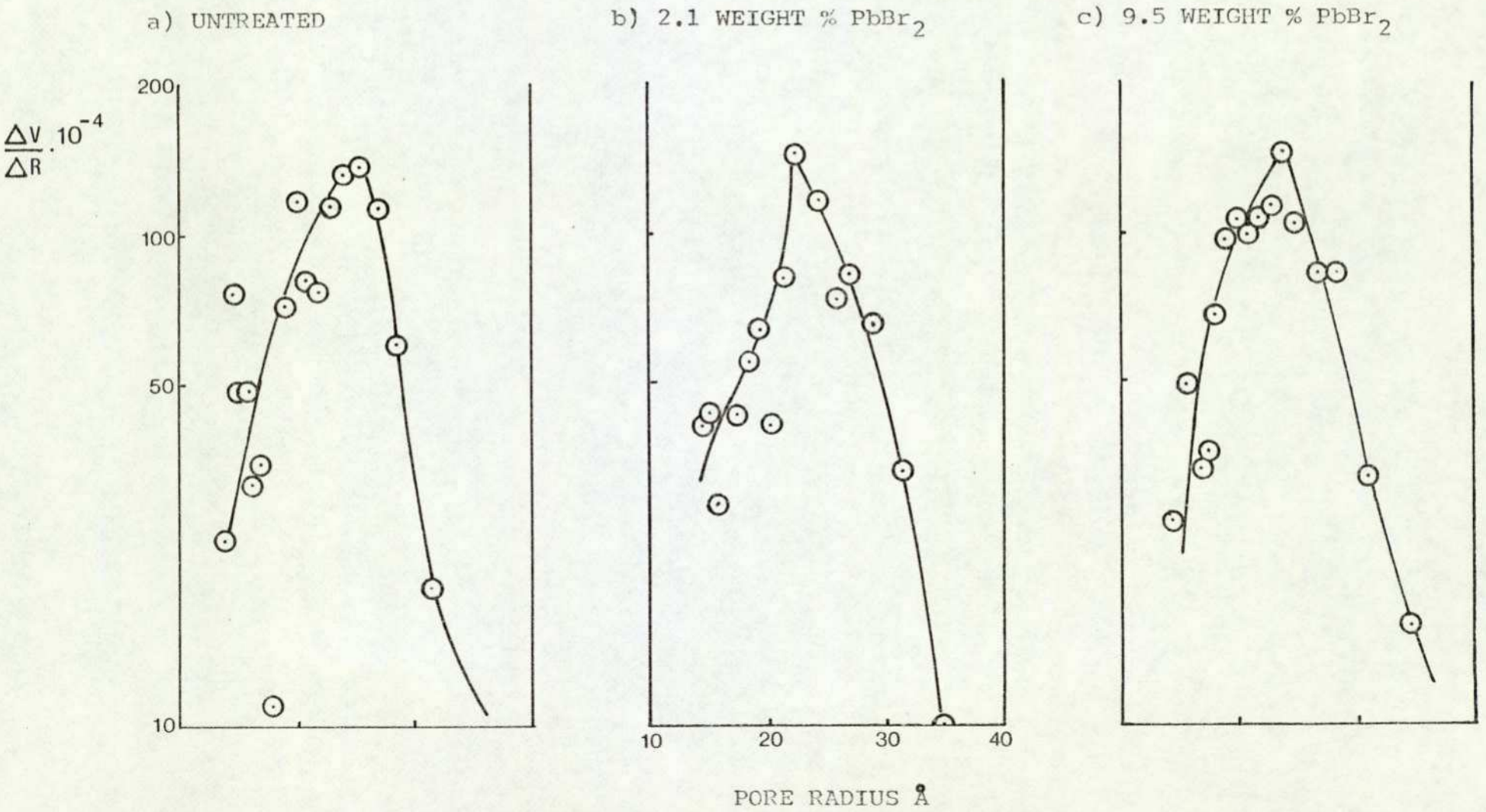

FIGURE 3.46. DIFFERENTIAL PORE SIZE DISTRIBUTION:- ALUMINA SUPPORTED COBALT(II,III,III)OXIDE

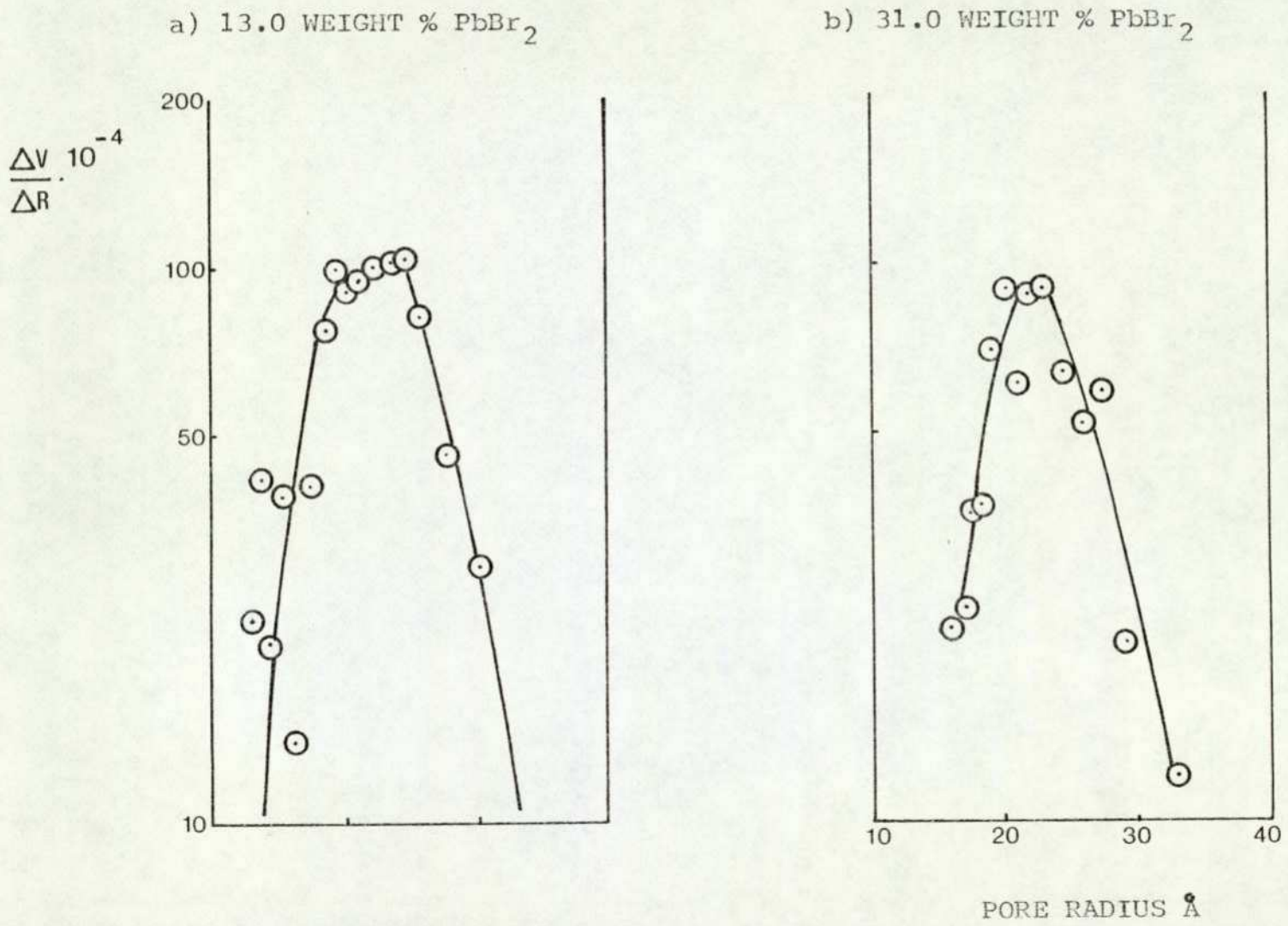

FIGURE 3.47. DIFFERENTIAL PORE SIZE DISTRIBUTION:- ALUMINA SUPPORTED COBALT(II,III,III)OXIDE

a) 43.7 WEIGHT % $PbBr_2$ b) FIRST REMOVAL (5.4 Wt % $PbBr_2$) c) SECOND REMOVAL (4.4 Wt% $PbBr_2$)

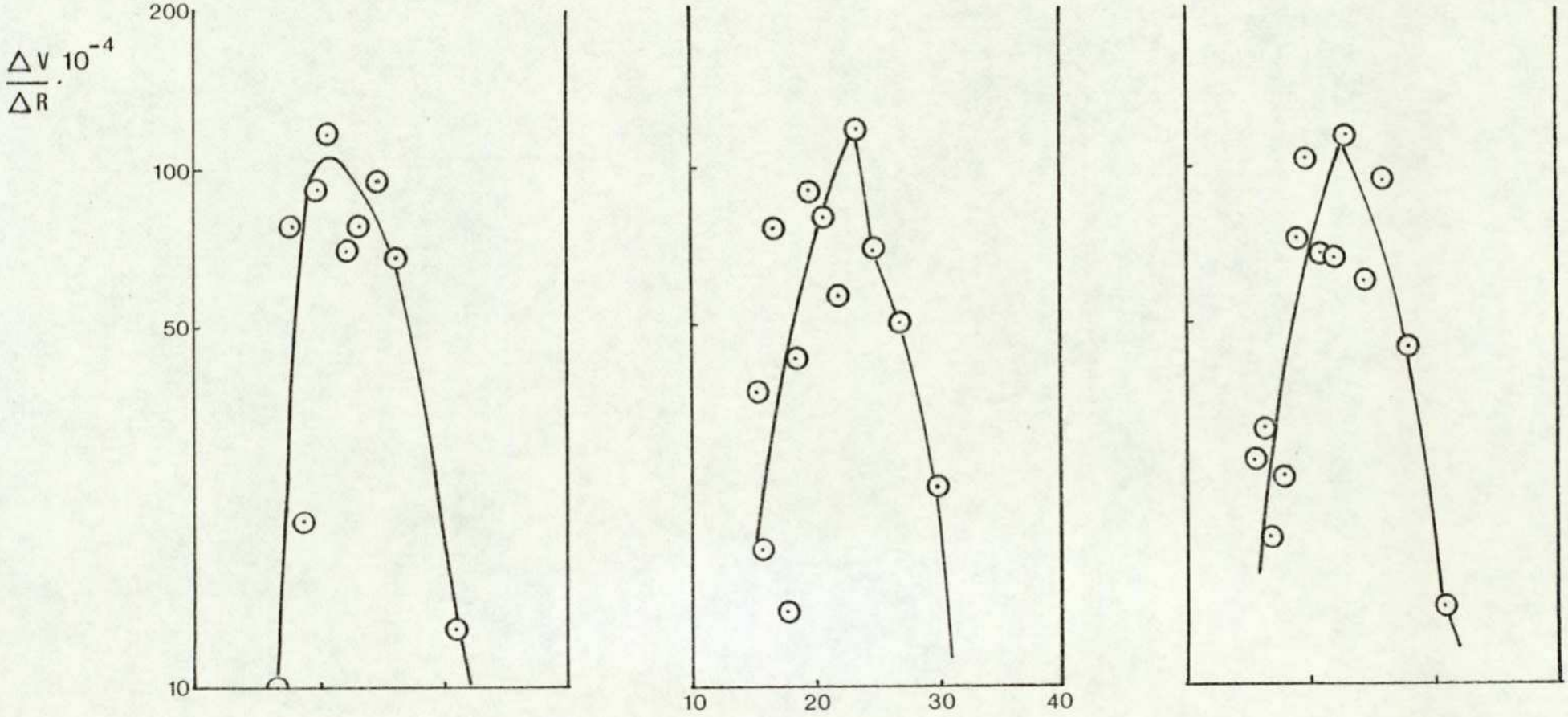

FIGURE 3.48. DIFFERENTIAL PORE SIZE DISTRIBUTION:- ALUMINA SUPPORTED COBALT(II,III,III)OXIDE

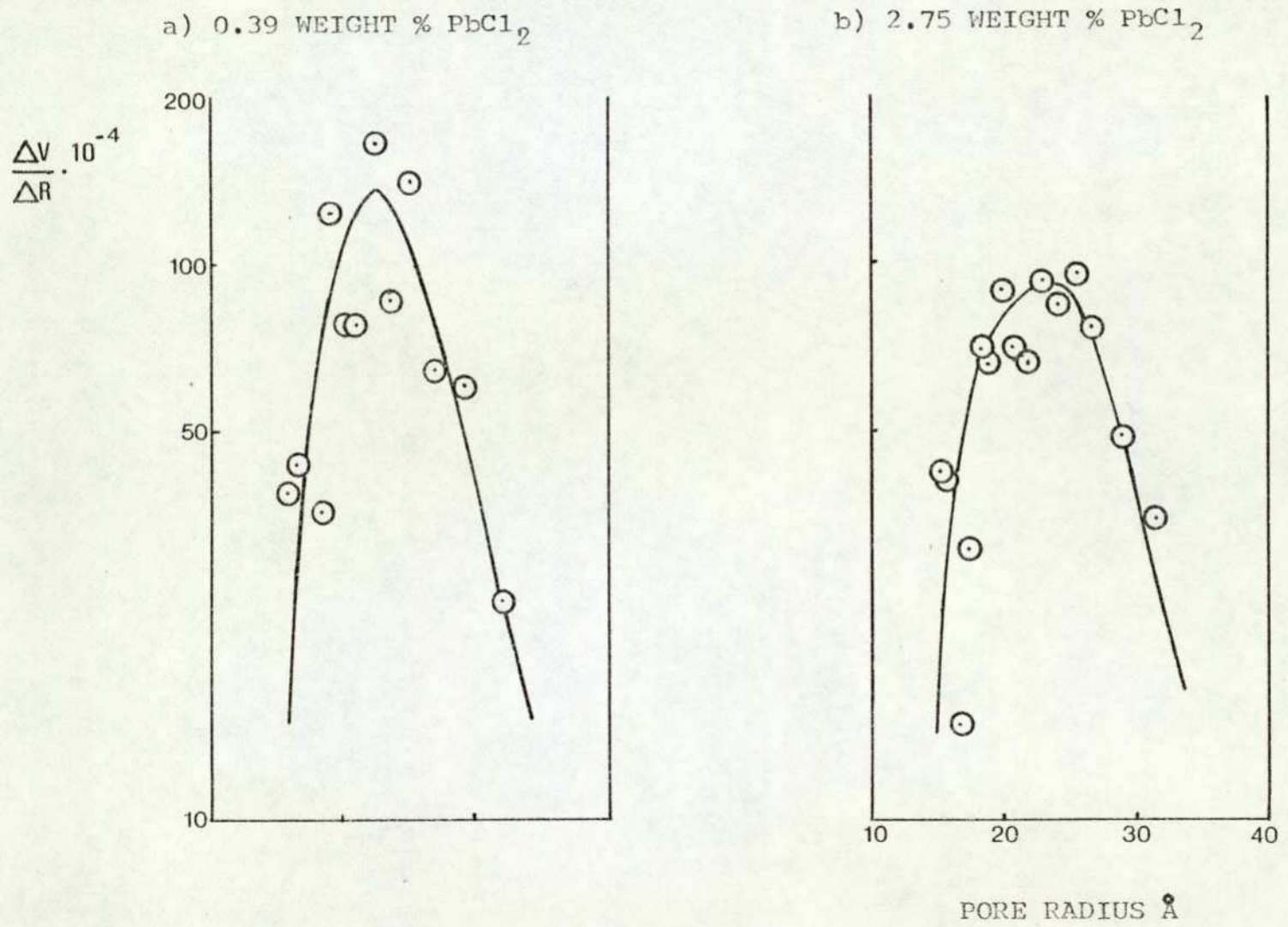

FIGURE 3.49. DIFFERENTIAL PORE SIZE DISTRIBUTION:-ALUMINA SUPPORTED COBALT(II,III,III)OXIDE

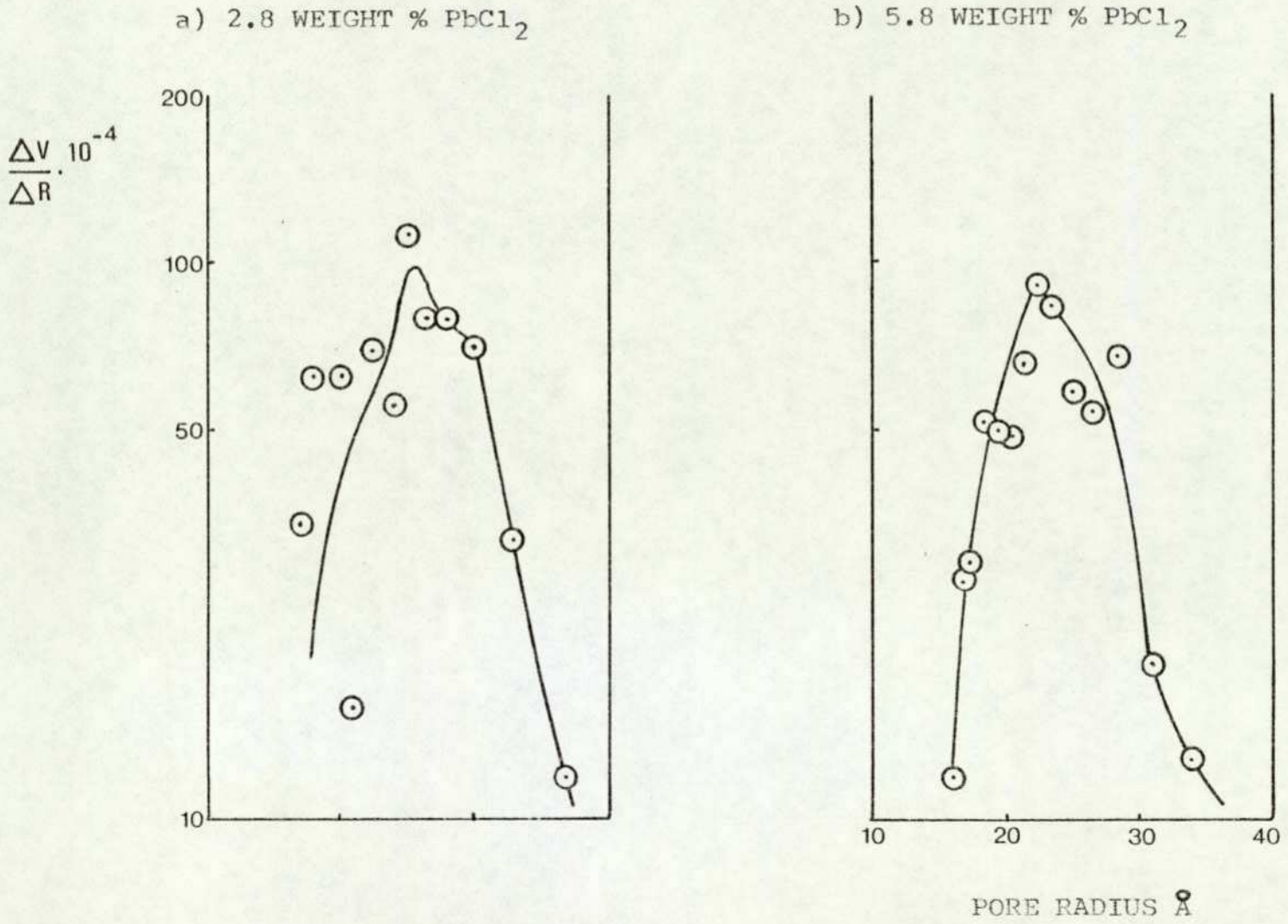

a) Co_3O_4 SAMPLE Wt 35.85 mg

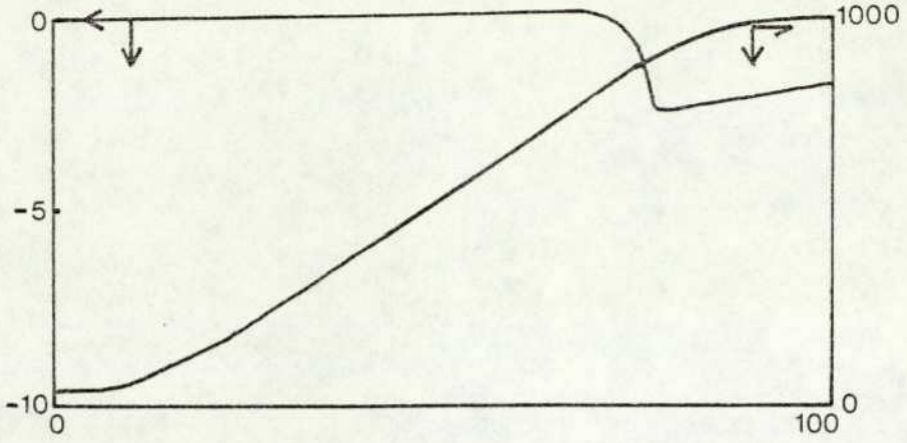

b) Co_3O_4 WITH 4.2 Wt% $PbBr_2$.SAMPLE Wt 209 mg

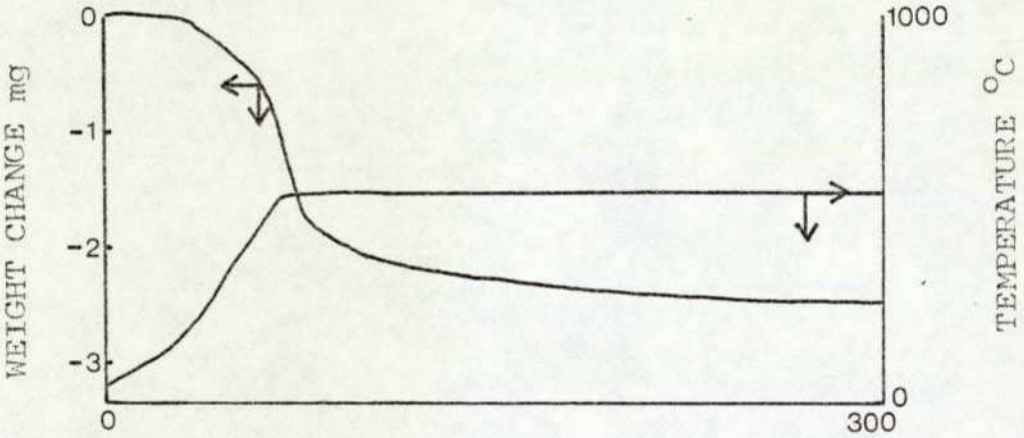

c) Co_3O_4 WITH 6.2 Wt% $PbBr_2$.SAMPLE Wt 108 mg

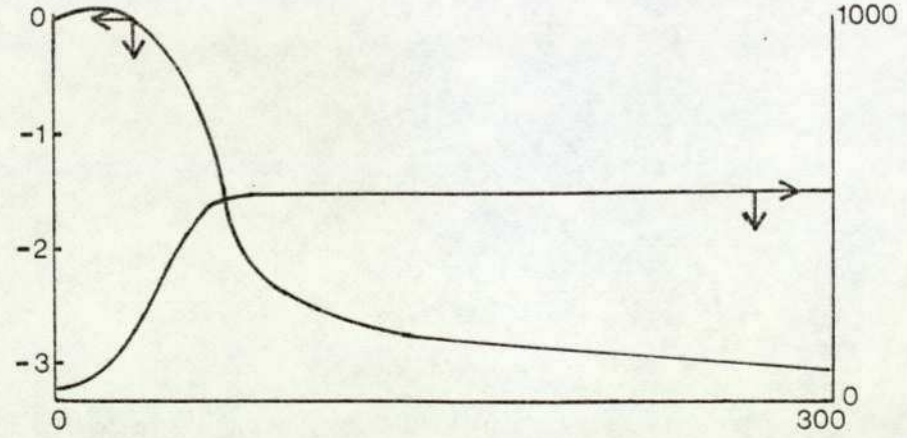

TIME min

FIGURE 3.50. THERMOGRAVIMETRIC ANALYSIS

HEATING RATE 10°C min^{-1}

a) Co_3O_4 WITH 11.3 Wt% $PbBr_2$.SAMPLE Wt 34.72 mg

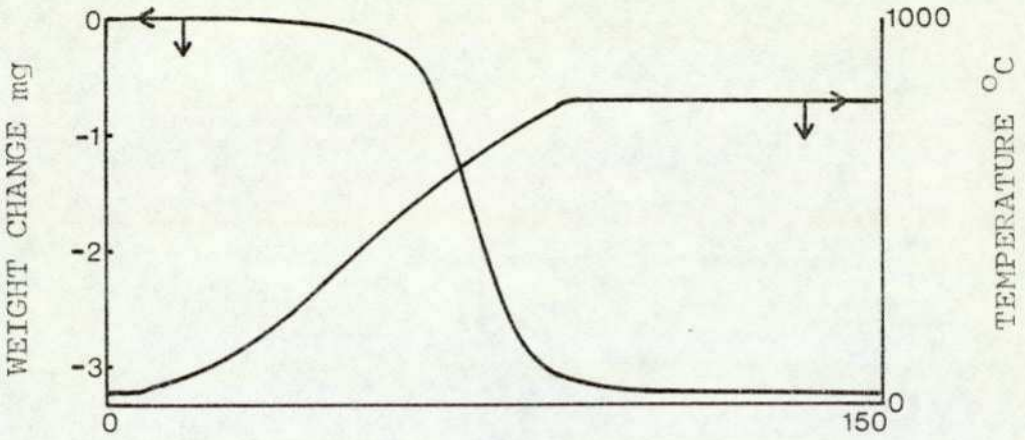

b) Co_3O_4 WITH 15.1 Wt% $PbBr_2$.SAMPLE Wt 35.6 mg

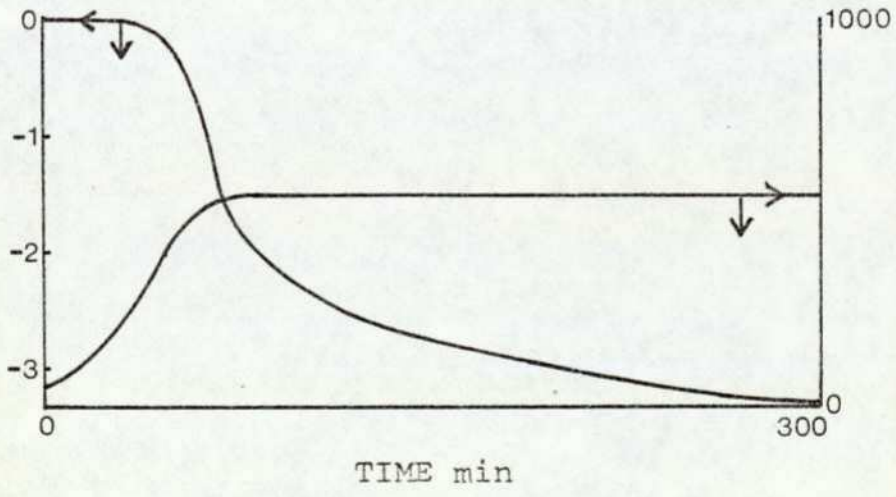

FIGURE 3.51. THERMOGRAVIMETRIC ANALYSIS

HEATING RATE $10^{o}C\ min^{-1}$

FIGURE 3.52. DIFFERENTIAL THERMAL ANALYSIS:- COBALT(II,III,III)OXIDE

SAMPLE WEIGHT 40.53 mg.HEATING RATE $5^{o}C\ min^{-1}$

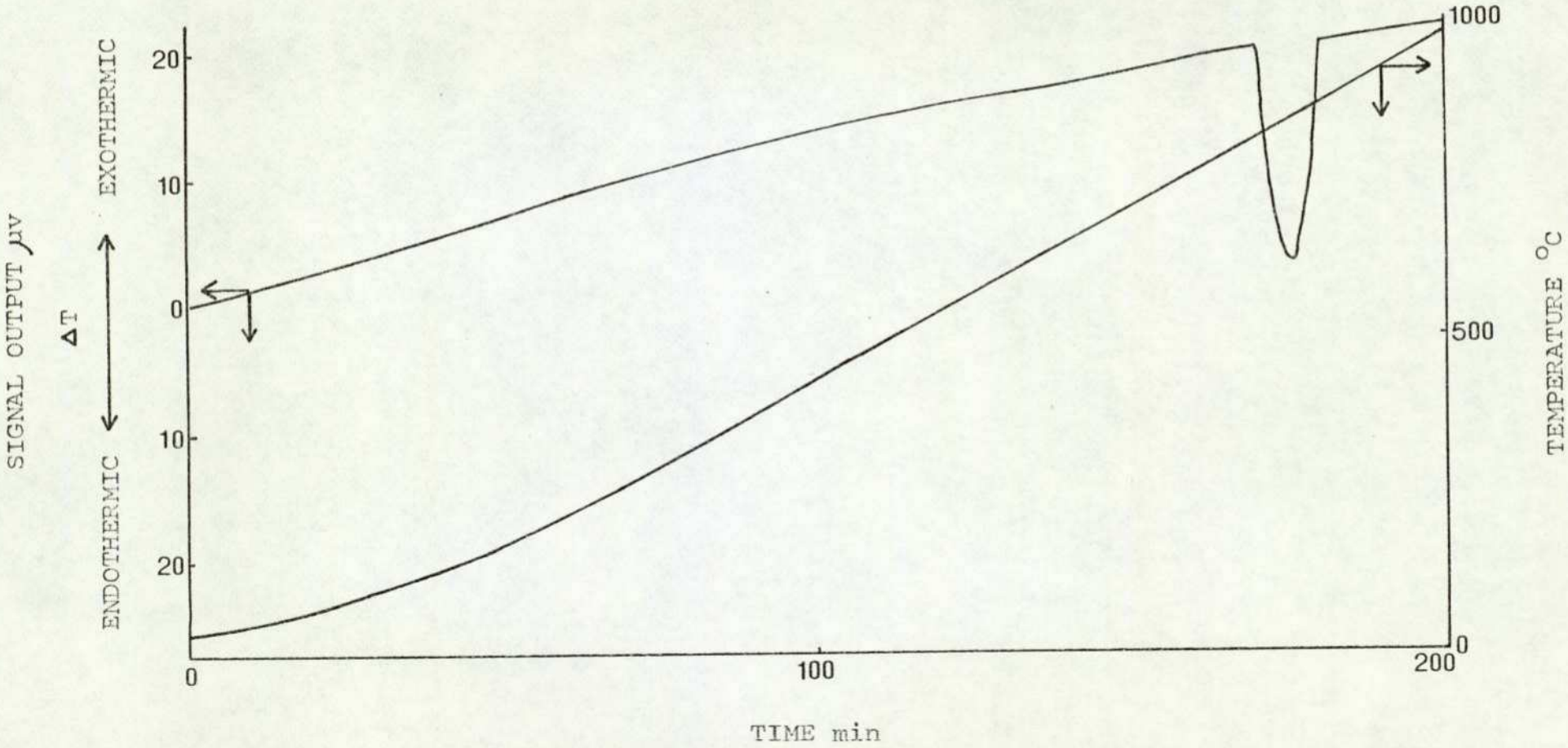

FIGURE 3.53. DIFFERENTIAL THERMAL ANALYSIS:- LEAD(II)CHLORIDE

SAMPLE WEIGHT 50.0 mg. HEATING RATE $5^{o}C\ min^{-1}$

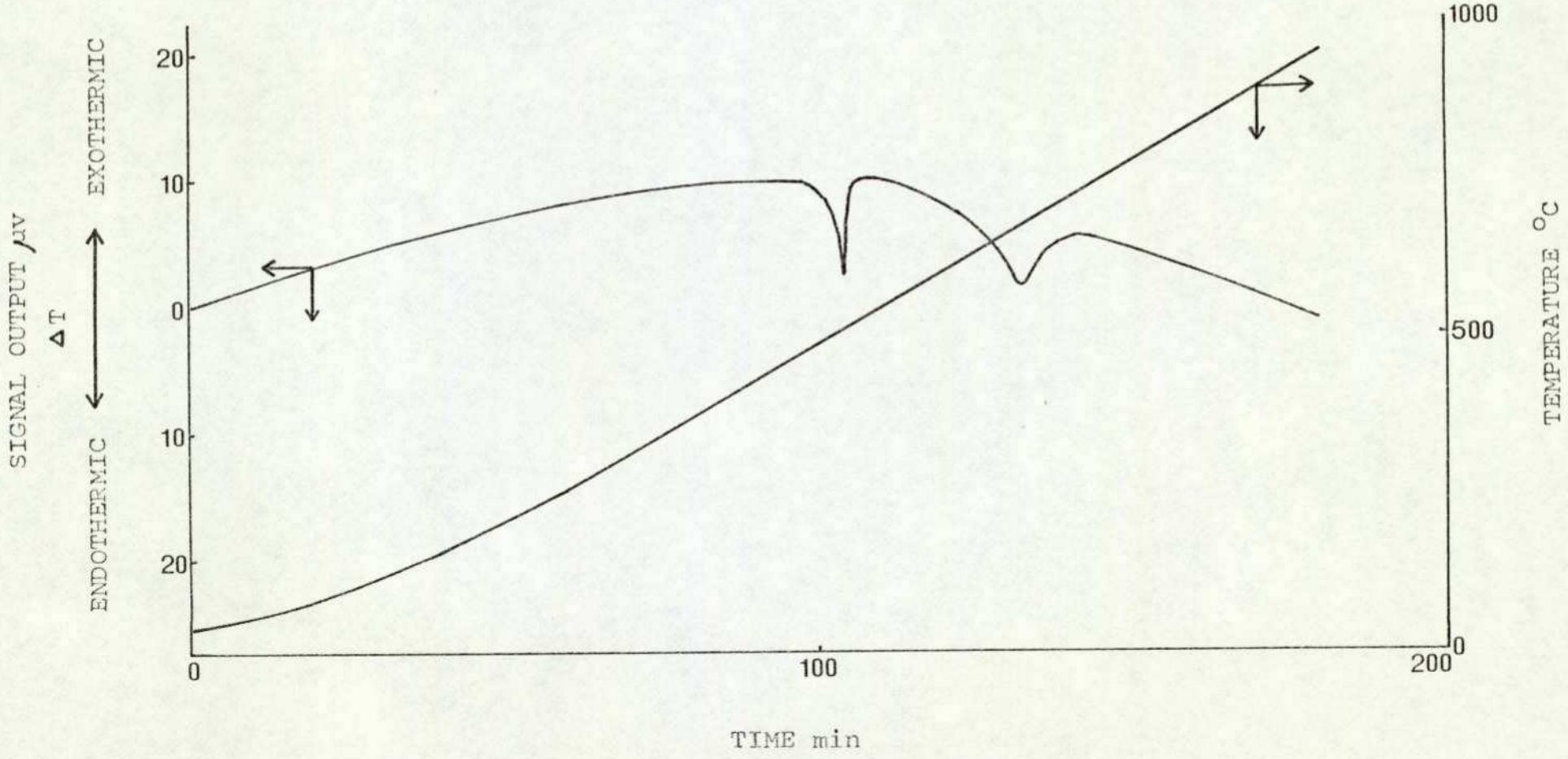

FIGURE 3.54. DIFFERENTIAL THERMAL ANALYSIS:- ALUMINA SUPPORTED COBALT(II,III,III)OXIDE

SAMPLE WEIGHT 38.8 mg. HEATING RATE 5°C min^{-1}

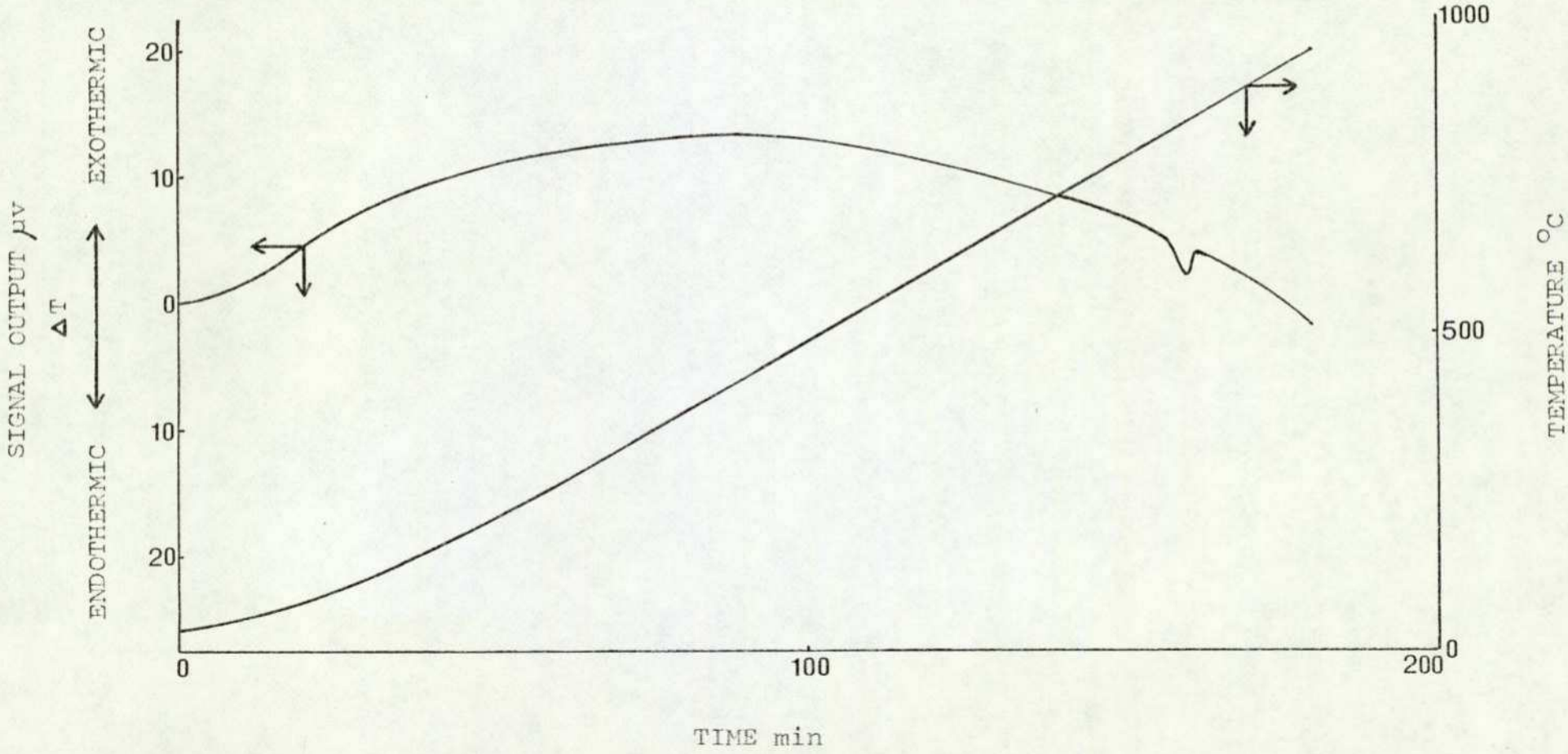

FIGURE 3.55. DIFFERENTIAL THERMAL ANALYSIS:- PHYSICAL MIXTURE OF Co_3O_4 (50 Wt %) AND $PbBr_2$. SAMPLE WEIGHT 43.8 mg. HEATING RATE $5^{o}C\ min^{-1}$

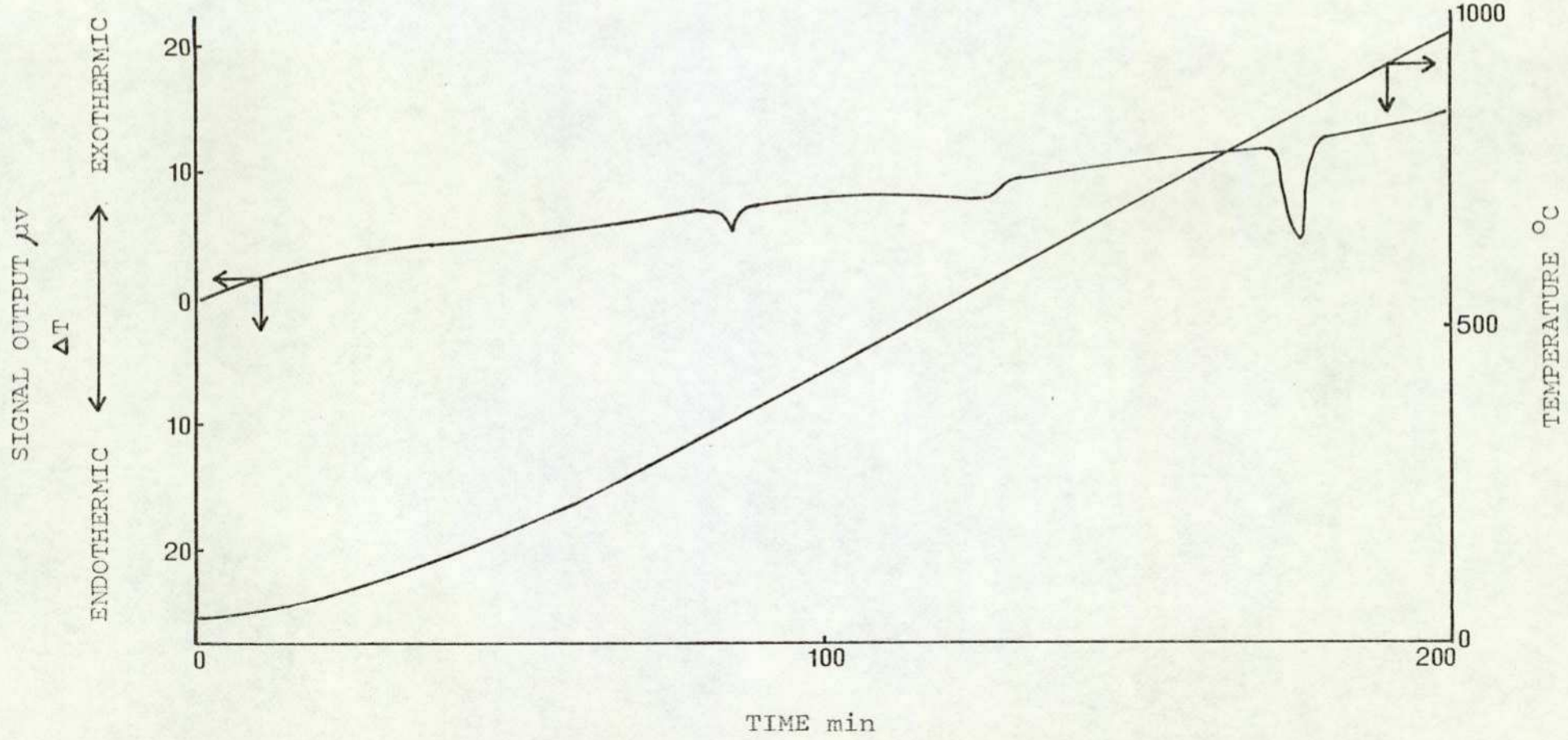

FIGURE 3.56. DIFFERENTIAL THERMAL ANALYSIS:-

PHYSICAL MIXTURE OF ALUMINA SUPPORTED Co_3O_4 (50 Wt %) AND $PbBr_2$

SAMPLE WEIGHT 79.0 mg. HEATING RATE $5^{o}C\ min^{-1}$

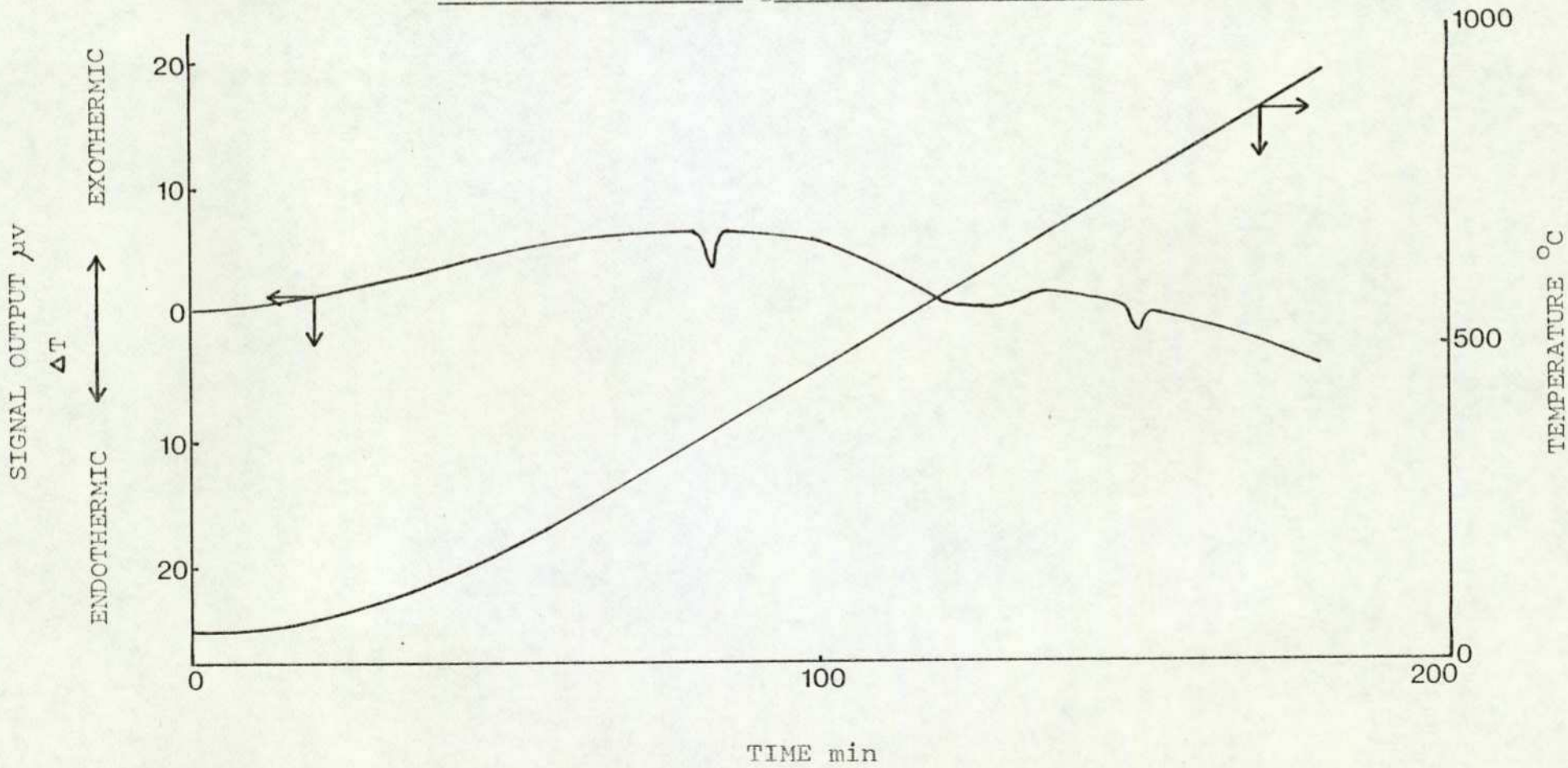

FIGURE 3.57. DIFFERENTIAL THERMAL ANALYSIS:-

PHYSICAL MIXTURE OF ALUMINA SUPPORTED Co_3O_4 (50 Wt %) AND $PbCl_2$

SAMPLE WEIGHT 67.0 mg. HEATING RATE $5^{o}C\ min^{-1}$

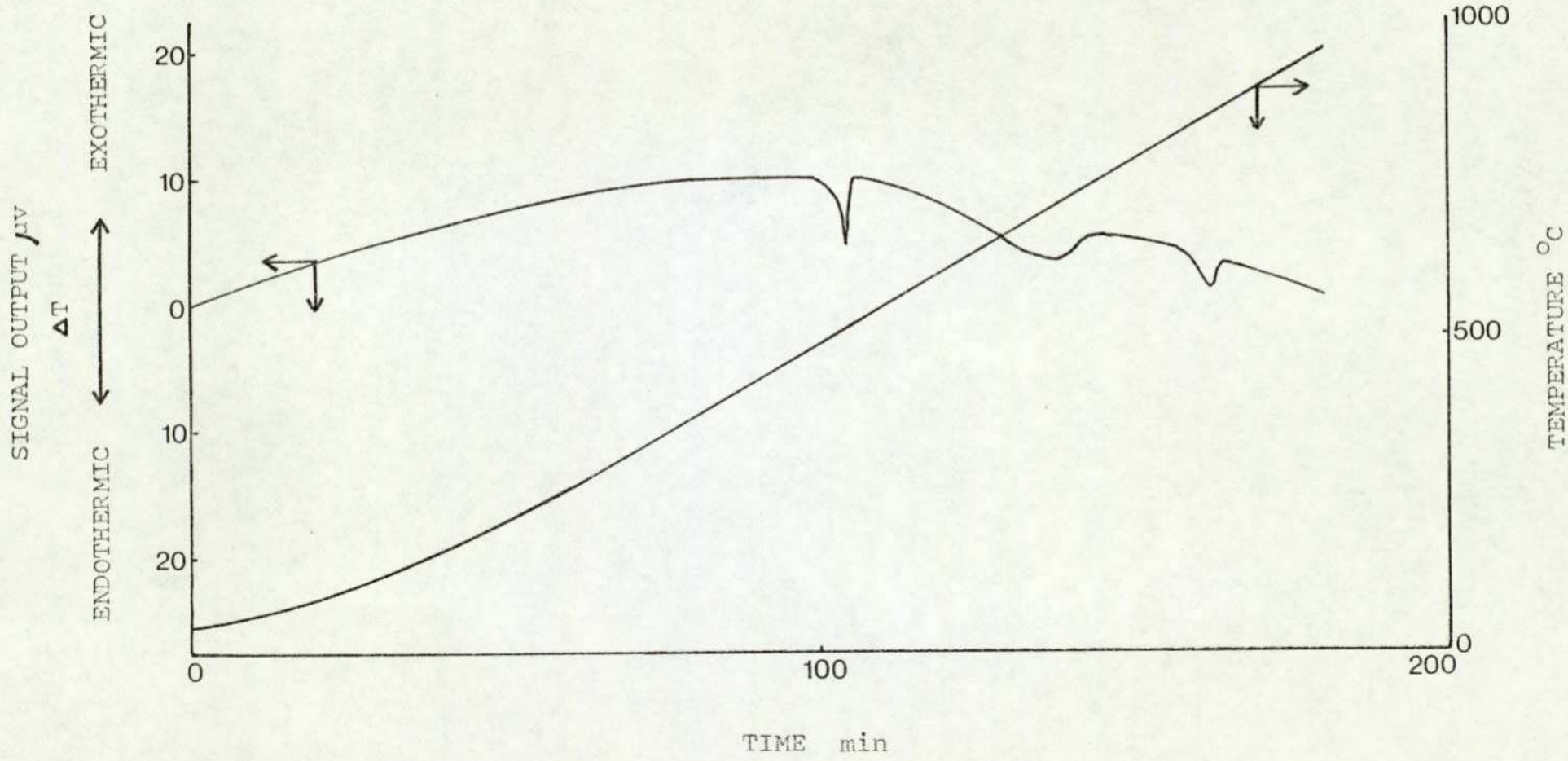

FIGURE 3.58. CATALYTIC ACTIVITY OF MANGANESE(IV)OXIDE

VARYING WITH LEAD(II)BROMIDE CONTENT

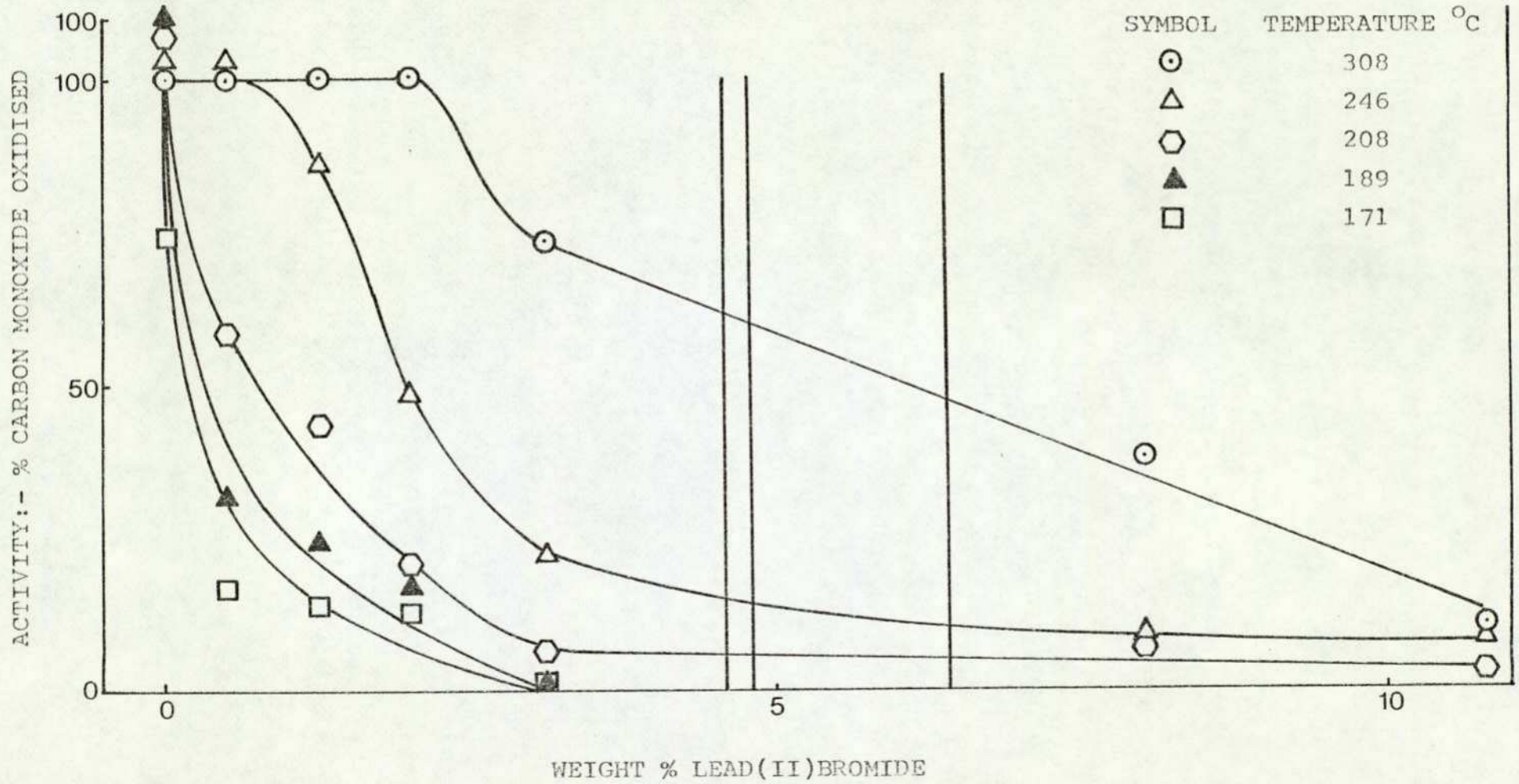

FIGURE 3.59. SURFACE AREA OF MANGANESE(IV)OXIDE

VARYING WITH LEAD(II)BROMIDE CONTENT

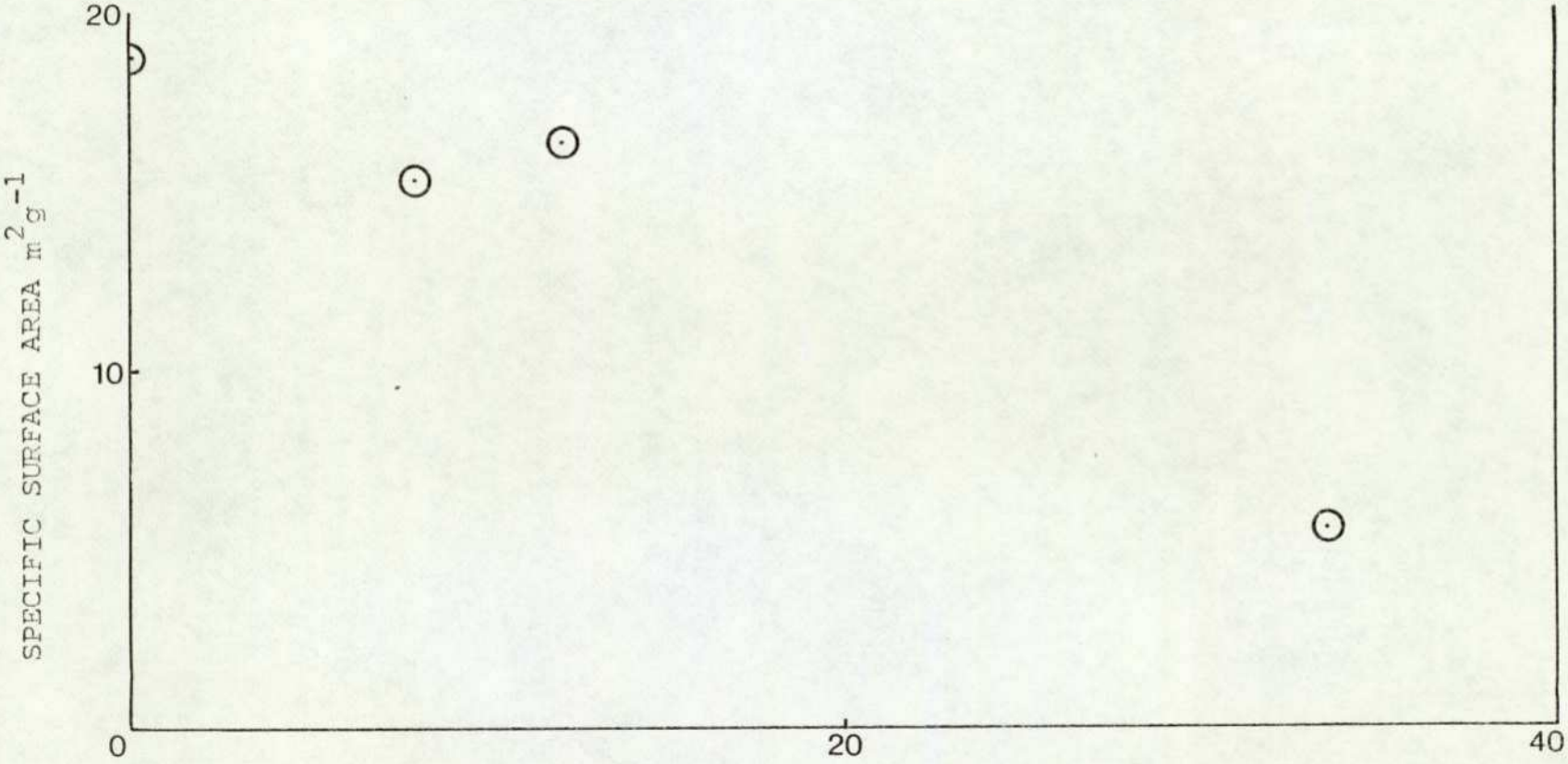

FIGURE 3.60. DIFFERENTIAL THERMAL ANALYSIS:- MANGANESE(IV)OXIDE

SAMPLE WEIGHT 33.6 mg. HEATING RATE $5^{o}C\ min^{-1}$

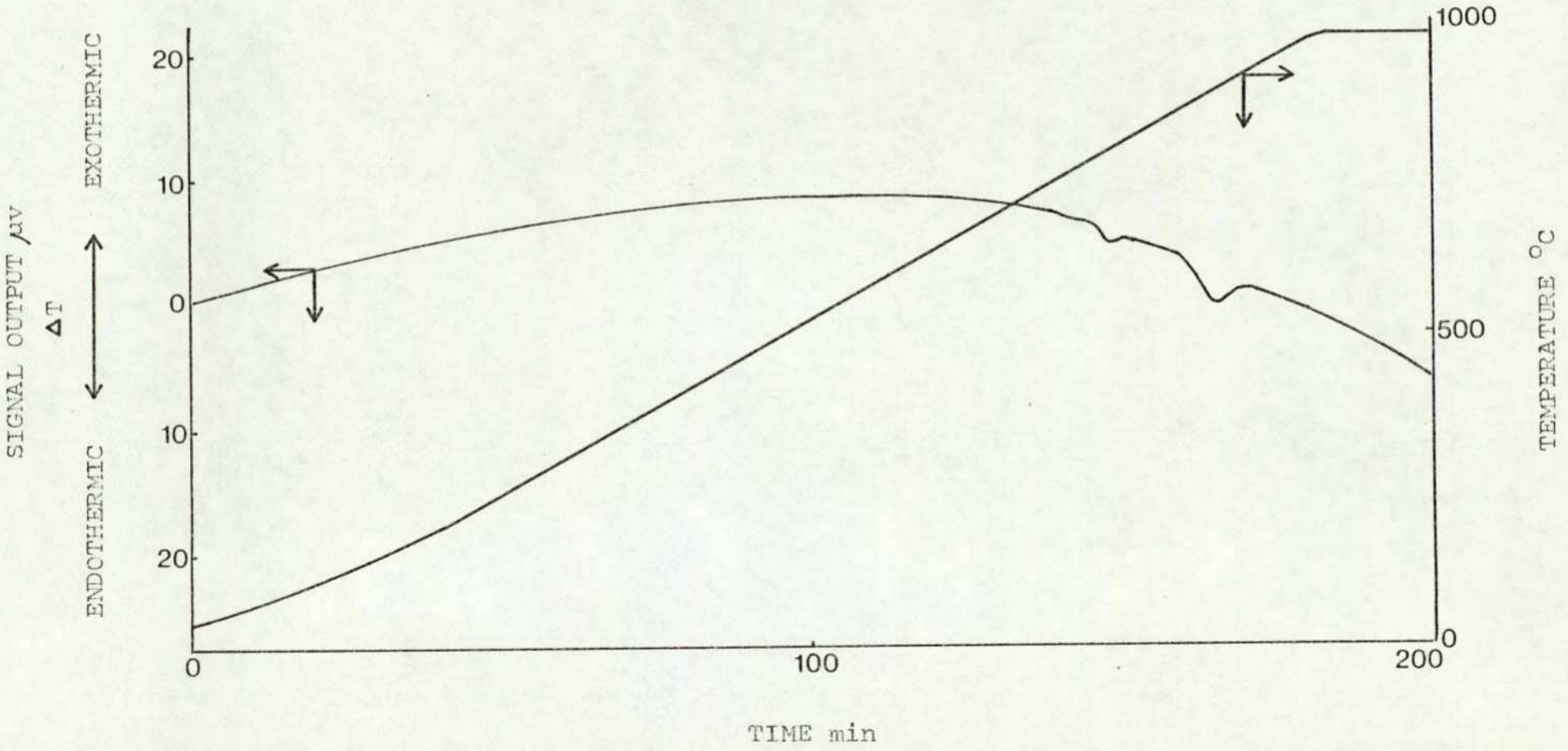

FIGURE 3.61. DIFFERENTIAL THERMAL ANALYSIS:-

PHYSICAL MIXTURE OF MANGANESE(IV)OXIDE (50 WEIGHT %) AND LEAD(II)BROMIDE

SAMPLE WEIGHT 37.9 mg. HEATING RATE $5^{o}C\ min^{-1}$

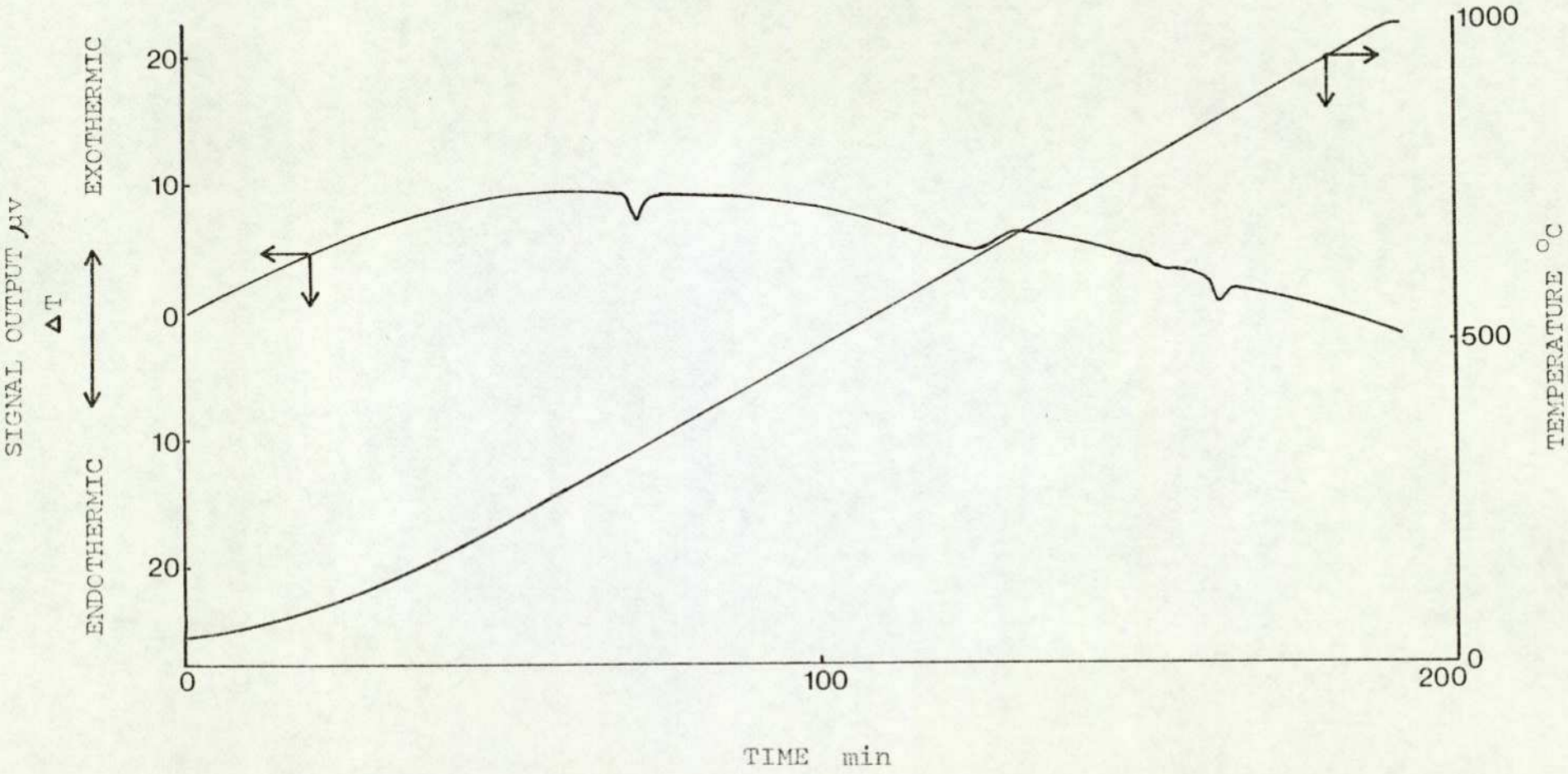

FIGURE 3.62. ELECTRICAL CONDUCTIVITY OF MANGANESE(IV)OXIDE VARYING WITH LEAD(II)BROMIDE CONTENT

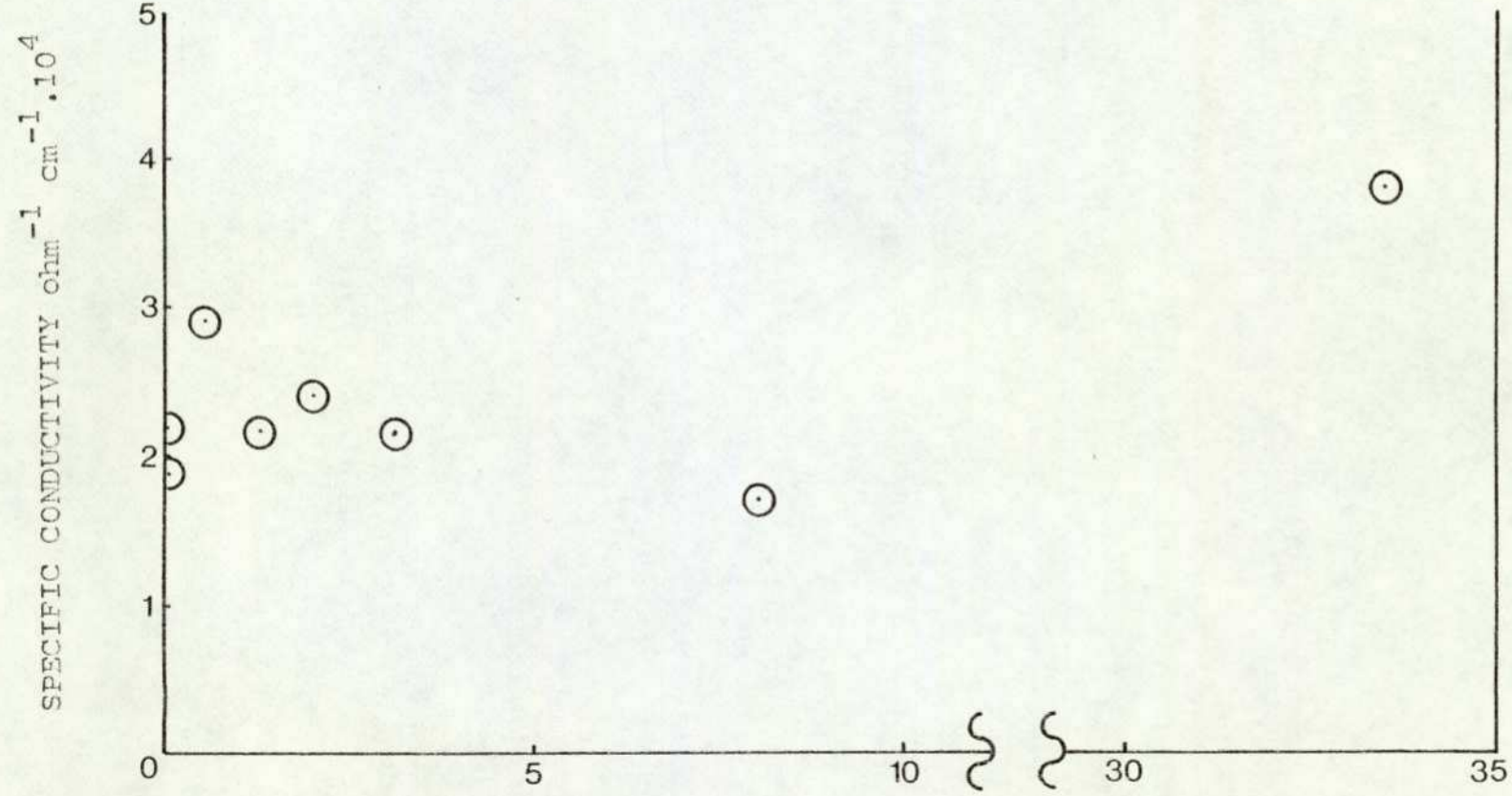

SECTION 4

DISCUSSION

SECTION 4

4.1. PREVIOUS THEORIES OF THE DEACTIVATION OF OXIDATION CATALYSTS BY LEAD COMPOUNDS

In Section 1.3.6. the deactivation of catalysts used in automotive pollution control, by various chemicals including lead compounds, was discussed in some detail. It is convenient, however, at this stage to summarize those theories which are specifically relevant to the deactivation of oxidation catalysts by lead compounds. The main theories, which have been reviewed by Yolles and Wise (152), involve: (1) physical adsorption on catalyst with monolayer formation, (2) pore plugging, and (3) reaction with catalyst and/or support to produce an inactive phase or compound.

The results of the present work have shown that relatively large quantities of lead halides are required to reduce the activity of the catalysts studied. For this reason it would appear to be inappropriate to use the term "poisoning", which, it is generally accepted, implies severe reduction of catalytic activity by a small quantity of a material selectively adsorbed on active sites. Thus the term "deactivation" is used in this Section to describe the effect of lead halides as the catalysts investigated. Furthermore, in view of the relatively large quantities of lead halides required to deactivate the catalysts examined, it is convenient to compare this quantity with the amount required to form a monolayer. This procedure has the dual advantages of testing an important theory of deactivation, whilst at the same time providing a useful point of reference

from which to examine other possible deactivation mechanisms.

4.1.1. CALCULATION OF CATALYST MONOLAYER CAPACITY WITH RESPECT TO LEAD HALIDES

In order to calculate the monolayer capacity of a catalyst with respect to any adsorbate, it is necessary to know the surface area of the catalyst and the cross-sectional area of the adsorbate molecule. The surface areas of unsupported and supported catalysts have been determined and are given in Section 3. There are, however, no published values for the cross-sectional areas of lead halide molecules. For this reason it is necessary to consider methods of calculating such areas for lead (II) bromide and lead (II) chloride, the specific lead halides used in this research.

Studies have been made of the structures of lead (II) chloride and lead (II) bromide both in the solid and gaseous phases (153,154). The two compounds have the same basic structure, the solids consisting of lead ions at the centre of a trigonal prism with six halide ions at the corners and three outside the face centres. The lead-halogen distances are, however, unequal, resulting in a distorted structure. Using electron diffraction methods, Lister and Sutton (154) have determined the structures of lead (II) bromide and lead (II) chloride in the gas phase. It was established that the vapours contained individual, bent (X-Pb-X = 95°) molecules, the Pb-X distance being 2.60 Å and 2.46 Å in the bromide and chloride respectively. Using Pauling's electronegativities, the percentage ionic characters of lead (II) chloride and lead (II) bromide are found to be 30% and 22% respectively. However, the ionic character of the solid would appear to be more pronounced than that of the vapour, as the interatomic distances of the solid are consistent

FIGURE 4.1.

a) A SINGLE LEAD HALIDE MOLECULE

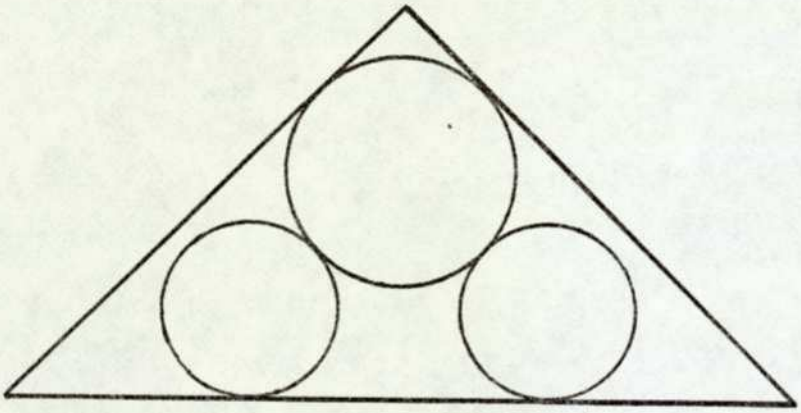

b) A POSSIBLE MODE OF PACKING

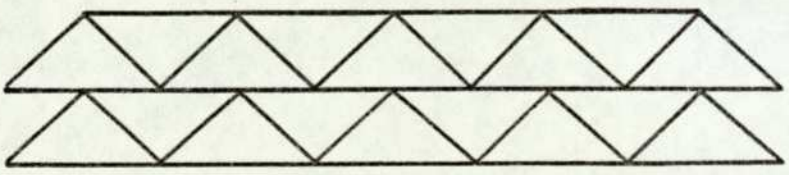

with an ionic model, whereas the lead-halogen distances for the vapour are more consistent with a covalent model.

In view of the differences in structure between the solid and gaseous phases of the lead halides, it is important to establish which model to use in the calculations of cross-sectional areas. Since deactivation of the catalysts by lead halides occurs from the gas phase, it is probably better (initially) to use the gas-phase structure as a basis for calculation. If the lead halide molecule is deposited on the surface of a catalyst, three simple orientations are possible. The molecule may either lie "flat" with all three atoms in contact with the surface, or, on the assumption that the lead atom forms the apex of a triangle, lie with the lead atom in contact with the surface and the halogen atoms projecting upwards. In the third model, the two halogen atoms may lie in contact with the surface with the lead atom projecting upwards from the surface. However for the purpose of calculating the cross-sectional area of the molecule, the last two possibilities are identical. Other orientations are possible but are not considered here. Using the data of Lister and Sutton (154), and assuming that the molecules lie "flat" and are packed in such a way that each lies within a 45^{o} right-angled triangle, as shown in figure 4.1.(a), then the cross-sectional areas of the lead (II) bromide and lead (II) chloride molecules are 24.7 Å^2 and 21.4 Å^2 respectively. If the alternative packing arrangement is employed, however, then each molecule will lie within an oblong with sides of 6.12 Å and 2.92 Å for lead (II) bromide and sides of 5.6 Å and 2.94 Å for lead (II) chloride. Thus the cross-sectional areas are 17.9 Å^2 and 16.45 Å^2 for the bromide and chloride

respectively.

The results obtained from this approach probably represent the extremes of a range of possible values. Furthermore, the smaller value would seem likely to represent the lower limit, as comparison of it with that normally assigned to diatomic nitrogen (i.e. 16.268 Å^2 at 77.36 K) reveals that the triatomic lead halide molecules would have only slightly larger cross-sectional areas. An alternative procedure for calculating the cross-sectional areas is based on the method of Emmett and Brunauer (155) who derived an equation (4.1.) having the form:-

$$X = 4 \times 0.866 \left(M/4\,N\,d\sqrt{2} \right)^{\frac{2}{3}} \quad \ldots\ldots\ldots\ldots\ldots\ldots \quad (4.1.)$$

where X = cross-sectional area of adsorbate in Å^2

M = molecular weight of adsorbate

N = Avogadro's Constant

d = density of the liquified adsorbate in g cm^{-3}

A difficulty which frequently arises with the use of this equation, however, is the scarcity of reliable data concerning the density. In this case, however, the densities of molten lead (II) bromide and lead (II) chloride, at the relevant temperature, are known to be 5.545 g cm^{-3} and 4.792 g cm^{-3} respectively (156).

Using equation (4.1.) values for the cross-sectional areas of lead (II) bromide and lead (II) chloride molecules were calculated (25 Å^2 and 24.2 Å^2 respectively). These values are similar to those calculated assuming a "flat" orientation of the halide molecules on the catalyst surface. Finally, it is possible to use equation (4.1.) to calculate the cross-sectional area of lead halide molecules assuming that they possess the dimensions of the solid phase when they are present on the catalyst surface.

The values obtained in this way are 22.4 $Å^2$ for lead (II) bromide and 20.0 $Å^2$ for lead (II) chloride.

In order to calculate the monolayer capacity of lead halide-poisoned catalysts, a value for the cross-sectional area of the lead halide molecules must be selected from the four calculated values. In the case of lead (II) bromide, it is desirable, in view of the close agreement between two of the values, i.e. 25 $Å^2$ and 24.7 $Å^2$, that a mean should be used. Of the remaining values (22.4 $Å^2$, 17.9 $Å^2$) one is particularly low and, if this is eliminated, the resulting mean of the remaining values may represent the most significant single value. However, the lowest value would also be relevant for calculating the maximum amount of lead (II) bromide which could exist as a monolayer. For these reasons the entire range of the four values i.e. 25.0 $Å^2$ - 17.9 $Å^2$ was used for calculating the monolayer capacity of catalysts, and the mean of the three closest values viz. 24.$Å^2$ was taken as representing the most probable single value for lead (II) bromide. Using a similar argument the range of values for the cross-sectional area of the lead (II) chloride molecule was 16.5 $Å^2$ - 24.2 $Å^2$. However, the spread of values within this range is distinctly more symmetrical about the mid point than was the case for lead (II) bromide, and therefore the most probable single value for lead (II) chloride will be taken as the mean of all four values i.e. 20.5 $Å^2$.

4.2. NICKEL (II) OXIDE

Nickel (II) oxide is the only anhydrous oxide of nickel. It is a non-stoichiometric compound, deficient in nickel, and is an important catalyst for the oxidation of carbon monoxide and of

Table 4.1. PROPERTIES OF NICKEL(II)OXIDE

Chemical Formula	NiO
Melting Point	2230 K
Boiling Point	-
Thermal Stability	Stable
Density	7.45 g cm^{-3}
Standard Heat of Formation	-244.5 kJ mol^{-1}
Free Energy of Formation	-216.5 kJ mol^{-1}
Heat of Dissociation at 298 K	410.3 kJ mol^{-1}

hydrocarbons. Nickel (II) oxide is also an active catalyst for other reactions, such as the decomposition of dinitrogen oxide and the oxidation of ammonia. The structure of nickel (II) oxide is that of an ionic lattice with a face-centred cubic unit cell (sodium chloride structure). A summary of some of this compound's other properties is shown in Table 4.1.

Of the three main theories of deactivation discussed in Section 4.1., the possibility of lead halides reacting with the catalyst to produce an inactive phase or compound is conveniently considered first. In order to investigate this, the techniques of differential thermal analysis (DTA) and X-ray powder diffraction were employed. The differential thermal analysis of various physical mixtures of nickel (II) oxide and lead (II) bromide (figures 3.12.- 3.15.) revealed no peaks which could be attributed to the formation of a new phase or compound. In addition such mixtures, when heated and subsequently analyzed using X-ray powder diffraction, yielded no evidence of compound formation.

Thus the possibility of bulk reaction occurring between lead halide and catalyst, in the mixtures examined, may be eliminated, at least under the conditions of the present experiments. A detailed account of these experiments, together with the results has been given in Section 3.2.

With regard to the possibility of pore-blocking causing catalyst deactivation, the surface properties and physical structure of the nickel (II) oxide catalysts were examined. The BET surface areas of poisoned and unpoisoned nickel (II) oxide catalysts are shown in figures 3.4. and 3.5. These results show that the surface area is not significantly affected by lead (II) bromide levels sufficient for

complete deactivation of the catalysts. Furthermore, in the case of nickel (II) oxide prepared via the hydroxide (figure 3.4.) a lead (II) bromide level of three times that required for complete deactivation was found to have reduced the surface area by only 16%.

In addition to the BET surface area results obtained for nickel (II) oxide, the surface area of this catalyst was calculated using the results of electron microscopy measurements. This examination (plate 3.1.) revealed that the catalyst consists of some apparently cubic-shaped particles, although most were irregular in appearance. A surface area within the range 4.2 - 10 m^2g^{-1} was obtained, however. The BET surface area of the nickel (II) oxide catalyst was 4.4 m^2g^{-1}, which is within the range of values obtained by electron microscopy. This agreement, which may be to some extent fortuitous due to errors arising from the assumption of a reasonably typical particle-size distribution, suggests that this catalyst is non-porous. Thus the outer surfaces of the particles may well constitute the entire surface area of the catalyst.

The pore-size distribution curves for both poisoned and unpoisoned nickel (II) oxide are shown in figures 3.6. and 3.7. respectively. Initially these results appear to suggest that this catalyst has a porous structure, with the most frequently occurring pore radius being 13.3 Å for the unpoisoned catalyst and 12.5 Å for the poisoned catalyst. However, in view of the electron microscopic examination of these catalysts, this interpretation must be considered incorrect. If the catalyst particles are in very close contact with each other, then the spaces between them would form a pseudo-porous structure, which could explain this apparent contradiction. Having established then that the nickel (II) oxide catalyst structure is particulate

and non-porous, the possibility of pore-blocking contributing to catalyst deactivation can therefore be eliminated.

Using values for the cross-sectional area of the lead (II) bromide molecule, calculated in Section 4.1.1. and the BET surface area, the monolayer capacity of nickel (II) oxide prepared via the hydroxide route is found to be 1.06 - 1.48 weight % lead (II) bromide, with the most probable value being 1.11 weight %. Figure 3.1. shows the variation of the catalytic activity of this nickel (II) oxide sample, with weight % lead (II) bromide; the vertical lines drawn at right angles to the abscissae represent the previously mentioned monolayer capacity values. It can be seen that the activity of the catalyst decreases in such a way as to approach zero at a lead (II) bromide content slightly smaller than, or within, the possible range for monolayer formation. The activity, however, having reached a value of less than 10% of its original value, decreases less sharply and eveentually reaches zero at a lead (II) bromide content approximately 30% in excess of the monolayer capacity of this catalyst. Thus, the activity of the catalyst initially decreases in such a way as to approach zero at, or slightly before, the monolayer capacity of the catalyst but later deviates from the monolayer range and reaches zero at a lead (II) bromide content greater than the monolayer capacity. Similar behaviour occurs with the nickel (II) oxide catalyst prepared by decomposition of the nitrate (figure 3.2.) although in this case the catalytic activity decreases more sharply. Furthermore, this catalyst has a smaller monolayer capacity due to its lower surface area.

In order to test the theory of catalyst deactivation involving adsorption of lead (II) bromide with monolayer formation (both physical adsorption and chemisorption are possible), it is convenient to consider

the following idealised case and to compare its predictions with the results actually obtained. Thus, if adsorption of the lead halide takes place and the entire catalyst surface is homogeneous with respect to the adsorbate, then for a non-porous catalyst, the deactivation curve will be a straight line with catalytic activity being eliminated at the point of monolayer formation. However, the deactivation curves of the nickel (II) oxide samples deviate somewhat from this idealised situation. Both curves, for example, exhibit "tail off", an effect which Ashmore (157) has suggested may be due to the difficulty of filling all the sites with comparatively bulky inhibitor molecules. In addition, it can be seen from figure 3.2. that the activity of the catalyst decreases much more sharply at low lead (II) bromide levels (this effect being much less pronounced for the other nickel oxide catalyst). A possible explanation for this behaviour would be selective adsorption on a small fraction of the catalyst sites. Winter (158) proposed that the activity of various oxide catalysts is confined to a relatively few sites. If initial adsorption of the poison were to occur preferentially on a small fraction of the catalyst surface, e.g. on that part with the most strongly attractive forces, then it is reasonable to assume that this fraction would contain a high proportion of sites which are active in bringing about oxidation of carbon monoxide. Thus the initial rate of deactivation with respect to the amount of poison adsorbed would be more rapid than that occurring at a later stage. These results, therefore, suggest that, although monolayer formation in the strict sense is unlikely to occur, a single molecular layer of

lead (II) bromide may cover most of the catalyst surface, possibly being formed initially at active sites, before subsequent layers of lead (II) bromide are deposited.

Figure 3.3. shows the effect on catalyst activity of removing lead (II) bromide from a nickel (II) oxide catalyst, using a stream of nitrogen at the temperature used during the original poisoning operation. The two curves represent the behaviour of two samples of the catalyst, treated with differing amounts of lead (II) bromide. In both cases, a significant reduction in lead (II) bromide content is observed, as well as a corresponding increase in catalytic activity. With the more heavily contaminated of the two catalysts (catalyst A), a significant increase in activity caused by the removal of approximately one third of the halide, indicates that an appreciable proportion of the active catalyst surface is exposed by this process. However, the lead (II) bromide which remains is still more than sufficient for a single molecular layer to cover completely the surface of the catalyst. Thus there appears to be a possibility of the remaining lead (II) bromide existing as a layer from one to several molecules thick but covering only a part of the surface. In addition, the relative ease of removal of approximately one third of the lead halide suggests that at least some of the lead halide is present as a result of physical adsorption or condensation rather than chemisorption.

The less heavily contaminated of the two catalysts (catalyst B) does not increase in activity to the same extent, although it again loses a significant proportion of the original lead (II) bromide content. However, in this case, since an insufficient quantity of lead (II) bromide remains on the surface, the existence

of a monolayer seems to be impossible. Thus, again, during the removal process a significant proportion of the active catalyst may have become exposed and available for reaction.

It is of interest to note that, for a given quantity of lead (II) bromide, the activities of the nickel (II) oxide catalyst samples shown in figure 3.3. are higher than those of the catalyst samples shown in figure 3.2. In view of the fact that all these samples were taken from a single batch of nickel (II) oxide, these results appear to suggest that the distribution of the lead (II) bromide on the catalyst surface can also vary. Variation of the lead (II) bromide distribution on the catalyst could be interpreted as indicating that physical adsorption of the lead halide was a contributing factor in the mechanism of catalyst deactivation. For example the well known phenomenon of hysteresis, which is a feature of physical adsorption, is caused by a difference in the distribution of the adsorbate on the adsorbent surface. Alternatively, if the distribution of the lead (II) bromide on the surface of nickel (II) oxide does not vary, it is possible that the catalytic activity of the surface could vary. One suggestion along these lines is that migration of positive holes in nickel (II) oxide (a p-type semiconductor) may be induced if static electricity builds up on the catalyst as the result of friction between this and the nitrogen gas stream. If this were to happen, the formation of new "active" sites (i.e. recently transferred positive holes) on the remaining uncontaminated nickel (II) oxide surface would explain the higher catalytic activity of nickel (II) oxide, for a given lead (II) bromide content, after the removal process.

The results shown in figure 3.3. indicate that a proportion of lead (II) bromide is relatively weakly held by the catalyst surface. This part of the adsorbate may be held by physical adsorption, with the remainder (which is much more difficult to remove) possibly being chemisorbed. The amount of residual lead (II) bromide in the case of catalyst A is 27% more than the maximum monolayer capacity and for catalyst B it is 29% less than the minimum monolayer capacity. This indicates that the monolayer capacity of nickel oxide for lead (II) bromide is significant, and that the formation of an adsorbed layer of lead (II) bromide approximately one molecule thick may be an important stage of the deactivation process. However, the concept of the formation during deactivation of sufficiently tightly-packed molecular layer, which would completely prevent nickel (II) oxide taking part in the reaction is not supported by the experimental results.

Figures 3.8. - 3.11. show the results of thermogravimetric analysis (TGA) of various nickel (II) oxide samples. The data shown in figures 3.8a. - 3.8c. refer to pure nickel (II) oxide heated in air, an empty crucible and pure nickel (II) oxide heated in nitrogen. At temperatures up to 800°C no weight loss is observed; at higher temperatures, however, a small loss in weight (probably due to release of oxygen) occurs in a nitrogen atmosphere. The result of a typical TGA run on a 0.9 mg sample of lead (II) bromide is shown in figure 3.9a. Figures 3.9b. - 3.11b. show the results of various TGA runs for nickel (II) oxide samples treated with lead (II) bromide. These all contain 0.9 mg of lead (II) bromide, although the relative quantities of lead (II) bromide and nickel (II) oxide vary. The sample of pure lead (II) bromide is shown by TGA to have completely volatilized at a temperature of 600°C. However, in the

case of lead (II) bromide-treated nickel (II) oxide samples, the TGA results show that the halide is not completely volatilized even at 1000°C. Furthermore, the weight loss sustained at this temperature is due, in part, to loss of oxygen.

Table 3.2a.shows some results of bulk lead (II) bromide analysis. These were obtained from the lead (II) bromide treated nickel (II) oxide samples both before and after thermal analysis, and show that even after a temperature of 1000°C has been reached, between 45% and 89% of the original lead (II) bromide still remains on the nickel (II) oxide. Furthermore, it is interesting to note that in figure 3.11a., the nickel (II) oxide sample with the largest initial lead (II) bromide content of 1.76 weight % (corresponding to 80% more than the monolayer capacity) is shown to lose less than a third of the lead halide as being heated to 550°C and maintained at that temperature for 100 minutes. In addition, upon a detailed analysis of the TGA results shown in figures 3.9b. - 3.11b. (Table 3.2b.), it can be seen that the loss of lead (II) bromide from nickel (II) oxide at temperatures up to 600°C is lower than 25% of the total halide for samples containing less than the monolayer capacity of lead (II) bromide.

Finally, if the TGA results of those samples heated to 1000°C are considered from the point of view of their surface area, it can be shown that the loss of lead (II) bromide correlates quite well with the reduction of catalyst surface area, from 2.85 to 1.25 m^2g^{-1}, caused by sintering. Figure 3.11c. shows the monolayer range of nickel (II) oxide with respect to lead (II)

bromide, calculated for both surface area values, and also plots the loss of lead (II) bromide which occurs during TGA. It can be seen therefore that lead (II) bromide is removed in large quantity only from those samples containing a significant excess over the monolayer capacity calculated on the basis of the lower surface area of the sintered catalyst, i.e. 1.25 m^2g^{-1}. Thus, again, the monolayer capacity of the catalyst is shown to be significant, a result which supports the idea of an adsorbed layer approximately one molecule thick, playing an important part in the deactivation process.

The possibility of lead (II) bromide forming a chemisorbed layer on nickel (II) oxide was investigated using spectroscopic techniques and also by measuring the electrical conductivity of the deactivated and untreated catalysts. The results of the spectroscopic study, which included the ultra-violet, visible and infra-red regions, are shown in figures 3.16.- 3.20. The variation of electrical conductivity with lead (II) bromide content is shown in figure 3.21.

Lead (II) bromide was found to have useful absorption characteristics only in the ultra-violet region, although nickel (II) oxide, both deactivated and untreated, yielded a useful spectrum over the entire range. However, no significant differences were observed between the spectra of deactivated and untreated nickel (II) oxide. Despite the absence of new absorption bands, these results do not, for reasons discussed in Section 1.2.5.3., necessarily indicate that chemisorption has not occurred. Furthermore, the relatively low surface area of the catalyst may render this technique too insensitive to detect absorption bands due to

Table 4.2. PROPERTIES OF COBALT(II,III,III)OXIDE

Chemical Formula	Co_3O_4
Melting Point	1240 K
Boiling Point	Decomposes
Thermal Stability	Loses Oxygen at 1173 K
Density	6.07 g cm^{-3}
Standard Heat of Formation	-857.1 kJ mol^{-1}
Free Energy of Formation	-466.4 kJ mol^{-1}

chemisorption of lead (II) bromide on the catalyst surface.

The electrical conductivity measurements on lead (II) bromide-treated nickel (II) oxide (figure 3.21.) show virtually no variation with lead (II) bromide content. This may indicate that lead (II) bromide has no effect on the conductivity of this catalyst and therefore that chemisorption has not occurred. However, the low surface area of the nickel (II) oxide may again have obscured any change in the conductivity of this catalyst.

4.3. COBALT (II, III, III) OXIDE

Cobalt forms two anhydrous oxides, cobalt (II) oxide and cobalt (II, III,III) oxide, but there is no evidence for the existence of pure cobalt (II) oxide. Cobalt (II, III, III) oxide is a normal spinel which consists of a face-centred cubic lattice of oxygen ions, containing cobalt (II) ions in one eighth of the tetrahedral sites and cobalt (III) ions in one half of the octahedral sites. This oxide is an intrinsic semiconductor and is an important catalyst for the oxidation of carbon monoxide and hydrocarbons. Table 4.2. summarizes some of its other important properties.

4.3.1. UNSUPPORTED COBALT (II,III,III) OXIDE

The possibility of bulk reaction between lead halides and cobalt (II,III,III) oxide causing deactivation was examined by means of DTA and X-ray diffraction, using the methods described in Section 4.2. for nickel (II) oxide. From the results of this investigation (see Section 3.5.) it was concluded that bulk reaction did not take place under the conditions investigated. Furthermore the result of an EDAX examination of a lead (II) bromide

treated sample of cobalt (II,III,III) oxide (Section 3.5.) indicated that both lead and bromine were present and that the ratio of these two elements was consistent with the existence of lead (II) bromide. This result, whilst not eliminating the possibility of a reaction between lead (II) bromide and cobalt (II,III,III) oxide, does rule out any chemical reaction which would result in the presence of lead only in a sample of lead (II) bromide treated cobalt (II,III,III) oxide. Thus the EDAX result is helpful in supporting the results of DTA and X-ray diffraction, and therefore also the conclusion that bulk reaction between lead (II) bromide and cobalt (II,III,III) oxide does not contribute towards the deactivation process.

In order to decide whether deactivation of cobalt (II,III,III) oxide by lead halides occurs via the mechanism of pore-blocking, an investigation of its surface properties and physical structure was carried out, similar to that described for nickel (II) oxide. An electron microscope investigation of cobalt (II,III,III) oxide (plate 3.4.) clearly reveals a particulate structure, similar to that of nickel (II) oxide. Thus the catalyst consists of solid rather than porous particles, and the external surface of these particles constitutes the entire surface area of the catalyst. Further confirmation of this is obtained from an estimate of the surface area of the catalyst by means of electron microscopy and comparison of this with the BET surface area. For example, the surface area calculated from electron microscopy lies within the range 5-25 m^2g^{-1}, the precise value depending on the particle size distribution. The BET surface area is 6.2 m^2g^{-1}, and, although

this lies towards the lower end of the range calculated from the electron microscopy results, the possibility of a porous structure being involved is again virtually excluded. One reason for this conclusion is that the presence of a porous structure would be detected by the BET method and reflected in the value for the surface area, whilst only the external surface area of particles would contribute to the result calculated from electron microscopy measurements. Thus, for a porous structure, a relatively high BET surface area would be expected. These results, by discounting the possibility of the catalyst having a porous structure, show that pore-blocking cannot be responsible for the deactivation of unsupported cobalt (II,III,III) oxide.

The BET surface area values obtained for various lead (II) bromide-treated samples of cobalt (II,III,III) oxide catalysts (figure 3.42.) reveal that the surface area is virtually unaffected by the range of lead halide concentrations found to be effective in reducing and eliminating catalytic activity. This result tends to confirm the previous conclusion that pore-blocking cannot occur with this catalyst, as a pore-blocking mechanism would be expected to cause a significant decrease in surface area. Finally, the consistency of these surface area values suggests that the lead (II) bromide cannot be present in the form of small particles as the surface area would be expected to increase with lead (II) bromide content. The presence of lead (II) bromide as large particles must also be considered unlikely as, although the surface area of cobalt (II,III,III) oxide would be virtually unaffected by the presence of a few

large particles of lead (II) bromide, some evidence would then have been expected for a lead (II) bromide phase in the electron microscopy results (plates3.4. - 3.5.). The absence of this, together with the surface area results, therefore suggests that lead (II) bromide may be present on the surface of the catalyst as a thin layer. Such a distribution of the lead halide would not be expected to alter significantly the surface area of the catalyst, nor would this distribution be easily seen in an electron micrograph of the catalyst.

Using a procedure identical to that used for nickel (II) oxide catalysts (Section 4.2.) it can be shown that the calculated monolayer capacity of the cobalt (II,III,III) oxide catalyst, with respect to lead (II) bromide, lies within the range 1.49-2.07 weight %, the most probable value being 1.56 weight %. Figure 3.34.shows the variation of catalytic activity of this cobalt (II,III,III) oxide sample, at several temperatures, with weight % lead (II) bromide; the vertical lines in this figure again represent the various calculated values of monolayer capacity. The activity of this catalyst decreases in a manner similar to that found with nickel (II) oxide, although zero activity is approached at values considerably greater than the monolayer capacity. However, at the higher temperatures, the catalytic activity decreases very slowly yielding deactivation curves of a more convex shape compared with those obtained for nickel (II) oxide.

In order to understand the reason for the apparently widely differing shapes of these deactivation curves, it is necessary to consider the effect of increasing temperature on catalytic activity. A temperature range of about 100°C was used in the case of cobalt (II,III,III) oxide and it would be expected, from the usual Arrhenius dependence of reaction rate on temperature, that an increase

of this size would greatly increase the rate of the catalyzed reaction. Now the activity of catalysts at all temperatures was measured using the same fixed quantity of reactants. Thus, at a sufficiently low temperature, even the untreated catalyst would not be capable of causing complete reaction of this quantity of reactants, and catalysts treated with the lead halide would cause even less reaction to take place. Thus a deactivation curve could be plotted showing catalyst activity decreasing in some way with increase in lead halide content. However, at higher temperatures the untreated catalyst would not only be able to cause complete reaction of the given quantity of reactants but also to cause the reaction of an extra, but unknown, quantity. Furthermore, even a catalyst treated with a small quantity of lead halide may be capable, at this higher temperature, of causing complete reaction of the fixed quantity of reactants. The deactivation curve obtained at the higher temperature would therefore start with a catalytic activity level at 100% which would continue to have this value, until the lead halide content was sufficiently great to cause the activity of the catalyst to start to decrease. At this stage the deactivation curve would be expected to have a similar shape at the higher temperature as at the lower temperature. Thus the deactivation curves obtained at high temperature can be considered as "magnified" versions of the low temperature curves, but with the initial section of the curve showing a constant activity level of 100% due to the use of too small an amount of reactants for the capacity of the catalyst.

If, as has been suggested, the high temperature deactivation curves are basically similar to the low temperature curves and can therefore be explained in the same way, it is only necessary to propose a single explanation for the whole family of curves. It has already been mentioned that, at the lower temperatures (109°C and 140°C) the deactivation curves are similar to those obtained for nickel (II) oxide. In the initial section of these curves the activity decreases in such a way as to approach zero at approximately the monolayer capacity of the catalyst. However, the activity curve veers sharply away from this point at higher lead (II) bromide levels. This suggests that, if adsorption of lead halide is responsible for deactivation of the catalyst, then at the appropriate stage of deactivation a layer approximately one molecule thick may cover the surface of the catalyst and that this layer is packed in such a way as to allow access for reactant molecules to a small fraction of the catalyst surface. There are, however, drawbacks to this theory, e.g. the presence of catalytic activity at a temperature as low as 109°C at a lead (II) bromide level of approximately twice the monolayer capacity. It is of course possible that the close packing of the lead halide may be much more difficult on the surface of this catalyst, compared with that of nickel (II) oxide, and that two or more layers of the halide may be necessary to prevent completely access of reactants to the catalyst surface. Alternatively, deposition of the lead halide on the surface of cobalt (II,III,III) oxide may not take place layer by layer. For example, deposition of the lead halide may take place initially in selected areas and at a certain stage, when a sufficient proportion of the catalyst surface is covered with halide, preferential deposition of lead halide may

take place on those areas already covered with lead halide. Thus "islands" of lead (II) bromide, several molecules thick, may build up on the surface of cobalt (II,III,III) oxide and the entire surface may not be sufficiently effectively covered to prevent catalysis occurring until the monolayer capacity has been exceeded by a substantial margin. Of these two mechanisms of deactivation of cobalt (II,III,III) oxide by lead (II) bromide, the latter is clearly the preferred one.

In the case of lead (II) chloride-treated cobalt (II,III,III) oxide, the range proposed for the monolayer capacity is 1.17 - 1.72 weight %, with the most probable single value being 1.38 weight %. From figure 3.35. it can be seen that at temperatures of 140, 170 and 190°C, the catalytic activity approaches zero at a lead halide content near to or within the monolayer range. However, at the higher temperatures of 227 and 265°C, the activity, although initially decreasing rapidly, later falls off more slowly with increasing lead (II) chloride content, so that a level of even eight times the monolayer capacity is insufficient to eliminate completely the catalytic activity.

The results shown in figure 3.35. again show, to a limited extent, the effect of temperature on the deactivation curves as discussed earlier in this Section. However, the elimination of catalytic activity, at the lower temperatures and at almost exactly the lead halide content corresponding to the monolayer capacity of this catalyst, strongly suggests the presence of a layer of lead (II) chloride with an average thickness of one molecule. The presence of significant activity at the higher

temperatures indicates that the packing of lead (II) chloride, even at the highest concentration, is not significantly coherent to prevent completely access to the catalyst surface by reactant molecules.

The effect of removing lead (II) bromide from cobalt (II,III,III) oxide is shown in figures 3.38. and 3.39. The results obtained for this catalyst are, in some respects, similar to those for nickel (II) oxide. For example, with both samples of cobalt (II,III,III) oxide, a significant reduction in lead (II) bromide content is observed concurrently with an increase in catalytic activity. However these results do not really indicate which of the two, previously mentioned, alternative explanations of deactivation is the more likely. However, the tenacity of the last fraction of the lead halide towards the cobalt (II,III,III) oxide does suggest that the monolayer capacity of cobalt (II,III,III) oxide, with respect to lead (II) bromide, is of some significance and that a relatively strong attraction exists between the residual lead (II) bromide and the catalyst surface. However, the presence of a strongly adherent, close-packed, single molecular layer of lead (II) bromide capable of excluding reactant molecules from the cobalt (II,III,III) oxide surface would appear to be impossible.

There is an interesting contrast between the lead (II) bromide removal results obtained for cobalt (II,III,III) oxide and those for nickel (II) oxide. Thus, cobalt (II,III,III) oxide yields a similar activity curve for both the addition and removal of lead (II) bromide, whereas the corresponding curves for nickel (II) oxide differ according to whether the lead halide is being added or

removed from the catalyst. The similarity of the activity curves obtained for both addition and removal of lead (II) bromide from cobalt (II,III,III) oxide, indicates that the surface distribution of the poison is the same for increasing and decreasing amounts of lead (II) bromide. In addition it suggests that the catalytic activity of the uncontaminated surface does not vary. The last point is consistent with the stoichiometric structure of cobalt (II,III,III) oxide and thus with the absence of potentially mobile defects as a possible explanation of the nickel (II) oxide results.

Figures 3.50a. - 3.51b., show the results of thermogravimetric analyses of untreated and four lead (II) bromide-treated samples of cobalt (II,III,III) oxide. In figure 3.50a. (TGA of pure cobalt (II,III,III) oxide) the weight loss occurring at 800 - 900°C can be attributed to decomposition of the catalyst. The weight losses in figures 3.50b. - 3.51b. (lead (II) bromide treated catalysts) are due to vaporization of lead (II) bromide. The results shown in figure 3.50b. were obtained by heating the sample and then maintaining the temperature constant at 550°C until no further weight loss had occurred; the reduction of lead (II) bromide content during this experiment ranged from 4.2 to 3.0 weight %. In figures 3.50c. and 3.51b. the results of similar experiments show that lead (II)bromide levels decreased from 6.4 to 3.6 weight % and 15.1 to 6.2 weight % respectively. However, in figure 3.51a., where the temperature was kept at 800°C, the lead (II) bromide content was reduced from 11.3 to 2.08 weight %. In this experiment, the comparatively low residual lead (II) bromide content may indicate sintering of the catalyst,

with corresponding loss in surface area.

These results also indicate that removal of lead (II) bromide from cobalt (II,III,III) oxide becomes progressively more difficult at levels approaching the monolayer capacity of the catalyst, i.e. 1.49 - 2.07 weight %.

In view of the large quantities of lead (III) bromide initially present on cobalt (II,III,III) oxide before TGA, it would be reasonable to assume that the lead halide exists at least on a proportion of the surface, as a layer several molecules thick. Thus the lead (II) bromide present in the uppermost layers is probably relatively easily removed during TGA and the first layer is more difficult to remove, due to the attractive forces between the catalyst and the first lead (II) bromide layer being stronger than between successive layers of lead (II) bromide. In conclusion, these TGA results can be interpreted as supporting the evidence derived from the lead (II) bromide removal experiments, although they are of little use in extending, or clarifying, the previously proposed ideas of deactivation of cobalt (II,III,III) oxide by lead (II) bromide.

4.3.2. SUPPORTED COBALT (II,III,III) OXIDE

The possibility of bulk reaction between lead halides and supported cobalt (II,III,III) oxide contributing towards deactivation was investigated in the usual way, namely by differential thermal analysis (DTA) and X-ray powder diffraction of mixtures of lead halides and the catalyst. The results of DTA (figures 3.54. - 3.57.) and X-ray diffraction (see text Section 3.5.) yielded no evidence of compound formation. Furthermore an EDAX analysis of alumina-supported cobalt (II,III,III) oxide treated with 8.9 weight %

lead (II) bromide (see Section 3.5.) showed that lead and bromine were present in relative quantities which are consistent with the presence of lead (II) bromide.

The mechanism of pore-blocking cannot be considered in isolation at this stage owing to the relatively complex nature of the results obtained during the study of this catalyst. However, in contrast to the unsupported cobalt (II,III,III) oxide, the supported catalyst has a distinct porous structure due to the porous nature of the alumina support as revealed by electron microscopy.

The deactivation curves shown in figures 3.36. and 3.37. refer to alumina-supported cobalt (II,III,III) oxide deactivated with lead (II) bromide and lead (II) chloride respectively. The shapes of the deactivation curves obtained for these supported catalysts bear a close relationship to those for the unsupported catalysts. In addition, lead (II) chloride is shown to be more effective than lead (II) bromide for deactivating supported cobalt (II,III,III) oxide, a result similar to that obtained for the unsupported catalysts.

If the shapes of these deactivation curves are examined by the method of Wheeler (see Section 1.2.3.6.) which was developed for application to porous catalysts, then their concave nature suggests that selective poisoning is occurring at the mouths of the pores. In addition it may be concluded that the rate of reaction is controlled by diffusion into the porous structure of the catalyst. However, as the more concave deactivation curves were obtained at the lowest temperatures, where diffusion control is least likely to be in evidence, it would appear that this explanation contains an implicit contradiction. However, from an examination of supported cobalt (II,III,III) oxide (see text Section 3.5. and plates 3.6. - 3.13.)

by means of an electron microscope, it would appear that the major part of the active catalyst exists as particles dispersed on the outer surface of the porous support. Furthermore, the unsupported catalysts, again from the results of electron microscopy and also from surface area calculations, are believed to be particulate rather than porous. In view of the similarity between the shapes of the deactivation curves for supported and non-porous unsupported catalysts, and the contradiction arising from the assumption that the active element of the supported catalyst is genuinely porous, the use of the Wheeler method would probably not be applicable to the analysis of the deactivation curves of the supported catalysts. Thus the mechanism of deactivation by pore blocking, at least for that proportion of the active catalyst present as solid particles can be discounted.

With supported catalysts, calculation of the quantity of lead halide required for the formation of a monolayer and comparison of this with the amount required for complete deactivation, is unlikely to be as useful as with unsupported catalysts. The reason for this limitation is the difficulty in deciding what proportion of lead halide is deposited on the support, compared with that deposited on the active catalyst. Despite this, some useful information can be obtained from this approach and the monolayer capacity has therefore been calculated for supported catalysts.

The monolayer capacity of supported cobalt (II,III,III), oxide treated with lead (II) chloride lies within the range 24.5 - 32.0 weight %, the most probable single value being 27.8 weight %.

The activity of this catalyst is reduced by at least 85% (figure 3.37.) by only 5.8 weight % lead (II) chloride, even at the highest temperature used. This quantity of lead (II) chloride is very much smaller than is necessary for monolayer-formation over the entire surface. Now, as the majority of the cobalt (II,III,III) oxide exists at the outer surface of the porous support, and in view of the effective deactivating action of the relatively small quantity of lead (II) chloride, it would appear that the halide is also concentrated at the outer surface of the support.

In the case of supported cobalt (II,III,III) oxide treated with lead (II) bromide, even a lead halide content of 43.7 weight % is insufficient to eliminate catalytic activity at the three highest temperatures (figures 3.36.). In addition, the monolayer capacity of the catalyst with respect to lead (II) bromide lies within the range 29.3 - 36.6 weight %, the most probable value being 30 weight %. However, in contrast to the preceding case, it is not possible to deduce from this information, with any degree of certainty, the distribution of lead (II) bromide on this catalyst. The possibility of the halide again being concentrated mainly on the outer surface of the support cannot however be ruled out, in view of the almost complete elimination of the catalytic activity by only 12 weight % of lead (II) bromide at the two lowest temperatures.

It is interesting to compare the effects of each of the two lead halides on the activity and surface properties of the supported cobalt (II,III,III) oxide and also where possible to

compare these results with those obtained in the case of the unsupported catalyst. For example, the effects of the lead halides on the surface area of supported cobalt (II,III,III) oxide are shown in figures 3.61.and 3.62. In both cases the maximum loss in surface area is approximately 50% of the initial value. However, this is achieved in the case of lead chloride with only 5.8 weight %, whereas with the bromide 43.7 weight % is required. Similarly the pore volume of this catalyst is reduced to a much greater extent for a given quantity of lead (II) chloride (figures 3.45a, 3.48a, - 49b.) than for the same quantity of the bromide (figures 3.45a. - 3.47a.). Furthermore, the decrease in catalytic activity at these lead halide levels and at the same temperature, i.e. at 308°C, is 100% in the case of the chloride, but only 68% for the bromide (figures 3.37.and 3.36. respectively).

These results show that lead (II) chloride, on a weight % basis, is approximately seven times more effective in reducing catalytic activity, surface area and pore volume than is lead (II) bromide. Similarly it was shown, in Section 4.3.1., that lead (II) chloride is considerably more effective than the bromide in deactivating cobalt (II,III,III) oxide. Now it was suggested that lead (II) chloride was adsorbed on the surface of unsupported cobalt (II,III,III) oxide as a layer approximately one molecule thick. In other words, at the monolayer capacity of cobalt (II,III,III) oxide, with respect to lead (II) chloride, a layer one molecule thick covers most, but not all, of the surface. Those areas not covered with a single molecular layer would either be completely free of lead halide or covered with a thicker layer.

In view of the structure of the supported cobalt (II,III,III) oxide consisting mainly of cobalt (II,III,III) oxide particles dispersed on the alumina support, it is possible that the results obtained for the supported catalyst may also be due to the formation of a layer approximately one molecule thick on the active (i.e. cobalt oxide) part of the catalyst. In addition there is some indication that lead (II) chloride forms a very thin adsorbed layer on the pure alumina support, as a heated mixture of lead (II) chloride and alumina yields an X-ray diffraction photograph with a significant line-broadening effect for those lines generated by lead (II) chloride. This effect is characteristic of samples with a high surface area, and a very thin layer of lead (II) chloride adsorbed on the alumina support would have such a surface area.

The likelihood of lead (II) bromide being adsorbed on unsupported cobalt (II,III,III) oxide in the same way as lead (II) chloride was considered to be small and an alternative mechanism, involving the formation of "islands", of lead (II) bromide was proposed. Similarly, in the case of supported cobalt (II,III,III) oxide, the results examined so far indicate that lead (II) bromide is not adsorbed on the catalyst in the same way as lead (II) chloride, but again forms "islands" of the lead halide, several molecules thick, on the active part of the catalyst. Only at high concentrations do these link up to cover the entire surface.

Figure 3.40. shows the effect of the removal of lead (II) bromide on the activity of supported cobalt (II,III,III) oxide. The corresponding effects on surface area and pore-size distribution

are shown in figures 3.41., and 3.47. respectively. It is again interesting to note the similarity of these results with those for the unsupported catalyst. For example, the first stage of lead (II) bromide removal results in a substantial loss of the lead halide from 43.7 to 5.4 weight %. The effect of this is to cause a corresponding substantial increase in catalytic activity and surface area, although the effect on pore-size distribution is not clear. In addition, the second stage of lead (II) bromide removal results in little or no improvement in activity or change in surface properties. Thus the similarity of these results, with those obtained for the unsupported catalyst, once more indicates that the explanation for the deactivation of the supported catalyst is probably similar to that previously outlined for the unsupported catalyst.

It has already been mentioned that supported cobalt (II,III,III) oxide is a porous catalyst deriving its porosity from the support rather than from the catalyst. Furthermore, it is known that the active cobalt (II,III,III) oxide exists mainly as solid particles situated on the external surface of the larger support particles (see Plate 3.9.). However, as mentioned in Section 3.5. an EDAX examination of the supported catalyst revealed that a small proportion of cobalt (II,III,III) oxide is more intimately associated with the support, i.e. trapped in the porous structure. Now the mechanism of pore-blocking cannot operate in the case of that proportion of cobalt (II,III,III) oxide existing as solid particles. However, the small proportion of cobalt (II,III,III) oxide trapped in the porous structure of the support can clearly

be deactivated by this mechanism. Thus the pore-size distribution results, shown in figures 3.45. - 3.49. and indicating decreasing pore-volume with increasing lead halide content, also show that pore-blocking by lead halides must contribute towards deactivation, although this mechanism must be considered to be of little importance in view of the relatively small quantities of cobalt (II,III,III) oxide contained within the pores of this catalyst.

Electron micrographs (plate 3.6. - 3.9.) of a lead (II) bromide-treated supported cobalt (II,III,III) oxide catalyst, with an overall lead (II) bromide content of 8.9 weight %, whilst clearly showing the alumina and cobalt (II,III,III) oxide phases, reveal no evidence of a third phase of lead (II) bromide. This result is not unexpected in view of the previously outlined mechanism of lead (II) bromide deposition. However, it is clear that several other modes of lead (II) bromide deposition would also lead to an apparent absence of a lead (II) bromide phase and that only deposition of the bromide in the form of relatively large particles can be ruled out on the basis of this evidence.

In Section 3.5. it was mentioned that an EDAX examination of this catalyst showed that lead and bromine, although detected in conjunction with both the cobalt (II,III,III) oxide and alumina phases, was primarily associated with the alumina

phase. Thus it would appear that the lead halide is deposited preferentially on the alumina support. However it is not clear whether the reason for this is a greater affinity between alumina and lead (II) bromide, than exists between cobalt (II,III,III) oxide and lead (II) bromide, or simply the larger surface area of alumina which would provide more opportunities for collision between vapour phase lead (II) bromide and the solid surface.

4.4. OTHER UNSUPPORTED CATALYSTS

4.4.1. COPPER (II) OXIDE

Copper forms two commonly known anhydrous oxides, i.e. copper (I) oxide and copper (II) oxide, although others have been reported (159). Copper (II) oxide has a distorted platinum sulphide structure (Monoclinic system) in which the copper atoms form four coplanar bonds with the oxygen atoms which in turn form four approximately tetrahedral bonds with copper. Copper (II) oxide is an insulator and catalyses a wide variety of reactions e.g. the complete oxidation of carbon monoxide and hydrocarbons, the partial oxidation of benzene by hydrogen peroxide to benzoquinone and maleic acid, the dehydrogenation of alkanes and cycloalkanes, the dehydration of alcohols, the decomposition of dinitrogen oxide, the synthesis of methanol and the hydration of anthracene.

Table 4.3. PROPERTIES OF COPPER(II)OXIDE

Chemical Formula	CuO
Melting Point	-
Thermal Stability	Decomposes above 1073 K
Density	6.45 g \cm^{-3}
Standard Heat of Formation	-155.3 kJ mol^{-1}
Free Energy of Formation	-127.3 kJ mol^{-1}
Heat of Dissociation at 298 K	339.1 kJ mol^{-1}

Table 4.3. summarizes some of its other important properties.

Unsupported copper (II) oxide, as stated in Section 3.3., was found to have good catalytic activity with respect to carbon monoxide oxidation, but very few results were obtained, because the smallest amount of lead (II) bromide which could be applied to it, i.e. 0.32 weight %, completely eliminated its catalytic activity. The BET surface area of this catalyst was found to be only 0.145 m^2g^{-1} and its monolayer capacity, calculated in the usual way, lay within the range 0.035 - 0.049 weight %. Thus the minimum amount of lead (II) bromide which could be applied to this catalyst exceeds the monolayer capacity by a factor of almost ten. An excess of lead (II) bromide of this magnitude would presumably be sufficient to exclude reactant molecules from the surface of the catalyst. The mode of lead (II) bromide deposition cannot be inferred from these limited results, although the possibility of bulk reaction of lead (II) bromide with copper (II oxide can be eliminated on the basis of the results of differential thermal analysis of various mixtures of these two compounds (See Section 3.3. and Table 3.1.).

4.4.2. MANGANESE (IV) OXIDE

Manganese (IV) oxide is one of the five oxides of manganese, which include MnO, Mn_3O_4, Mn_2O_3, MnO_2, and Mn_2O_7.

Table 4.4. PROPERTIES OF MANGANESE(IV)OXIDE

Chemical Formula	MnO_2
Melting Point	1120 K
Thermal Stability	Loses Oxygen above 808 K
Density	5.03 g cm^{-3}
Standard Heat of Formation	-521.3 kJ mol^{-1}
Free Energy of Formation	-466.4 kJ mol^{-1}
Heat of Dissociation at 298 K	921.1 kJ mol^{-1}

Manganese (IV) oxide exists naturally as the mineral pyrolusite (β-MnO_2) which has the rutile structure. A number of other forms of manganese (IV) oxide can exist and have been prepared in the laboratory (153). β-MnO_2 was the form used in this study; its structure is complex but it can be described as consisting of infinite chains of octahedra (each octahedron consisting of a central manganese atom coordinated by six oxygen atoms) joined up along their lengths by sharing corners. Manganese (IV) oxide is non-stoichometric, being oxygen-deficient, and is an important catalyst, particularly for oxidation reactions, e.g. the complete oxidation of carbon monoxide and hydrocarbons, the oxidation of ammonia and the partial oxidation of toluene to benzaldehyde. Other reactions catalysed by manganese (IV) oxide include the decomposition of potassium hypochlorite and of hydrogen peroxide. Table 4.4. summarizes some of the other properties of manganese (IV) oxide.

The variation of the catalytic activity of the manganese (IV) oxide catalyst with weight % lead (II) bromide content is shown in figure 3.58. The monolayer capacity of this catalyst, with respect to lead (II) bromide, occurs within the range 4.4 - 6.0 weight %, the most probable value being 4.5 weight %. Thus, at the two lowest temperatures, catalytic activity is eliminated at a lead halide content slightly below the monolayer capacity, although activity at the higher temperature occurs at a lead halide content of up to twice the monolayer capacity. These results

suggest that a layer of one molecule thick is responsible for the principal part of the deactivation process. However, "tail off" is evident at the higher temperatures, which suggests that a layer of, perhaps, two or even three molecules thick is necessary for complete elimination of catalytic activity. It is interesting to note that the high-temperature curves (246 and 308°C) are, in general, similar to the deactivation curves obtained for nickel (II) oxide at 306.5°C.

The results in figure 3.59. show the variation of BET surface area of manganese (IV) oxide with weight % lead (II) bromide content. It can be seen from these results that the surface area of manganese (IV) oxide is only slightly reduced by lead (II) bromide at levels sufficient to eliminate almost entirely the catalytic activity, although the surface area is substantially reduced at the highest lead (II) bromide level (greater than 30 weight % lead (II) bromide).

For a non-porous catalyst it would be expected that the surface area would be virtually unaffected by the formation of a thin layer consisting of only one or two molecules. However, due to the absence of electron microscopy data, it is not possible to decide whether or not this catalyst has a porous structure. Thus the contribution of pore-blocking to the mechanism of deactivation cannot be ruled out, although such limited evidence as is available does not suggest that this is likely.

The differential thermal analysis (DTA) of manganese (IV) oxide, shown in figure 3.60., and that of a physical mixture of manganese (IV) oxide and lead (II) bromide, shown in figure 3.61., whilst indicating that manganese (IV) oxide decomposes at approximately 800°C, and that

lead (II) bromide is appreciably volatile, does not show any evidence of compound formation. Thus, the bulk reaction between manganese (IV) oxide and lead (II) halide appears not to occur and can therefore be eliminated as a possible deactivation mechanism.

Figure 3.62. shows the results of electrical conductivity measurements on lead (II) bromide-treated manganese (IV) oxide. These show no evidence of any well-defined trend over the range of lead (II) bromide concentrations responsible for deactivation of the catalyst. Furthermore, the results exhibit a certain degree of scatter, which does not assist interpretation. Thus it can be concluded that this technique may not be sufficiently sensitive to detect any change in the conductivity of the catalyst, due to the presence of lead (II) bromide. Alternatively, it is possible that the lead (II) halide does not affect the conductivity of manganese (IV) oxide and that there is no correlation between the conductivity of the catalyst and its activity.

4.5. OTHER SUPPORTED CATALYSTS

Two supported catalysts are included in this Section, namely alumina-supported copper (II) oxide and alumina-supported platinum. The possibility of bulk reaction between the catalysts and the lead (II) halides is considered first. This was investigated in the case of supported copper (II) oxide by differential thermal analysis of various physical mixtures of copper (II) oxide, alumina and lead (II) bromide, which are listed in Table 3.1. However, no evidence of compound formation was found from this

examination at temperatures up to 600°C. In addition, X-ray diffraction studies on a sample of supported copper (II) oxide containing 87 weight % lead (II) bromide revealed no lines which might be attributable to a new compound. Unfortunately no DTA or X-ray diffraction results were obtained for the supported platinum catalyst and thus the possibility of bulk reaction occurring cannot be ruled out, although the inert character of platinum would suggest that bulk reaction with lead (II) bromide is unlikely. In addition, bulk reaction of lead halides with the alumina support has already been ruled out from the results obtained for other supported catalysts.

Figure 3.22. shows the deactivation curve for supported copper (II) oxide at a temperature of 241°C. The initial section of this deactivation curve is flat, indicating that the activity of the catalyst remains almost unaffected by lead (II) bromide levels of up to 45 weight %. The monolayer capacity lies within the range 28.6 - 36.0 weight %, with the most probable value being 29.5 weight %. Thus the quantity of lead (II) bromide required for deactivation, i.e. 90 weight %, is very high and well in excess of the monolayer capacity. The initial flat region is not easily explained in view of the lack of information concerning the distribution of copper (II) oxide on the support. However, if, as is the case with supported cobalt (II,III,III) oxide, the copper (II) oxide lies mainly on the outer surface of the porous support, in the form of particles, then the lead (II) bromide may be preferentially deposited on the support rather than on the

catalyst. This view is supported by both the surface area and pore-size distribution results, shown in figures 3.23. - 3.27., as both surface area and pore volume decrease approximately linearly with increasing lead (II) bromide content up to 45 weight %, whilst catalytic activity remains virtually unaffected.

Thus lead (II) bromide may initially be deposited preferentially on the alumina support but in only insignificant quantity on the copper (II) oxide when a large proportion of the support is already covered. This stage would appear to be reached at a lead halide content of about 50 weight %, as the activity of the catalyst decreases sharply at this point.

The variation of catalytic activity of the alumina-supported platinum catalyst, at various temperatures, is shown in figure 3.28. The shapes of these deactivation curves are, in general, smoother than those for the supported copper (II) oxide catalyst, although complete deactivation again occurs at a very high lead (II) bromide content i.e. between 80 and 90 weight % lead (II) bromide. The monolayer capacity of the platinum catalyst lies within the range 31.4 - 39.0 weight %, the most probable value being 32.3 weight %. Again the monolayer capacity of the platinum catalyst is exceeded by a substantial amount before elimination of catalytic activity is complete.

The distribution of platinum on the alumina support was also not established by electron microscopy and therefore the distribution must be assumed. Evidence is available (160) to show that alumina-supported platinum, prepared by reduction of alumina

treated with hydrogen hexachloroplatinate (IV) hydrate, consists of platinum particles situated mainly on the outer surface of the alumina support. This distribution arises from the tendency of hydrogen hexachloroplatinate (IV) hydrate to be adsorbed preferentially on the outer surface of the support rather than to penetrate deeper into the porous structure.

The effects of lead (II) bromide on the total surface area, active surface area and pore-size distribution of the alumina supported catalyst are shown in figures 3.29., 3.30. and 3.31. - 3.33. respectively. With this catalyst the amount of lead (II) bromide required for complete deactivation is virtually the same as that required to block the porous structure of the catalyst and to reduce both active and total surface areas to zero, i.e. to such a low value as to be undetectable. Furthermore all of these parameters i.e. catalytic activity, active surface area etc., would appear to be reduced at the same rate as the increase in lead (II) bromide content. Thus, whatever the mode of lead (II) bromide deposition and if account is taken of the larger surface area of the alumina compared with that of the platinum, there would appear to be little tendency for preferential deposition of lead (II) bromide on either the platinum or the alumina phase.

If the mode of lead (II) bromide deposition is now considered and it is assumed that the lead halide is deposited at an equal rate, per unit surface area, on both platinum and alumina, it would appear unlikely that monolayer formation could be responsible for

deactivation of this catalyst. The reason for this is a simple comparison of the monolayer capacity of the catalyst with respect to lead (II) bromide (i.e. 31.4 - 39.0 weight %) with the amount of lead (II) bromide required for complete deactivation i.e. 80 - 90 weight %. This evidence would indicate that a layer of lead (II) bromide of approximately two molecules average thickness is required for complete deactivation. Alternatively, if it is assumed that lead (II) bromide is deposited preferentially on the outer surface of the alumina, then it must be concluded that a layer of considerably greater average thickness than two molecules is responsible for catalyst deactivation.

It is of interest to note that, despite the lack of evidence suggesting decomposition of lead (II) bromide or reaction of the lead halides with any of the catalysts examined in this investigation, the lead compounds are decomposed by light (156). In addition, Williams and Baron (130) have suggested that lead halides decompose on the surface of platinum and leave a residue of metallic lead strongly bonded to the platinum surface. Indeed it is conceivable, under certain conditions, say in an actual car exhaust system, that the formation of a platinum lead alloy may contribute to deactivation as these two elements are known to form binary alloys at temperatures as low as 300 - 400°C. (161). However, in view of the massive quantities of lead (II) bromide required to deactivate the alumina-supported platinum catalyst, under the conditions used in this work, and the absence of any apparent tendency of lead (II) bromide to be deposited preferentially on platinum rather than alumina, this mechanism is

unlikely to be important.

4.6. CONCLUSIONS

Bulk reaction of lead (II) bromide with nickel (II) oxide, unsupported cobalt (II,III,III) oxide, supported cobalt (II,III,III) oxide, manganese (IV) oxide and alumina-supported copper (II) oxide has not been found, on the basis of DTA and X-ray diffraction results, to be responsible for the deactivation of these catalysts. In addition bulk reaction of lead (II) chloride has similarly not been found to cause deactivation of supported cobalt (II,III,III) oxide. In the case of supported platinum, deactivation by bulk reaction is thought to be unlikely, although no direct evidence has been obtained. However a deactivation mechanism has been described, based on the work of Williams and Baron (130), which involves the formation of a lead platinum alloy, or at least the decomposition of lead halide on the platinum surface, leaving a residue of metallic lead. This mechanism is, however, thought to be unlikely to contribute significantly to the deactivation observed under the conditions used.

The mechanism of pore blocking cannot occur in the case of unsupported nickel (II) oxide and cobalt (II,III,III) oxide, as neither of these catalysts has a porous structure. The other two unsupported catalysts are also unlikely to have a porous structure, and are therefore equally unlikely to be deactivated by a pore-blocking mechanism. However, this has not been established experimentally. With regard to alumina-supported catalysts, the mechanism of pore-blocking cannot be ruled out as the alumina phase

has a definite porous structure. Furthermore, pore-size distribution results, for all the supported catalysts examined, have clearly shown that the porous structure is progressively blocked by increasing quantities of lead halides. However, in view of the proven or inferred distribution of the active catalysts, which suggests that they exist mainly in particulate form on the outer alumina surface with only small amounts located internally, the mechanism of pore-blocking must be considered to be only of limited importance.

The mechanism of deactivation by adsorption of lead halides leading to monolayer formation, has not been proved to operate in the case of the unsupported catalysts. However, a layer of lead halide approximately one molecule thick (i.e. with most of the surface covered with a single molecular layer and the remainder either free of lead halide or covered with a thicker layer) is believed to form during the deactivation of nickel (II) oxide and manganese (IV) oxide by lead (II) bromide and also during the deactivation of cobalt (II,III,III) oxide by lead (II) chloride. Thus the complete deactivation of these catalysts must be caused by a lead halide layer somewhat more than one molecule thick. With nickel (II) oxide this layer would not greatly exceed one molecule in thickness as complete deactivation at the relatively high temperature of 306.5°C occurs for a lead (II) bromide content only slightly in excess of the monolayer capacity of the catalyst.

The deactivation of cobalt (II,III,III) oxide by lead (II) bromide appears to be a somewhat different process from that outlined for the previous systems, although it is envisiged that the formation of a lead halide layer approximately one molecule thick would initially be formed on a part of the catalyst surface. However, subsequent deposition of lead (II) bromide is believed to produce "islands" of greater thickness than one molecule surrounded by areas still free of lead (II) bromide. These "islands" would, on addition of still more lead halide, link up and eventually completely cover the surface of the catalyst. The final layer of lead (II) bromide would be expected on average to be considerably thicker than a monolayer.

The mechanisms outlined for the deactivation of nickel (II) oxide, manganese (IV) oxide and cobalt (II,III,III) oxide by lead (II) bromide suggest that adsorption of the lead halide is stronger, or at least takes place more readily on nickel (II) oxide and manganese (IV) oxide than on cobalt (II,III,III) oxide. There are a number of factors which may contribute to, or explain this difference, and for this reason it is possible to propose several reasonable explanations. However, it is conceivable that the most important factor is the presence or absence of defect structures in these catalysts. For example, nickel (II) oxide and manganese (IV) oxide are non-stoichiometric compounds, the former being deficient in nickel and the latter deficient in oxygen. In contrast to this, cobalt (II,III,III) oxide is a stoichiometric compound and thus has no defect structure due to non-stoichiometry. It is therefore possible that the apparently

greater ease with which lead (II) bromide is adsorbed on nickel (II) oxide compared with cobalt (II,III,III) oxide, is due to adsorption at the sites of lattice defects caused by non-stoichiometry.

In the case of cobalt (II,III,III) oxide, the apparently greater tendency for lead (II) chloride to be adsorbed may be explained in terms of a greater affinity of this halide for cobalt (II,III,III) oxide. Certainly if lead halides are chemisorbed on cobalt (II,III,III) oxide then it is reasonable to expect the strongest interactions to occur between elements with the greatest electronegativity differences. Thus the interactions between cobalt and halogen and lead and oxygen would be stronger than those between halogen and oxygen and lead and cobalt. In addition the interaction between lead and oxygen would occur in both systems so that the greater electronegativity difference between cobalt and chlorine, compared with that between cobalt and bromine would lead to a greater affinity of lead (II) chloride for cobalt (II,III,III) oxide.

The mechanism of deactivation of alumina-supported cobalt (II,III,III oxide by lead (II) bromide is considered to be fundamentally similar to that for the unsupported catalysts. This deduction arises simply from the structure of alumina-supported cobalt (II,III,III) oxide, which consists of separate cobalt (II,III,III) oxide particles situated at the outer surface of the alumina support with only a small part of the cobalt (II,III,III) oxide more intimately associated with the alumina phase. The main difference between the deactivation of supported and unsupported catalysts arises from the

influence of the support in providing a very large surface area for the adsorption of lead (II) bromide. However, lead (II) bromide appears to be concentrated mainly on the outer surface of the supported catalyst particles, with relatively little deep penetration into the porous structure. In addition the available evidence indicates that a similar situation exists for the deactivation of alumina-supported cobalt (II,III,III) oxide by lead (II) chloride. This lead compound is also concentrated mainly on the outer surface of the porous catalyst. Another point of similarity between the deactivation of supported and unsupported cobalt (II,III,III) oxide is that lead (II) chloride is considered to form a thinner layer than lead (II) bromide on supported cobalt (II,III,III) oxide. This last finding, therefore, indicates that lead (II) chloride is adsorbed more readily than lead (II) bromide on alumina, as well as on cobalt (II,III,III) oxide.

The deactivation by lead (II) bromide of both alumina-supported copper (II) oxide and alumina-supported platinum is believed to involve a mechanism which is, in essence, similar to that proposed for supported cobalt (II,III,III) oxide. According to this, lead (II) bromide is deposited on the outer surface of the support particles with relatively little deep penetration into the porous structure. Again, it is suggested that the active constituents of these catalysts are found mainly on the outer surface of the support particles. Finally, total deactivation in both cases has been found to be the result of a massive deposition of lead (II) bromide, which it is thought, renders the active parts of the catalysts completely inaccessible to reactant molecules.

REFERENCES

1. Encyclopaedia Britannica, 1975, 14, 750.

2. R. M. E. Diamant, "The Prevention of Pollution", page 112, Pitman, London, 1974.

3. World Health Organization Technical Report Series No. 506, "Air Quality Criteria and Guides for Urban Air Pollutants", 1972.

4. E. Challis, Chem. Brit., 1971, 7, 237.

5. Reference 2, page 181.

6. A. Curtis, Motor, September 8 1973, page 17.

7. R. S. Yolles, H. Wise, Critical Reviews in Environmental Control, 1971, 2 (1), 125.

8. Reference 2, pages 189, 195.

9. D. Bryce-Smith, Chem. Brit., 1971, 7, 54.

10. G. S. Parkinson, Chem. Brit., 1971, 7, 242.

11. Reference 6, page 16.

12. Reference 10, page 241.

13. A. Curtis, Motor, June 16 1973, page 27.

14. A. Curtis, New Scientist, May 3 1973, page 271.

15. J. J. Mikita, N. E. Cantwell, "Exhaust Manifold Thermal Reactors - A solution to the Automobile Emissions Problem", presented at the National Petroleum Refiners Association, San Antonio, Texas, April, 1970.

16. Reference 2, page 144.

17. D. R. Fussell, Petroleum Review, 1970, 24, 199.

18. F. G. Dwyer, Catalysis Reviews, 1972, 6 (2), 279.

19. J. M. Thomas and W. J. Thomas, "Introduction to the Principles of Heterogeneous Catalysis", page 9, Academic Press, London, 1967.

20. J. H. de Boer, Bull Soc. chim. Pays-Bas Belg. 1958,67, 284.

21. B. M. W. Trapnell, "Chemisorption" Chapter 1, Butterworths, London 1955.

22. Reference 19, page 33.

23. S. Brunauer, "The Adsorption of Gases and Vapours" University Press, Princeton, 1943.

24. K. J. Laidler, "Catalysis", Ed. P.H. Emmett, Vol.1, page 75, Reinhold, New York, 1954.

25. R. N. Pease and R. Stewart, J. Am.Chem.Soc. 1925, 47, 1235.

26. J. B. Newkirk and J. H. Wernick (Eds.), "Direct Observations of Imperfections in Crystals", Interscience, New York, 1962.

27. J. H. de Boer (Ed.) "Reactivity of Solids", Elsevier, Amsterdam, 1961.

28. P. Sabatier, "La Catalyse en Chemie Organique", Librairie Polytechnique, Paris, 1913.

29. N. W. Cant and W. K. Hall, J. Catalysis, 1970, 16,220.

30. D. A. Dowden and D. Wells, Actes 2^{e} Congr.Int. Catalysis, p. 1499, Paris, 1961.

31. D. A. Dowden, 2nd Int. Congr. Catalysis, Moscow, 1961.

32. J. Haber and F. S. Stone, Trans. Faraday Soc., 1962, 59, 192.

33. P. G. Ashmore "Catalysis and Inhibition of Chemical Reactions", page 188, Butterworths, London 1963.

34. K. C. Campbell and S. J. Thomson, Trans.Faraday Soc. 1959, 55, 306.

35. S. Affrossman, D. Cormack and S. J. Thomson, J.Chem.Soc. 1962, 3217.

36. S. J. Thomson and J. L.Wishlade, Trans.Faraday Soc. 1962, 58, 1170.

37. E. B. Maxted, K. L. Moon and E. Overagage, Discuss. Faraday Soc. 1950, 8, 135.

38. T. Kivan, Advan. Catalysis, 1954, 67, 103.

39. E. B. Maxted and H. C. Evans, J. Chem. Soc. 1937, 603.

40. A. Wheeler, Advan. Catalysis, 1951, 3, 249.

41. O.V. Krylov, "Catalysis by Nonmetals", Academic Press, New York, 1970.

42. C. F. Cullis, Ind. and Eng. Chem., 1967, 59, 20.

43. Reference 41, page 180.

44. Reference 18, page 263.

45. Y. Morooka and A. Ozaki, J. Catalysis, 1966, 5, 116.

46. Reference 33, page 190.

47. V. A. Shuets, W. M. Vorotinzev and V. B. Kazansky, J. Catalysis 1969, 15, 214.

48. T. Wolkenstein, Advan. Catalysis, 1960, 12 189.

49. D. A. Dowden, Chem. Eng. Prog. Symp. Ser., 1967, 63, 90.

50. Reference 41, page 63.

51. K. S. De and F. S. Stone, Nature, 1962, 194, 570.

52. E. P. Barrett, L. G. Joyner and P.P. Halenda, J. Am. Chem. Soc., 1951, 73, 373.

53. S. Brunauer, P. H. Emmett and E. Teller, J. Am. Chem. Soc. 1938, 60, 309.

54. F. M. Nelson and F. T. Eggertsen, Anal. Chem. 1958, 30, 1387.

55. C. Pierce, J. Phys. Chem. 1953, 57, 149.

56. L. S. Ettre, "Applications of the Continuous Flow Method and the model 212-D Sorptometer for Surface Studies", Perkin Elmer, Application No. SO - AP - 002, 1966.

57. Reference 19, page 69.

58. Reference 19, page 79.

59. R. P. Eischens and W. A. Pliskin, Advan. Catalysis, 1958, 10, 1.

60. H. P. Leftin, J. Phys. Chem. 1960, 64, 1714.

61. K. Siegbahn, Phil. Trans. Roy. Soc. London, Ser. A 1970, 268 (1184), 33-57.

62. D. L. Trimm, Private communication, 1974.

63. L. S. Birks, "Electron Probe Microanalysis", Interscience, New York, 1963.

64. R. L. Moss, M. J. Duell and D. H. Thomas, Trans. Faraday Soc. 1963, 59, 216.

65. I. Langmuir, J. Am. Chem. Soc. 1916, 38, 2221; 1917, 39, 1848; 1918, 40, 1361.

66. J. Deren and R. Mania, J. Catalysis, 1974, 35, 369.

67. D. E. Keene, Ph.D. Thesis, The City University, London, 1969, page 59.

68. R. J. Kokes, H. Tobin and P.H. Emmett, J.Am.Chem.Soc. 1955, 77, 5860.

69. J. H. Jones et al., Joint Meeting of AIChE and Instituto Mexicano de Ingenieros Quimcos, Denver,August 30, 1970.

70. R. L. Klimisch and J. M. Komarmy, "Approaches to Catalytic Control of Automotive NO_x Emissions", presented at the General Motors Research Symposium on "The Catalytic Chemistry of Nitrogen Oxides", October 8, 1974.

71. S. Z. Roginskii, Acta Physicochim. USSR, 1938, 9, 475.

72. S. Z. Roginskii and J. Zeldowitch, Acta Physicochim. USSR, 1934, 1, 554.

73. C. S. Brooks, J. Catalysis, 1967, 8, 272.

74. W. E. Gainer, T. J. Gray and F.S. Stone, Discuss. Faraday Soc., 1950, 8, 246.

75. E. D. Pierron, J. A. Rashkin and J. P. Roth, J. Catalysis 1967, 9, 38-44.

76. W. Hertl, J. Catalysis, 1973, 31, 231.

77. H. Praliand, J. Rousseau, F. Figueras and M.V. Mathieu, J. Chim. Phys. Physicochim. Biol. 1973, 70 (7-8), 1053-8.

78. M. J. Fuller, and M. E. Warwick, J. Catalysis, 1976, 42, 418.

79. N. Pacia, A. Cassuto, A. Dentenero and B. Weber, J. Catalysis, 1976, 41, 455-65.

80. E. McCarthy, J. Zahradnik, G. C. Kuczynski, and J.J. Carberry, J. Catalysis, 1975, 39, 29.

81. G. W. Keulks and C.C. Chang, J. Phys. Chem., 1970, 74 (13), 2590.

82. G. C. Bond, "Catalysis by Metals", Academic Press, London, page 460, 1962.

83. G. M. Schwab and K. Gossner, Z. Phys.Chem. (Frankfurt), 1958, 16, 39.

84. A. J. Grodsel, J. Catalysis, 1973, 30, 175-86.

85. Y.F. Yu Yao, J. Catalysis, 1973, 28, 139-49.

86. R. Mezaki and C. C.Watson, Ind. Eng. Chem. Proc. Des. Dev. 1966, 5(1), 62.

87. O. P. Ahuja and G. P. Mathur, Canad. J. Chem. Eng. 1967,45, 367.

88. L. Hiam, H. Wise and S. Chaikin, J. Catalysis, 1968, 9, 272.

89. B. A. Sazanov, V.V. Popovskii and G. K. Boreshov, Kinetika i Kataliz, 1968, 9 (2), 312.

90. B. Dmuchovsky, M. C. Freerks and F. B. Zienty, J. Catalysis, 1965, 4, 577.

91. Y. Morooka and A. Ozaki, J. Catalysis, 1966, 5, 116.

92. Y. F. Yu Yao and J. T. Kummer, J. Catalysis, 1973, 28, 124-38.

93. Y. F. Yu Yao, J. Catalysis, 1974 33, 108-22.

94. Reference 18, page 285.

95. E.R.S. Winter, J. Catalysis, 1971, 22, 158.

96. K. Jellinek, Z. Anorg. Allgem. Chem. 1906, 49, 229.

97. M. Shelef, K. Otto and H. Gandhi, J. Catalysis, 1968, 12, 361.

98. D. T. Clay and S. Lynn, "Iron-Catalyzed Reduction of NO by CO and H_2 in Simulated Flue Gas", presented at the General Motors Research Symposium on "The Catalytic Chemistry of Nitrogen Oxides", October 8, 1974.

99. E. L. Force and R. J. Ayen, Am. Inst. Chem. Eng., Symp. Ser. 1972, 68, 80.

100. R. T. Rewick and H. Wise, J. Catalysis, 1975, 40, 301-11.

101. R. A. Baker and R. C. Doerr, Ind. Eng. Chem. Proc. Res. Dev., 1965, 4(2), 188.

102. R. L. Klimisch and G. Barnes, J. Environ. Sci. Tech. 1972, 6, 543.

103. G. H. Megurian and C. R. Lang, SAE Automotive Congress, Paper No. 710291, January 1971.

104. R. L. Klimisch and K. C. Taylor, Environ. Sci. Tech. 1973, 7, 127.

105. M. Shelef and H. S. Gandhi, Ind. Eng. Chem. Prod. Res. Dev. 1972, 11, 393.

106. T. P. Kobylinski and B. W. Taylor, J. Catalysis, 1974, 33, 376.

107. K. C. Taylor, "Simultaneous NO and CO Conversion over Rhodium", presented at the General Motors Research Symposium on "The Catalytic Chemistry of Nitrogen Oxides" October 8, 1974.

108. D. R. Ashmead, J. S. Campbell, P. Davies and K. Farmery, SAE paper No. 740249, Detroit, 1974.

109. Reference 18, page 277.

110. Reference 7, page 140.

111. R. J. Leak, J. T. Brandenburg and M. D. Behrens, Environ.Sci. Tech. 1968, 2, 10.

112. E. I. du Pont de Nemours and Company, British Patent 1,068, 186, May 10, 1967.

113. W. A. Cannon and C. E. Welling, SAE Meeting, Detroit, Paper 297, January 1959.

114. E. E. Weaver, SAE Int. Automotive Eng. Congress, Detroit, Paper 690016, January 1969.

115. K. I. Jagel and F. G. Dwyer, SAE Automotive Congress, Paper 710290, January 1971.

116. Reference 7, page 138.

117. R. E. Stephens, U.S. Patent 3,425,792, February 4, 1969.

118. Y. Oda and M. Suhara, Japanese Patent 74,134,569, December 25, 1974.

119. P. K. Gallagher, D. W. Johnson, E. M. Vogel and F. Schrey, Mater. Res. Bull. 1975, 10(7), 623-7.

120. M. Kobayashi and H. Kobayashi, J. Catalysis, 1975, 36, 74-80.

121. J. F. Roth, Division of Petr. Chem., ACS, Los Angeles Meeting, March 1971, Preprint, Vol. 16, 2, page E 53.

122. L. L. Hegedus and K. Baron, J. Catalysis, 1975, 37, 129.

123. J. L. Bomback, M. A. Wheeler, J. Tabock and J. Janowski, Environ. Sci. Techn. 1975, 9(2), 139-43.

124. J. Mooi, J. P. Kuebrich, M.F.L. Johnson and F.J. Chloupek, Proc., Div., Refining, Am. Petrol. Inst., 1973, 53, 14-25.

125. E.C. Su, E. E. Weaver, SAE (Tech. Paper), Paper 730594, 1973.

126. R. L. Klimisch, C. Jerry and J. C. Schlatler, Adv. Chem. Ser. 1975, 143, 103-15.

127. D. McArthur, Adv. Chem. Ser. 1975, 143, 85-101.

128. G. J. K. Acres, B. J. Cooper, E. Shutt and B. W. Malerbi, Adv. Chem. Ser. 1975, 143, 55-71.

129. W. Fitzgerald and J. V. D. Wilson SAE (Tech. Paper), Paper 750447, 1975.

130. F. Williams and K. Baron, J. Catalysis, 1975, 40, 108-16.

131. M. A. Wheeler and M. Bettman, J. Catalysis, 1975, 40, 124-28.

132. D. M. Teague, Report to Chrysler Corporation, No. E-8546-1, May 14, 1974.

133. K. Otto and C. N. Montreuil, Environ. Sci. Tech. 1976, 10(2), 154-8.

134. D. M. Teague, L. B. Clougherty and A. N. Speca, Environ. Health Perspect., 1975, 10, 113-16.

135. Reference 128, page 55.

136. D. P. McArthur, "NO_x Catalyst Degradation by Contaminant Poisoning" presented at the General Motors Research Symposium on"The Catalytic Chemistry of Nitrogen Oxides", October 8, 1974.

137. D. A. Hirschler, L. F. Gilbert, F. W. Lamb and L. M.Niebylski, Ind. Eng. Chem. 1957, 49, 1131-1142.

138. W. E. Newby and L. F. Dumont, Ind. Eng. Chem. 1953, 45, 1336.

139. F. S. Stone, Advan. Catalysis, 1962, 13, 1.

140. F. M. Vainshtein and G. Y. Turovskii, Dokl. Akad. Nank S.S.S.R. 1950, 72 297: 1951, 78, 1173.

141. Reference 19, page 370.

142. A. B. Littlewood, "Gas Chromatography", Academic Press, London, 1962.

143. R. Alan Jones, "Gas-Liquid Chromatography" Academic Press, London, 1970.

144. H. L. Gruber, J. Phys. Chem., 1962, 66, 48.

145. H. L. Gruber, Anal. Chem., 1962, 34, 1848.

146. J. J. F. Scholten and A. Van Montfoort, J. Catalysis, 1962, 1, 85.

147. H. W. Daeschner and F. H. Stross, Anal. Chem. 1962, 34, 1150.

148. M. G. Farey and B. G. Tucker, Anal. Chem., 1971, 43, 1307.

149. B. G. Tucker, Private communication, 1972.

150. International Critical Tables, 1928, 3, 309.

151. R. Duckworth, Ph.D. Thesis, The City University, London, 1975, page 78.

152. Reference 7, page 138.

153. A. F. Wells, "Structural Inorganic Chemistry", 4th Edition, Clarenden Press, Oxford, 1975.

154. M. W. Lister, and L. E. Sutton, Trans. Faraday Soc. 1941, 37, 406.

155. P. H. Emmett and S. Brunauer, J. Am. Chem. Soc., 1937, 59, 1553.

156. J. W. Mellor, "A Comprehensive Treatise on Inorganic and Theoretical Chemistry" 1970, 7, p. 712, 748.

157. Reference 33, page 189.

158. E. R. S. Winter, Advan. Catalysis, 1958, 10, 196.

159. G. V. Samsonov, "The Oxide Handbook", Translated by C.N.Turton and T. I. Turton, IFI/Plenium, New York, 1973, p. 108, 215.

160. J. R. Anderson, "Structures of Metallic Catalysts", Academic Press, 1975 p. 193.

161. M. Hansen, "Constitution of Binary Alloys", McGraw-Hill Book Co., 1958.

--oOo--

APPENDIX

```
      MASTER PORE SIZE DISTRIBUTION
C
C     PROGRAMME TO COMPUTE PORE SIZE DISTRIBUTION FOR
C     CONTINUOUS FLOW SURFACE AREA APPARATUS
C
C     SYMBOLS USED
C
C     W = WEIGHT OF SAMPLE
C     A = RELATIVE PRESSURE
C     B = PORE DIAMETER UNCORRECTED
C     C = VOLUME OF NITROGEN PER GRAM OF SOLID
C     X = GASEOUS VOLUME OF NITROGEN
C     D = APPARENT PORE VOLUME
C     E = INCREMENTAL REDUCTIONS OF D
C     F = AVERAGE PORE DIAMETER
C     G = INCREMENTS OF SURFACE AREA UNCORRECTED
C     H = SUMMATION OF SURFACE AREA UNCORRECTED
C     O = N STATISTICAL LAYERS
C     P = CORRECTION FOR PORE DIAMETER
C     Q = CORRECTED PORE VOLUME
C     R = INCREMENTAL REDUCTIONS OF Q
C     S = INCREMENTS OF SURFACE AREA
C     T = SUMMATION OF SURFACE AREA
C     U = DELTA PORE RADIUS
C     V = PORE SIZE DISTRIBUTION ORDINATE
C
      DIMENSION A(20),B(20),C(20),D(20),H(20),O(20),
     1P(20),Q(20),R(20),S(20),T(20),U(20),V(20),G(20),
     2X(20),F(20)
   65 DO 13 I = 1,20
      A(I) = 0.0
      X(I) = 0.0
      B(I) = 0.0
      C(I) = 0.0
      D(I) = 0.0
      E(I) = 0.0
      F(I) = 0.0
      G(I) = 0.0
      H(I) = 0.0
      O(I) = 0.0
      P(I) = 0.0
      Q(I) = 0.0
      R(I) = 0.0
      S(I) = 0.0
      T(I) = 0.0
      U(I) = 0.0
   13 V(I) = 0.0
      READ (1,100)(X(I),B(I),A(I),I = 2,20)
  100 FORMAT(3F9.4)
      READ (1,101)(O(I),I =2,19)
  101 FORMAT(F4.1)
      READ(1,102)W
  102 FORMAT(F6.4)
      X(2) = X(3)*1.02
      DO 10 I = 2,20
      C(I) = X(I)/W
   10 D(I) = C(I)*0.00155
      CONTINUE
C
C     CONTINUED ON NEXT PAGE
```

```
C
      DO 21 J = 2,19
      I = 1+J
      E(J) = D(J)-D(I)
      F(J) = (B(J)+B(I))/2
      G(J) = (E(J)*40000.0)/F(J)
      N = J-1
      H(J) = H(N)+G(J)
      P(J) = (H(J)*O(J))/10000.0
   21 Q(J) = D(J)-P(N)
      CONTINUE
      DO 20 J = 2,19
      N = J-1
      I = J+1
      R(J) = Q(J)-Q(I)
      S(J) = (R(J)*40000.0)/F(J)
      T(J) = T(N)+S(J)
      U(J) = (B(J)-B(I))/2
   20 V(J) = (R(J)/U(J))*10000.0
      CONTINUE
      WRITE(2,200)
  200 FORMAT(1H1,////,8X,4HPORE,12X,8HAPPARENT,8X,4HPORE,
     112X,7HAVERAGE,6X,4HPORE,1X,4HSIZE,6X,8HRELATIVE,7X,
     23HGAS,1X,3HVOL,/,7X,8HDIAMETER,8X,4HPORE,1X,6HVOLUME,
     36X,6HVOLUME,8X,4HPORE,1X,8HDIAMETER,5X,7HDISTRIB,1X,
     43HORD,5X,8HPRESSURE,8X,4HGRAM,1X,5HSOLID,/)
      WRITE(2,201)(B(I),D(I),Q(I),F(I),V(I),A(I),C(I),
     1I = 2,20)
  201 FORMAT(7F16.6,/)
      READ(1,30)N
   30 FORMAT(I1)
      IF(N-1)65,66,65
   66 CONTINUE
      STOP
      END
```

```
      MASTER SURFACE PROPERTIES(CARLO ERBA)
C
C     PROGRAMME TO COMPUTE NITROGEN ADSORPTION ISOTHERMS,
C     SPECIFIC SURFACE AREAS, AND PORE SIZE DISTRIBUTIONS
C     FOR THE CARLO ERBA SORPTOMATIC SERIES 1800
C
C     SYMBOLS USED
C
C      W = WEIGHT OF SAMPLE GRAM
C     PE = INTRODUCTION PRESSURE TORR
C     PO = ATMOSPHERIC PRESSURE TORR
C     NA = NUMBER OF INTRODUCTIONS
C     NR = NUMBER OF REDUCED STROKES
C     ND = NUMBER OF DESORPTIONS
C     PA = ADSORPTION PRESSURE
C     PD = DESORPTION PRESSURE
C     VA/W = VOLUME OF NITROGEN ADSORBED/GRAM OF SAMPLE
C     PA/PO = PARTIAL PRESSURE OF NITROGEN (ADSORPTION)
C     VD/W = VOLUME OF NITROGEN STILL ADSORBED/GRAM OF SAMPLE
C     PD/PO = PARTIAL PRESSURE OF NITROGEN (DESORPTION)
C     DV/DRP = A MEASURE OF PORE VOLUME AT GIVEN PORE RADIUS
C     RPB = MEAN PORE RADIUS
C     SS = SPECIFIC SURFACE AREA M2/G
C     VTOT = TOTAL VOLUME INTRODUCED
C     RM = MEAN PORE RADIUS
C
C     NOTE
C (1)
C     THE INTRODUCTION VOLUME FOR A COMPLETE STROKE (VS) AND
C     FOR A REDUCED STROKE (VSR) ARE SPECIFIC FOR THE
C     INSTRUMENT USED IN THIS WORK
C
C (2)
C     THE EQUATIONS USED TO CALCULATE VGA AND VGD ARE SPECIFIC
C     FOR THE BURETTE USED IN THIS WORK
C
      DIMENSION PA(31),PD(31),VGA(31),VA(31),VAW(31)
      DIMENSION PPNA(31),RPB(31),X(31),Y(31),VGD(31),VK(31)
      DIMENSION VD(31),VDW(31),PPND(31),VLIQ(31),RK(31)
      DIMENSION T(31),RP(31),DV(31),DRP(31),DVDR(31)
C
C       SET ARRAYS TO ZERO
C
  98  DO 99 I = 1,31
      PA(I) = 0.0
      PD(I) = 0.0
      VGA(I) = 0.0
      VA(I) = 0.0
      VAW(I) = 0.0
      PPNA(I) = 0.0
      X(I) = 0.0
      Y(I) = 0.0
      VK(I) = 0.0
      VGD(I) = 0.0
      VD(I) = 0.0
      VDW(I) = 0.0
      PPND(I) = 0.0
      VLIQ(I) = 0.0
      RK(I) = 0.0
      T(I) = 0.0
      RP(I) = 0.0
      DV(I) = 0.0
      DRP(I) = 0.0
      DVDR(I) = 0.0
  99  RPB(I) = 0.0
C
C     CONTINUED ON NEXT PAGE
```

```
C
C     READ IN DATA
C
  127 READ (1,100) W,PE,PO
  100 FORMAT (F6.4,F6.1,F5.1)
      READ (1,101) NA,NR,ND
  101 FORMAT (3I2)
      READ (1,102) (PA(I), I = 1,NA)
  102 FORMAT (F5.1)
      N = ND + 1
      PD(1) = 0.0
      READ (1,103) (PD(I), I = 2,N)
  103 FORMAT (F5.1)
C
C    CALCULATE ADSORPTION ISOTHERM
C
      VS = 17.081
      VSR = 8.56
      AK = 0.001159
      CPA = 200.0
      AN = 0.0
      NB = 0
      NSS = 0
      SSN = 0.0
      SVI = 0.0
      DO 104 I = 1,NA
      AN = AN + 1.0
      IF(NR.EQ.0) GO TO 105
      VI = VSR*PE*AK
      SVI = SVI + VI
      VGA(I) = 0.2846*PA(I) + 0.226
  107 VA(I) = SVI - VGA(I)
      VAW(I) = VA(I)/W
      PPNA(I) = PA(I)/PO
      IF(PPNA(I).GT.0.3) GO TO 130
      NSS = NSS + 1
      SSN = SSN + 1.0
  130 NR = NR - 1
      NB = NB + 1
      GO TO 108
  105 VI = VS*PE*AK
      SVI = SVI + VI
      VGA(I) = 0.2846*PA(I) + 0.226
  110 VA(I) = SVI - VGA(I)
      VAW(I) = VA(I)/W
      PPNA(I) = PA(I)/PO
      IF(PPNA(I).GT.0.3) GO TO 108
  129 NSS = NSS + 1
      SSN = SSN + 1.0
  108 CONTINUE
  104 CONTINUE
C
C     CONTINUED ON NEXT PAGE
C
```

```
C
C     CALCULATE SPECIFIC SURFACE AREA, AND MEAN PORE RADIUS
C
      SX = 0.0
      SY = 0.0
      SXX = 0.0
      SXY = 0.0
      DO 111 I = 1,NSS
      X(I) = PO - PA(I)
      Y(I) = PA(I)/((VA(I)*X(I))/W
      SX = SX + X(I)
      SY = SY + Y(I)
      SXY = SXY + (X(I)*Y(I))
  111 SXX = SXX + (X(I)*X(I))
      AM = ((SSN*SXY)-(SX*SY))/((SSN*SXX)-(SX*SX))
      XB = SX/SSN
      YB = SY/SSN
      B = YB - (AM*XB)
      VM = 1.0/(AM + B)
      SS = VM*4.39
      RM = 2.0*VA(NA)*15.5/(W*SS)
C
C     CALCULATE VTOT
C
      VTOT = 0.0
      IF(NB.EQ.0) GO TO 112
      VTOT = VSR*PE*AK*NB
      NA = NA - NB
  112 VTOT = VTOT + (VS*PE*AK*NA)
      IF(NB.EQ.0) GO TO 113
      NA = NA + NB
C
C     CALCULATE DESORPTION ISOTHERM
C
  113 ND = ND + 1
      SVK = 0.0
      DO 114 I = 2,ND
      VK(I) = PD(I)*VS*AK
      SVK = SVK + VK(I)
      VGD(I) = 0.2846*PD(I) + 0.226
  116 VD(I) = VTOT - VGD(I) - SVK
      VDW(I) = VD(I)/W
  114 PPND(I) = PD(I)/PO
C
C     CALCULATE PORE SIZE DISTRIBUTION
C
      VLIQ(1) = 0.0
      RP(1) = 0.0
      DO 117 I = 2,ND
      J = I - 1
      VLIQ(I) = VD(I)*0.00155/W
      DV(I) = VLIQ(J) - VLIQ(I)
      RK(I) = (-4.14/(ALOG10(PPND(I))))
      T(I) = (-172.6/(ALOG10(PPND(I))))**(1.0/3.0)
      RP(I) = RK(I) + T(I)
      DRP(I) = RP(J) - RP(I)
      DVDR(I) = DV(I)/DRP(I)
  117 RPB(I) = (RP(J) + RP(I))/2.0
C
C     CONTINUED ON NEXT PAGE
C
```

```
C
C   PRINT OUT RESULTS
C
      WRITE (2,122) W,PE,PO
  122 FORMAT (1H1,9X,20H WEIGHT OF SAMPLE = ,F6.4,
     1//,28H INTRODUCTION PRESSURE PE = ,F6.1,5H TORR,//,
     124H ATMOSPHERIC PRESSURE = ,F5.15H TORR)
      WRITE (2,125) SS,VTOT,RM
  125 FORMAT (1H0,///,25H SPECIFIC SURFACE AREA = ,F6.2,
     15H M2/G,//,8H VTOT = ,F6.2,4H CM3,//,6H RM = ,
     1F7.4,3H A )
      WRITE (2,123)
  123 FORMAT (1H0,84X,10HPORE SIZE,/,13X,10HADSORPTION,
     130X,10HDESORPTION,20X,12HDISTRIBUTION,//,4X,2HPA,10X,
     14HVA/W,10X,5HPA/PO,9X,2HPD,10X,4HVD/W,8X,5HPD/PO,8X,
     16HDV/DRP,8X,3HRPB,/)
      WRITE (2,124) (PA(I),VAW(I),PPNA(I),PD(I),VDW(I),
     1PPND(I),DVDR(I),RPB(I), I = 1,31)
  124 FORMAT ((1H0,F9.3,5X,7(F8.4,5X)))
      READ (1,126) NS
  126 FORMAT (I1)
      IF(NS.EQ.0) GO TO 128
      GO TO 98
  128 CONTINUE
      STOP
      END
```